UNIVERSITAT POLITÈCNICA DE CATALUNYA

Programa de Doctorat:

AUTOMÀTICA, ROBÒTICA I VISIÓ

Tesi Doctoral

DISTANCE-BASED FORMULATIONS FOR THE POSITION ANALYSIS OF KINEMATIC CHAINS

Nicolás Rojas

Director: Federico Thomas

Abril de 2012

Universitat Politècnica de Catalunya

Programa de Doctorat:
Automàtica, Robòtica i Visió

Aquesta tesi ha estat realitzada a:
Institut de Robòtica i Informàtica Industrial, CSIC-UPC

Director de tesi:
Federico Thomas

© Nicolás Rojas 2012

To all those Colombians abroad that day by day, with their work, intelligence, and initiative, project a new image of our country

"Nothing in the world can take the place of persistence. Talent will not; nothing is more common than unsuccessful men with talent. Genius will not; unrewarded genius is almost a proverb. Education will not; the world is full of educated derelicts. Persistence and determination alone are omnipotent"

Calvin Coolidge

Abstract

This thesis addresses the kinematic analysis of mechanisms, in particular, the position analysis of kinematic chains, or linkages, that is, mechanisms with rigid bodies (links) interconnected by kinematic pairs (joints). This problem, of completely geometrical nature, consists in finding the feasible assembly modes that a kinematic chain can adopt. An assembly mode is a possible relative transformation between the links of a kinematic chain. When an assignment of positions and orientations is made for all links with respect to a given reference frame, an assembly mode is called a configuration. The methods reported in the literature for solving the position analysis of kinematic chains can be classified as graphical, analytical, or numerical.

The graphical approaches are mostly geometrical and designed to solve particular problems. The analytical and numerical methods deal, in general, with kinematic chains of any topology and translate the original geometric problem into a system of kinematic equations that defines the location of each link based, mainly, on independent loop equations. In the analytical approaches, the system of kinematic equations is reduced to a polynomial, known as the *characteristic polynomial* of the linkage, using different elimination methods —*e.g.*, Gröbner bases or resultant techniques. In the numerical approaches, the system of kinematic equations is solved using, for instance, polynomial continuation or interval-based procedures.

In any case, the use of independent loop equations to solve the position analysis of kinematic chains, almost a standard in *kinematics of mechanisms*, has seldom been questioned despite the resulting system of kinematic equations becomes quite involved even for simple linkages. Moreover, stating the position analysis of kinematic chains directly in terms of poses, with or without using independent loop equations, introduces two major disadvantages: arbitrary reference frames has to be included, and all formulas involve translations and rotations simultaneously. This thesis departs from this standard approach by, instead of directly computing Cartesian locations, expressing the original position problem as a system of distance-based constraints that are then solved using analytical and numerical procedures adapted to their particularities.

In favor of developing the basics and theory of the proposed approach, this thesis focuses on the study of the most fundamental planar kinematic chains, namely, Baranov trusses, Assur kinematic chains, and pin-jointed Grübler kinematic chains. The results obtained have shown that the novel developed techniques are promising tools for the position analysis of kinematic chains and related problems. For example, using these techniques, the *characteristic polynomials* of most of the cataloged Baranov trusses can be obtained without relying on variable eliminations or trigonometric substitutions and using no other tools than elementary algebra. An outcome in clear contrast with the complex variable eliminations require when independent loop equations are used to tackle the problem.

The impact of the above result is actually greater because it is shown that the *characteristic polynomial* of a Baranov truss, derived using the proposed distance-based techniques, contains all the necessary and sufficient information for solving the position

analysis of all the Assur kinematic chains resulting from replacing some of its revolute joints by slider joints. Thus, it is concluded that the polynomials of all fully-parallel planar robots can be derived directly from that of the widely known 3-R<u>P</u>R robot. In addition to these results, this thesis also presents an efficient procedure, based on distance and oriented area constraints, and geometrical arguments, to trace coupler curves of pin-jointed Grübler kinematic chains. All these techniques and results together are contributions to *theoretical kinematics of mechanisms*, robot kinematics, and distance plane geometry.

Abstract in Spanish

Resumen

Esta tesis aborda el problema de análisis cinemático de mecanismos, en particular, el análisis de posición de cadenas cinemáticas, es decir, mecanismos con cuerpos rígidos (enlaces) interconectados por pares cinemáticos (articulaciones). Este problema, de naturaleza completamente geométrica, consiste en encontrar los modos de ensamblaje factibles que una cadena cinemática puede adoptar. Un modo de ensamblaje es una transformación relativa posible entre los enlaces de una cadena cinemática. Cuando una asignación de posiciones y orientaciones se hace para todos los enlaces con respecto a un marco de referencia dado, un modo de ensamblaje recibe el nombre de configuración. Los métodos reportados en la literatura para la solución del análisis de posición de cadenas cinemáticas se pueden clasificar como gráficos, analíticos o numéricos.

Los enfoques gráficos son en su mayoría geométricos y se diseñan para resolver problemas particulares. Los métodos analíticos y numéricos tratan, en general, con cadenas cinemáticas de cualquier topología y traducen el problema geométrico original en un sistema de ecuaciones cinemáticas que define la ubicación de cada enlace, basado generalmente en ecuaciones de bucle independientes. En los enfoques analíticos, el sistema de ecuaciones cinemáticas se reduce a un polinomio, conocido como el *polinomio característico* de la cadena cinemática, utilizando diferentes métodos de eliminación —*e.g.*, bases de Gröbner o técnicas de resultantes. En los métodos numéricos, el sistema de ecuaciones cinemáticas se resuelve utilizando, por ejemplo, la continuación polinomial o procedimientos basados en intervalos.

En cualquier caso, el uso de ecuaciones de bucle independientes para resolver el análisis de posición de cadenas cinemáticas, prácticamente un estándar en *cinemática de mecanismos*, rara vez ha sido cuestionado a pesar de que el sistema resultante de ecuaciones cinemáticas es bastante complicado incluso para cadenas cinemáticas simples. Por otra parte, establecer el análisis de la posición de cadenas cinemáticas directamente en términos de poses, con o sin el uso de ecuaciones de bucle independientes, presenta dos inconvenientes principales: sistemas de referencia arbitrarios deben ser introducidos, y todas las fórmulas implican traslaciones y rotaciones de forma simultánea. Esta tesis se aparta de este enfoque estándar expresando el problema de posición original como un sistema de restricciones basadas en distancias, en lugar de directamente calcular posiciones cartesianas. Estas restricciones son posteriormente resueltas mediante procedimientos analíticos y numéricos adaptados a sus particularidades.

Con el propósito de desarrollar los conceptos básicos y la teoría del enfoque propuesto, esta tesis se centra en el estudio de las cadenas cinemáticas planas más fundamentales, a saber, estructuras de Baranov, cadenas cinemáticas de Assur, y cadenas cinemáticas de Grübler con articulaciones de revolución. Los resultados obtenidos han demostrado que las novedosas técnicas desarrolladas son herramientas prometedoras para el análisis

de posición de cadenas cinemáticas y problemas relacionados. Por ejemplo, usando dichas técnicas, los *polinomios característicos* de la mayoría de las estructuras de Baranov catalogadas se puede obtener sin realizar eliminaciones de variables o sustituciones trigonométricas, y utilizando solo herramientas de álgebra elemental. Un resultado en claro contraste con las complejas eliminaciones de variables que se requieren cuando las ecuaciones de bucle independientes se utilizan para abordar el problema.

El impacto del resultado anterior es en realidad mayor porque se demuestra que el *polinomio característico* de una estructura de Baranov, derivado a partir de las técnicas propuestas basadas en distancias, contiene toda la información necesaria y suficiente para resolver el análisis de posición de todas las cadenas cinemáticas de Assur que resultan de la sustitución de algunas de sus articulaciones de revolución por articulaciones prismáticas. De esta forma, se concluye que los polinomios de todos los robots planares totalmente paralelos se pueden derivar directamente del *polinomio característico* del ampliamente conocido robot 3-R$\underline{\text{P}}$R. Además de estos resultados, esta tesis también presenta un procedimiento eficaz, basado en restricciones de distancias y áreas orientadas, y argumentos geométricos, para trazar curvas de acoplador de cadenas cinemáticas de Grübler con articulaciones de revolución. En conjunto, todas estas técnicas y resultados constituyen contribuciones a la *cinemática teórica de mecanismos*, la cinemática de robots, y la geometría plana de distancias.

Acknowledgments

Federico (Fede) Thomas, my director and the man whose novel ideas and guidance shaped this thesis, deserves my infinite gratitude. Thanks to his passion for research and his, literally, open door policy, we have formed a team that has made big steps in a few time. Fede, I have learned a lot of things from you but, without doubt, it is your commitment of conducting research of high quality, the teaching that will mark my scientific career. Thank you so much!

A special recognition has to be given to Lluís Ros. I am very much indebted to him. Lluís opened me the door to the great place that is the *Institut de Robòtica i Informàtica Industrial (IRI)* by suggesting my name to Fede in late summer 2009. Moreover, since I met him during his graduate course "Kinematic Geometry of Robot Mechanisms" (formerly called "Geometry and Computational Kinematics in Robotics"), Lluís has always shown the attitude of someone I can count on.

I also thank my fellows at IRI for their support, the good times, and the interesting talks. My gratitude goes especially to the members of "D19+rodalies", "tupper world", and "IRIFutbol". The IRI's administrative and IT staff also deserve an acknowledgment, clearly their professionalism made my work easier. In these lines, I have to mention David Lavernia. I am very grateful for his open-minded attitude and companionship, particularly, during those times completely dedicated to graduate courses that were my first months in Barcelona.

Now Marta. Knowing you has been really the most important thing along this time. You are my partner in this journey called life. Living, sharing, and making plans with you are wonderful experiences I want to repeat every day! Thank you very much for your love, time, and unconditional support. I also want to greatly thank the help, kindness, and affection of Moreno and Benito families, especially to Ana, Chema, and Jordi.

Finally, I would like to thank my mother, María de los Ángeles, and my family in Cali and abroad:
Ma', aunque te lo he dicho muchas veces, nunca será suficiente: muchas gracias por todo tu amor, ayuda y ejemplo. Tus enseñanzas me alientan a no desfallecer y a continuar la lucha por mis sueños. A mi familia en Cali, mis tíos y primos, quiero agradecerles todo su apoyo, especialmente la tranquilidad que me brinda el saber que mi madre puede contar con ellos en los momentos que más se necesita. A mi primo (mi hermano) Lucho, en Miami, quiero agradecerle su amistad y compañía constante a través de la red. A mi tía y mi prima en México D.F. les agradezco, particularmente, el demostrarme que salir de tu país en busca de objetivos personales y profesionales es algo difícil, pero normal.

My doctoral studies and the research reported in this thesis have been partially developed under the activities of:

- The Catalonian Reference Network in Advanced Production Technologies (XaRTAP),

and have been partially supported by:

- The Colombian Ministry of Communications and Colfuturo through the Information and Communications Technology (ICT) National Plan of Colombia, and
- My own and my mother's savings.

Contents

Abstract **ix**

Figures **xx**

Tables **xxi**

1 Introduction **1**
1.1 On kinematics, mechanisms, and kinematic chains . . . 1
1.1.1 Theoretical kinematics and kinematics of mechanisms . . . 1
1.2 Position analysis of kinematic chains . . . 3
1.2.1 Solution approaches . . . 3
1.2.1.1 Analytical methods . . . 4
1.2.1.2 Numerical methods . . . 6
1.3 About distance geometry . . . 7
1.3.1 Why distance geometry? . . . 7
1.3.2 The graph embedding problem . . . 7
1.3.2.1 The Euclidean distance matrix completion problem . . . 8
1.4 A new approach to the position analysis of kinematic chains . . . 9
1.5 Planar kinematic chains . . . 9
1.5.1 Mobility . . . 10
1.5.2 Modular kinematics . . . 10
1.6 Overview of chapters . . . 13

2 Bilateration matrices and closure conditions **15**
2.1 Basic notation . . . 15
2.2 Cayley-Menger determinants . . . 15
2.3 Bilateration . . . 15
2.3.1 Bilateration matrices . . . 16
2.3.1.1 Basic properties of bilateration matrices . . . 17
2.4 Perpendicular matrices and fundamental properties . . . 17
2.5 Ruler and compass constructions . . . 19
2.5.1 Circle-circle, circle-line, and line-line intersections . . . 19
2.5.2 Bilateration, geometric constructions, and kinematic chains . . . 20
2.6 Strips of triangles . . . 20
2.6.1 Two triangles sharing one edge . . . 20
2.6.2 Squared distances in strips of triangles . . . 21
2.6.3 Strips of strips of triangles . . . 22
2.7 Closure conditions of kinematic chains using bilateration matrices . . . 23
2.7.1 Closure conditions and symmetries of kinematic chains . . . 24

3 Position analysis of Baranov trusses **27**
3.1 Position analysis of the triad or $3/B_1$ Baranov truss . . . 29
3.1.1 Example . . . 30
3.2 Position analysis of the pentad or $5/B_1$ Baranov truss . . . 31
3.2.1 Deriving the characteristic polynomial . . . 31
3.2.2 Computing configurations . . . 32
3.2.3 Example . . . 32
3.3 Position analysis of the seven-link Baranov trusses . . . 33
3.3.1 Position analysis of the $7/B_1$ Baranov truss . . . 33
3.3.1.1 Computing $s_{6,8}$ as a function of $s_{2,3}$ . . . 35
3.3.1.2 Deriving the characteristic polynomial . . . 36
3.3.1.3 Example . . . 37
3.3.2 Position analysis of the $7/B_2$ Baranov truss . . . 39
3.3.2.1 Computing $s_{1,6}$ as a function of $s_{4,8}$ . . . 39
3.3.2.2 Deriving the characteristic polynomial . . . 40
3.3.2.3 Example . . . 41
3.3.3 Position analysis of the $7/B_3$ Baranov truss . . . 41
3.3.3.1 Computing $s_{7,9}$ as a function of $s_{1,4}$ . . . 43
3.3.3.2 Deriving the characteristic polynomial . . . 44
3.3.3.3 Example . . . 44
3.4 Position analysis of four-loop Baranov trusses . . . 44
3.4.1 Solving a truss of coupling degree 2: The $9/B_{28}$ Baranov truss . . . 44
3.4.1.1 Computing $s_{6,10}$ as a function of $s_{1,4}$ and $s_{2,4}$ . . . 47
3.4.1.2 Computing $s_{7,9}$ as a function of $s_{1,4}$ and $s_{2,4}$ . . . 47
3.4.1.3 Deriving the characteristic polynomial . . . 48
3.4.1.4 Example . . . 49
3.4.2 All four-loop Baranov trusses . . . 50
3.5 Compendium: All the cataloged Baranov trusses . . . 50
3.6 Beyond four loops . . . 52
3.6.1 Baranov trusses of regular patterns . . . 52
3.6.2 Position analysis of the general n-link Watt-Baranov truss . . . 53
3.6.2.1 Example: A five-loop Watt-Baranov truss . . . 55
3.6.2.2 Example: A six-loop Watt-Baranov truss . . . 58

4 Position analysis of Assur kinematic chains **63**
4.1 Projective extensions of Baranov trusses . . . 64
4.2 Position analysis of a family of seven-link Assur kinematic chains . . . 66
4.2.1 The assembly modes of the $7/B_3$ Baranov truss . . . 66
4.2.2 Replacing one revolute joint . . . 67
4.2.3 Replacing two adjacent revolute joints . . . 70
4.2.4 Replacing a revolute joint involved in the variable distance . . . 71

5 The forward kinematics of all fully-parallel planar robots **75**
5.1 The forward kinematics of 3-RPR planar robots . . . 75
5.1.1 Distance-based formulation . . . 76
5.1.2 Analytic robots . . . 78
5.1.3 Examples . . . 79
5.1.3.1 Example I: A comparison with previous formulations . . . 79
5.1.3.2 Example II: Roots at $T = 0$ . . . 82
5.1.3.3 Example III: Coalescence of two attachments . . . 83
5.1.3.4 Example IV: Collinearity of base and platform . . . 84

5.1.3.5 Example V: Similar base and platform 84
5.1.3.6 Example VI: Mirrored base and platform 85
5.2 All fully-parallel planar robots and their forward kinematics 85
5.2.1 Replacing revolute by prismatic joints 88
5.2.1.1 Replacing one revolute joint 88
5.2.1.2 Replacing two revolute joints 90
5.2.1.3 Replacing three revolute joints 91
5.2.2 Example 92

6 Configuration spaces and coupler curves 99
6.1 Overview of the proposed approach 101
6.2 Tracing the double butterfly linkage configuration space 103
6.3 Example 105
6.3.1 Coupler curves 107
6.4 Other pin-jointed Grübler kinematic chains 108

7 Conclusions 111
7.1 Summary of contributions 111
7.2 Directions for future work 113

8 List of publications 115

A All the cataloged Baranov trusses 117

Bibliography 125

Figures

1.1 A Grübler kinematic chain. 11
1.2 The associated basic trusses of a Grübler kinematic chain. 12

2.1 The bilateration problem. 16
2.2 Circle-circle, circle-line, and line-line intersections. 19
2.3 Two triangles sharing one edge. 21
2.4 Strips of triangles. 22
2.5 Closure conditions using bilateration. 24
2.6 Automorphisms of a planar truss. 25

3.1 The cataloged Baranov trusses. 28
3.2 The triad and the pentad. 30
3.3 The configurations of the analyzed $3/B_1$ Baranov truss. 30
3.4 The configurations of the analyzed $5/B_1$ Baranov truss. 34
3.5 The $7/B_1$ Baranov truss and its associated notation. 35
3.6 The configurations of the analyzed $7/B_1$ Baranov truss. 38
3.7 The $7/B_2$ Baranov truss and its associated notation. 39
3.8 The configurations of the analyzed $7/B_2$ Baranov truss. 42
3.9 The $7/B_3$ Baranov truss and its associated notation. 43
3.10 The configurations of the analyzed $7/B_3$ Baranov truss. 45
3.11 The $9/B_{28}$ Baranov truss and its associated notation. 46
3.12 The configurations of the analyzed $9/B_{28}$ Baranov truss. 51
3.13 Baranov trusses of regular patterns. 52
3.14 The general n-link Watt-Baranov truss. 53
3.15 The configurations of the analyzed 11-link Watt-Baranov truss. 58
3.16 The configurations of the analyzed 13-link Watt-Baranov truss (Part 1/3). 60
3.17 The configurations of the analyzed 13-link Watt-Baranov truss (Part 2/3). 61
3.18 The configurations of the analyzed 13-link Watt-Baranov truss (Part 3/3). 62

4.1 The 3-link and 5-link Assur kinematic chains. 64
4.2 Geometric transformation between revolute and slider joints. 65
4.3 The $7/B_3$ Baranov truss. 67
4.4 Substitution of one and two revolute joints in a $7/B_3$ Baranov truss. . . . 68
4.5 The configurations of the $7/B_3$ Baranov truss used as reference truss. . . 69
4.6 The configurations of the Assur kinematic chain with one slider joint. . . 70
4.7 The configurations of the Assur kinematic chain with two slider joints. . . 72
4.8 Replacing a revolute joint involved in the variable distance. 73
4.9 The configurations of a seven-link Assur kinematic chain. 74

5.1 A general planar 3-R$\underline{\text{P}}$R parallel robot and its associated notation. 77
5.2 Configuration analyzed in Example I. 81

5.3 The four moving platform poses obtained in Example II. 82
5.4 The four moving platform poses obtained in Example III. 83
5.5 The two moving platform poses obtained in Example IV. 84
5.6 The four moving platform poses obtained in Example V. 85
5.7 One revolute joint is substituted by a prismatic joint. 89
5.8 Two revolute joints are substituted by prismatic joints. 90
5.9 The three revolute joints are substituted by prismatic joints. 91
5.10 The moving platform poses of the analyzed planar robots (Part 1/2). . . . 93
5.11 The moving platform poses of the analyzed planar robots (Part 2/2). . . . 97

6.1 Some types of singular points of algebraic plane curves. 100
6.2 The predictor-corrector method. 100
6.3 The four-bar linkage and its configuration space. 102
6.4 Configuration space of a double butterfly linkage. 103
6.5 The double butterfly linkage. 104
6.6 Configuration space of the analyzed double butterfly linkage 106
6.7 Coupler curves of the analyzed double butterfly linkage. 109

Tables

3.1 Number of Baranov trusses and coupling degrees. 27

5.1 The known 3-R$\underline{P}$R analytic planar robots. 80
5.2 Fully-parallel planar robot leg types. 86
5.3 The 10 fully-parallel planar robot families. 87
5.4 Distance substitutions for each robot family (Part 1/3). 94
5.5 Distance substitutions for each robot family (Part 2/3). 95
5.6 Distance substitutions for each robot family (Part 3/3). 96

6.1 Code of colors used in the analyzed double butterfly linkage. 107
6.2 Eight-bar linkages whose configuration space is two dimensional. 110

A.1 Position analysis of all the cataloged Baranov trusses (Part 1/8). 117
A.2 Position analysis of all the cataloged Baranov trusses (Part 2/8). 118
A.3 Position analysis of all the cataloged Baranov trusses (Part 3/8). 119
A.4 Position analysis of all the cataloged Baranov trusses (Part 4/8). 120
A.5 Position analysis of all the cataloged Baranov trusses (Part 5/8). 121
A.6 Position analysis of all the cataloged Baranov trusses (Part 6/8). 122
A.7 Position analysis of all the cataloged Baranov trusses (Part 7/8). 123
A.8 Position analysis of all the cataloged Baranov trusses (Part 8/8). 124

Chapter 1
Introduction

1.1 On kinematics, mechanisms, and kinematic chains

André-Marie Ampère, the famous French physicist and mathematician, proposed in 1834 the name **kinematics** for a new science dedicated to "everything that can be said about the different sorts of motions independent of the forces that can produce them" [8, p. 51] (translation cited in [96]). In this way, the analytical study of motion, kinematics, started a process of institutionalization, that is, entire courses on kinematics began to be taught at universities and the first books dedicated to kinematics were written [96]. A constantly overlooked aspect in the history of kinematics is that the underlying idea of Ampère's proposal was actually to give a scientific support to the development of mechanical systems for the transmission of power or force: "this is a science (kinematics) where motions are considered in themselves as they are when we observe them in the instances that surround us, especially in the devices that we call machines"[1] [8, p. 52].

From a practical viewpoint, a **kinematic chain** is essentially the skeleton of a machine, namely, the system that supports its physical elements and constrains its motion when exposed to forces and displacements. Kinematic chains can be classified as specializations of mechanisms. Formally, according to the International Federation for the Promotion of Mechanism and Machine Science (IFToMM), a mechanism is a constrained system of bodies designed to convert motions of, and forces on, one or several bodies into specific motions of, and forces on, the remaining ones [83]. Thus, kinematic chains are mechanisms with rigid bodies interconnected by kinematic pairs —*i.e.*, contact constraints, or, in simpler words, assemblages of links and joints [83].

It can be properly said that kinematic chains, also known as linkages, came into existence early in the age of the power revolution, by the 13th century [134]. The term kinematic chain was coined in the mechanical engineering community, ostensibly, in the 19th century. Franz Reuleaux, often called the 'father of kinematics' [128], and one of the firsts 'engineer-scientists' [129], already used it in his major book *The Kinematics of Machinery* [155]. Since kinematics and kinematic chains are the object of research of this thesis, at this point of discussion, it is important to distinguish between two relevant and connected areas of the study of motion: *theoretical kinematics* and *kinematics of mechanisms* [96].

1.1.1 Theoretical kinematics and kinematics of mechanisms

Theoretical kinematics is the branch of kinematics that deals with the more general geometrical properties of motion [96]. The golden age of this subject was between the 19th century and the first quarter of the 20th century. In that period, several mathematicians interested in geometry successfully turned their attention to kinematics, to name a few,

[1] Translation made with the help of Léonard Jaillet.

Julius Plücker, Arthur Cayley, Jean Victor Poncelet, and Henri Résal, author of the first book entirely dedicated to the branch [154]. In 1829, Michel Chasles probably presented the first contribution to theoretical kinematics, the geometrical proof of the existence of the instantaneous center of rotation [32]. The last relevant contribution in the subject has possibly been the development of the so-called screw theory by, principally, Robert Ball [10], Raoul Bricard [22], and Eduard Study [178] during the turn of the 20th century. A modern treatment of theoretical kinematics, based on classical geometry, was developed by the Dutch geometer Oene Bottema in the sixties of the 20th century [20].

The specific study of motion in mechanisms is known as *kinematics of mechanisms*. This branch had its origins by the late 18th century and first part of the 19th century when some French mathematicians such as Gaspard de Prony and Alexandre Joseph Hidulphe Vincent began to study the approximate straight-line linkages of the Scottish inventor James Watt [94]. However, the prominent fathers of this subject were the already mentioned German engineering scientist Franz Reuleaux and the Russian mathematician Pafnuty Chebyshev (see [116] for a compilation of his results) who worked in the area during the second half of the 19th century. Many of the current ideas about kinematics of mechanisms and multi-body systems stem from the approaches of Reuleaux and Chebyshev.

Among Reuleaux's main ideas are the novel concept of machine as a chain of geometrical constraints between kinematic pairs, and the distinction between open and closed kinematic chains [128, 129]. Chebyshev, for his part, was probably the first in using mathematical formulations for the study of mechanisms [28, 117] while worked in the design of straight-line linkages, his relevance in kinematics is even greater because, due to his authority, he aroused the interest for the subject of linkages of several leading mathematicians in France and England, including the distinguished James Sylvester [95]. Other key researchers in the development of *kinematics of mechanisms* are, among many others, the English geometer Samuel Roberts [156], the English engineering scientist Robert Willis [213], and the American (German-born) engineering scientist Ferdinand Freudenstein [47].

It is convenient to stand out that some authors, such as Bottema and Roth [21], consider the *kinematics of mechanisms* as a type of *applied kinematics*, the application of *theoretical kinematics*. Although the results of *theoretical kinematics* can be applied to the study of motion in mechanisms, as presently happens widely with screw theory, it is also true that a simple application of those results cannot solve, in general, the problems that arise in *kinematics of mechanisms*, moreover, some of those problems can be even solved without resorting to *theoretical kinematics*. As a consequence, this thesis agrees with the Dutch mathematical historian Teun Koetsier in the aforementioned differentiation between *theoretical kinematics* and *kinematics of mechanisms* [96].

Furthermore, since a mechanism, and in particular a kinematic chain, is indeed a system of geometrical constraints, that is, a group of geometrical elements —*e.g*, points, lines, circles, polygons— subject to geometrical measures —*e.g.*, angles, lengths, areas, volumes— and geometrical relations —*e.g.*, ratios, congruences, tangencies, contacts, it is argued in this thesis that the study of mechanisms doesn't belong exclusively to the study of machines. Hence, this thesis considers that *kinematics of mechanisms* actually divides in two complement and different branches: *theoretical kinematics of mechanisms* and *applied kinematics of mechanisms*.

Theoretical kinematics of mechanisms refers to the study of the geometry of motion in general mechanisms, namely, open or closed chains of geometrical constraints. The German geometer Ludwig Burmester can be considered the father of this branch, he was probably the pioneer in the study of complex compound mechanisms [24], that is,

mechanisms with more than two independent loops in which at least one geometrical element is connected through kinematic pairs to more than two others [29], a loop is a subset of geometrical elements that forms a closed circuit [83]. *Applied kinematics of mechanisms* employs theoretical results in specific mechanisms that emerge in areas such as, for instance, robotics, mechatronics, or Computer-Aided Design (CAD), or directly studies the motion on those particular instances. *Applied kinematics of mechanisms* is nowadays the most fruitful branch of kinematics. The outcomes of this thesis can be principally cataloged in *theoretical kinematics of mechanisms*, but significant results are also made to *applied kinematics of mechanisms*, specifically, in robot kinematics.

1.2 Position analysis of kinematic chains

Kinematics of mechanisms, regardless of the theoretical and applied perspectives, can be widely divided into two big problems: i) *kinematic analysis* and ii) *kinematic synthesis*. *Kinematic analysis* is the examination and determination of the motion —position, velocity, and acceleration— of a mechanism, *kinematic synthesis* is the development of a mechanism whose motion holds a desired set of characteristics. This thesis addresses the *kinematic analysis* problem, in particular, the **position analysis of kinematic chains**. This problem consists basically in finding the feasible assembly modes that a kinematic chain can adopt. An assembly mode is a possible relative transformation between the geometrical elements —*i.e.*, the links— of a kinematic chain. When an assignment of positions and orientations is made for all links, an assembly mode is called a configuration.

The position analysis problem of kinematic chains is a high impact research subject because important problems of several domains can be reduced to it. For example, the problem arises in robotics, specifically, in robot kinematics when solving the inverse/forward displacement analysis of serial/parallel manipulators [9, Ch. 8], in grasping and path planning when planning the coordinated manipulation of an object or the locomotion of a reconfigurable robot [220], in simultaneous localization and map-building (SLAM) [144], or in the relational positioning module of robotized teleoperated tasks [13, 157]. Other research areas where the problem appears include, at least, the simulation and control of complex deployable structures [139], the design of mechanical hands [38], the theoretical study of rigidity [17, 18], the location of points on a plane in CAD programs [136], and the conformational analysis of biomolecules [97, 150, 205].

1.2.1 Solution approaches

The methods to solve the position analysis of kinematic chains can be classified, broadly speaking, as graphical, analytical, or numerical [78]. The graphical approaches are completely geometrical and specially designed to solve particular problems. This approach was extensively used at the beginning of *kinematics of mechanisms*, during the 19th century, based on the descriptive geometry of French mathematician Gaspard Monge [28, 117]. These methods principally use dyadic decomposition for solving the position analysis problem. In a kinematic chain, a dyad is any connection of two links with a revolute joint or a prismatic pair (also called a slider joint). The dyadic decomposition approach consists in the identification of a loop of four links in the kinematic chain under study for then calculating the position of the other dyads using arc intersections. In modern times, the procedure has been combined with other techniques —*e.g.*, interpolation methods— for improving its results and scope [78].

In contrast to graphical approaches, the analytical and numerical methods deal, in

general, with kinematic chains of any topology. Typically, these methods use analytical geometry to translate closure conditions of the original geometrical problem —*i.e.*, conditions that are fulfilled if and only if the kinematic chain can be assembled— into a system of equations, normally nonlinear, that constraints the location, or coordinates, of each link respect to a particular reference frame. These coordinates can be defined using *reference point coordinates*, *natural coordinates*, or *relative coordinates* [88, Ch. 2]. In *reference point coordinates* and *natural coordinates*, the location of each geometrical element is directly defined in absolute form with respect to a common reference frame. The closure condition in these approaches is given by a mathematization of a proper selection of the geometrical measures and geometrical relations of the kinematic chain —*e.g*, the distance constraints between kinematic pairs.

In *relative coordinates*, the location of each link is defined in relation to the previous element in the kinematic chain. The closure condition in this approach is normally given by an independent set of the vector closure relations that naturally arise from each loop in a kinematic chain. The mathematization with *relative coordinates* of this closure condition is widely known as *independent loop equations* or *loop closure equations*. This technique is currently, by far, the most common practice in *kinematics of mechanisms* because, principally, the emerging system of equations is more compact —*i.e*, less number of equations and variables— than the resulting system using other approaches such as, for example, those based on equations that express constancy of distance between kinematic pairs. The use of *independent loop equations* in kinematic chains was probably introduced in the second half of 19th century, inspired by Chebyshev's work on parallelograms (see, for instance, [116, pp. 52-53]).

1.2.1.1 Analytical methods

In position analysis, the difference between analytical and numerical methods lies in the procedure used to solve the system of equations that characterizes the valid configurations of a kinematic chain. In the analytical approaches, the system of equations is transformed into a system of polynomial equations that is then reduced to a univariate polynomial using variable elimination. The polynomial transformation is performed using substitution of variables and the variable elimination is implemented using either Gröbner bases or elimination and resultant methods. In any case, the analytical approaches are complete —*i.e.*, they are able to find all the valid configurations of a kinematic chain.

The concept of Gröbner Bases was introduced in 1966 by Bruno Buchberger in his doctoral thesis [23]. The basic idea of the method is to eliminate the highest-ordered terms in a given set of polynomial equations by adding multiples of the other equations in the set, this process is known as reduction [133]. In the method, the system of polynomial equations $f_1 = 0, f_2 = 0, \ldots, f_n = 0$ in the variables $x_1, x_2, \ldots, x_n$ is written as a triangular form $g_n(x_n) = 0, g_{n-1}(x_n, x_{n-1}) = 0, \ldots, g_1(x_1, x_2, \ldots, x_n)$ called a Gröbner basis [123]. Gröbner bases generalize three familiar techniques: Gaussian elimination for solving linear systems of equations, the Euclidean algorithm for computing the greatest common divisor of two univariate polynomials, and the Simplex algorithm for linear programming [179]. This technique has been successfully used in the position analysis of different kinematic chains, see for instance [43, 45, 51].

Elimination and resultant methods use algorithms for computing the solutions of a system of polynomial equations in several variables based on resultants. Resultants, or eliminants, are polynomial expressions in the coefficients of a system of polynomial equations that are derived after eliminating variables. The importance of resultants lies in that their vanishing is a necessary and sufficient condition for the system to have a

solution [206]. Resultants expressions for two polynomials $f(x) = a_m x^m + \ldots + a_0$ and $g(x) = b_n x^n + ... + b_0$ of degrees m and n, respectively, are:

1. *The Sylvester resultant.* The Sylvester matrix is an $(m+n)\times(m+n)$ matrix formed by filling the matrix beginning with the upper left corner with the coefficients of $f(x)$, then shifting down one row and one column to the right and filling in the coefficients starting there until they hit the right side. The process is then repeated for the coefficients of $g(x)$ [210]. The determinant of this matrix is the Sylvester resultant.

2. *The Bézout determinant.* Assuming that $m > n$, the Bézout determinant is formed with a system of m equations derived from $f(x)$ and $g(x)$. The first $m-n$ equations are formed from $g(x)$ by multiplication with $x^{m-n-1}, x^{m-n-1}, \ldots, x^0$ in sequence. The remaining n equations are derived from $f(x)$ and $x^{m-n}\, g(x)$, both of which are of degree m. These latter polynomials are set equal to zero, and each of the resulting equations, $f(x) = 0$ and $x^{m-n}\, g(x) = 0$, is solved explicitly for its highest degree term in x, its two highest degree terms in x, and so on. After taking ratios and cross multiplying these equations, n polynomials of degree $m-1$ are obtained. The Bézout determinant is the determinant of the coefficient matrix of these m equations [101].

In addition, given a system of $n+1$ polynomial equations $P_i(X) = f_i(x_1, x_2, \ldots x_n) = 0$, $i = 1, ..., n+1$, the methods that simultaneously and efficiently eliminate several variables from it at a time include:

1. *The Dixon resultant.* Let $\hat{X} = \{\hat{x}_1, \hat{x}_2, \ldots \hat{x}_n\}$ be a new set of variables and

$$\delta(\hat{X}) = \begin{vmatrix} Q_{1,1} & \ldots & Q_{1,n+1} \\ Q_{2,1} & \ldots & Q_{2,n+1} \\ \vdots & \vdots & \vdots \\ Q_{n,1} & \ldots & Q_{n,n+1} \\ P_1(\hat{X}) & \ldots & P_{n+1}(\hat{X}) \end{vmatrix},$$

   where

$$Q_{j,i} = \left(f_i(\hat{x}_1, \ldots, \hat{x}_{j-1}, x_j, \ldots, x_n) - f_i(\hat{x}_1, \ldots, \hat{x}_j, x_{j+1}, \ldots, x_n)\right) / \left(x_j - \hat{x}_j\right).$$

   $\delta(\hat{X})$ is known as the Dixon polynomial. Now, if D is the set of polynomials formed by the set of all coefficients (which are polynomials in X) of terms in $\delta(\hat{X})$, then the coefficient matrix of D is the Dixon matrix and its determinant is known as the Dixon resultant [90].

2. *The Macaulay resultant.* For $1 \leq i \leq n+1$, let d_i the total degree of polynomial $P_i(X)$ and $d_m = 1 + \sum_1^{n+1}(d_i - 1)$. Let T denote the set of all terms of degree d_m in the variables $x_1, x_2, \ldots x_n$, that is, $T = \{{x_1}^{\alpha_1}\, {x_2}^{\alpha_2} \ldots {x_n}^{\alpha_n} | \alpha_1 + \alpha_2 + \ldots + \alpha_n = d_m\}$. Now, let $T^{(i)}$ the terms of degree $d_m - d_i$ that are not divisible by $\{{x_1}^{d_1}, {x_2}^{d_2}, \ldots, {x_{i-1}}^{d_{i-1}}\}$. Then, the multiplication of terms in $T^{(i)}$ by $P_i(X)$ gives a set of polynomials whose coefficients formed the Macaulay matrix. The determinant of this matrix is the Macaulay resultant [224].

Elimination and resultant methods has been extensively used to solve the position analysis of kinematic chains. In the context of planar kinematic chains —*i.e.*, kinematic chains whose geometrical elements lie in parallel planes, the general methods developed

by Nielsen and Roth [133], and Charles Wampler [190, 191] stand out. Both methods are notable for their uniform treatment of planar kinematic chains by variable elimination techniques. The method of Nielsen and Roth uses a modification of Dixon resultant applied to independent loop equations formulated in terms of sines and cosines. Charles Wampler proposed first a Sylvester-type elimination procedure applied to independent loop equations formulated in the complex plane [190]. He improved the method later by applying the Dixon determinant procedure of Nielsen and Roth to the set of complex equations [191].

1.2.1.2 Numerical methods

The numerical techniques developed in the literature for solving the system of equations that define the feasible configurations of a kinematic chain can be divided in incomplete and complete methods. The incomplete methods, that only provide some solutions (typically one) of the system of equations, commonly are gradient-based iterative methods that require an initial guess of a solution [26]. The complete methods —*i.e.*, procedures that find all solutions of a system— are, for instance, the approaches that solve the problem using polynomial continuation or interval-based techniques based on branch-and-prune methods, as explained below:

1. *Polynomial continuation.* The basic premise of this procedure, originally known as "bootstrap method" and developed by Roth and Freudenstein in 1963 [167], is that small perturbations in the coefficients of a system of equations lead to small changes in the solutions [133]. The method begins with an initial system whose solutions are all known, then the system is modified, in a step-by-step process, to the system whose solutions are sought, while tracking all solutions paths along the way [148]. Polynomial continuation is also known as homotopy continuation.

   General continuation-based solvers that can be applied to solve the position analysis of kinematic chains include the PHCPACK of Jan Verschelde [187] and the Bertini software of Bates et. al. [14].

2. *Interval-based techniques.* The branch-and-prune approach, a technique developed to solve optimization problems, consists in using approximate bounds of the solution set for discarding the parts of the search space that contain no solution [68]. It employs a successive decomposition of the initial problem into smaller disjoint subproblems that are solved iteratively until a criterion is achieved and the optimal solution is found [177]. The convergence of this approach is guaranteed because the bounds get tighter as the intermediate domains get smaller [149].

   The interval-based techniques develop iterative algorithms that combine interval methods with the branch-and-prune principle for determining all solutions of a system of equations within a given search space. The interval methods integrate interval arithmetic with analytic estimation techniques to solve a system of equations, two main classes of interval methods have been explored in the position analysis of kinematic chains: those based on the interval version of the Newton method [27, 122] and those based on polytope approximations of the solution set [148].

   The CUIK project developed by the Kinematics and Robot Design Group at the *Institut de Robòtica i Informàtica Industrial* [92], a software package able to deal with the most complex kinematic chains [149], can be cataloged as an interval-based technique.

1.3 About distance geometry

1.3.1 Why distance geometry?

Classically, as it was discussed in the last section, closure conditions of kinematic chains has been directly stated in terms of Cartesian poses —*i.e.*, location and orientation— of the links using analytical geometry techniques. This widely accepted approach has two major disadvantages:

1. Arbitrary reference frames has to be introduced
2. All formulas involve translations and rotations simultaneously

The first drawback is very relevant because the numerical conditioning of the system of equations derived from the closure conditions, that is, the best possible accuracy of a solution given approximations by the computation [186], depends on the selected reference frames. This drawback affects all the analytical and numerical methods based on analytical geometry. The second disadvantage affects those methods that use the tangent-half angle substitution or normalized homogeneous coordinates to transform the original system of equations into a system of polynomial equations because problems to reconstruct $\pm\pi$ roots, and other roots occurring in conjunction with them, arise [106].

This thesis departs from the usual analytical-geometry-based approach to solve the position analysis of kinematic chains by expressing the original geometrical problem as a graph with vertices subject to polytope content constraints —*e.g.*, distances, areas, volumes. The content of a polytope, the generalized concept of volume, or hypervolume, can be always expressed in terms of distances between points, using Cayley-Menger determinants (see Chapter 2). Then, the solution of the position problem of a kinematic chain reduces to determine the feasible distinct embeddings of a graph of Euclidean distance constraints in the corresponding problem's dimension. A graph embedding, in simple terms, is a particular drawing of a graph [209].

The embedding problem of a graph of Euclidean distance constraints is equivalent to the problem of determining the point conformation (configuration, relative position or location) by inference from interpoint Euclidean distance information. This problem is studied by the so-called distance geometry, a term coined by the American mathematician Leonard Blumenthal during the first half of the 20th century [15, 16]. This relatively new branch of mathematics concerns about the classification and study of geometric spaces by means of the metrics —*i.e.*, distances— that can be defined on them [70]. Distance geometry has successfully been used to intrinsically characterize Euclidean spaces, providing proves of theorems of Euclidean geometry without imposing arbitrary reference frames [69].

1.3.2 The graph embedding problem

In a graph of Euclidean distance constraints with n vertices and m edges, the graph distance matrix, also called the all-pairs shortest path matrix, is a $n \times n$ matrix with zero diagonal entries consisting of all Euclidean distances from vertex i to vertex j. The graph distance matrix corresponds to a symmetric partial matrix —*i.e.*, a symmetric matrix in which only some of its entries are specified. Then, the embedding problem of a graph of distance constraints in a specific dimension reduces to determine whether its graph distance matrix with the entries squared can be completed to a proper Euclidean Distance Matrix (EDM). This problem is called the Euclidean Distance Matrix completion problem (EDM completion problem, for short).

1.3.2.1 The Euclidean distance matrix completion problem

An $n \times n$ matrix $\mathbf{D} = (s_{i,j})$ is called an EDM if and only if there are n points $P_1, P_2 \dots P_n$ in some Euclidean space, such that $s_{i,j} = \|P_j - P_i\|^2$ —*i.e.*, the squared distance between P_i and P_j. A proper EDM is a symmetric matrix with positive entries and with zero diagonal that is negative semidefinite on the subspace $\mathbf{e}^T x = 0$ where $x \in \mathbb{R}^n$ and $\mathbf{e}$ is the vector of all ones of appropriate dimension [1]. A symmetric partial matrix is a symmetric matrix in which only some of its entries are specified, the unspecified entries are said to be free.

Given a $n \times n$ symmetric partial matrix $\mathbf{A}$, a $n \times n$ matrix $\mathbf{D}$ is an EDM completion of $\mathbf{A}$ if and only if $\mathbf{D}$ is EDM. Thus, the EDM completion problem, in its general form, is the problem of determining whether or not a symmetric partial matrix $\mathbf{A}$ has an EDM completion [2]. The reported methods to solve this problem can be classified as:

1. *Global methods.* In these methods, all feasible EDM completions of a given symmetric partial matrix are determined in a specific dimension. An example of solution for $\mathbb{R}^3$ is the branch-and-prune procedure developed by Porta et. al. [151, 152]. In this algorithm, the original problem of distance constraints is transform into a system of multilinear equalities and inequalities using criteria based on the theory of Cayley-Menger determinants, then all possible values for the unknown distances are established via a bound smoothing process [146].

   In [182, 183], Thomas et. al. presented an ingenious approach of a global method for the EDM completion problem in $\mathbb{R}^d$. The idea of the algorithm is to iteratively reduce and expand the dimension of the problem using projection and backprojection operations based on the cosine theorem. In the approach, given a $n \times n$ symmetric partial matrix, all entries are converted to real compact intervals by putting lower and upper bounds for the unknown entries using triangle and/or tetrangle inequalities. The squared distance intervals —*i.e.*, the entries of the transformed symmetric partial matrix— are repetitively projected onto the hyperplane orthogonal to the axis defined by the entry $1, n$ and their bounds are reduced through backprojections or divided by bisection. The branches of the process that after d iterations of projection yield null matrices are finally backprojected, they correspond to all feasible EDM completions of the problem.

2. *Local methods.* The local methods only find a single EDM completion. These algorithms are based mainly on semidefinite programming, a subfield of convex optimization [3, 104, 219]. In this approach, given a partial symmetric matrix $\mathbf{A}$ with nonnegative elements and zero diagonal, one of its feasible EDM completions, the matrix $\mathbf{D}$, is computed by solving the convex optimization problem

$$\begin{aligned} &\text{minimize} \quad \|\mathbf{H} \circ (\mathbf{A} - \mathbf{D})\|_F^2 \\ &\text{subject to} \quad \mathbf{D} \in \xi, \end{aligned}$$

   where $\mathbf{H}$ is an $n \times n$ symmetric matrix with nonnegative elements, $\circ$ denotes the Hadamard product, F indicates the Frobenius norm, and ξ represents the cone of EDMs. In this approach the dimension of the completion can not be specified. Other similar methods for a local solution of the EDM completion problem, but in which the desired dimension of embedding can be constrained, include the dissimilarity parameterized formulation [58, 185] and the nonconvex position formulation [227].

1.4 A new approach to the position analysis of kinematic chains

The total number of pairwise distances between n points is $\frac{n(n-1)}{2}$ [39]. Hence, finding all possible solutions of the EDM completion problem is, in general, extremely complex. In fact, James Saxe in [168] showed that this problem is NP-complete for dimension 1 and NP-hard for higher dimensions. However, determining all the set of unknown squared distances is normally unnecessary because, for instance, to solve a distance constraint problem between n spatial points, only $3\,n - 6$ distances are usually enough [221]. An example of this characteristic is the approach presented by Porta et. al. in [147] where the set of kinematic chains, associated with spatial serial and parallel robot manipulators, whose EDM can be derived following a constructive geometric process through trilaterations is identified.

Given the location of n points in a space, n-lateration is a method to determine the location of another point whose distance to these n points is known. In three-dimensional space, for $n < 3$ the problem is indeterminate, for $n = 3$ the problem, called trilateration, has two feasible solutions, and for $n > 3$ the problem is overconstrained. Analogously, in the case of plane geometry, for $n < 2$ the problem is indeterminate, for $n = 2$ the problem, called bilateration in this thesis, has two feasible solutions, and for $n > 2$ the problem is overconstrained.

The trilateration problem, using analytical geometry, can be trivially formulated as the intersection of three spheres, that is, as the solution of a system of quadratic equations. Alternatively, Thomas and Ros in [184], using barycentric coordinates and a distance geometry approach, developed a more elegant formulation, namely, a vectorial expression in terms of Cayley-Menger determinants. This formulation was proven to be mathematically more tractable than previous ones because of, in contrast to other approaches, all its terms have a geometrical meaning.

This thesis, in order to solve the position analysis problem, introduces a further twist to the idea developed in [147] by, instead of solving the EDM completion problem, obtaining closure conditions of kinematic chains using n-laterations and constructive geometric arguments. The mathematization of these closure conditions, a fundamental step in the whole process, is performed using formulations of n-laterations inspired by the idea developed in [184] for trilateration. The resulting system of equations are then solved using analytical and numerical procedures adapted to its particularities. In favor of developing the basics and theory of this new approach for solving the position analysis of kinematic chains, this thesis focuses on the study of the most fundamental planar kinematic chains.

1.5 Planar kinematic chains

Kinematic chains can be characterized as planar, spherical, or spatial, depending on if the axes of their rotational joints, see as lines in three-dimensional Euclidean space, coincide at an infinite point, coincide at a finite one, or do not coincide at all, respectively. In this thesis, planar kinematic chains as taken as case study to develop the approach for the position analysis of kinematic chains discussed in the last section. These kind of linkages can also be defined as kinematic chains whose links lie in parallel planes. The kinematics study of these linkages is relevant because most kinematic chains found in practice are, in fact, planar [118]. Examples of planar kinematic chains can be found in, to name a few, the suspension system of an automobile, the feeding device of a multifunction

domestic sewing machine, or the end-effector of a robot arm.

1.5.1 Mobility

The main structural parameter of a kinematic chain, regardless if it is planar, spherical, or spatial, is its mobility [52]. IFToMM defines it as the number of independent coordinates needed to define the configuration of a kinematic chain [83]. Alternatively, in this thesis, mobility is defined as the minimum (maximum) number of geometrical constraints that has to be added to (subtracted from) a kinematic chain with given side link lengths to get (maintain) a discrete relative transformation between their links —*i.e*, a finite number of assembly modes. Moreover, instantaneous mobility, or local mobility, is defined as the mobility of a kinematic chain in a particular configuration. The definition and distinction here presented are made taking into account results recently published for the mobility calculation of kinematic chains [131, 171, 193].

A problem that has attracted the attention of several researchers since the dawn of *kinematics of mechanisms* is the derivation of a simple equation for the quick and correct identification of the mobility of mechanisms. However, although a large number of formulas have been indeed proposed for the calculation of mobility (see [52] for an exhaustive collection of these equations); unfortunately, in general, they are not able to correctly predict the mobility of a mechanism for all its particular instances —*e.g.*, local mobility cases. A solution to this problem seems the approach based on mechanism's topology and inner forces proposed by Offer Shai [171] but it is a result that requires further research.

The most widely used formula for the quick calculation of the mobility of a kinematic chain is the Chebychev-Grübler-Kutzbach's criterion [131]. In the case of planar kinematic chains composed only by revolute and prismatic joints, this formula states that the mobility F can be computed as [118]:

$$F = 3\,l - 2\,j - 3, \tag{1.1}$$

where l and j are the number of links and joints, respectively. Altough it is well known that this formula does not give the correct mobility for special cases of planar kinematic chains such as overconstrained planar linkages or some planar kinematic chains with particular link side lengths —the formula actually yields a lower bound on the mobility of a specific planar kinematic chain [131], it is quite general for the purposes of this thesis.

1.5.2 Modular kinematics

In position analysis of kinematic chains, modular kinematics refers to the idea of analyzing a linkage by dividing it into a sequence of fundamental modules —*i.e.*, basic elements in which a planar kinematic chain can be built up— in order to obtain a decoupled system of kinematic equations for the kinematic chain under studied [50]. This idea was introduced by the Russian engineering scientist Leonid Assur in 1914 [169] by stating that any planar kinematic chain can always be divided in simpler linkages. Nowadays, these basic modules are called Assur groups, formally defined as the minimal group of links that can be connected to any kinematic chain without modifying its mobility [30].

Presently, it is widely known that any kinematic chain with positive mobility is equivalent to a linkage of mobility zero, that is, a structure, when its input joints are fixed, or in other words, a planar kinematic chain of mobility F is constituted of F input links and one linkage of mobility zero. In any case, the resulting structure is composed by Assur groups [12, Ch. 4]. The automatic decomposition of a planar kinematic chain

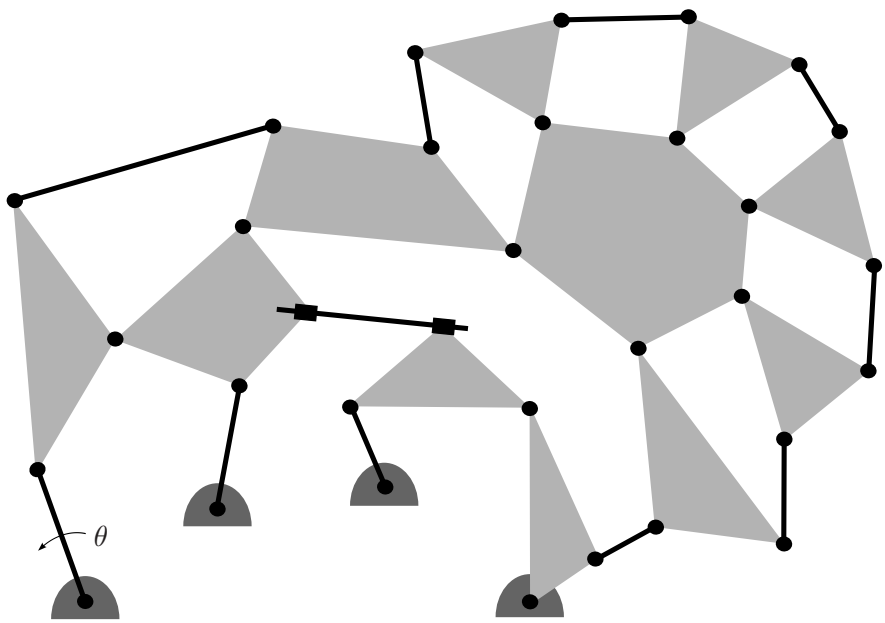

Figure 1.1. A Grübler kinematic chain of 22 links, 1 prismatic joint, and 30 revolute joints.

into Assur groups can be made using the procedure, based on the pebble game algorithm developed in structural rigidity, recently reported by Sljoka and colleagues [175]. A non-overconstrained closed planar linkage with mobility zero from which an Assur group can be obtained by removing any of its links is defined as an Assur kinematic chain, basic truss [30, 50], or Baranov truss when no slider joints are considered. Hence, an Assur kinematic chain (or a Baranov truss) corresponds to multiple Assur groups.

The relevance of Assur kinematic chains (and Baranov trusses) derive from the fact that, if the position analysis of an Assur kinematic chain (or of a Baranov truss) is solved, the same process can be applied to solve the position analysis of all its corresponding Assur groups. Therefore, by solving the position analysis of Assur kinematic chains (and Baranov trusses), the position analysis of any planar kinematic chain can be solved. As a consequence, this thesis focuses in the study of these fundamental kinematic chains.

By way of motivating example, let us consider the planar linkage depicted in Fig. 1.1. This kinematic chain has 22 links, 1 prismatic joint, and 30 revolute joints. Then, according to equation (1.1), $F = 3\,(22) - 2\,(31) - 3 = 1$. Therefore, the linkage is a Grübler kinematic chain, that is, a closed planar kinematic chain with mobility one. For a given value θ of the input link —labeled with the arrow in Fig. 1.1, it can be verified that the resulting linkage of mobility zero [Fig. 1.2(top)] is composed of:

- One Assur kinematic chain of seven links [Fig. 1.2(center-left)]. In Chapter 4, it is shown how the position analysis of this kinematic chain reduces to solve a scalar radical equation in a single variable.

- Six Baranov trusses of three links, or triads [Fig. 1.2(center-right)]. The triad is the simplest Baranov truss, a one-loop structure with three links and two feasible configurations. This kinematic chain is analyzed in Chapter 3.

- One Baranov truss of thirteen links [Fig. 1.2(bottom)]. This kinematic chain is indeed a Watt-Baranov truss, a linkage whose position analysis, regardless the number of independent loops, reduces to solve a scalar radical equation in a single variable. This kinematic chain is also analyzed in Chapter 3.

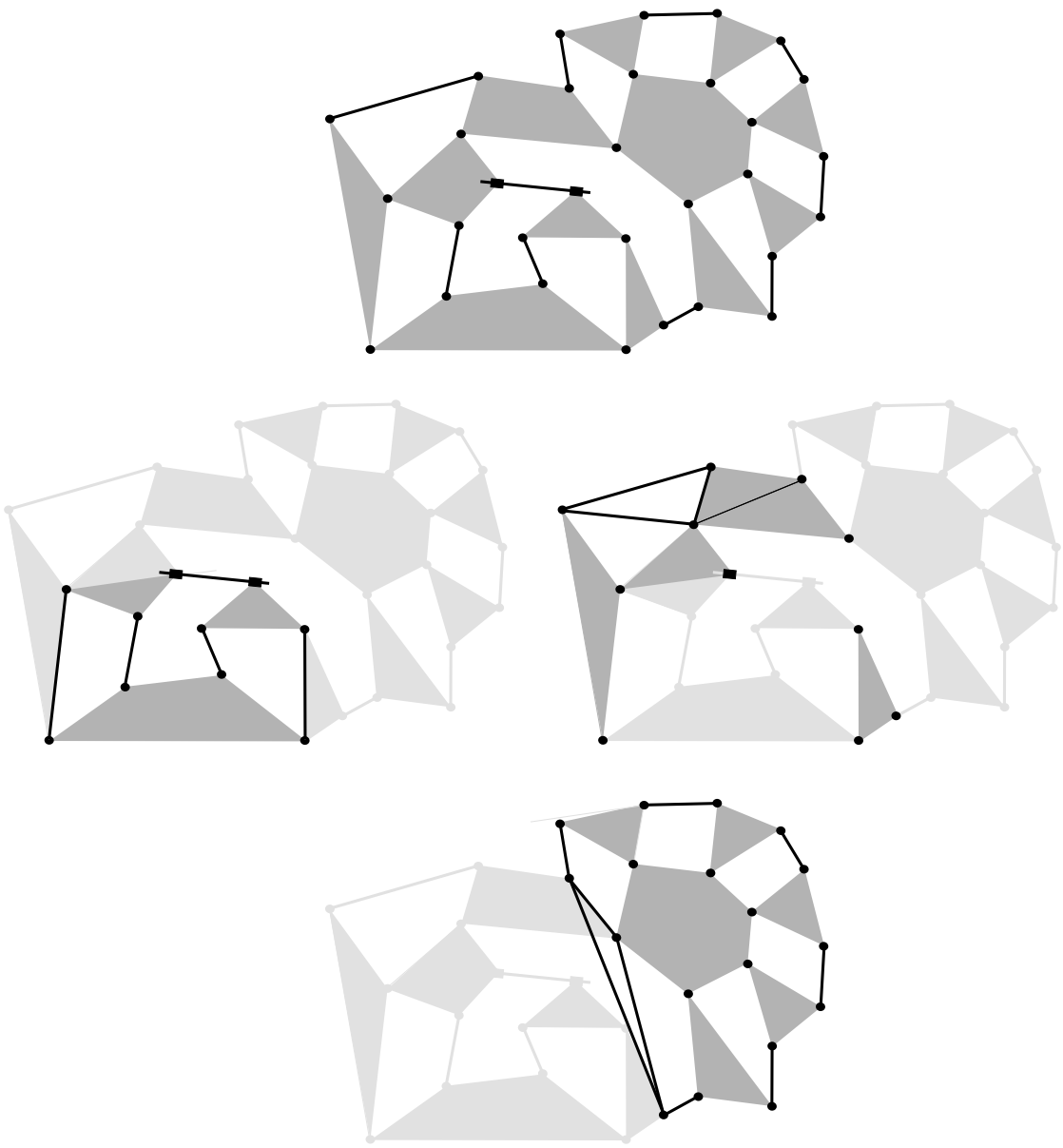

Figure 1.2. For a given value θ of the input link in the Grübler kinematic chain depicted in Fig. 1.1, the resulting linkage of mobility zero **(top)** is composed of: one Assur kinematic chain of seven links **(center-left)**, six triads **(center-right)**, and one Watt-Baranov truss of thirteen links **(bottom)**.

Then, by solving in cascade the position analysis of each of the above Assur kinematic chains and Baranov trusses, the position analysis of the Grübler kinematic chain under study, for a given value of θ, can be solved. The movement of the Grübler kinematic chain, starting from an initial configuration, can be followed by varying discretely the θ angle and then solving the position analysis problem for each of its new values. Thus, a finite set of locations is obtained for any arbitrary point on the Grübler kinematic chain. If θ is changed continuously, rather than discretely, these finite sets become plane curves.

In Grübler kinematic chains, the curve traced by a point at a link during the continuous movement of the linkage —*i.e.*, when the joint variable of a input link changes continuously— is known as coupler curve. Tracing this curve is a problem of great interest in the study of this kind of linkages because their properties plays a fundamental

role in, for example, the design of machines or the simulation of mechanisms. As it was discussed, a sampled coupler curve —*i.e.*, a finite set of locations for a point— of a Grübler kinematic chain can be readily obtained using the modular approach above presented. However, find the correct connection between neighboring samples of such sampled curve is not a trivial problem at all. This thesis focuses in the study of pin-jointed Grübler kinematic chains, that is, closed planar kinematic chains with mobility one connected by revolute joints, in order to find an efficient solution to the coupler curve tracing problem.

1.6 Overview of chapters

The rest of this thesis is structured as follows:

- Chapter 2 introduces the basic tools for the application of the proposed technique in kinematic chains: the concept of bilateration matrices and the idea of deriving closure conditions in terms of them.
- Chapter 3 shows how the position analysis of Baranov trusses can be solved using the theory developed in Chapter 2. A comprehensive review of the solutions reported in the literature for the position analysis of Baranov trusses is also presented.
- Chapter 4 discusses how to transform an Assur kinematic chain with slider joints into a Baranov truss with revolute joint centers located at infinity to obtain closure conditions in terms of bilateration matrices. The position analysis of Assur kinematic chains is then solved.
- In Chapter 5, the ideas developed in Chapters 3 and 4 are applied and extended to solve the forward kinematics of all fully-parallel planar robots.
- Chapter 6 presents an approach, based on bilateration techniques and geometrical arguments, to trace the configuration space —*i.e.* the possible values of the set of parameters that define a configuration— and coupler curves of pin-jointed Grübler kinematic chains.
- In Chapter 7, the conclusions summarize the main contributions and propose prospects for further research.
- Finally, in Chapter 8, a list of the publications resulting from the research reported in this thesis is presented.

Chapter 2

Bilateration matrices and closure conditions

2.1 Basic notation

Throughout this thesis, P_i and $\mathbf{p}_i$ will denote a point and its position vector in a given reference frame, $\overline{P_iP_j}$ the segment defined by P_i and P_j, $\triangle P_iP_jP_k$ the triangle defined by P_i, P_j, and P_k, $\angle P_iP_jP_k$ the angle defined by P_i, P_j, and P_k with P_j as reference, and $A_{i,j,k}$ the oriented area of $\triangle P_iP_jP_k$. Moreover, $\mathbf{p}_{i,j} = \overrightarrow{P_iP_j}$ is the vector going from P_i to P_j and $s_{i,j} = d_{i,j}^2 = \|\mathbf{p}_{i,j}\|^2$ is the squared distance between P_i and P_j.

2.2 Cayley-Menger determinants

Karl Menger in 1928 [119] proposed an intrinsic characterization of the Euclidean metric, or Euclidean distance, in the form of a system of polynomial equations and inequalities in terms of squared interpoint distances [70]. These polynomials can be written as

$$D(i_1,\ldots,i_n;j_1,\ldots,j_n) = 2\left(\frac{-1}{2}\right)^n \begin{vmatrix} 0 & 1 & \ldots & 1 \\ 1 & s_{i_1,j_1} & \ldots & s_{i_1,j_n} \\ \vdots & \vdots & \ddots & \vdots \\ 1 & s_{i_n,j_1} & \ldots & s_{i_n,j_n} \end{vmatrix}. \tag{2.1}$$

This determinant is known as the *Cayley-Menger bi-determinant* of the point sequences $P_{i_1},\ldots,P_{i_n}$, and $P_{j_1},\ldots,P_{j_n}$ and its geometric interpretation plays a fundamental role in distance geometry. When the two point sequences are the same, it is convenient to abbreviate $D(i_1,\ldots,\ i_n;i_1,\ldots,i_n)$ by $D(i_1,\ldots,i_n)$, which is simply called the *Cayley-Menger determinant* of the involved points.

The evaluation of $D(i_1,\ldots,i_n)$ gives $(n-1)!^2$ times the squared hypervolume, or squared content, of the simplex spanned by the points $P_{i_1},\ldots,P_{i_n}$ in $\mathbb{R}^{n-1}$ [120, pp. 737-738]. Therefore, the squared distance between P_i and P_j can be expressed as $D(i,j)$ and the oriented area of $\triangle P_iP_jP_k$ as $\pm\frac{1}{2}\sqrt{D(i,j,k)}$, which is defined as positive if P_k is to the left of vector $\mathbf{p}_{i,j}$, and negative otherwise. It can also be verified that $D(i_1,i_2;j_1,j_2)$ is equivalent to the dot product between the vectors $\mathbf{p}_{i_1,i_2}$ and $\mathbf{p}_{j_1,j_2}$. Then, $\cos\theta = D(i,j;i,k)/\sqrt{D(i,j)D(i,k)}$, θ being the angle between $\mathbf{p}_{i,j}$ and $\mathbf{p}_{i,k}$. For more properties of Cayley-Menger determinants, the interested reader is referred to [70, 124, 184].

2.3 Bilateration

Many geometric problems can be elegantly formulated using Cayley-Menger determinants, see, for instance, [70, §2]. The bilateration problem is one of them. It consists of

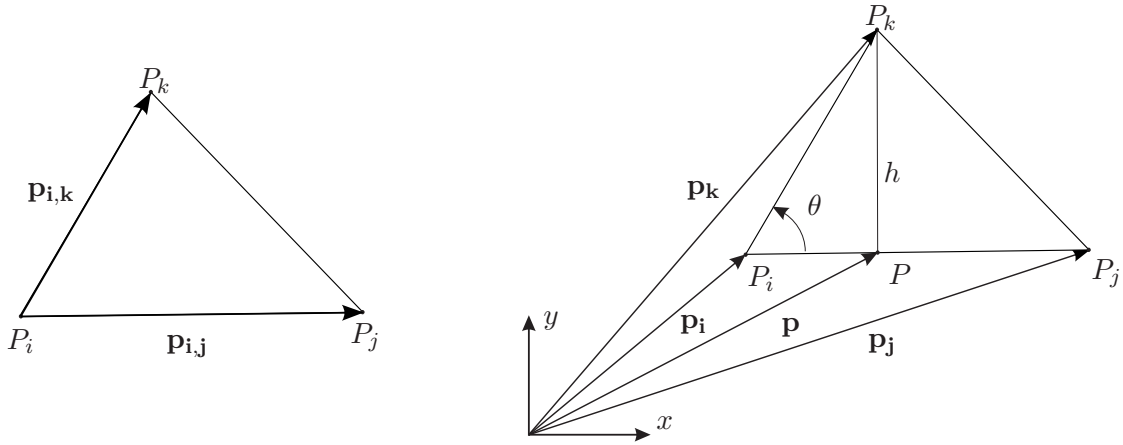

Figure 2.1. The bilateration problem **(left)** and associated notation **(right)**

finding the feasible locations of a point, say P_k, given its distances to two other points, say P_i and P_j, whose locations are known [Fig. 2.1(left)]. Then, according to notation of Fig. 2.1(right), the position vector of the orthogonal projection of P_k onto $\overline{P_iP_j}$ can be expressed as

$$\mathbf{p} = \mathbf{p}_i + \sqrt{\frac{D(i,k)}{D(i,j)}}\cos\theta\,\mathbf{p}_{i,j} = \mathbf{p}_i + \frac{D(i,j;i,k)}{D(i,j)}\,\mathbf{p}_{i,j}. \tag{2.2}$$

Moreover, the position vector of P_k can be expressed as

$$\mathbf{p}_k = \mathbf{p} \pm \frac{\sqrt{D(i,j,k)}}{D(i,j)}\,\mathbf{S}\,\mathbf{p}_{i,j}, \tag{2.3}$$

where $\mathbf{S} = \begin{pmatrix} 0 & -1 \\ 1 & 0 \end{pmatrix}$ and the $\pm$ sign accounts for the two mirror symmetric locations of P_k with respect to the line defined by $\overline{P_iP_j}$. Then, substituting (2.2) in (2.3), we get

$$\mathbf{p}_k = \mathbf{p}_i + \frac{D(i,j;i,k)}{D(i,j)}\,\mathbf{p}_{i,j} \pm \frac{\sqrt{D(i,j,k)}}{D(i,j)}\,\mathbf{S}\,\mathbf{p}_{i,j}. \tag{2.4}$$

Therefore,

$$\begin{aligned}\mathbf{p}_{i,k} &= \frac{D(i,j;i,k)}{D(i,j)}\,\mathbf{p}_{i,j} \pm \frac{\sqrt{D(i,j,k)}}{D(i,j)}\,\mathbf{S}\,\mathbf{p}_{i,j} \\ &= \frac{1}{D(i,j)}\left(D(i,j;i,k) \pm \sqrt{D(i,j,k)}\,\mathbf{S}\right)\mathbf{p}_{i,j}. \end{aligned}\tag{2.5}$$

2.3.1 Bilateration matrices

Equation (2.5) is the bilateration problem formulated in terms of Cayley-Menger determinants. However, a more compact and suitable representation is obtained by expressing this equation in matrix form, that is

$$\mathbf{p}_{i,k} = \mathbf{Z}_{i,j,k}\,\mathbf{p}_{i,j} \tag{2.6}$$

where

$$\begin{aligned}\mathbf{Z}_{i,j,k} &= \frac{1}{D(i,j)}\left(D(i,j;i,k)\,\mathbf{I} \pm \sqrt{D(i,j,k)}\,\mathbf{S}\right) \\ &= \frac{1}{D(i,j)}\begin{pmatrix} D(i,j;i,k) & \mp\sqrt{D(i,j,k)} \\ \pm\sqrt{D(i,j,k)} & D(i,j;i,k) \end{pmatrix}\end{aligned}$$

is called a *bilateration matrix* [161]. $\mathbf{I}$ is the 2×2 identity matrix. If the Cayley-Menger determinants involved in $\mathbf{Z}_{i,j,k}$ are expanded, a more amenable expression is obtained [163]:

$$\mathbf{Z}_{i,j,k} = \frac{1}{2\,s_{i,j}} \begin{pmatrix} s_{i,j} + s_{i,k} - s_{j,k} & -4\,A_{i,j,k} \\ 4\,A_{i,j,k} & s_{i,j} + s_{i,k} - s_{j,k} \end{pmatrix}$$

where

$$A_{i,j,k} = \pm\frac{1}{4}\sqrt{(s_{i,j}+s_{i,k}+s_{j,k})^2 - 2\,({s_{i,j}}^2+{s_{i,k}}^2+{s_{j,k}}^2)} \tag{2.7}$$

is the oriented area of $\triangle P_i P_j P_k$.

2.3.1.1 Basic properties of bilateration matrices

Given the triangle in Fig. 2.1(left), it is possible to compute six different bilaterations. Expressly,

$$\mathbf{p}_{i,k} = \mathbf{Z}_{i,j,k}\,\mathbf{p}_{i,j} \tag{2.8}$$
$$\mathbf{p}_{j,k} = \mathbf{Z}_{j,i,k}\,\mathbf{p}_{j,i} \tag{2.9}$$
$$\mathbf{p}_{i,j} = \mathbf{Z}_{i,k,j}\,\mathbf{p}_{i,k} \tag{2.10}$$
$$\mathbf{p}_{k,i} = \mathbf{Z}_{k,j,i}\,\mathbf{p}_{k,j} \tag{2.11}$$
$$\mathbf{p}_{k,j} = \mathbf{Z}_{k,i,j}\,\mathbf{p}_{k,i} \tag{2.12}$$
$$\mathbf{p}_{j,i} = \mathbf{Z}_{j,k,i}\,\mathbf{p}_{j,k}. \tag{2.13}$$

From these equations, three interesting properties arise:

1. $\mathbf{Z}_{i,j,k} = \mathbf{I} - \mathbf{Z}_{j,i,k}$

Proof. Since $\mathbf{p}_{i,k} = \mathbf{p}_{i,j} + \mathbf{p}_{j,k}$, then, using equation (2.9), $\mathbf{p}_{i,k} = \mathbf{p}_{i,j} + \mathbf{Z}_{j,i,k}\,\mathbf{p}_{j,i} = \mathbf{p}_{i,j} - \mathbf{Z}_{j,i,k}\,\mathbf{p}_{i,j}$. Hence, $\mathbf{p}_{i,k} = (\mathbf{I} - \mathbf{Z}_{j,i,k})\,\mathbf{p}_{i,j}$. Substituting equation (2.8) in this last result, we get $\mathbf{Z}_{i,j,k}\,\mathbf{p}_{i,j} = (\mathbf{I} - \mathbf{Z}_{j,i,k})\,\mathbf{p}_{i,j}$. Therefore, $\mathbf{Z}_{i,j,k} = \mathbf{I} - \mathbf{Z}_{j,i,k}$. Note that if $\mathbf{A}\,x = \mathbf{B}\,x$ for all x with $\mathbf{A}$ and $\mathbf{B}$ $n \times n$ matrices and x an appropriate non-zero vector, then $\mathbf{A}\,x - \mathbf{B}\,x = (\mathbf{A} - \mathbf{B})\,x = 0$. Thus, $\mathbf{A} = \mathbf{B}$. □

2. $\mathbf{Z}_{i,j,k}\mathbf{Z}_{i,k,j} = \mathbf{I}$

Proof. Substituting equation (2.10) in equation (2.8), we get $\mathbf{p}_{i,k} = \mathbf{Z}_{i,j,k}\mathbf{Z}_{i,k,j}\,\mathbf{p}_{i,k}$. Therefore, $\mathbf{Z}_{i,j,k}\mathbf{Z}_{i,k,j} = \mathbf{I}$. □

3. $\mathbf{Z}_{i,j,k} = -\mathbf{Z}_{k,j,i}\mathbf{Z}_{j,i,k}$

Proof. Since $\mathbf{p}_{i,k} = -\mathbf{p}_{k,i}$, from equations (2.8) and (2.11), we get $\mathbf{Z}_{i,j,k}\,\mathbf{p}_{i,j} = -\mathbf{Z}_{k,j,i}\,\mathbf{p}_{k,j} = \mathbf{Z}_{k,j,i}\,\mathbf{p}_{j,k}$. Replacing equation (2.9) in this last result, we obtain $\mathbf{Z}_{i,j,k}\,\mathbf{p}_{i,j} = \mathbf{Z}_{k,j,i}\mathbf{Z}_{j,i,k}\,\mathbf{p}_{j,i} = -\mathbf{Z}_{k,j,i}\mathbf{Z}_{j,i,k}\,\mathbf{p}_{i,j}$. Therefore, $\mathbf{Z}_{i,j,k} = -\mathbf{Z}_{k,j,i}\mathbf{Z}_{j,i,k}$. □

2.4 Perpendicular matrices and fundamental properties

Bilateration matrices can be seen as perpendicular matrices, namely, 2×2 matrices whose columns and rows are orthogonal vectors of the same magnitude, specifically, matrices of the form $\begin{pmatrix} a & -b \\ b & a \end{pmatrix}$. Some fundamental properties of these special matrices are:

Let two perpendicular matrices $\mathbf{A} = \begin{pmatrix} a_{1,1} & -a_{1,2} \\ a_{1,2} & a_{1,1} \end{pmatrix}$ and $\mathbf{B} = \begin{pmatrix} b_{1,1} & -b_{1,2} \\ b_{1,2} & b_{1,1} \end{pmatrix}$, then

1. **Perpendicular matrix addition is closed and commutative.** $\mathbf{A}+\mathbf{B}=\mathbf{B}+\mathbf{A}$, $\mathbf{A}+\mathbf{B}$ is a perpendicular matrix

   Proof. The expansion of $\mathbf{A}+\mathbf{B}$ and $\mathbf{B}+\mathbf{A}$ yields $\begin{pmatrix} a_{1,1}+b_{1,1} & -(a_{1,2}+b_{1,2}) \\ a_{1,2}+b_{1,2} & a_{1,1}+b_{1,1} \end{pmatrix}$, that is, a perpendicular matrix. □

2. **Perpendicular matrix product is closed and commutative.** $\mathbf{AB}=\mathbf{BA}$, $\mathbf{AB}$ is a perpendicular matrix

   Proof. The expansion of $\mathbf{AB}$ and $\mathbf{BA}$ yields

$$\begin{pmatrix} a_{1,1}\,b_{1,1}-a_{1,2}\,b_{1,2} & -(a_{1,1}\,b_{1,2}+a_{1,2}\,b_{1,1}) \\ (a_{1,1}\,b_{1,2}+a_{1,2}\,b_{1,1} & a_{1,1}\,b_{1,1}-a_{1,2}\,b_{1,2} \end{pmatrix},$$

   that is, a perpendicular matrix. □

To sum up, perpendicular matrices constitute a commutative group —*i.e.*, an abelian group— under product and addition operations. Additionally,

3. **Orthogonality.** $\mathbf{AA}^T=\mathbf{A}^T\mathbf{A}=\det(\mathbf{A})\,\mathbf{I}$

   Proof. The expansion of $\mathbf{AA}^T$ and $\mathbf{A}^T\mathbf{A}$ yields

$$\begin{pmatrix} a_{1,1}^2+a_{1,2}^2 & 0 \\ 0 & a_{1,1}^2+a_{1,2}^2 \end{pmatrix}=\left(a_{1,1}^2+a_{1,2}^2\right)\mathbf{I}=\det(\mathbf{A})\,\mathbf{I}.$$

   □

   This property is a consequence of the columns and rows in a perpendicular matrix are orthogonal vectors. Note that, since the determinant of a perpendicular matrix is always positive, the special orthogonal group of order 2, $SO(2)$, namely, the set of rotation matrices of size 2, is a particular case of perpendicular matrices.

4. **Scaling.** If $\mathbf{v}=\mathbf{Aw}$ with $\mathbf{u}$ and $\mathbf{v}$ appropriate vectors, then $\|\mathbf{v}\|^2=\det(\mathbf{A})\,\|\mathbf{w}\|^2$

   Proof. Let choose a reference frame, without lost of generality, whose x axis is collinear to vector $\mathbf{w}$, so $\mathbf{w}=(x_w,0)^T$. Thus, $\mathbf{v}=\mathbf{Aw}=\begin{pmatrix} a_{1,1} \\ a_{1,2} \end{pmatrix} x_w$. Therefore,

$$\begin{aligned} \|\mathbf{v}\|^2 &= \left(a_{1,1}^2+a_{1,2}^2\right){x_w}^2=\left(a_{1,1}^2+a_{1,2}^2\right)\|\mathbf{w}\|^2 \\ &= \det(\mathbf{A})\,\|\mathbf{w}\|^2. \end{aligned}$$

   □

Of these four fundamental properties of perpendicular matrices, the properties of closure and commutation under product and addition operations, and the scaling property, especially, will be useful throughout this thesis.

2.5 Ruler and compass constructions

Classical geometric constructions, or Euclidean constructions, refer to precisely draw geometrical shapes, angles, or lines using a ruler[1] and a compass only. The geometrical problems of antiquity, namely, circle squaring, cube duplication, and angle trisection, were restricted to be solved using uniquely a finite set of this kind of constructions. Although each of these three problems cannot be solved with that condition, other interesting geometrical problems such as, for instance, the bisector of a line segment, the construction of an equilateral triangle, or the square root of a number, can be. In fact, in the geometrical problems whose solution can be constructed using a ruler and a compass alone, each point is determined by only three basic operations: the intersection of two lines, the intersection of a line and a circle, or the intersection of two circles [91].

2.5.1 Circle-circle, circle-line, and line-line intersections

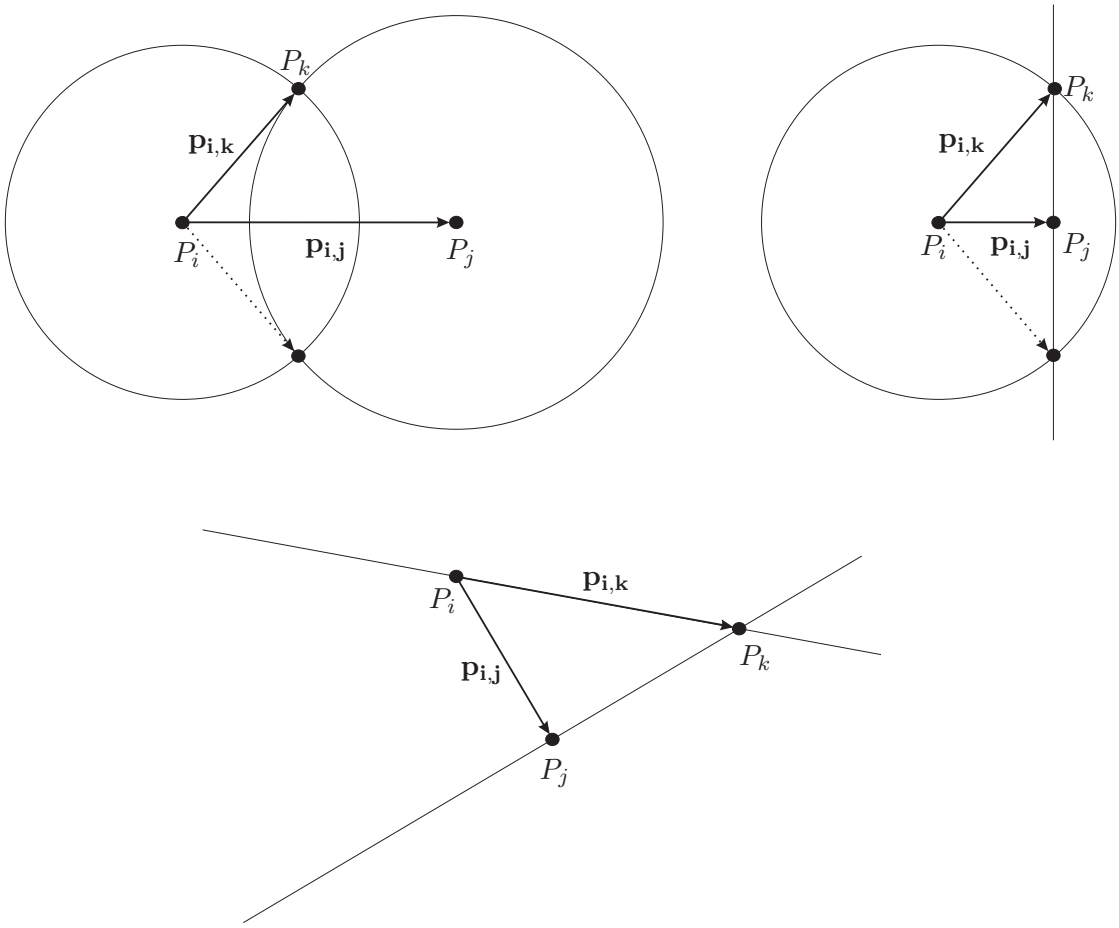

Figure 2.2. The intersection of two circles **(top-left)**, and the intersection of a circle and a line **(top-right)** can have up to two possible solutions which can be expressed in vector form using bilateration matrices. Two lines intersect, in general, in a single point **(bottom)**, this solution can also be expressed in vector form using bilateration matrices.

[1]The ruler is assumed to be infinite in length, has no markings on it, and has only one edge, that is, a straightedge.

The intersection of two circles is a classical geometrical problem whose solution implies the resolution of a system of two quadratic equations. According to notation of Fig. 2.2(left), the result to this problem can be expressed in terms of bilateration matrices as

$$\mathbf{p}_{i,k} = \mathbf{Z}_{i,j,k}\,\mathbf{p}_{i,j}. \tag{2.14}$$

A line and a circle may intersect in two imaginary points, a single degenerate point, or two distinct points. Then, let us suppose, according to notation of Fig. 2.2(right), that we want to obtain the intersection of a circle centered at P_i and a line whose nearest point to P_i is P_j. In this case $s_{i,k} = s_{i,j} + s_{j,k}$, so, substituting this relationship in expression (2.14), we get

$$\mathbf{p}_{i,k} = \mathbf{Y}_{i,j,k}\mathbf{p}_{i,j} \tag{2.15}$$

where

$$\mathbf{Y}_{i,j,k} = \frac{1}{s_{i,j}} \begin{bmatrix} s_{i,j} & -2A'_{i,j,k} \\ 2A'_{i,j,k} & s_{i,j} \end{bmatrix} \tag{2.16}$$

and

$$A'_{i,j,k} = \pm\frac{1}{2}\sqrt{s_{i,j}s_{i,k}} \tag{2.17}$$

is the oriented area of right triangle $\triangle P_iP_jP_k$.

Two lines intersect, in general, in a single point. Then, let us suppose, according to the notation in Fig. 2.2(bottom), that we want to obtain the intersection between a line that passes through point P_i and a line that passes through point P_j which is the projection point of P_i onto this second line. This problem can be solved in terms of bilateration matrices using equation (2.15), taking into account that the orientation of $\triangle P_iP_jP_k$ is fixed and that the angle between two lines is given by the dot product between their direction vectors.

2.5.2 Bilateration, geometric constructions, and kinematic chains

Since bilateration matrices permit to represent the result of the three basic operations of geometric constructions in a vector form, where the sign of the square roots account for all possible solutions that are generated along the constructive process, they constitute an interesting tool to solve this type of geometrical problems. As an example, the position analysis of a planar kinematic chain is a geometrical problem that sometimes can be solved with no further help than a compass and a ruler. This kind of kinematic chains is called quadratically-solvable linkages. Unfortunately, the position analysis of complex planar kinematic chains —*e.g.*, Baranov trusses with more than 3 links (1 loop)— cannot be solved using only a ruler and a compass. However, bilateration matrices are still of great practical interest because, as it will be shown later, their use permits to derive efficient closure conditions.

2.6 Strips of triangles

2.6.1 Two triangles sharing one edge

Let us consider the two triangles sharing one edge depicted in Fig. 2.3. Then, $\mathbf{p}_{i,l}$ can be expressed in terms of $\mathbf{p}_{i,j}$ by applying two consecutive bilaterations, as

$$\mathbf{p}_{i,l} = \mathbf{Z}_{i,k,l}\,\mathbf{p}_{i,k} = \mathbf{Z}_{i,k,l}\,\mathbf{Z}_{i,j,k}\,\mathbf{p}_{i,j}. \tag{2.18}$$

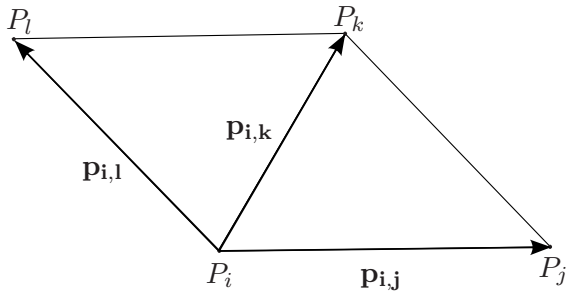

Figure 2.3. Two triangles sharing one edge.

Actually, a vector involving any two different points in the set $\{P_i, P_j, P_k, P_l\}$ can be expressed in function of $\mathbf{p}_{i,j}$ using bilateration matrices. For example,

$$\mathbf{p}_{j,l} = \mathbf{p}_{i,l} - \mathbf{p}_{i,j} = (\mathbf{Z}_{i,k,l}\,\mathbf{Z}_{i,j,k} - \mathbf{I})\,\mathbf{p}_{i,j}. \tag{2.19}$$

Therefore, since $\mathbf{Z}_{i,k,l}\,\mathbf{Z}_{i,j,k} - \mathbf{I}$ is a perpendicular matrix, the unknown squared distance between P_j and P_l can be obtained as:

$$s_{j,l} = \det(\mathbf{Z}_{i,k,l}\,\mathbf{Z}_{i,j,k} - \mathbf{I})s_{i,j}. \tag{2.20}$$

If this result is compared to the approached presented for example in [57, pp. 65-69], the ability of bilateration matrices to represent the solution of complex problems in a very compact form starts to be appreciated.

2.6.2 Squared distances in strips of triangles

The result presented in the previous subsection can be extended to strips of triangles —*i.e.*, series of connected triangles that share one edge with one neighbor and another with the next— to obtain the squared distance between any couple of their vertices as a function of known edge lengths. As an example, first, let us suppose that we are interested in finding $\mathbf{p}_{4,3}$ as a function of $\mathbf{p}_{2,4}$ for the strip of three triangles $\{\triangle P_1P_{10}P_2, \triangle P_2P_{10}P_4, \triangle P_{10}P_3P_4\}$ appearing in Fig. 2.4(top-left). Then, clearly,

$$\begin{aligned}\mathbf{p}_{4,3} &= \mathbf{Z}_{4,10,3}\,\mathbf{p}_{4,10}\\ &= \mathbf{Z}_{4,10,3}\,\mathbf{Z}_{4,2,10}\,\mathbf{p}_{2,4}.\end{aligned}$$

Now, let us suppose that we want to compute $\mathbf{p}_{1,3}$ as a function of $\mathbf{p}_{2,4}$. In this case $\overline{P_1P_3}$ is not an edge of any triangle in the strip, but

$$\begin{aligned}\mathbf{p}_{1,3} &= -\mathbf{p}_{2,1} + \mathbf{p}_{2,4} + \mathbf{p}_{4,3}\\ &= -\mathbf{Z}_{2,10,1}\,\mathbf{p}_{2,10} + \mathbf{p}_{2,4} + \mathbf{Z}_{4,10,3}\,\mathbf{p}_{4,10}\\ &= -\mathbf{Z}_{2,10,1}\,\mathbf{Z}_{2,4,10}\,\mathbf{p}_{2,4} + \mathbf{p}_{2,4} + \mathbf{Z}_{4,10,3}\,\mathbf{p}_{4,10}\\ &= (-\mathbf{Z}_{2,10,1}\,\mathbf{Z}_{2,4,10} + \mathbf{I} - \mathbf{Z}_{4,10,3}\,\mathbf{Z}_{4,2,10})\,\mathbf{p}_{2,4}.\end{aligned}$$

Therefore, the squared distance $s_{1,3}$ can be expressed as:

$$s_{1,3} = \det(\mathbf{\Omega}_1)\,s_{2,4}, \tag{2.21}$$

where $\mathbf{\Omega}_1 = -\mathbf{Z}_{2,10,1}\,\mathbf{Z}_{2,4,10} + \mathbf{I} - \mathbf{Z}_{4,10,3}\,\mathbf{Z}_{4,2,10}$. Note that $\mathbf{\Omega}_1$ is a function of all the known edge lengths in the strip of triangles.

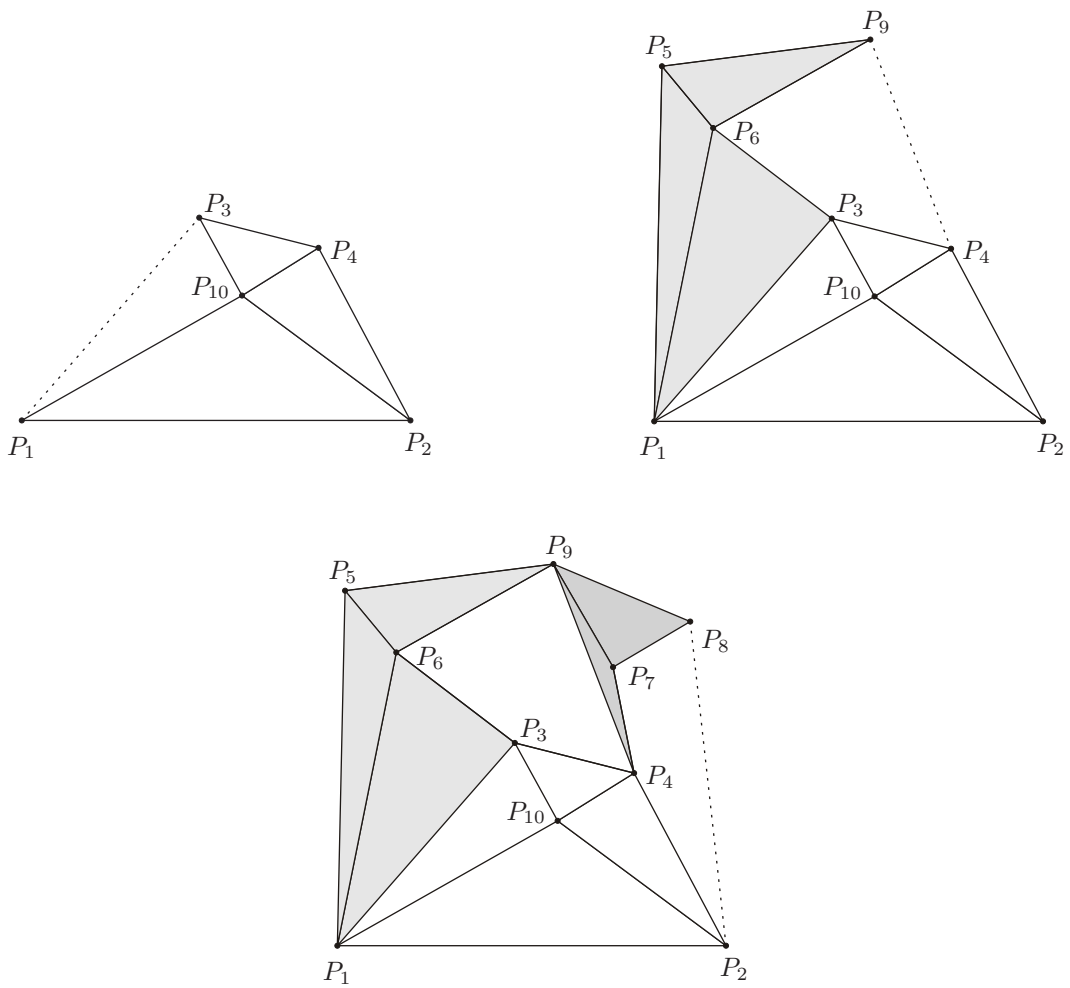

Figure 2.4. In the strip of triangles $\{\triangle P_1P_{10}P_2, \triangle P_2P_{10}P_4, \triangle P_{10}P_3P_4\}$, $s_{1,3}$ can be obtained from bilateration matrices **(top-left)**. After affixing the strip of triangles $\{\triangle P_1P_6P_3, \triangle P_1P_5P_6, \triangle P_6P_5P_9\}$ to the previous one, $s_{4,9}$ can also be obtained using bilateration matrices **(top-right)**. Likewise, $s_{2,8}$ can be obtained after affixing the strip of triangles $\{\triangle P_4P_9P_7, \triangle P_7P_9P_8\}$ **(bottom)**.

2.6.3 Strips of strips of triangles

The possibility of computing squared distances that involve arbitrary couples of vertices, using sequences of bilaterations, is not limited to strips of triangles. This can also be applied, for example, to two strips sharing two arbitrary vertices —*i.e.*, a strip of strips of triangles. To exemplify this, let us suppose that we are interested in finding $\mathbf{p}_{4,9}$ as a function of $\mathbf{p}_{2,4}$ after attaching the strip of triangles defined by $\{\triangle P_1P_6P_3, \triangle P_1P_5P_6, \triangle P_6P_5P_9\}$ to the strip $\{\triangle P_1P_{10}P_2, \triangle P_2P_{10}P_4, \triangle P_{10}P_3P_4\}$ depicted in Fig. 2.4(top-left), so that they share vertices P_1 and P_3 [see Fig. 2.4(top-right)]. Then,

$$\begin{aligned}
\mathbf{p}_{4,9} &= -\mathbf{p}_{2,4} + \mathbf{p}_{2,1} + \mathbf{p}_{1,6} + \mathbf{p}_{6,9} \\
&= -\mathbf{p}_{2,4} + \mathbf{Z}_{2,10,1}\,\mathbf{p}_{2,10} + \mathbf{p}_{1,6} + \mathbf{Z}_{6,5,9}\,\mathbf{p}_{6,5} \\
&= (-\mathbf{I} + \mathbf{Z}_{2,10,1}\,\mathbf{Z}_{2,4,10})\mathbf{p}_{2,4} + (\mathbf{I} - \mathbf{Z}_{6,5,9}\mathbf{Z}_{6,1,5})\mathbf{p}_{1,6} \\
&= (-\mathbf{I} + \mathbf{Z}_{2,10,1}\,\mathbf{Z}_{2,4,10})\mathbf{p}_{2,4} + (\mathbf{I} - \mathbf{Z}_{6,5,9}\,\mathbf{Z}_{6,1,5})\mathbf{Z}_{1,3,6}\,\mathbf{p}_{1,3}
\end{aligned}$$

$$
\begin{aligned}
&= (-\mathbf{I} + \mathbf{Z}_{2,10,1}\,\mathbf{Z}_{2,4,10})\mathbf{p}_{2,4} + (\mathbf{I} - \mathbf{Z}_{6,5,9}\,\mathbf{Z}_{6,1,5})\mathbf{Z}_{1,3,6}\,\mathbf{\Omega}_1\,\mathbf{p}_{2,4} \\
&= (-\mathbf{I} + \mathbf{Z}_{2,10,1}\,\mathbf{Z}_{2,4,10} + (\mathbf{I} - \mathbf{Z}_{6,5,9}\,\mathbf{Z}_{6,1,5})\mathbf{Z}_{1,3,6}\,\mathbf{\Omega}_1)\mathbf{p}_{2,4}.
\end{aligned}
$$

Therefore,

$$
s_{4,9} = \det\left(\mathbf{\Omega}_2\right) s_{2,4}, \tag{2.22}
$$

where

$$
\mathbf{\Omega}_2 = -\mathbf{I} + \mathbf{Z}_{2,10,1}\,\mathbf{Z}_{2,4,10} + (\mathbf{I} - \mathbf{Z}_{6,5,9}\,\mathbf{Z}_{6,1,5})\mathbf{Z}_{1,3,6}\,\mathbf{\Omega}_1.
$$

The process of adding a strip of triangles sharing two arbitrary vertices with the obtained structure can be iterated further. For example, we can now add the strip of triangles defined by $\{\triangle P_4P_9P_7, \triangle P_7P_9P_8\}$, as shown in Fig. 2.4(bottom). In this case, we might be interested in obtaining $s_{2,8}$ as a function of $s_{2,4}$. To this end, we could compute

$$
\begin{aligned}
\mathbf{p}_{2,8} =& \mathbf{p}_{2,4} + \mathbf{p}_{4,9} + \mathbf{p}_{9,8} \\
=& \mathbf{p}_{2,4} + \left(\mathbf{I} - \mathbf{Z}_{9,7,8}\,\mathbf{Z}_{9,4,7}\right)\mathbf{p}_{4,9} \\
=& \left(\mathbf{I} + \left(\mathbf{I} - \mathbf{Z}_{9,7,8}\,\mathbf{Z}_{9,4,7}\right)\mathbf{\Omega}_2\right)\mathbf{p}_{2,4}.
\end{aligned}
$$

Thus,

$$
s_{2,8} = \det\left(\mathbf{\Omega}_3\right) s_{2,4}, \tag{2.23}
$$

where

$$
\mathbf{\Omega}_3 = \mathbf{I} + \left(\mathbf{I} - \mathbf{Z}_{9,7,8}\,\mathbf{Z}_{9,4,7}\right)\mathbf{\Omega}_2.
$$

Observe that, if $s_{2,8}$ is fixed to a given value, the above equation can be seen as a closure equation, a condition that is fulfilled if and only if the strip of triangles can be constructed so that the distance between P_2 and P_8 is the desired one. This idea can be applied to obtain closure conditions of planar kinematic chains, as presented in the next section.

2.7 Closure conditions of kinematic chains using bilateration matrices

Considering the 9-bar pin-jointed planar truss —*i.e.*, a planar kinematic chain of mobility zero with nine binary links (links with two points of connection) connected by revolute joints— depicted in Fig. 2.5(a). The points P_1, P_2, P_3, P_4, and P_5 are the revolute pair centers of the nine binary links. In this truss, note that once P_1 and P_4 have been located on the plane, points P_2 and P_5 can be positioned in 8 and 4 different locations, respectively. Taking $\mathbf{p}_{1,6}$ as a reference, since the revolute pair centers and the nine binary links of this truss define the strip of triangles $\{\triangle P_1P_3P_2, \triangle P_1P_6P_3, \triangle P_1P_4P_6, \triangle P_4P_5P_6\}$, we have that

$$
\begin{aligned}
\mathbf{p}_{2,5} &= -\mathbf{p}_{1,2} + \mathbf{p}_{1,6} + \mathbf{p}_{6,5} \\
&= -\mathbf{Z}_{1,3,2}\,\mathbf{p}_{1,3} + \mathbf{p}_{1,6} + \mathbf{Z}_{6,4,5}\,\mathbf{p}_{6,4} \\
&= -\mathbf{Z}_{1,3,2}\,\mathbf{Z}_{1,6,3}\,\mathbf{p}_{1,6} + \mathbf{p}_{1,6} + \mathbf{Z}_{6,4,5}\,\mathbf{Z}_{6,1,4}\,\mathbf{p}_{6,1} \\
&= \left(\mathbf{I} - \mathbf{Z}_{1,3,2}\,\mathbf{Z}_{1,6,3} - \mathbf{Z}_{6,4,5}\,\mathbf{Z}_{6,1,4}\right)\mathbf{p}_{1,6}.
\end{aligned} \tag{2.24}
$$

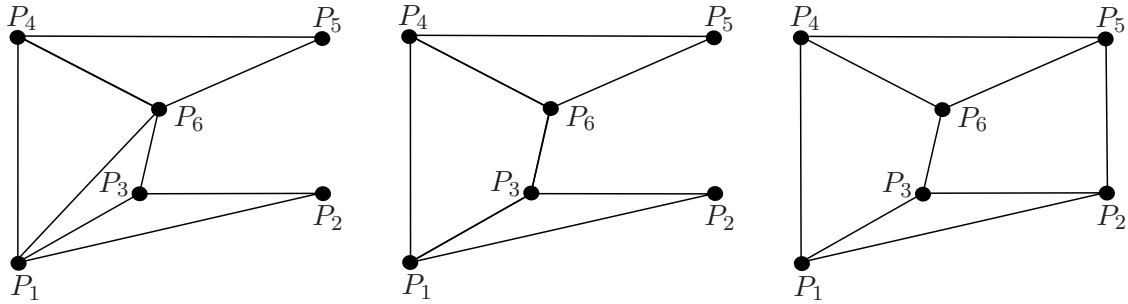

Figure 2.5. If the binary link between the revolute pair centers P_1 and P_6 is removed in the 9-bar pin-jointed planar truss **(left)**, a planar linkage of mobility 1 is obtained **(center)**. If a binary link is then added between P_2 and P_5, a truss is again obtained **(right)** whose closure condition can be expressed as the squared distance $s_{2,5}$ as a function of $s_{1,6}$.

Thus, the possible values of the squared distance between points P_2 and P_5 can be computed as a function of the lengths of the binary links as:

$$s_{2,5} = \det\Big(\mathbf{I} - \mathbf{Z}_{1,3,2}\,\mathbf{Z}_{1,6,3} - \mathbf{Z}_{6,4,5}\,\mathbf{Z}_{6,1,4}\Big)s_{1,6}. \tag{2.25}$$

Now, if the binary link between the revolute pair centers P_1 and P_6 is removed, as presented in Fig. 2.5(b), the planar pin-jointed truss becomes a planar linkage of mobility 1 (observe the 4-bar linkage formed between P_1, P_3, P_4, and P_6). But, if a binary link is then added between P_2 and P_5, a truss is again obtained [Fig. 2.5(c)]. What are the assembly modes of this new truss? Note that the closure condition of this truss is given by equation (2.25). The solution of this equation gives the set of values of $s_{1,6}$ compatible with the lengths of all the binary links of this new truss. Actually, when $\triangle P_1P_3P_2$ and $\triangle P_4P_5P_6$ are oriented —*i.e.*, when $\triangle P_1P_3P_2$ and $\triangle P_4P_5P_6$ are ternary links— this truss corresponds to a well-known kinematic chain, the Baranov truss of two loops, or pentad.

As it will be presented in next chapters, the above process can be extended to compute closure conditions of complex planar kinematic chains. It will be shown how the resulting formulations greatly simplify the position analysis problem of planar linkages.

2.7.1 Closure conditions and symmetries of kinematic chains

The symmetries of a kinematic chain are given by its automorphisms. An automorphism of a kinematic chain is a set of permutations of its joints that map the kinematic chain onto itself while preserving the connectivity between joints. Since the composition of two automorphisms is clearly another automorphism, the set of automorphisms of a given kinematic chain, under the composition operation, forms a group, the automorphism group of the kinematic chain.

Finding the automorphism group and an irreducible set of its generators for a kinematic chain is an easy task using any of the available open-source software tools for computing graph automorphisms. For instance, the truss of Fig. 2.5(right) has twelve automorphisms: $\{1,2,3,4,5,6\}$, $\{1,3,2,4,6,5\}$, $\{2,1,3,5,4,6\}$, $\{2,3,1,5,6,4\}$, $\{3,1,2,6,4,5\}$, $\{3,2,1,6,5,4\}$, $\{4,5,6,1,2,3\}$, $\{4,6,5,1,3,2\}$, $\{5,4,6,\ 2,1,3\}$, $\{5,6,4,2,3,1\}$, $\{6,4,5,3,1,2\}$, and $\{6,5,4,3,2,1\}$ (Fig. 2.6 depicts the first three).

Observe that the closure condition of any of the symmetric trusses above discussed is obtained by the simple application of the corresponding permutation to equation (2.25).

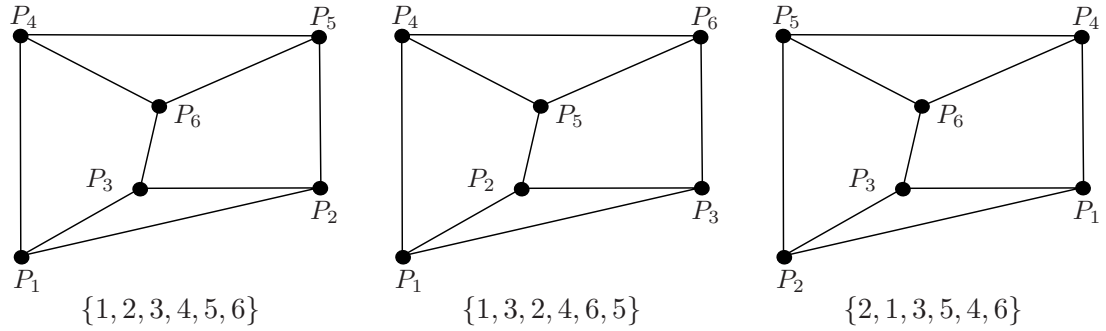

Figure 2.6. Three of the twelve automorphisms of the planar truss presented in Fig. 2.5(right).

For example, the closure condition of the truss in Fig. 2.6(center) is obtained by applying the permutation

$$\begin{bmatrix} 1 & 2 & 3 & 4 & 5 & 6 \\ 1 & 3 & 2 & 4 & 6 & 5 \end{bmatrix}.$$

That is,

$$s_{3,6} = \det\Big(\mathbf{I} - \mathbf{Z}_{1,2,3}\mathbf{Z}_{1,5,2} - \mathbf{Z}_{5,4,6}\mathbf{Z}_{5,1,4}\Big)s_{1,5}.$$

The application of permutations to closure conditions will be useful later to solve the position analysis of complex planar kinematic chains.

Chapter 3

Position analysis of Baranov trusses

An Assur group, a key concept in *kinematics of mechanisms* introduced by the Russian engineering scientist Leonid Assur in 1914 [169], is a minimal group of links that can be connected to any kinematic chain without modifying its mobility [30]. A non-overconstrained closed planar linkage with mobility zero from which an Assur group can be obtained by removing any of its links is defined as an Assur kinematic chain, basic truss [30, 50], or Baranov truss when no slider joints are considered [138]. Hence, a Baranov truss, named after the Russian kinematician G.G. Baranov who first presented the idea of this kind of truss in 1952 [11], corresponds to multiple Assur groups. The relevance of the Baranov trusses derive from the fact that, if the position analysis of a Baranov truss is solved, the same process can be applied to solve the position analysis of all its corresponding Assur groups.

The simplest Baranov trusses are the triad, a one-loop structure with three links and two feasible configurations, and the pentad, a truss with two loops and up to six assembly modes. Baranov, in his seminal paper, presented 3 trusses of 7 links and 26 trusses of 9 links. In 1971, Manolescu and Erdelean identified two additional trusses of 9 links that were missing in the initial categorization [115], thus completing the classification of Baranov trusses with up to 4 loops. In 1994, Yang and Yao found that the number of Baranov trusses with 11 links is 239 [223]. Unfortunately, their topologies were not made available and, to the best of the author's knowledge, they have not been published yet. Thus, strictly speaking, only the Baranov trusses with up to 9 links have been cataloged (see Table 3.1). This catalog appears in Fig. 3.1 where each truss is identified using the nomenclature suggested by Manolescu [114].

Links	Loops	Baranov trusses	Available topology	Coupling degree 0	1	2	3	Resulting Assur groups
3	1	1	Yes	1	0	0	0	1
5	2	1	Yes	0	1	0	0	2
7	3	3	Yes	0	3	0	0	10
9	4	28	Yes	0	24	4	0	173
11	5	239	No	0	197	42	0	5442
13	6	?	No	0	?	?	?	251638

Table 3.1. Number of Baranov trusses as a function of the number of links (alternatively, number of loops), indication of whether the topologies are available in the literature, number of trusses with different coupling degrees, and number of different Assur groups resulting from eliminating one link from the trusses in each class.

The position analysis problem for a planar truss consists in, given the dimensions of all links, calculating all relative possible transformations between them all. This analysis, in the analytical methods (§1.2.1.1), reduces to finding the roots of a polynomial in one

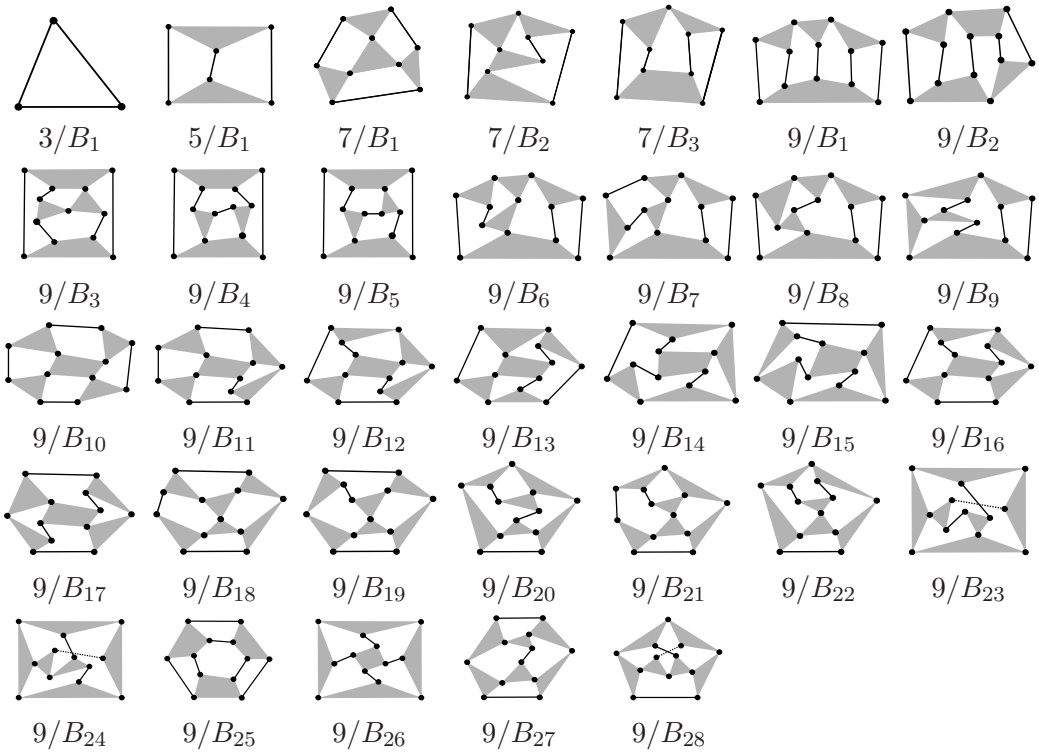

Figure 3.1. The cataloged Baranov trusses.

variable, the *characteristic polynomial* of the truss. When this polynomial is obtained, it is said that the problem is solved in *closed form*. This approach is usually preferred to numerical approaches (§1.2.1.2), although obtaining the polynomial with standard methods is in general a cumbersome task, because the degree of the polynomial specifies the greatest possible number of assembly modes of the linkage and modern software provides guaranteed and fast computation of all real roots of a polynomial equation and hence of all assembly modes of the analyzed linkage.

The closed-form solution to the position analysis of the cataloged Baranov trusses is known for 22 of them. They have been solved on an ad hoc basis by several authors (see §3.1, Tables A.1-A.8, and the references therein) using mainly elimination techniques, as those based on Sylvester or Dixon resultants, applied to vector loop equations expressed in trigonometric or complex number terms. Some of those approaches are in fact variations of the general methods developed by Nielsen and Roth [133], and Wampler [190, 191]. Up to author's knowledge, the closed-form position analysis of the trusses identified as $9/B_2$, $9/B_3$, $9/B_4$, $9/B_5$, $9/B_6$, $9/B_8$, $9/B_9$, $9/B_{13}$, $9/B_{18}$, $9/B_{19}$, and $9/B_{22}$ has not been reported in the literature. Nevertheless, the number of assembly modes of these trusses was studied in [67] using homotopy continuation. However, as it will be shown later, some of the reported results are erroneous. Beyond four loops, the closed-form position analysis of only one 11-link Baranov truss has been previously reported. In [109], Lösch solved the five-loop version of the $9/B_1$ Baranov truss with a procedure based on trigonometric-based vector loop equations and Gröbner basis. The same truss was analyzed by Wohlhart using Sylvester elimination [217]. In Section 3.6, the position analysis of the five-loop (11-link) and six-loop (13-link) versions of the $9/B_{10}$ Baranov truss are solved.

An n-ary link in a Baranov truss introduces a set of distance constraints between the n involved joints. This translates into a set of quadratic equations from which an elimi-

nant can be obtained to get a single equation in one variable. In this case, each equation is simple but the elimination process involves a large number of equations. A more compact elimination process is obtained when the set of $\frac{n-1}{2}$ independent loop equations is derived. This has been the dominating technique in *kinematics of mechanisms* which, in general, requires not only complex eliminations but also tangent-half-angle substitutions. It is relevant to stand out that the use of independent loop equations is too the standard technique in numerical approaches.

Observe that an even more compact formulation is obtained by a applying the following constructive process. Take one loop with a low number of joints and some of its joint variables as parameters which, when assigned to particular values, make the loop rigid. Then, the position of all links in the neighboring loops to this loop can also be obtained as a function of the chosen parameters taking, if needed, more joint variables as parameters. This process can be repeated till the locations of all links are expressed as functions of a set of parameters. Along the process, the locations of some links can be computed using different sets of parameters. This give rise to constraints between the parameters which translate into equations. The number of these equations is called the *coupling degree* of the truss [222, 223].

For non-overconstrained trusses, as is the case of Baranov trusses, the number of resulting constraints always equals the number of joint variables taken as parameters. Since the coupling degree is always lower than the number of loops (see Table 3.1), the elimination process to get a characteristic polynomial is simplified. Actually, when the coupling degree is 1, eliminations are no longer required. Moreover, there are some trusses that form regular patterns whose coupling degree is independent from the number of its loops, as discussed in Section 3.6.

Although the above idea is simple, its implementation using displacement transformations —*i.e.*, a collection of rotations and translations— is not. This is probably why this approach has been belittled but, in this chapter, we show how, by expressing the position analysis problem fully in terms of distances, this idea recovers interest because its implementation becomes straightforward. Moreover, as it will be presented in Sections 3.2, 3.3, and 3.4, for all the cataloged Baranov trusses with positive coupling degree[1], the system of kinematic equations is reduced to a single scalar equation in one variable, except for the Baranov trusses $9/B_{25}$, $9/B_{26}$, $9/B_{27}$, and $9/B_{28}$ for which the system is formed by two scalar equations in two variables, a result in agreement with their coupling degrees found by Yang and Yao [223].

3.1 Position analysis of the triad or $3/B_1$ Baranov truss

The simplest Baranov truss is the $3/B_1$ truss or triad. This one-loop truss has three binary links and up to two assembly modes, its position analysis problem is equivalent to the bilateration problem. Thus, according to the notation used in Fig. 3.2(left), given the dimensions of the three binary links and the locations of the revolute pair centers P_1 and P_2, the location of the revolute pair center P_3 can be computed as:

$$\mathbf{p}_{1,3} = \mathbf{Z}_{1,2,3}\,\mathbf{p}_{1,2}. \tag{3.1}$$

Other approaches to solve the position analysis problem of the triad can be found, for instance, in [49, 180].

[1]The position analysis of the triad, whose coupling degree is 0, reduces to the bilateration problem

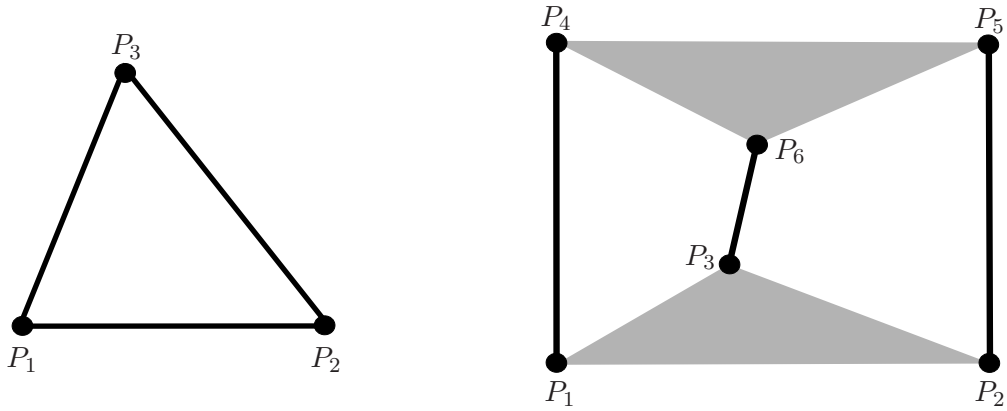

Figure 3.2. The triad **(left)** and the pentad **(right)**.

3.1.1 Example

As an example, let us suppose that we are interested in solve the position analysis problem of a triad whose link squared lengths are $s_{1,2} = 50$, $s_{1,3} = 20$, and $s_{2,3} = 18$. In this case,

$$\begin{aligned}\mathbf{Z}_{1,2,3} &= \frac{1}{2\,s_{1,2}}\begin{pmatrix} s_{1,2}+s_{1,3}-s_{2,3} & -4\,A_{1,2,3} \\ 4\,A_{1,2,3} & s_{1,2}+s_{1,3}-s_{2,3}\end{pmatrix} \\ &= \begin{pmatrix} \frac{13}{25} & \mp\frac{9}{25} \\ \pm\frac{9}{25} & \frac{13}{25}\end{pmatrix}.\end{aligned}$$

Then, if P_1 and P_2 are located, for instance, in $(1,3)^T$ and $(6,8)^T$, respectively, we get

$$P_3 = \left(\frac{9}{5}, \frac{37}{5}\right)^T \text{ or } P_3 = \left(\frac{27}{5}, \frac{19}{5}\right)^T.$$

This two configurations appear in Fig. 3.3.

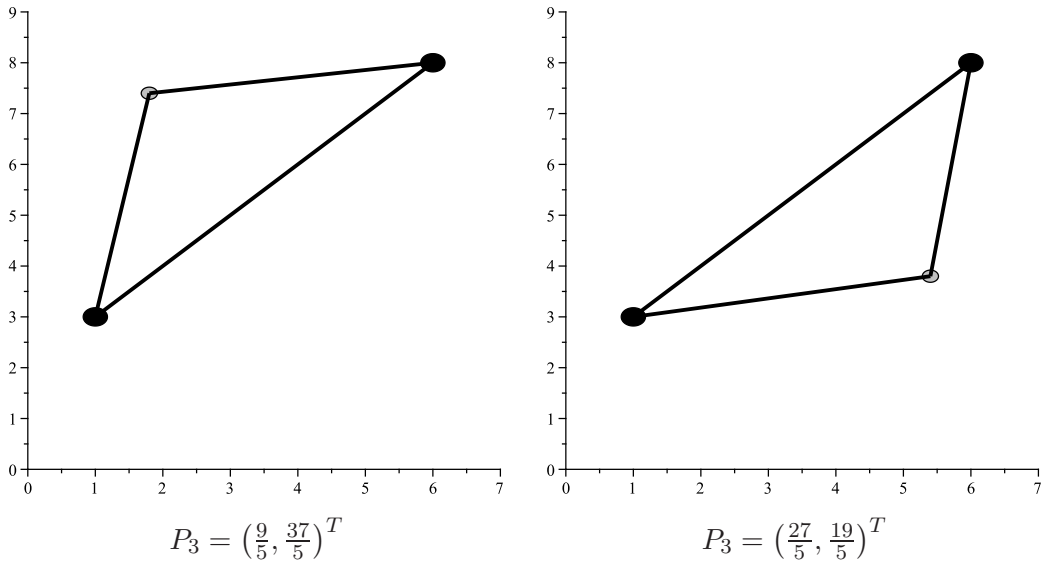

Figure 3.3. The configurations of the analyzed $3/B_1$ Baranov truss.

3.2 Position analysis of the pentad or $5/B_1$ Baranov truss

The pentad or $5/B_1$ Baranov truss is a two-loop structure of two ternary links and three binary links with up to six assembly modes. This truss has been, by far, the most studied Baranov truss in the literature. The Russian kinematician Eduard Peisach is credited to be the first researcher in obtaining a characteristic polynomial for this structure in 1985 [137]. After Peisach's work, a characteristic polynomial for the pentad has been obtained independently at least by Li and Matthew [105], Pennock and Kassner [142], Gosselin *et. al.* [55, 56], Wohlhart [214], Husty [81], Kong and Gosselin [98], Collins [37], Han *et. al.* [66], Liu *et. al.* [108], and Luo [110]. Numerical approaches has also been reported, for instance, Hang *et. al.* [67] used homotopy continuation, Luo *et. al.* [111] used a Newton iterative method, and Chandra and Rolland [31] used an hybrid metaheuristic.

In the $5/B_1$ Baranov truss depicted in Fig. 3.2(right), the revolute pair centers of the two ternary links define the line segments $\overline{P_1P_4}$, $\overline{P_2P_5}$, and $\overline{P_3P_6}$, and the triangles $\triangle P_1P_3P_2$ and $\triangle P_6P_4P_5$. The closure condition of this truss using bilateration techniques, as presented in Section 2.7, equation (2.25), reduces to compute $s_{2,5}$ as a function of all the link side lengths in the Baranov truss and the unknown squared distance $s_{1,6}$, namely:

$$s_{2,5} = \det\Big(\mathbf{I} - \mathbf{Z}_{1,3,2}\,\mathbf{Z}_{1,6,3} - \mathbf{Z}_{6,4,5}\,\mathbf{Z}_{6,1,4}\Big)s_{1,6}. \tag{3.2}$$

This equation is fulfilled if and only if the $5/B_1$ Baranov truss can be assembled. The expansion of equation (3.2) yields

$$s_{2,5} = \frac{1}{s_{1,6}}\left(\Psi + \Phi_2\,A_{1,4,6} + \Phi_3\,A_{1,6,3} + \Phi_4\,A_{1,4,6}\,A_{1,6,3}\right), \tag{3.3}$$

that is,

$$(\Psi - s_{2,5}\,s_{1,6}) + \Phi_2\,A_{1,4,6} + \Phi_3\,A_{1,6,3} + \Phi_4\,A_{1,4,6}\,A_{1,6,3} = 0$$

or

$$\Phi_1 + \Phi_2\,A_{1,4,6} + \Phi_3\,A_{1,6,3} + \Phi_4\,A_{1,4,6}\,A_{1,6,3} = 0, \tag{3.4}$$

where $\Phi_1 = \Psi - s_{2,5}\,s_{1,6}$, and Ψ, Φ_2, Φ_3, and Φ_4 are polynomials in $s_{1,6}$, of at most second order, whose coefficients are algebraic functions of the link side lengths. Hence, equation (3.4) is a scalar radical equation in a single variable: $s_{1,6}$, that is, the pentad has coupling degree 1.

The roots of equation (3.4), in the range in which the signed areas of the triangles $\triangle P_1P_4P_6$ and $\triangle P_1P_6P_4$ are real, that is, the range

$$\Big[\max\{(d_{1,4} - d_{4,6})^2\,,(d_{1,3} - d_{3,6})^2\}, \min\{(d_{1,4} + d_{4,6})^2\,,(d_{1,3} + d_{3,6})^2\}\Big]\,,$$

determine the assembly modes of the $5/B_1$ Baranov truss. These roots can be readily obtained for the four possible combinations of signs for the oriented areas $A_{1,4,6}$ and $A_{1,6,3}$ using a **numerical approach**, for example, an interval Newton method. If a polynomial representation is preferred, we proceed as explained in the next subsection.

3.2.1 Deriving the characteristic polynomial

In order to obtain a polynomial expression from the scalar equation (3.4), we just have to clear the radicals associated with the oriented areas $A_{1,4,6}$ and $A_{1,6,3}$. To this end,

the terms in equation (3.4) are arranged as

$$\Phi_2\, A_{1,4,6} + \Phi_3\, A_{1,6,3} = -\left(\Phi_1 + \Phi_4\, A_{1,4,6}\, A_{1,6,3}\right).$$

Now, by squaring both sides of the above equation, expanding the result, and rearranging terms, we get

$$\Phi_2^2\, A_{1,4,6}^2 + \Phi_3^2\, A_{1,6,3}^2 - \Phi_4^2\, A_{1,4,6}^2\, A_{1,6,3}^2 - \Phi_1^2 = 2\left(\Phi_1\, \Phi_4 - \Phi_2\, \Phi_3\right) A_{1,4,6}\, A_{1,6,3}.$$

Finally, if both sides of the above equation are again squared and expanded, the following equation is obtained:

$$\begin{aligned} &-\Phi_4^4 A_{1,4,6}^4 A_{1,6,3}^4 + 2\Phi_4^2\Phi_2^2 A_{1,4,6}^4 A_{1,6,3}^2 + 2\Phi_4^2\Phi_3^2 A_{1,4,6}^2 A_{1,6,3}^4 - \Phi_2^4 A_{1,4,6}^4 - \Phi_3^4 A_{1,6,3}^4 \\ &-\Phi_1^4 + \left(2\Phi_2^2\Phi_3^2 - 8\Phi_2\Phi_3\Phi_4\Phi_1 + 2\Phi_4^2\Phi_1^2\right) A_{1,4,6}^2 A_{1,6,3}^2 + 2\Phi_1^2\Phi_2^2 A_{1,4,6}^2 + 2\Phi_1^2\Phi_3^2 A_{1,6,3}^2 = 0. \end{aligned} \tag{3.5}$$

which, when fully expanded, leads to

$$s_{1,6}^2\, \mathcal{P}_{5B1} = 0, \tag{3.6}$$

where $\mathcal{P}_{5B1}$ is a 6th-degree polynomial in $s_{1,6}$. The double extraneous root at $s_{1,6} = 0$ was introduced when clearing denominators to obtain equation (3.4), so they can be dropped. $\mathcal{P}_{5B1}$ is the distance-based characteristic polynomial of the $5/B_1$ Baranov truss. The form of equation (3.4) as well as the twice squaring process for clearing radicals explained above will be recurrent along this thesis to solve the position analysis of kinematic chains in closed form.

3.2.2 Computing configurations

The roots of equation (3.4) or polynomial $\mathcal{P}_{5B1}$ correspond to the assembly modes of the $5/B_1$ Baranov truss. For each of these roots, given the location of the ternary link associated to the triangle $\triangle P_1P_3P_2$ —*i.e.*, given the locations of the revolute pair centers P_1, P_2, and P_3, the Cartesian position of the revolute pair centers P_4, P_5, and P_6 can be computed using the following sequence of bilaterations:

$$\begin{aligned} \mathbf{p}_{1,6} &= \mathbf{Z}_{1,3,6}\, \mathbf{p}_{1,3}, \\ \mathbf{p}_{1,4} &= \mathbf{Z}_{1,6,4}\, \mathbf{p}_{1,6}, \\ \mathbf{p}_{4,5} &= \mathbf{Z}_{4,6,5}\, \mathbf{p}_{4,6}. \end{aligned}$$

This process leads up to four possible locations for P_5, and at least one of them must satisfy the distance imposed by the binary link connecting P_2 and P_5.

To compute the configurations of a $5/B_1$ Baranov truss given the location of a link different to the one associated to $\triangle P_1P_3P_2$, we simply have to calculate the Euclidean transformation between the constant values of the new link of reference, or ground link, and the values computed with the above set of bilaterations.

3.2.3 Example

According to the notation used in Fig. 3.2(right), let us suposse that $s_{1,2} = 50$, $s_{1,3} = 20$, $s_{1,4} = 52$, $s_{2,3} = 18$, $s_{2,5} = 73$, $s_{3,6} = 18$, $s_{4,5} = 81$, $s_{4,6} = 40$, and $s_{5,6} = 13$. In this case,

$$\mathbf{Z}_{1,3,2} = \begin{pmatrix} \frac{13}{10} & \frac{9}{10} \\ -\frac{9}{10} & \frac{13}{10} \end{pmatrix},$$

$$\mathbf{Z}_{1,6,3} = \frac{1}{2\,s_{1,6}} \begin{pmatrix} s_{1,6}+2 & \mp\sqrt{-s_{1,6}^2+76\,s_{1,6}-4} \\ \pm\sqrt{-s_{1,6}^2+76\,s_{1,6}-4} & s_{1,6}+2 \end{pmatrix},$$

$$\mathbf{Z}_{6,4,5} = \begin{pmatrix} -\frac{7}{20} & \frac{9}{20} \\ -\frac{9}{20} & -\frac{7}{20} \end{pmatrix}, \text{ and}$$

$$\mathbf{Z}_{6,1,4} = \frac{1}{2\,s_{1,6}} \begin{pmatrix} s_{1,6}-12 & \mp\sqrt{-s_{1,6}^2+184\,s_{1,6}-144} \\ \pm\sqrt{-s_{1,6}^2+184\,s_{1,6}-144} & s_{1,6}-12 \end{pmatrix}.$$

Note that the orientation of triangles $\triangle P_1P_3P_2$ and $\triangle P_6P_4P_5$ is fixed.

Now, substituting the link side lengths of the analyzed pentad in equation (3.4), we obtain

$$\begin{aligned} &-40\,{s_{1,6}}^2+26480\,s_{1,6}-960\pm 1440\sqrt{-s_{1,6}^2+184\,s_{1,6}-144} \\ &\pm(8640-2160\,s_{1,6})\sqrt{-s_{1,6}^2+76\,s_{1,6}-4} \\ &\pm 40\sqrt{-s_{1,6}^2+76\,s_{1,6}-4}\sqrt{-s_{1,6}^2+184\,s_{1,6}-144}=0 \end{aligned}$$

that is a scalar equation in $s_{1,6}$ which can be numerically solved for the four possible combinations of signs of the two involved squared roots. Alternatively, substituting the above values in $\mathcal{P}_{5B1}$, the following characteristic polynomial is obtained:

$$\begin{aligned} &266085\,{s_{1,6}}^6-44959860\,{s_{1,6}}^5+2314950740\,{s_{1,6}}^4-35686383040\,{s_{1,6}}^3 \\ &+210282384000\,{s_{1,6}}^2-482011052800\,s_{1,6}+366616640000. \end{aligned}$$

The real roots of this polynomial are 1.6525, 2.3684, 5.9939, 10.6876, 73.7712, and 74.4945. The corresponding configurations for the case in which $P_1=(0,0)^T$, $P_2=(5\sqrt{2},0)^T$, and $P_3=(\frac{13}{5}\sqrt{2},\frac{9}{5}\sqrt{2})^T$ appear in Fig. 3.4.

3.3 Position analysis of the seven-link Baranov trusses

There are three seven-link (three-loop) Baranov trusses, namely, the $7/B_1$ Baranov truss, $7/B_2$ Baranov truss, and $7/B_3$ Baranov truss. Next, it is shown how the position analysis of each of them can be solved using the bilateration techniques presented in Chapter 2. In this section, the product $\mathbf{Z}_{i,j,k}\mathbf{Z}_{i,k,l}$ is abbreviated as $\mathbf{\Omega}_{i,j,k,l}$.

3.3.1 Position analysis of the $7/B_1$ Baranov truss

The $7/B_1$ Baranov truss is a three-loop structure of four ternary links and three binary links with up to fourteen assembly modes. The position analysis of this truss has been solved in closed form, following standard analytical methods, at least by Kong and Yang [99], Innocenti [87], and Dhingra *et. al.* [41]. Numerical approaches based on homotopy continuation have been reported by Liu and Yang [107] and Hang *et. al.* [67].

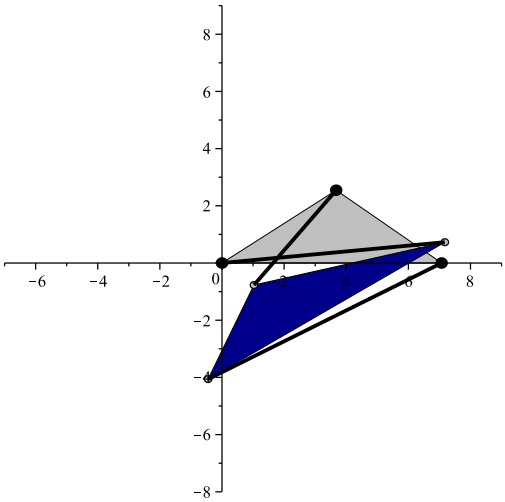

$s_{1,6} = 1.6525$

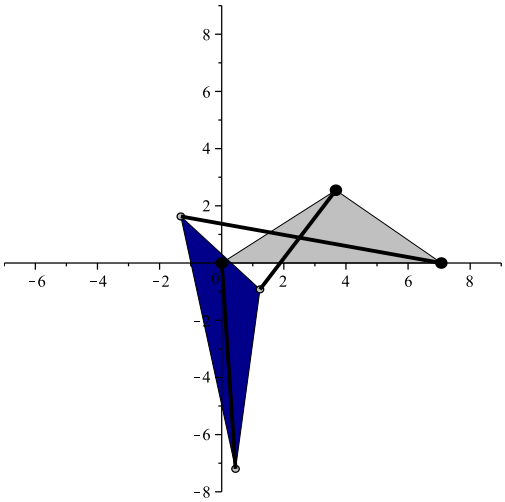

$s_{1,6} = 2.3684$

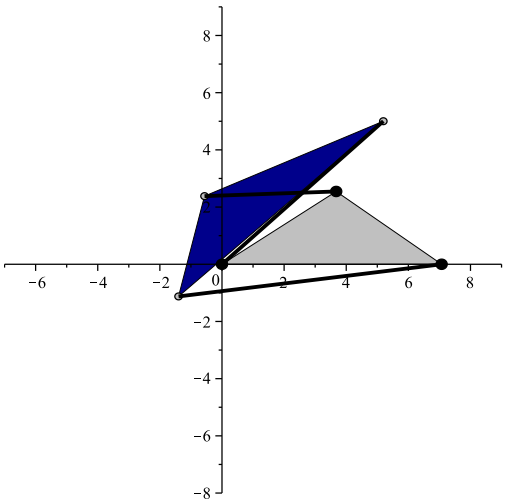

$s_{1,6} = 5.9939$

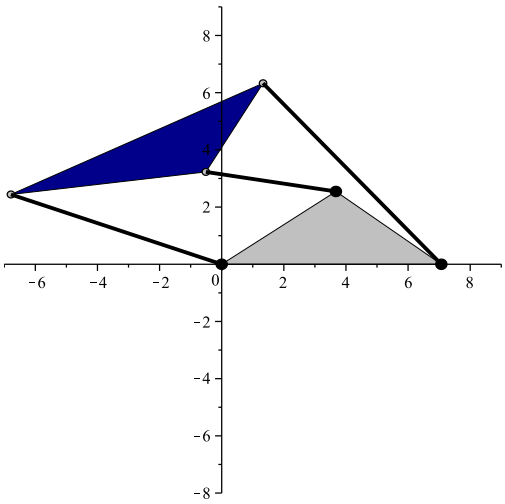

$s_{1,6} = 10.6876$

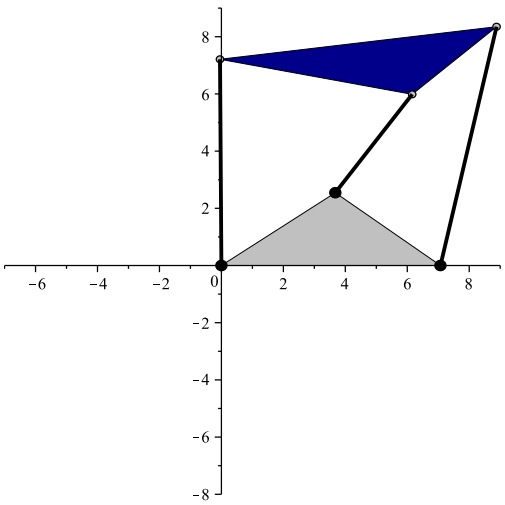

$s_{1,6} = 73.7712$

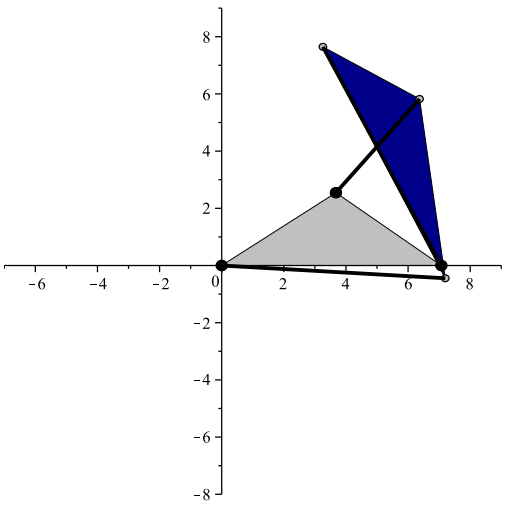

$s_{1,6} = 74.4945$

Figure 3.4. The configurations of the analyzed $5/B_1$ Baranov truss.

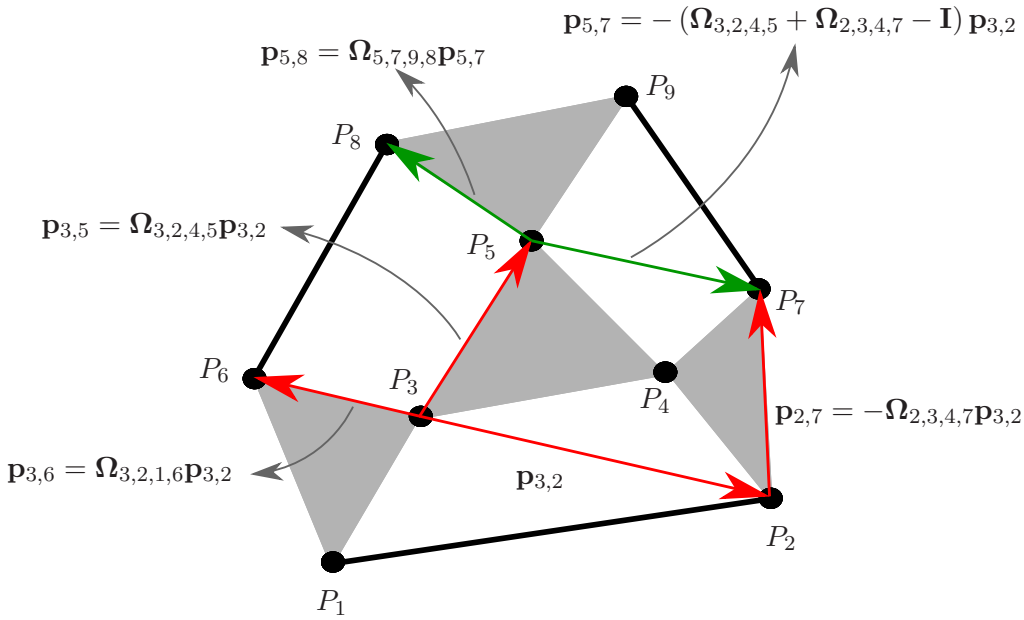

Figure 3.5. The $7/B_1$ Baranov truss and its associated notation.

In the $7/B_1$ Baranov truss depicted in Fig. 3.5, the revolute pair centers of the three ternary links define the triangles $\triangle P_2P_4P_7$, $\triangle P_3P_5P_4$, $\triangle P_3P_1P_6$, and $\triangle P_5P_8P_9$. Next, it is shown how the kinematic equations of this truss can be reduced to compute $s_{6,8}$ as a function of $s_{2,3}$. That is, $s_{2,3}$ is used as a parameter in terms of which the location of all other links of the truss can be expressed. Since one parameter is needed, the truss is said to have coupling degree 1, as already observed by [223].

3.3.1.1 Computing $s_{6,8}$ as a function of $s_{2,3}$

Considering the two strips of triangles $\{\triangle P_3P_1P_6, \triangle P_1P_3P_2, \triangle P_3P_2P_4, \triangle P_2P_7P_4, \triangle P_3P_4P_5\}$ and $\{\triangle P_5P_7P_9, \triangle P_5P_9P_8\}$ in Fig. 3.5, we have

$$\mathbf{p}_{2,7} = \mathbf{Z}_{2,4,7}\mathbf{p}_{2,4} = -\mathbf{Z}_{2,4,7}\mathbf{Z}_{2,3,4}\mathbf{p}_{3,2} = -\mathbf{\Omega}_{2,3,4,7}\mathbf{p}_{3,2} \tag{3.7}$$

$$\mathbf{p}_{3,5} = \mathbf{Z}_{3,4,5}\mathbf{p}_{3,4} = \mathbf{Z}_{3,4,5}\mathbf{Z}_{3,2,4}\mathbf{p}_{3,2} = \mathbf{\Omega}_{3,2,4,5}\mathbf{p}_{3,2} \tag{3.8}$$

$$\mathbf{p}_{3,6} = \mathbf{Z}_{3,1,6}\mathbf{p}_{3,1} = \mathbf{Z}_{3,1,6}\mathbf{Z}_{3,2,1}\mathbf{p}_{3,2} = \mathbf{\Omega}_{3,2,1,6}\mathbf{p}_{3,2} \tag{3.9}$$

$$\mathbf{p}_{5,8} = \mathbf{Z}_{5,9,8}\mathbf{p}_{5,9} = \mathbf{Z}_{5,9,8}\mathbf{Z}_{5,7,9}\mathbf{p}_{5,7} = \mathbf{\Omega}_{5,7,9,8}\mathbf{p}_{5,7}. \tag{3.10}$$

Since

$$\mathbf{p}_{6,8} = -\mathbf{p}_{3,6} + \mathbf{p}_{3,5} + \mathbf{p}_{5,8} \tag{3.11}$$

and

$$\begin{aligned}\mathbf{p}_{5,7} &= -\mathbf{p}_{3,5} + \mathbf{p}_{3,2} + \mathbf{p}_{2,7}\\ &= -\mathbf{\Omega}_{3,2,4,5}\mathbf{p}_{3,2} + \mathbf{p}_{3,2} - \mathbf{\Omega}_{2,3,4,7}\mathbf{p}_{3,2}\\ &= \left(\mathbf{I} - \mathbf{\Omega}_{3,2,4,5} - \mathbf{\Omega}_{2,3,4,7}\right)\mathbf{p}_{3,2}\end{aligned} \tag{3.12}$$

then

$$\begin{aligned}\mathbf{p}_{6,8} &= -\mathbf{\Omega}_{3,2,1,6}\mathbf{p}_{3,2} + \mathbf{\Omega}_{3,2,4,5}\mathbf{p}_{3,2} + \mathbf{\Omega}_{5,7,9,8}\mathbf{p}_{5,7}\\ &= \left(-\mathbf{\Omega}_{3,2,1,6} + \mathbf{\Omega}_{3,2,4,5} - \mathbf{\Omega}_{5,7,9,8}\left(\mathbf{\Omega}_{3,2,4,5} + \mathbf{\Omega}_{2,3,4,7} - \mathbf{I}\right)\right)\mathbf{p}_{3,2}.\end{aligned}$$

Therefore,

$$s_{6,8} = \det\left(-\mathbf{\Omega}_{3,2,1,6} + \mathbf{\Omega}_{3,2,4,5} - \mathbf{\Omega}_{5,7,9,8}\left(\mathbf{\Omega}_{3,2,4,5} + \mathbf{\Omega}_{2,3,4,7} - \mathbf{I}\right)\right) s_{2,3}. \tag{3.13}$$

The expansion of the right hand side of the above equation is a function of the unknown squared distances $s_{2,3}$ and $s_{5,7}$. Since, from equation (3.12),

$$s_{5,7} = \det\left(\mathbf{\Omega}_{3,2,4,5} + \mathbf{\Omega}_{2,3,4,7} - \mathbf{I}\right) s_{2,3}, \tag{3.14}$$

then the substitution of (3.14) in (3.13) yields a scalar radical equation in a single variable: $s_{2,3}$. The roots of this equation, in the range in which the signed areas of the triangles $\triangle P_1P_3P_2$ and $P_3P_2P_4$ are real, that is, the range

$$\left[\max\{(d_{1,2} - d_{1,3})^2, (d_{2,4} - d_{3,4})^2\}, \min\{(d_{1,2} + d_{1,3})^2, (d_{2,4} + d_{3,4})^2\}\right]$$

determine the assembly modes of the $7/B_1$ Baranov truss. These roots can be quickly obtained for the eight possible combinations of signs for the signed areas of the triangles $\triangle P_1P_3P_2$, $\triangle P_3P_2P_4$, and $\triangle P_5P_7P_9$ using a standard numerical procedure. For each of these roots, given the location of the ternary link associated to the triangle $\triangle P_3P_5P_4$, we can determine the Cartesian position of the six revolute pair centers P_1, P_2, P_6, P_7, P_8, and P_9 using equations (3.7)-(3.10) and the equation $\mathbf{p}_{2,3} = \mathbf{Z}_{3,4,2}\mathbf{p}_{3,4}$. This process leads up to eight combinations of locations for P_6 and P_8, and at least one of them must satisfy the distance imposed by the binary link connecting them. If a polynomial representation is preferred, we can proceed as described next.

3.3.1.2 Deriving the characteristic polynomial

By expanding equation (3.14), we get

$$s_{5,7} = \Gamma_1 + \Gamma_2\, A_{3,2,4} \tag{3.15}$$

where Γ_1 and Γ_2 are polynomials in $s_{2,3}$ whose coefficients are algebraic functions of the known squared distances $s_{3,4}$, $s_{3,5}$, $s_{4,5}$, $s_{4,7}$, $s_{2,7}$, and $s_{2,4}$. On the other hand, by expanding equation (3.13), we obtain

$$\begin{aligned} s_{6,8} = \frac{1}{s_{2,3}\, s_{5,7}} \big(&\Upsilon_1 + \Upsilon_2\, A_{3,2,1} + \Upsilon_3\, A_{3,2,4} + \Upsilon_4\, A_{3,2,1}\, A_{3,2,4} \\ &+ (\Upsilon_5 + \Upsilon_6\, A_{3,2,1} + \Upsilon_7\, A_{3,2,4} + \Upsilon_8\, A_{3,2,1}\, A_{3,2,4})\, A_{5,7,9}\big), \end{aligned} \tag{3.16}$$

that is,

$$\begin{aligned} &- s_{6,8}\, s_{2,3}\, s_{5,7} + \Upsilon_1 + \Upsilon_2\, A_{3,2,1} + \Upsilon_3\, A_{3,2,4} + \Upsilon_4\, A_{3,2,1}\, A_{3,2,4} \\ &+ (\Upsilon_5 + \Upsilon_6\, A_{3,2,1} + \Upsilon_7\, A_{3,2,4} + \Upsilon_8\, A_{3,2,1}\, A_{3,2,4})\, A_{5,7,9} = 0 \end{aligned} \tag{3.17}$$

where Υ_i, $i = 1, \ldots, 8$, are polynomials in $s_{2,3}$ and $s_{5,7}$ whose coefficients are algebraic functions of known distances.

Now, by properly squaring equation (3.17), that is, by clearing the square root related to $A_{5,7,9}$, we obtain a polynomial equation in $s_{5,7}$ whose coefficients are radical expressions in $s_{2,3}$. Therefore, by replacing (3.15) into this polynomial equation, we get

$$\Phi_1 + \Phi_2\, A_{3,2,1} + \Phi_3\, A_{3,2,4} + \Phi_4\, A_{3,2,1}\, A_{3,2,4} = 0 \tag{3.18}$$

where Φ_1, Φ_2, Φ_3 and Φ_4 are polynomials in $s_{2,3}$ of degree 6, 5, 5, and 4, respectively. Finally, the square roots in (3.18) can be eliminated by properly twice squaring it, using the procedure explained in §3.2.1. This operation yields

$$\begin{aligned}&-\Phi_4^4 A_{3,2,1}^4 A_{3,2,4}^4 + 2\Phi_4^2\Phi_2^2 A_{3,2,1}^4 A_{3,2,4}^2 + 2\Phi_4^2\Phi_3^2 A_{3,2,1}^2 A_{3,2,4}^4 - \Phi_2^4 A_{3,2,1}^4 - \Phi_3^4 A_{3,2,4}^4\\&-\Phi_1^4 + \left(2\Phi_2^2\Phi_3^2 - 8\Phi_2\Phi_3\Phi_4\Phi_1 + 2\Phi_4^2\Phi_1^2\right) A_{3,2,1}^2 A_{3,2,4}^2 + 2\Phi_1^2\Phi_2^2 A_{3,2,1}^2 + 2\Phi_1^2\Phi_3^2 A_{3,2,4}^2 = 0.\end{aligned} \tag{3.19}$$

which, when fully expanded, leads to

$$s_{2,3}^4\, s_{5,7}^2\, \mathcal{P}_{7B1} = 0 \tag{3.20}$$

where $\mathcal{P}_{7B1}$ is a 14th-degree polynomial in $s_{2,3}$. The extraneous roots at $s_{2,3} = 0$ and $s_{5,7} = 0$ were introduced when clearing denominators to obtain equation (3.17), so they can be dropped.

3.3.1.3 Example

According to the notation used in Fig. 3.5, let us suppose that $s_{1,2} = 101$, $s_{1,3} = 17$, $s_{1,6} = 34$, $s_{2,4} = 25$, $s_{2,7} = 36$, $s_{3,4} = 37$, $s_{3,5} = 25$, $s_{3,6} = 17$, $s_{4,5} = 20$, $s_{4,7} = 13$, $s_{5,8} = 25$, $s_{5,9} = 20$, $s_{6,8} = 61$, $s_{7,9} = 45$, and $s_{8,9} = 25$. Substituting these values in (3.18), we obtain

$$\Phi_1 + \Phi_2\, A_{3,2,1} + \Phi_3\, A_{3,2,4} + \Phi_4\, A_{3,2,1}\, A_{3,2,4} = 0 \tag{3.21}$$

where

$$\begin{aligned}\Phi_1 &= 3.6378\,10^5\, s_{2,3}^6 - 8.2798\,10^7\, s_{2,3}^5 - 6.2189\,10^8\, s_{2,3}^4 + 1.4591\,10^{12}\, s_{2,3}^3\\&\quad - 1.2227\,10^{14}\, s_{2,3}^2 + 2.8811\,10^{15}\, s_{2,3} - 5.5415\,10^{15}\\\Phi_2 &= -9.9850\,10^5\, s_{2,3}^5 + 3.1519\,10^8\, s_{2,3}^4 - 3.2834\,10^{10}\, s_{2,3}^3 + 1.2528\,10^{12}\, s_{2,3}^2\\&\quad - 1.5430\,10^{13}\, s_{2,3} + 6.0248\,10^{13}\\\Phi_3 &= 9.9850\,10^5\, s_{2,3}^5 - 4.1383\,10^8\, s_{2,3}^4 + 6.1116\,10^{10}\, s_{2,3}^3 - 3.7134\,10^{12}\, s_{2,3}^2\\&\quad + 6.6516\,10^{13}\, s_{2,3} + 4.2174\,10^{14}\\\Phi_4 &= 1.4551\,10^6\, s_{2,3}^4 - 3.5852\,10^8\, s_{2,3}^3 + 3.4064\,10^{10}\, s_{2,3}^2 - 1.5972\,10^{12}\, s_{2,3}\\&\quad + 2.1990\,10^{13}\end{aligned}$$

Equation (3.21) is a scalar equation in $s_{2,3}$ which can be numerically solved for the four possible combinations of signs of the two involved squared roots. Alternatively, proceeding as explained above, we obtain the characteristic polynomial

$$\begin{aligned}&119.5503\,10^{12}\, s_{2,3}^{14} - 132.8081\,10^{15}\, s_{2,3}^{13} + 67.7507\,10^{18}\, s_{2,3}^{12} - 20.9729\,10^{21}\, s_{2,3}^{11}\\&+ 4.3875\,10^{24}\, s_{2,3}^{10} - 654.0472\,10^{24}\, s_{2,3}^{9} + 71.4151\,10^{27}\, s_{2,3}^{8} - 5.7830\,10^{30}\, s_{2,3}^{7}\\&+ 347.7941\,10^{30}\, s_{2,3}^{6} - 15.4050\,10^{33}\, s_{2,3}^{5} + 492.8930\,10^{33}\, s_{2,3}^{4} - 11.0051\,10^{36}\, s_{2,3}^{3}\\&+ 161.4709\,10^{36}\, s_{2,3}^{2} - 1.3884\,10^{39}\, s_{2,3} + 5.2641\,10^{39}.\end{aligned}$$

The real roots of this polynomial are 39.8353, 41.6616, 42.6537, 78.9181, 81.8425, 106.0000, 121.9444, and 122.6125. The corresponding configurations for the case in which $P_3 = (0,0)^T$, $P_4 = (6,-1)^T$, and $P_5 = (4,3)^T$ appear in Fig. 3.6. The coefficients of the above polynomial have to be computed in exact rational arithmetic. Otherwise, numerical problems make impracticable the correct computation of its roots. Although these coefficients are given here in floating point arithmetic for saving space, they could be of interest for comparison and reproducibility purposes. This observation applies to the rest of closed-form examples presented in this thesis.

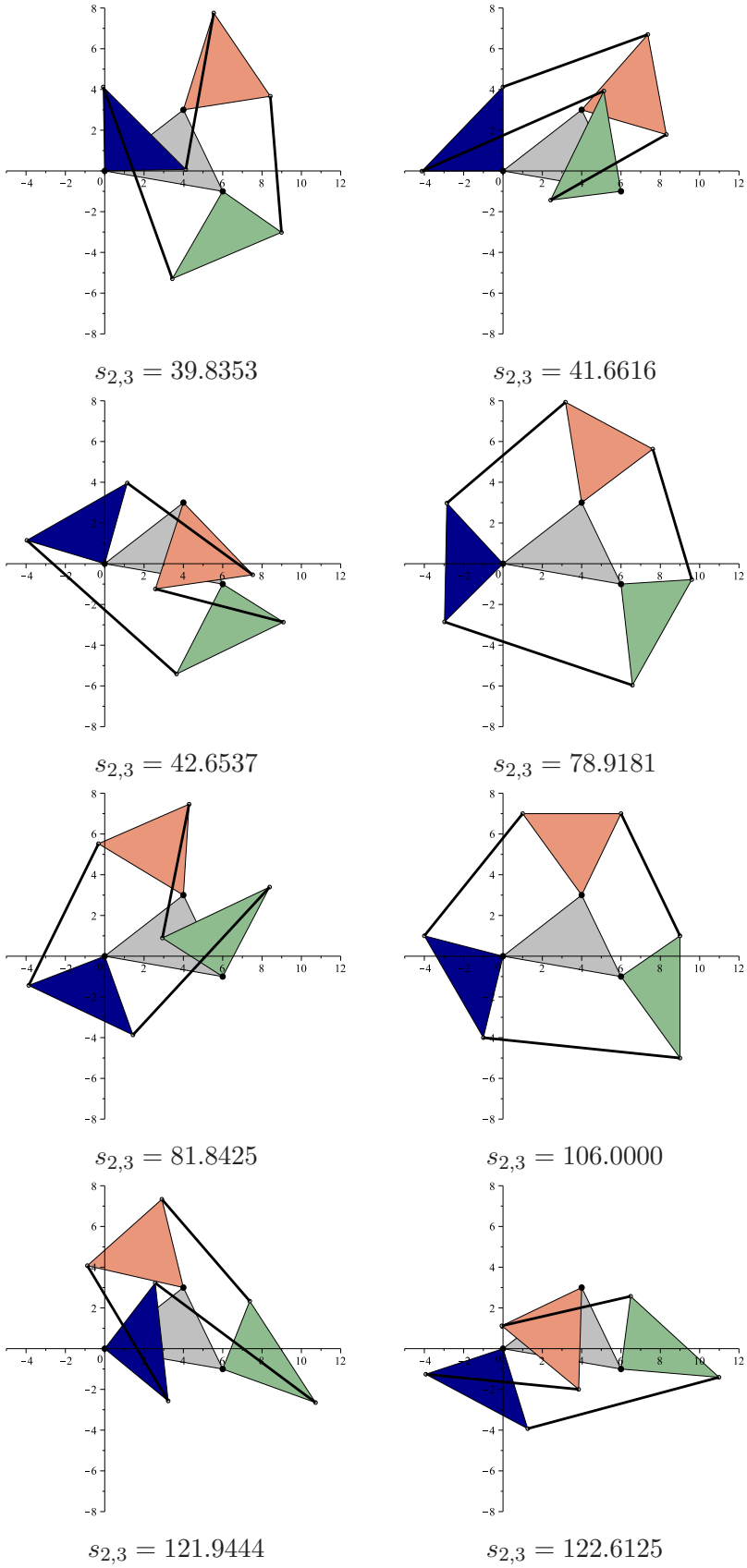

Figure 3.6. The configurations of the analyzed $7/B_1$ Baranov truss.

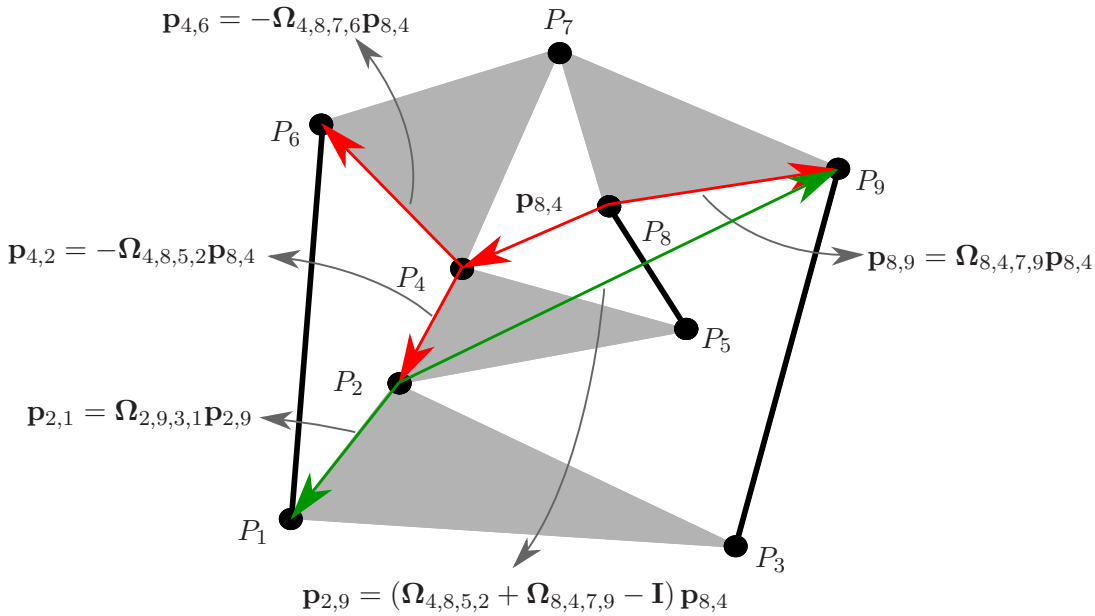

Figure 3.7. The $7/B_2$ Baranov truss and its associated notation.

3.3.2 Position analysis of the $7/B_2$ Baranov truss

The $7/B_2$ Baranov truss is a three-loop structure of four ternary links and three binary links with up to sixteen assembly modes. The position analysis of this truss was solved for the first time in closed form by Carlo Innocenti in [85] using an ad-hoc elimination procedure applied to trigonometric-based vector equations. The problem was also solved in closed form using Sylvester resultant by Almadi *et. al.* [7] and Dhingra *et. al.* [41]. A solution based on a combination of Gröbner basis and Sylvester resultant was presented in [42]. Wampler in [191] presented a solution using loop equations in the complex plane and the Dixon resultant. Numerical approaches have been reported, at least, by Hang *et. al.* [67] and Shen *et. al.* [172].

In the $7/B_2$ Baranov truss depicted in Fig. 3.7, the revolute pair centers of the three ternary links define the triangles $\triangle P_2P_4P_5$, $\triangle P_1P_2P_3$, $\triangle P_4P_6P_7$, and $\triangle P_8P_7P_9$. The kinematic equations of this truss can be reduced to compute $s_{1,6}$ as a function of $s_{4,8}$ when bilateration techniques are applied. That is, $s_{4,8}$ is used as a parameter in terms of which the location of all other links of the truss can be expressed. Since one parameter is needed, the truss is said to have coupling degree 1, a value in accordance with the degree reported in [223].

3.3.2.1 Computing $s_{1,6}$ as a function of $s_{4,8}$

Considering the two strips of triangles $\{\triangle P_4P_6P_7, \triangle P_8P_4P_7, \triangle P_4P_8P_5, \triangle P_4P_5P_2, \triangle P_7P_9P_8\}$ and $\{\triangle P_2P_9P_3, \triangle P_2P_3P_1\}$ in Fig. 3.7, we have

$$\mathbf{p}_{4,2} = \mathbf{Z}_{4,5,2}\mathbf{p}_{4,5} = -\mathbf{Z}_{4,5,2}\mathbf{Z}_{4,8,5}\mathbf{p}_{8,4} = -\mathbf{\Omega}_{4,8,5,2}\mathbf{p}_{8,4} \tag{3.22}$$

$$\mathbf{p}_{4,6} = \mathbf{Z}_{4,7,6}\mathbf{p}_{4,7} = -\mathbf{Z}_{4,7,6}\mathbf{Z}_{4,8,7}\mathbf{p}_{8,4} = -\mathbf{\Omega}_{4,8,7,6}\mathbf{p}_{8,4} \tag{3.23}$$

$$\mathbf{p}_{8,9} = \mathbf{Z}_{8,7,9}\mathbf{p}_{8,7} = \mathbf{Z}_{8,7,9}\mathbf{Z}_{8,4,7}\mathbf{p}_{8,4} = \mathbf{\Omega}_{8,4,7,9}\mathbf{p}_{8,4} \tag{3.24}$$

$$\mathbf{p}_{2,1} = \mathbf{Z}_{2,3,1}\mathbf{p}_{2,3} = \mathbf{Z}_{2,3,1}\mathbf{Z}_{2,9,3}\mathbf{p}_{2,9} = \mathbf{\Omega}_{2,9,3,1}\mathbf{p}_{2,9}. \tag{3.25}$$

Since

$$\mathbf{p}_{1,6} = -\mathbf{p}_{2,1} - \mathbf{p}_{4,2} + \mathbf{p}_{4,6} \tag{3.26}$$

and

$$\mathbf{p}_{2,9} = -\mathbf{p}_{4,2} - \mathbf{p}_{8,4} + \mathbf{p}_{8,9} \tag{3.27}$$

then

$$\begin{aligned}\mathbf{p}_{1,6} &= -\mathbf{\Omega}_{2,9,3,1}\mathbf{p}_{2,9} + \mathbf{\Omega}_{4,8,5,2}\mathbf{p}_{8,4} - \mathbf{\Omega}_{4,8,7,6}\mathbf{p}_{8,4} \\ &= \left(-\mathbf{\Omega}_{2,9,3,1}\left(\mathbf{\Omega}_{4,8,5,2} + \mathbf{\Omega}_{8,4,7,9} - \mathbf{I}\right) + \mathbf{\Omega}_{4,8,5,2} - \mathbf{\Omega}_{4,8,7,6}\right)\mathbf{p}_{8,4}.\end{aligned}$$

Therefore,

$$s_{1,6} = \det\left(-\mathbf{\Omega}_{2,9,3,1}\left(\mathbf{\Omega}_{4,8,5,2} + \mathbf{\Omega}_{8,4,7,9} - \mathbf{I}\right) + \mathbf{\Omega}_{4,8,5,2} - \mathbf{\Omega}_{4,8,7,6}\right) s_{4,8}. \tag{3.28}$$

The right hand side of the above equation is a function of the unknown squared distances $s_{2,9}$ and $s_{4,8}$. Since, from equation (3.27),

$$s_{2,9} = \det\left(\mathbf{\Omega}_{4,8,5,2} + \mathbf{\Omega}_{8,4,7,9} - \mathbf{I}\right) s_{4,8}, \tag{3.29}$$

then the substitution of (3.29) in (3.28) yields a scalar equation in $s_{4,8}$ whose roots in the range in which the signed areas of the triangles $\triangle P_4P_8P_5$ and $\triangle P_8P_4P_7$ are real, that is, the range

$$\left[\max\{(d_{5,8} - d_{4,5})^2, (d_{4,7} - d_{7,8})^2\}, \min\{(d_{5,8} + d_{4,5})^2, (d_{4,7} + d_{7,8})^2\}\right]$$

determine the assembly modes of the analyzed linkage. These roots can be obtained, as in the Baranov trusses previously studied, for the eight possible combinations of signs for the signed areas of the triangles $\triangle P_4P_8P_5$, $\triangle P_8P_4P_7$, and $\triangle P_2P_9P_3$. For each real root, taking as reference the link associated to triangle $\triangle P_2P_4P_5$, we can determine the Cartesian position of the six revolute pair centers P_1, P_3, P_6, P_7, P_8, and P_9 using equations (3.22)-(3.25) and the equation $\mathbf{p}_{4,8} = \mathbf{Z}_{4,5,8}\mathbf{p}_{4,5}$. This process leads up to eight combinations of locations for P_1 and P_6, and at least one of them must satisfy the distance imposed by the binary link connecting them. If a polynomial representation is preferred, we can proceed as described next.

3.3.2.2 Deriving the characteristic polynomial

By expanding equation (3.29), we get

$$s_{2,9} = \frac{1}{s_{4,8}}\left(\Gamma_1 + \Gamma_2\, A_{4,8,5} + \Gamma_3\, A_{8,4,7} + \Gamma_4\, A_{4,8,5}\, A_{8,4,7}\right) \tag{3.30}$$

where Γ_i, $i = 1, \ldots, 4$, are polynomials in $s_{4,8}$ whose coefficients are algebraic functions of the known squared distances $s_{2,4}$, $s_{2,5}$, $s_{4,5}$, $s_{4,7}$, $s_{5,8}$, $s_{7,8}$, $s_{7,9}$, and $s_{8,9}$. On the other hand, by expanding equation (3.28), we obtain

$$\begin{aligned}s_{4,8} = \frac{1}{s_{1,6}\, s_{2,9}}\big(&\Upsilon_1 + \Upsilon_2\, A_{4,8,5} + \Upsilon_3\, A_{8,4,7} + \Upsilon_4\, A_{4,8,5}\, A_{8,4,7} \\ &+ \left(\Upsilon_5 + \Upsilon_6\, A_{4,8,5} + \Upsilon_7\, A_{8,4,7} + \Upsilon_8\, A_{4,8,5}\, A_{8,4,7}\right) A_{2,9,3}\big),\end{aligned} \tag{3.31}$$

that is,

$$\begin{aligned}&\Upsilon_1 + \Upsilon_2\, A_{2,9,3} + \Upsilon_3\, A_{4,8,5} + \Upsilon_4\, A_{8,4,7} + \Upsilon_5\, A_{2,9,3}\, A_{4,8,5} \\ &+ \Upsilon_6\, A_{2,9,3}\, A_{8,4,7} + \Upsilon_7\, A_{4,8,5}\, A_{8,4,7} + \Upsilon_8\, A_{2,9,3}\, A_{4,8,5}\, A_{8,4,7} - s_{1,6}s_{2,9}s_{4,8} = 0\end{aligned} \tag{3.32}$$

where Υ_i, $i = 1, \ldots, 4$, are polynomials in the unknown distances $s_{2,9}$ and $s_{4,8}$ whose coefficients are algebraic functions of known squared distances.

Now, by properly squaring equation (3.32), that is, by clearing the square root related to $A_{2,9,3}$, we obtain a polynomial equation in $s_{2,9}$ whose coefficients are radical expressions in $s_{4,8}$. Therefore, by replacing (3.30) in this polynomial equation, we get

$$\Phi_1 + \Phi_2\, A_{4,8,5} + \Phi_3\, A_{8,4,7} + \Phi_4\, A_{4,8,5}\, A_{8,4,7} = 0, \tag{3.33}$$

where Φ_1, Φ_2, Φ_3, and Φ_4 are polynomials in $s_{4,8}$ of degree 8, 7, 7, and 6, respectively. Finally, to obtain a polynomial equation, the square roots in (3.33) can be eliminated by properly twice squaring it. When the result is fully expanded, we obtain

$$s_{4,8}^2\, s_{2,9}\, \mathcal{P}_{7B2} = 0, \tag{3.34}$$

where $\mathcal{P}_{7B2}$ is a 16th-degree polynomial in $s_{4,8}$. The extraneous roots at $s_{2,9} = 0$ and $s_{4,8} = 0$ were introduced when clearing denominators to obtain equation (3.32), so they can be dropped.

3.3.2.3 Example

According to the notation used in Fig. 3.7, let us suppose that $s_{1,2} = 25$, $s_{1,3} = 100$, $s_{1,6} = 97$, $s_{2,3} = 45$, $s_{2,4} = 13$, $s_{2,5} = 36$, $s_{3,9} = 97$, $s_{4,5} = 25$, $s_{4,6} = 13$, $s_{4,7} = 20$, $s_{5,8} = 16$, $s_{6,7} = 17$, $s_{7,8} = 13$, $s_{7,9} = 37$, and $s_{8,9} = 20$. Then, proceeding as explained above, we obtain the characteristic polynomial

$$\begin{aligned}
&18.8825\,10^{24}\, s_{4,8}^{16} - 5.9735\,10^{27}\, s_{4,8}^{15} + 818.5722\,10^{27}\, s_{4,8}^{14} - 64.1837\,10^{30}\, s_{4,8}^{13} \\
&+ 3.2137\,10^{33}\, s_{4,8}^{12} - 108.7285\,10^{33}\, s_{4,8}^{11} + 2.5531\,10^{36}\, s_{4,8}^{10} - 41.5239\,10^{36}\, s_{4,8}^{9} \\
&+ 452.6824\,10^{36}\, s_{4,8}^{8} - 3.1196\,10^{39}\, s_{4,8}^{7} + 12.6154\,10^{39}\, s_{4,8}^{6} - 28.2936\,10^{39}\, s_{4,8}^{5} \\
&+ 38.9353\,10^{39}\, s_{4,8}^{4} - 36.1341\,10^{39}\, s_{4,8}^{3} + 25.5007\,10^{39}\, s_{4,8}^{2} - 15.1151\,10^{39}\, s_{4,8} \\
&+ 5.2854\,10^{39}.
\end{aligned}$$

The real roots of this polynomial are 1.1161, 1.2002, 7.3517, 10.4180, 17.0000, 27.5995, 52.9281, 53.7863, 56.0905 and 61.5796. The corresponding configurations for the case in which $P_2 = (0,0)^T$, $P_4 = (2,3)^T$, and $P_5 = (6,0)^T$ appear in Fig. 3.8.

3.3.3 Position analysis of the $7/B_3$ Baranov truss

The $7/B_3$ Baranov truss is a three-loop structure of one quaternary link, two ternary links and four binary links with up to eighteen assembly modes. The position analysis of this truss was solved for the first time in closed form by Carlo Innocenti using a combination of Cramer's rule and Sylvester resultant applied to trigonometric-based vector equations [84, 86]. The problem has been also solved in closed form by, at least, Han *et. al.* [61] (complex-number-based vector loop equations with Sylvester resultant), Dhingra *et. al.* [41] (trigonometric-based vector loop equations with Sylvester resultant), Wang *et. al.* [196] (complex-number-based vector loop equations with Wu method), and Ni *et. al.* [132] (conformal-geometric-algebra-based vector equations with Dixon resultant). A numerical approach have been reported by Hang *et. al.* [67].

In the $7/B_3$ Baranov truss depicted in Fig. 3.9, the revolute pair centers of the quaternary link and the two ternary links define the triangles $\triangle P_1P_6P_7$, $\triangle P_1P_2P_6$, $\triangle P_3P_5P_4$, and $\triangle P_8P_5P_9$. Using bilateration techniques, the kinematic equations of this truss can be reduced to compute $s_{7,9}$ as a function of $s_{1,4}$. Since $s_{1,4}$ is used as a parameter in terms of which the location of all other links of the truss can be expressed, the truss is said to have coupling degree 1, as already observed by [223].

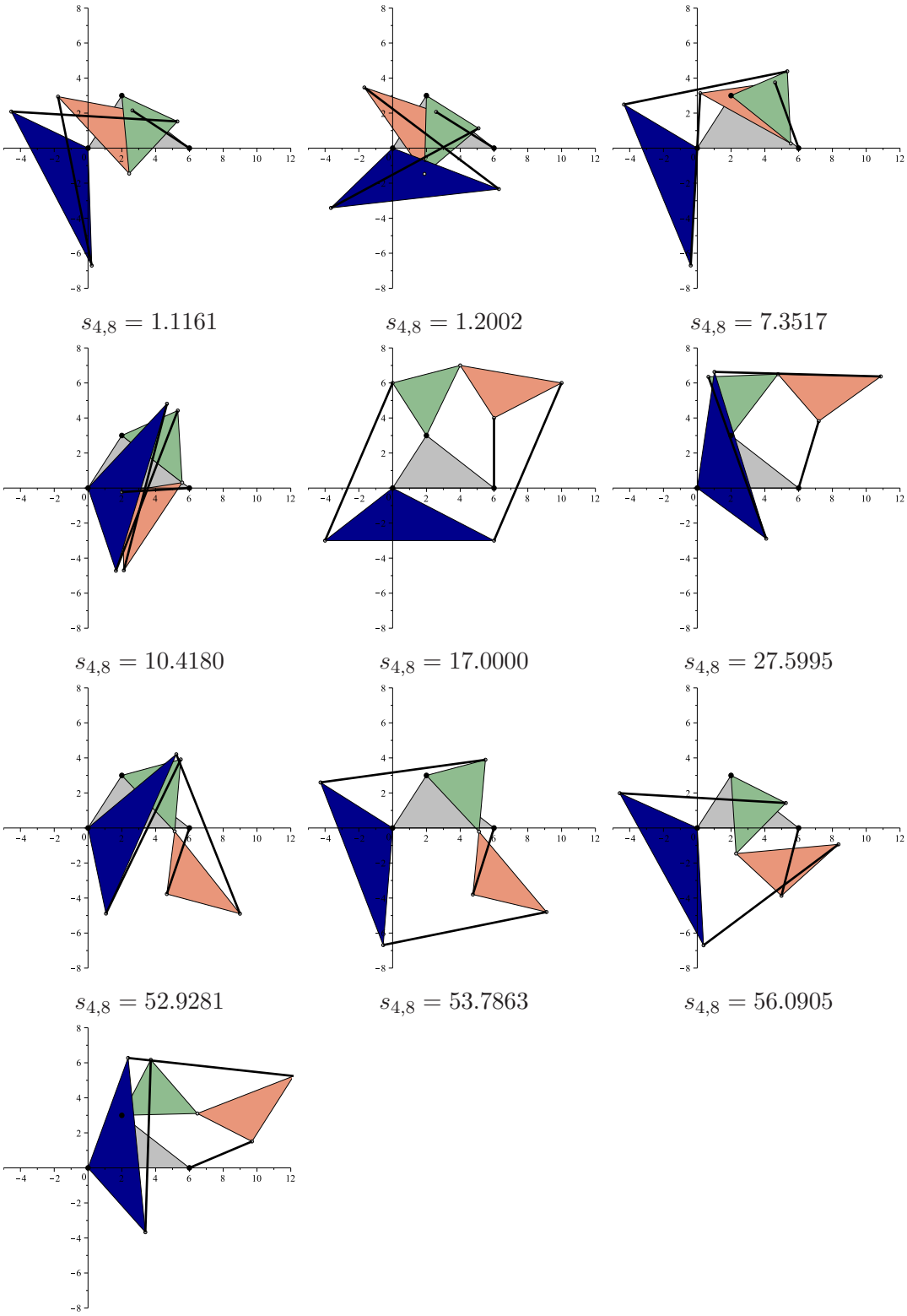

Figure 3.8. The configurations of the analyzed $7/B_2$ Baranov truss.

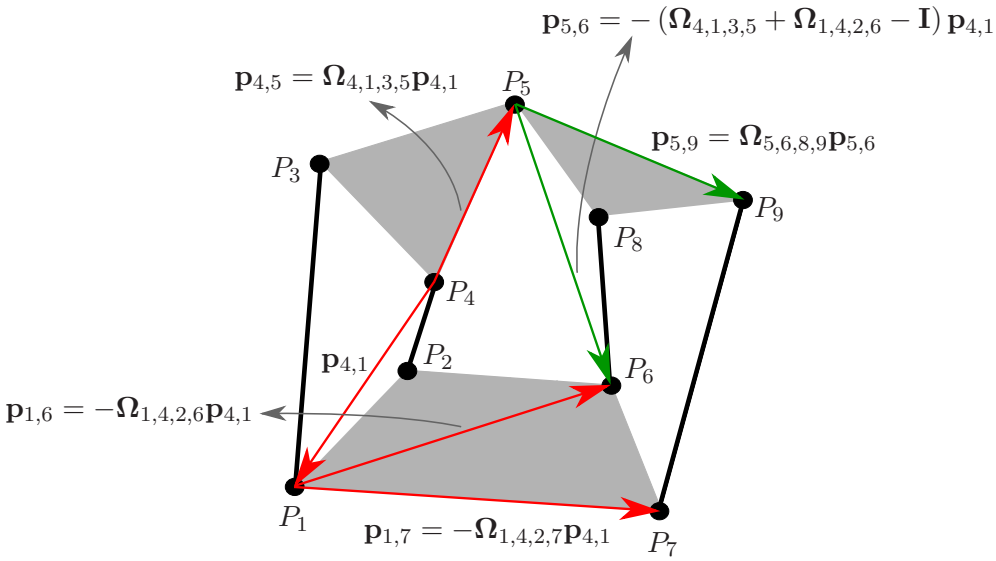

Figure 3.9. The $7/B_3$ Baranov truss and its associated notation.

3.3.3.1 Computing $s_{7,9}$ as a function of $s_{1,4}$

Considering the two strips of triangles $\{\triangle P_1P_6P_7, \triangle P_1P_2P_6, \triangle P_1P_4P_2, \triangle P_4P_1P_3, \triangle P_3P_5P_4\}$ and $\{\triangle P_5P_8P_6, \triangle P_8P_5P_9\}$ in Fig. 3.9, we have

$$\mathbf{p}_{1,6} = \mathbf{Z}_{1,2,6}\mathbf{p}_{1,2} = -\mathbf{Z}_{1,2,6}\mathbf{Z}_{1,4,2}\mathbf{p}_{4,1} = -\mathbf{\Omega}_{1,4,2,6}\mathbf{p}_{4,1}, \tag{3.35}$$
$$\mathbf{p}_{1,7} = \mathbf{Z}_{1,2,7}\mathbf{p}_{1,2} = -\mathbf{Z}_{1,2,7}\mathbf{Z}_{1,4,2}\mathbf{p}_{4,1} = -\mathbf{\Omega}_{1,4,2,7}\mathbf{p}_{4,1}, \tag{3.36}$$
$$\mathbf{p}_{4,5} = \mathbf{Z}_{4,3,5}\mathbf{p}_{4,3} = \mathbf{Z}_{4,3,5}\mathbf{Z}_{4,1,3}\mathbf{p}_{4,1} = \mathbf{\Omega}_{4,1,3,5}\mathbf{p}_{4,1}, \tag{3.37}$$
$$\mathbf{p}_{5,8} = \mathbf{Z}_{5,6,8}\mathbf{p}_{5,6} = \mathbf{Z}_{5,8,9}\mathbf{Z}_{5,6,8}\mathbf{p}_{5,6} = \mathbf{\Omega}_{5,6,8,9}\mathbf{p}_{5,6}. \tag{3.38}$$

Since

$$\mathbf{p}_{7,9} = \mathbf{p}_{1,6} - \mathbf{p}_{1,7} - \mathbf{p}_{5,6} + \mathbf{p}_{5,9} \tag{3.39}$$

and

$$\mathbf{p}_{5,6} = -\mathbf{p}_{4,5} + \mathbf{p}_{4,1} + \mathbf{p}_{1,6}, \tag{3.40}$$

then

$$\begin{aligned}\mathbf{p}_{7,9} &= -\mathbf{\Omega}_{1,4,2,6}\mathbf{p}_{4,1} + \mathbf{\Omega}_{1,4,2,7}\mathbf{p}_{4,1} - \mathbf{p}_{5,6} + \mathbf{\Omega}_{5,6,8,9}\mathbf{p}_{5,6} \\ &= \left(-\mathbf{\Omega}_{1,4,2,6} + \mathbf{\Omega}_{1,4,2,7} - \left(\mathbf{\Omega}_{5,6,8,9} - \mathbf{I}\right)\left(\mathbf{\Omega}_{4,1,3,5} + \mathbf{\Omega}_{1,4,2,6} - \mathbf{I}\right)\right)\mathbf{p}_{4,1}.\end{aligned}$$

Therefore,

$$s_{7,9} = \det\left(-\mathbf{\Omega}_{1,4,2,6} + \mathbf{\Omega}_{1,4,2,7} - \left(\mathbf{\Omega}_{5,6,8,9} - \mathbf{I}\right)\left(\mathbf{\Omega}_{4,1,3,5} + \mathbf{\Omega}_{1,4,2,6} - \mathbf{I}\right)\right) s_{1,4}. \tag{3.41}$$

The right hand side of the above equation is a function of the unknown squared distances $s_{1,4}$ and $s_{5,6}$. Since, from equation (3.40),

$$s_{5,6} = \det\left(\mathbf{\Omega}_{4,1,3,5} + \mathbf{\Omega}_{1,4,2,6} - \mathbf{I}\right) s_{1,4}, \tag{3.42}$$

then the substitution of (3.42) in (3.41) yields a scalar equation in $s_{1,4}$ whose roots in the range in which the signed areas of the triangles $\triangle P_1P_4P_2$ and $\triangle P_4P_1P_3$ are real, that is, the range

$$\left[\max\{(d_{2,4} - d_{1,2})^2, (d_{1,3} - d_{3,4})^2\}, \min\{(d_{2,4} + d_{1,2})^2, (d_{1,3} + d_{3,4})^2\}\right]$$

determine the assembly modes of the analyzed linkage. Similarly to previous sections, these roots can be obtained for the eight possible combinations of signs for the signed areas of the triangles $\triangle P_1P_4P_2$, $\triangle P_4P_1P_3$, and $\triangle P_5P_8P_6$ using a numerical procedure such as an interval Newton method. Alternatively, a polynomial representation is obtained as follows.

3.3.3.2 Deriving the characteristic polynomial

Following the procedure described in Section 3.3.2.2, from equations (3.41) and (3.42), we obtain

$$\Phi_1 + \Phi_2 A_{1,4,2} + \Phi_3 A_{4,1,3} + \Phi_4 A_{1,4,2} A_{4,1,3} = 0 \tag{3.43}$$

where Φ_1, Φ_2, Φ_3, and Φ_4 are polynomials in $s_{1,4}$ of degree 8, 7, 7, and 6, respectively. Finally, by properly twice squaring the above equation, we get

$$s_{1,4}^2\, s_{5,6}\, \mathcal{P}_{7B3} = 0 \tag{3.44}$$

where $\mathcal{P}_{7B3}$ is a 18th-degree polynomial in $s_{1,4}$. The extraneous roots at $s_{1,4} = 0$ and $s_{5,6} = 0$ were introduced when clearing denominators in this polynomial derivation, so they can be dropped. For each real root of $\mathcal{P}_{7B3}$, taking as reference the link associated to quadrilateral $\square P_1P_2P_6P_7$, we can determine the Cartesian position of the five revolute pair centers P_3, P_4, P_5, P_8, and P_9 using equations (3.35)-(3.38) and the equation $\mathbf{p}_{1,4} = \mathbf{Z}_{1,2,4}\mathbf{p}_{1,2}$. This process leads to up eight combinations of locations for P_7 and P_9, and at least one of them must satisfy the distance imposed by the binary link connecting them.

3.3.3.3 Example

According to the notation used in Fig. 3.9, let us suppose that $s_{1,2} = 20$, $s_{1,3} = 40$, $s_{1,6} = 65$, $s_{1,7} = 144$, $s_{2,4} = 13$, $s_{2,6} = 17$, $s_{2,7} = 68$, $s_{3,4} = 17$, $s_{3,5} = 40$, $s_{4,5} = 13$, $s_{5,8} = 18$, $s_{5,9} = 29$, $s_{6,7} = 17$, $s_{6,8} = 25$, $s_{7,9} = 37$, and $s_{8,9} = 5$. Then, proceeding as explained above, we obtain the characteristic polynomial

$$\begin{aligned}
&- 702.0669\,10^{12}\, s_{1,4}^{18} + 440.9551\,10^{15}\, s_{1,4}^{17} - 126.5260\,10^{18}\, s_{1,4}^{16} + 21.9306\,10^{21}\, s_{1,4}^{15} \\
&- 2.5592\,10^{24}\, s_{1,4}^{14} + 212.2835\,10^{24}\, s_{1,4}^{13} - 12.8945\,10^{27}\, s_{1,4}^{12} + 583.5044\,10^{27}\, s_{1,4}^{11} \\
&- 19.9010\,10^{30}\, s_{1,4}^{10} + 517.8331\,10^{30}\, s_{1,4}^{9} - 10.4725\,10^{33}\, s_{1,4}^{8} + 168.7340\,10^{33}\, s_{1,4}^{7} \\
&- 2.1961\,10^{36}\, s_{1,4}^{6} + 22.5420\,10^{36}\, s_{1,4}^{5} - 171.4717\,10^{36}\, s_{1,4}^{4} + 898.7415\,10^{36}\, s_{1,4}^{3} \\
&- 3.0279\,10^{39}\, s_{1,4}^{2} + 5.9942\,10^{39}\, s_{1,4} - 5.5218\,10^{39}.
\end{aligned}$$

The real roots of this polynomial are 5.2357, 6.7320, 9.8004, 16.9536, 39.1049, 45.3566, 48.4498, and 61.0000. The corresponding configurations for the case in which $P_1 = (0,0)^T$, $P_2 = (4,2)^T$, $P_6 = (8,1)^T$, and $P_7 = (12,0)^T$ appear in Fig. 3.10.

3.4 Position analysis of four-loop Baranov trusses

3.4.1 Solving a truss of coupling degree 2: The $9/B_{28}$ Baranov truss

The $9/B_{28}$ Baranov truss is one of the three cataloged Baranov trusses that cannot be represented as a planar graph (the other two are $9/B_{23}$ and $9/B_{24}$) [173, 223]. It was characterized for the first time by Baranov in 1952 [11] and Wang *et. al.* developed a procedure using complex-number-based vector loop equations and Dixon resultant to

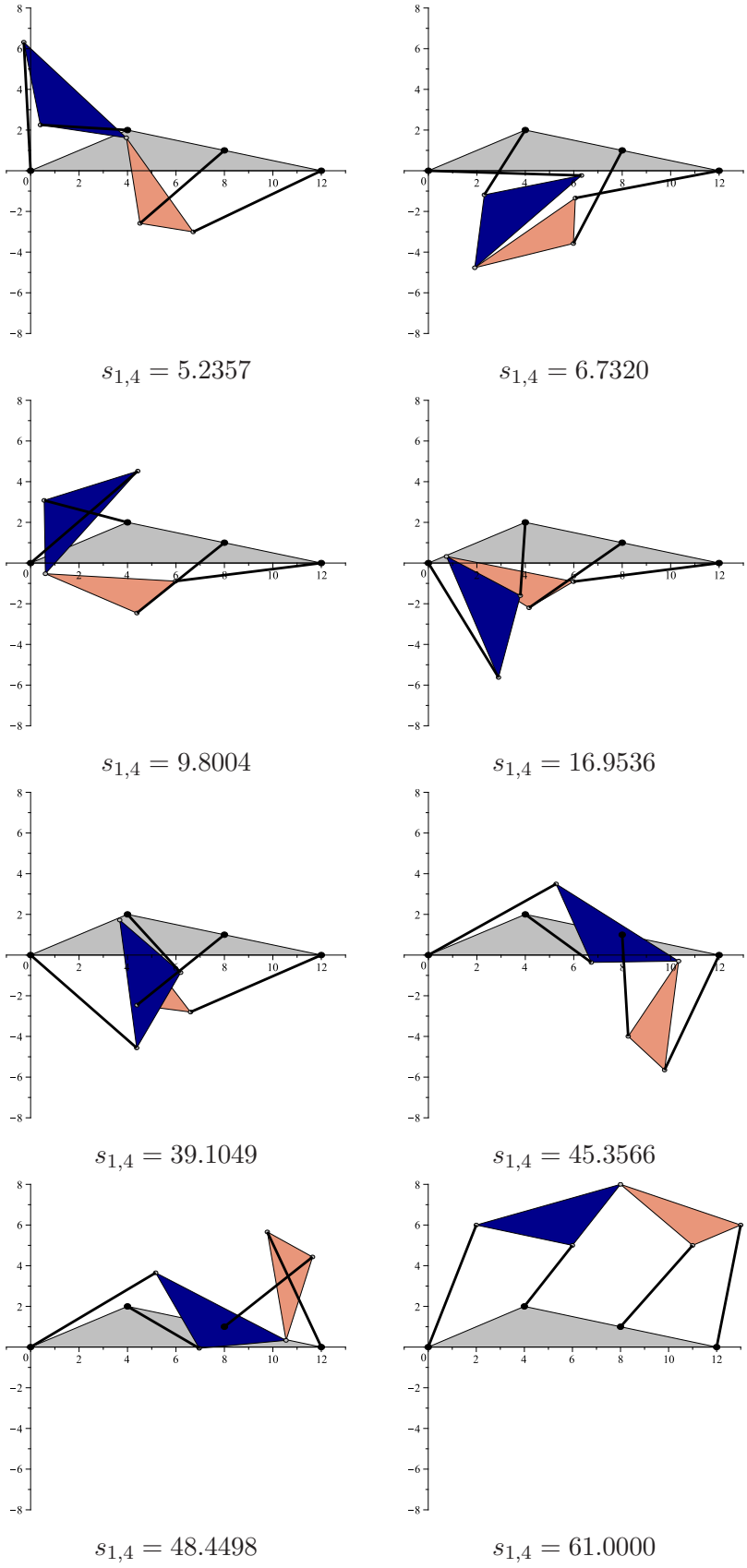

Figure 3.10. The configurations of the analyzed $7/B_3$ Baranov truss.

solve its position analysis in closed form [198]. They obtained a univariate polynomial of degree 64 but 6 extraneous roots were found, leading to the conclusion it can have up to 58 assembly modes —the largest number of assembly modes for a cataloged Baranov truss—, a result in agreement with that obtained by Hang *et. al.* using homotopy continuation [67].

In the $9/B_{28}$ Baranov truss depicted in Fig. 3.11(a), the revolute pair centers of the six ternary links define the triangles $\triangle P_1P_8P_3$, $\triangle P_3P_6P_4$, $\triangle P_4P_7P_5$, $\triangle P_2P_5P_{11}$, $\triangle P_8P_{12}P_9$, and $\triangle P_{10}P_{12}P_{11}$. Next, it is shown how the kinematic equations of this truss can be reduced to compute $s_{6,10}$ and $s_{7,9}$ as a function of $s_{1,4}$ and $s_{2,4}$. That is, $s_{1,4}$ and $s_{2,4}$ are used as parameters in terms of which the location of all other links of the truss can be expressed. Since two parameters are needed, the truss is said to have coupling degree 2, as already observed by [223].

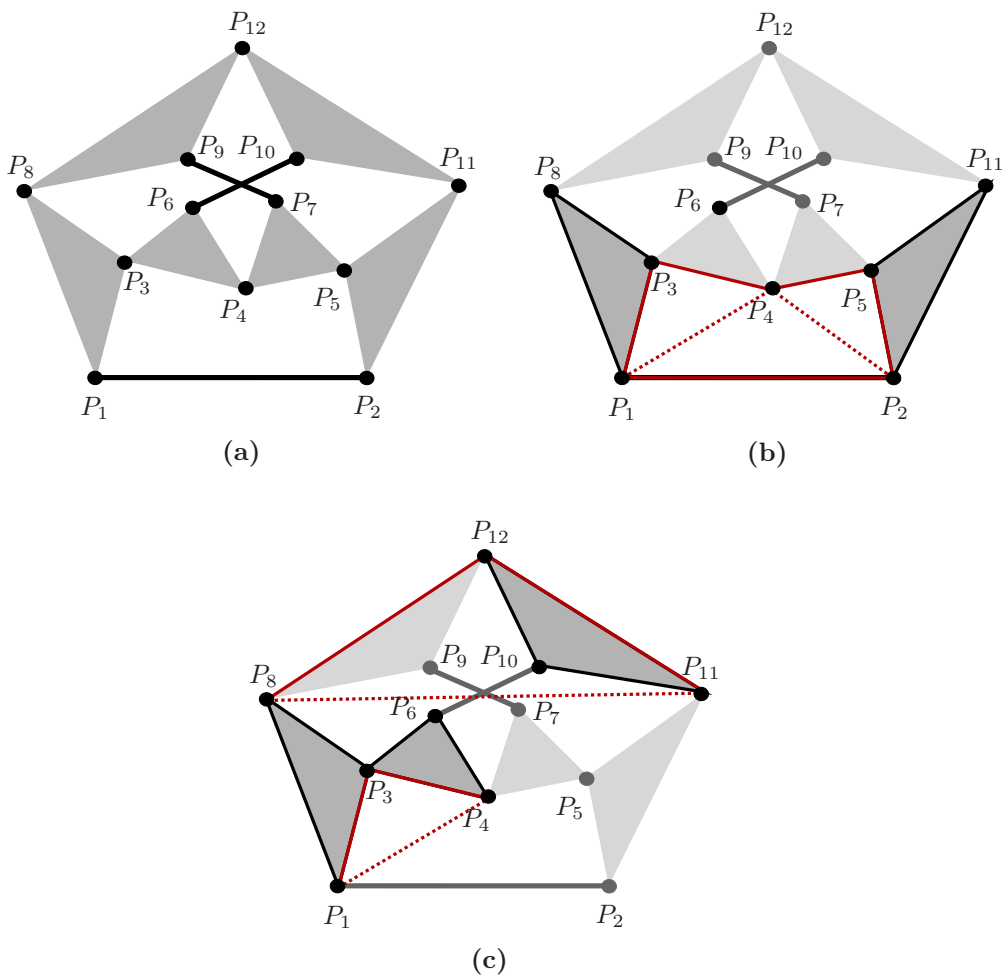

Figure 3.11. A $9/B_{28}$ Baranov truss **(a)**. The strip of triangles $\{\triangle P_1P_8P_3, \triangle P_1P_3P_4, \triangle P_1P_4P_2, \triangle P_4P_2P_5, \triangle P_2P_5P_{11}\}$ has been considered to compute $s_{8,11}$ as a function of $s_{1,4}$ and $s_{2,4}$ **(b)**. The strips of triangles $\{\triangle P_8P_{12}P_{11}, \triangle P_{10}P_{12}P_{11}\}$, $\{\triangle P_1P_8P_3, \triangle P_1P_3P_4\}$, and $\{\triangle P_3P_4P_6, \triangle P_1P_3P_4\}$ have also been considered to compute $s_{6,10}$ as a function of $s_{1,4}$ and $s_{2,4}$ **(c)**.

3.4.1.1 Computing $s_{6,10}$ as a function of $s_{1,4}$ and $s_{2,4}$

On the one hand, for the strip of triangles in Fig. 3.11(b), we have

$$\begin{aligned}\mathbf{p}_{8,11} &= -\mathbf{p}_{1,8} + \mathbf{p}_{1,4} - \mathbf{p}_{2,4} + \mathbf{p}_{2,11} \\ &= (-\mathbf{Z}_{1,3,8}\,\mathbf{Z}_{1,4,3} + \mathbf{I})\,\mathbf{p}_{1,4} + (\mathbf{Z}_{2,5,11}\,\mathbf{Z}_{2,4,5} - \mathbf{I})\,\mathbf{p}_{2,4} \\ &= (-\mathbf{Z}_{1,3,8}\,\mathbf{Z}_{1,4,3} + \mathbf{I} + (\mathbf{Z}_{2,5,11}\,\mathbf{Z}_{2,4,5} - \mathbf{I})\,\mathbf{Z}_{4,1,2})\;\mathbf{p}_{1,4}. \end{aligned} \tag{3.45}$$

Therefore,

$$s_{8,11} = f(s_{1,4}, s_{2,4}) = \det\Big(- \mathbf{Z}_{1,3,8}\,\mathbf{Z}_{1,4,3} + \mathbf{I} - \mathbf{Z}_{4,1,2} + \mathbf{Z}_{2,5,11}\mathbf{Z}_{2,4,5}\,\mathbf{Z}_{4,1,2}\Big) s_{1,4}. \tag{3.46}$$

On the other hand, from the three strips of triangles in Fig. 3.11(c),

$$\begin{aligned}\mathbf{p}_{6,10} &= -\,\mathbf{p}_{1,6} + \mathbf{p}_{1,8} + \mathbf{p}_{8,10} \\ &= (\mathbf{Z}_{4,3,6}\,\mathbf{Z}_{4,1,3} - \mathbf{I})\,\mathbf{p}_{1,4} + \mathbf{Z}_{1,3,8}\,\mathbf{Z}_{1,4,3}\,\mathbf{p}_{1,4} + (\mathbf{I} - \mathbf{Z}_{11,12,10}\,\mathbf{Z}_{11,8,12})\,\mathbf{p}_{8,11}. \end{aligned} \tag{3.47}$$

Then, the substitution of equation (3.45) in equation (3.47) yields

$$\begin{aligned}\mathbf{p}_{6,10} =& \big(- \mathbf{I} + \mathbf{Z}_{4,3,6}\,\mathbf{Z}_{4,1,3} + \mathbf{Z}_{1,3,8}\,\mathbf{Z}_{1,4,3} + \big(\mathbf{I} - \mathbf{Z}_{11,12,10}\,\mathbf{Z}_{11,8,12}\big)\big(- \mathbf{Z}_{1,3,8}\,\mathbf{Z}_{1,4,3} \\ &+ \mathbf{I} - \mathbf{Z}_{4,1,2} + \mathbf{Z}_{2,5,11}\mathbf{Z}_{2,4,5}\,\mathbf{Z}_{4,1,2}\big)\big)\,\mathbf{p}_{1,4}. \end{aligned} \tag{3.48}$$

Therefore,

$$\begin{aligned}s_{6,10} =& f(s_{1,4}, s_{2,4}, s_{8,11}) \\ =& \det\Big(- \mathbf{I} + \mathbf{Z}_{4,3,6}\,\mathbf{Z}_{4,1,3} + \mathbf{Z}_{1,3,8}\,\mathbf{Z}_{1,4,3} + \big(\mathbf{I} - \mathbf{Z}_{11,12,10}\,\mathbf{Z}_{11,8,12}\big)\big(- \mathbf{Z}_{1,3,8}\,\mathbf{Z}_{1,4,3} \\ &+ \mathbf{I} - \mathbf{Z}_{4,1,2} + \mathbf{Z}_{2,5,11}\mathbf{Z}_{2,4,5}\,\mathbf{Z}_{4,1,2}\big)\Big) s_{1,4}. \end{aligned} \tag{3.49}$$

Then, the substitution of equation (3.46) in equation (3.49) yields a scalar equation in two variables: $s_{1,4}$ and $s_{2,4}$.

3.4.1.2 Computing $s_{7,9}$ as a function of $s_{1,4}$ and $s_{2,4}$

The computation of $s_{7,9}$ as a function of $s_{2,4}$ and $s_{2,4}$ can be simplified by considering the symmetries of the analyzed truss. Indeed, by applying the permutation

$$\begin{bmatrix} 1 & 2 & 3 & 4 & 5 & 6 & 7 & 8 & 9 & 10 & 11 & 12 \\ 2 & 1 & 5 & 4 & 3 & 7 & 6 & 11 & 10 & 9 & 8 & 12 \end{bmatrix}$$

to equation (3.49), we conclude that

$$\begin{aligned}s_{7,9} =& f(s_{1,4}, s_{2,4}, s_{8,11}) \\ =& \det\Big(- \mathbf{I} + \mathbf{Z}_{4,5,7}\mathbf{Z}_{4,2,5} + \mathbf{Z}_{2,5,11}\mathbf{Z}_{2,4,5} + \big(\mathbf{I} - \mathbf{Z}_{8,12,9}\mathbf{Z}_{8,11,12}\big)\big(- \mathbf{Z}_{2,5,11}\mathbf{Z}_{2,4,5} \\ &+ \mathbf{I} - \mathbf{Z}_{4,2,1} + \mathbf{Z}_{1,3,8}\mathbf{Z}_{1,4,3}\mathbf{Z}_{4,2,1}\big)\Big) s_{2,4}. \end{aligned} \tag{3.50}$$

The expansion of the right hand side of equations (3.49) and (3.50), using equation (3.46) for substituting the unknown squared distance $s_{8,11}$, yields a system of two scalar equations in two variables: $s_{1,4}$ and $s_{2,4}$. Next, it is shown how to algebraically manipulate this system to obtain the characteristic polynomial of the $9/B_{28}$ Baranov truss.

3.4.1.3 Deriving the characteristic polynomial

The characteristic polynomial of the $9/B_{28}$ Baranov truss can be obtained by: (i) converting the scalar radical equations (3.49) and (3.50) in polynomials equations in $s_{1,4}$ and $s_{2,4}$, say $\mathcal{P}_1(s_{1,4}, s_{2,4}) = 0$ and $\mathcal{P}_2(s_{1,4}, s_{2,4}) = 0$, respectively, by clearing all the involved square roots; and (ii) eliminating $s_{2,4}$, or $s_{1,4}$, from the resulting polynomial system to get a single polynomial in one variable.

By expanding equation (3.46), we get

$$\begin{aligned} s_{8,11} =& \frac{1}{s_{1,4}\, s_{2,4}} \Big(\Lambda_1 + \Lambda_2\, A_{1,4,3} + \Lambda_3\, A_{1,4,2} + \Lambda_4\, A_{2,4,5} + \Lambda_5\, A_{1,4,3}\, A_{1,4,2} + \Lambda_6\, A_{1,4,3} \\ & A_{2,4,5} + \Lambda_7\, A_{1,4,2}\, A_{2,4,5} + \Lambda_8\, A_{1,4,3}\, A_{1,4,2}\, A_{2,4,5} \Big), \end{aligned} \tag{3.51}$$

where $A_{1,4,3}$, $A_{1,4,2}$, and $A_{2,4,5}$ are the unknown oriented areas of $\triangle P_1P_4P_3$, $\triangle P_1P_4P_2$, and $\triangle P_2P_4P_5$, respectively, and Λ_i, $i = 1, \ldots, 8$ are polynomials in $s_{1,4}$ and $s_{2,4}$.

Likewise, by expanding equation (3.49), we get

$$s_{6,10} = \frac{1}{s_{1,4}\, s_{2,4}\, s_{8,11}}\, \Psi, \tag{3.52}$$

that is,

$$\Psi - s_{6,10}\, s_{1,4}\, s_{2,4}\, s_{8,11} = 0, \tag{3.53}$$

where

$$\begin{aligned} \Psi =& \Psi_1 + \Psi_2 A_{1,4,3} + \Psi_3 A_{1,4,2} + \Psi_4 A_{2,4,5} + \Psi_5 A_{8,11,12} + \Psi_6 A_{1,4,3} A_{1,4,2} + \Psi_7 A_{1,4,3} \\ & A_{2,4,5} + \Psi_8 A_{1,4,3} A_{8,11,12} + \Psi_9 A_{1,4,2} A_{2,4,5} + \Psi_{10} A_{1,4,2} A_{8,11,12} + \Psi_{11} A_{2,4,5} \\ & A_{8,11,12} + \Psi_{12} A_{1,4,3} A_{1,4,2} A_{2,4,5} + \Psi_{13} A_{1,4,3} A_{1,4,2} A_{8,11,12} + \Psi_{14} A_{1,4,3} A_{2,4,5} \\ & A_{8,11,12} + \Psi_{15} A_{1,4,2} A_{2,4,5} A_{8,11,12} + \Psi_{16} A_{1,4,3} A_{1,4,2} A_{2,4,5} A_{8,11,12}, \end{aligned}$$

with Ψ_i, $i = 1, \ldots, 16$, polynomials in $s_{1,4}$, $s_{2,4}$ and $s_{8,11}$.

Now, by expressing equation (3.53) as a linear equation in $A_{8,11,12}$ (*i.e.*, $a + b\, A_{8,11,12} = 0$), squaring it (*i.e.*, $a^2 - b^2\, A_{8,11,12}^2 = 0$), and replacing equation (3.51) in the result, a equation in $A_{1,4,3}$, $A_{1,4,2}$, and $A_{2,4,5}$ is obtained. Repeating this process for $A_{2,4,5}$, we get

$$\Phi_1 + \Phi_2\, A_{1,4,3} + \Phi_3\, A_{1,4,2} + \Phi_4\, A_{1,4,3}\, A_{1,4,2} = 0, \tag{3.54}$$

where Φ_1, Φ_2, Φ_3, and Φ_4 are polynomials in $s_{1,4}$ of degree 16, 15, 15, and 14, respectively, and in $s_{2,4}$ of degree 8 in all cases. By properly twice squaring equation (3.54), the following equation is obtained:

$$\begin{aligned} & -\Phi_4^4 A_{1,4,3}^4 A_{1,4,2}^4 + 2\Phi_4^2\Phi_2^2 A_{1,4,3}^4 A_{1,4,2}^2 + 2\Phi_4^2\Phi_3^2 A_{1,4,3}^2 A_{1,4,2}^4 - \Phi_2^4 A_{1,4,3}^4 - \Phi_3^4 A_{1,4,2}^4 \\ & -\Phi_1^4 + \big(2\Phi_2^2\Phi_3^2 - 8\Phi_2\Phi_3\Phi_4\Phi_1 + 2\Phi_4^2\Phi_1^2\big) A_{1,4,3}^2 A_{1,4,2}^2 + 2\Phi_1^2\Phi_2^2 A_{1,4,3}^2 + 2\Phi_1^2\Phi_3^2 A_{1,4,2}^2 = 0. \end{aligned} \tag{3.55}$$

If the above procedure is applied to equation (3.51), we get a polynomial in $s_{1,4}$, $s_{2,4}$, and $s_{8,11}$, say $\mathcal{F}(s_{1,4}, s_{2,4}, s_{8,11})$. Finally, the full expansion of equation (3.55) factorizes as:

$$s_{1,4}^{16}\, s_{2,4}^{16}\, \mathcal{F}(s_{1,4}, s_{2,4}, 0)\, \mathcal{P}_1 = 0 \tag{3.56}$$

where $\mathcal{P}_1$ is a non-homogeneous bivariate polynomial in $s_{1,4}$ and $s_{2,4}$ with leading term $s_{1,4}^{32}\, s_{2,4}^{14}$. The roots of the term $s_{1,4}^{16}\, s_{2,4}^{16}\, \mathcal{F}(s_{1,4}, s_{2,4}, 0)$ were introduced when clearing denominators to obtain equation (3.53), so they can be dropped. To obtain $\mathcal{P}_2$, we can proceed in the same way as for the derivation of $\mathcal{P}_1$.

Finally, to obtain the characteristic polynomial, we have to eliminate either $s_{2,4}$ or $s_{1,4}$ from the polynomial system $\{\mathcal{P}_1(s_{1,4}, s_{2,4}) = 0, \mathcal{P}_2(s_{1,4}, s_{2,4}) = 0\}$. This can be implemented using, for example, Sylvester or Bézout resultants. If we eliminate either $s_{2,4}$ or $s_{1,4}$, the associated Sylvester and Bézout matrices have dimensions 68×68 and 36×36, respectively. In any case —*i.e.,* eliminating either $s_{2,4}$ or $s_{1,4}$ and using either Sylvester or the Bézout resultants— the result is a polynomial equation of degree 1826. When $s_{2,4}$ is the eliminated variable, this polynomial factors into 15 polynomials

$$\mathcal{P}_{9B28}(s_{1,4}) \prod_{i=1}^{14} \mathcal{D}_i(s_{1,4}) = 0 \tag{3.57}$$

where the roots of polynomials $\mathcal{D}_1, \ldots, \mathcal{D}_{14}$ are not solutions of the original system of radical equations formed by equations (3.49) and (3.50) and $\mathcal{P}_{9B28}$, the characteristic polynomial of the $9/B_{28}$ Baranov truss, is of degree 58 in $s_{1,4}$. As expected, the same result is obtained when $s_{1,4}$ is the eliminated variable.

For each of the real roots of $\mathcal{P}_{9B28}$, we can determine the Cartesian position of the revolute pair centers given by P_2, P_4, P_5, P_6, P_7, P_9, P_{10}, P_{11}, and P_{12}, with respect to the ternary link associated to $\triangle P_1 P_8 P_3$, computing $s_{2,4}$ from the system $\{\mathcal{P}_1(s_{1,4}, s_{2,4}) = 0, \mathcal{P}_2(s_{1,4}, s_{2,4}) = 0\}$ and using the set of equations

$$\begin{aligned}
\mathbf{p}_{1,4} &= \mathbf{Z}_{1,3,4}\, \mathbf{p}_{1,3} \\
\mathbf{p}_{3,6} &= \mathbf{Z}_{3,4,6}\, \mathbf{p}_{3,4} \\
\mathbf{p}_{1,2} &= \mathbf{Z}_{1,4,2}\, \mathbf{p}_{1,4} \\
\mathbf{p}_{2,5} &= \mathbf{Z}_{2,4,5}\, \mathbf{p}_{2,4} \\
\mathbf{p}_{5,7} &= \mathbf{Z}_{4,5,7}\, \mathbf{p}_{4,5} \\
\mathbf{p}_{2,11} &= \mathbf{Z}_{2,5,11}\, \mathbf{p}_{2,5} \\
\mathbf{p}_{8,12} &= \mathbf{Z}_{8,11,12}\, \mathbf{p}_{8,11} \\
\mathbf{p}_{8,9} &= \mathbf{Z}_{8,12,9}\, \mathbf{p}_{8,12} \\
\mathbf{p}_{11,10} &= \mathbf{Z}_{11,12,10}\, \mathbf{p}_{11,12}.
\end{aligned}$$

This process leads up to 16 combinations of locations for the couples P_6, P_{10} and P_7, P_9, and at least one of them must satisfy simultaneously the distances imposed by the binary links connecting them.

3.4.1.4 Example

According to the notation used in Fig. 3.11, let us suppose that $s_{1,2} = 3185$, $s_{1,3} = \frac{6610}{9}$, $s_{1,8} = \frac{16525}{9}$, $s_{2,5} = \frac{820}{9}$, $s_{2,11} = \frac{15826}{9}$, $s_{3,4} = 225$, $s_{3,6} = 180$, $s_{3,8} = 661$, $s_{4,5} = 400$, $s_{4,6} = 225$, $s_{4,7} = 452$, $s_{5,7} = 676$, $s_{5,11} = 1202$, $s_{6,10} = 625$, $s_{7,9} = 625$, $s_{8,9} = 305$, $s_{8,12} = 1600$, $s_{9,12} = 625$, $s_{10,11} = 676$, $s_{10,12} = 484$, and $s_{11,12} = 1600$. This corresponds to the example used by Wang *et. al.* in [198]. Then, proceeding as explained above, we obtain the characteristic polynomial

$$\begin{aligned}
&1.8481\,10^{239}\, {s_{1,4}}^{58} - 1.5725\,10^{244}\, {s_{1,4}}^{57} + 6.5857\,10^{248}\, {s_{1,4}}^{56} - 1.8099\,10^{253}\, {s_{1,4}}^{55} \\
&+ 3.6712\,10^{257}\, {s_{1,4}}^{54} - 5.8610\,10^{261}\, {s_{1,4}}^{53} + 7.6692\,10^{265}\, {s_{1,4}}^{52} - 8.4571\,10^{269}\, {s_{1,4}}^{51} \\
&+ 8.0199\,10^{273}\, {s_{1,4}}^{50} - 6.6413\,10^{277}\, {s_{1,4}}^{49} + 4.8604\,10^{281}\, {s_{1,4}}^{48} - 3.1737\,10^{285}\, {s_{1,4}}^{47}
\end{aligned}$$

$$
\begin{aligned}
&+ 1.8635\,10^{289}\, {s_{1,4}}^{46} - 9.9019\,10^{292}\, {s_{1,4}}^{45} + 4.7871\,10^{296}\, {s_{1,4}}^{44} - 2.1152\,10^{300}\, {s_{1,4}}^{43} \\
&+ 8.5737\,10^{303}\, {s_{1,4}}^{42} - 3.1985\,10^{307}\, {s_{1,4}}^{41} + 1.1012\,10^{311}\, {s_{1,4}}^{40} - 3.5073\,10^{314}\, {s_{1,4}}^{39} \\
&+ 1.0354\,10^{318}\, {s_{1,4}}^{38} - 2.8379\,10^{321}\, {s_{1,4}}^{37} + 7.2324\,10^{324}\, {s_{1,4}}^{36} - 1.7158\,10^{328}\, {s_{1,4}}^{35} \\
&+ 3.7930\,10^{331}\, {s_{1,4}}^{34} - 7.8194\,10^{334}\, {s_{1,4}}^{33} + 1.5042\,10^{338}\, {s_{1,4}}^{32} - 2.7012\,10^{341}\, {s_{1,4}}^{31} \\
&+ 4.5296\,10^{344}\, {s_{1,4}}^{30} - 7.0937\,10^{347}\, {s_{1,4}}^{29} + 1.0375\,10^{351}\, {s_{1,4}}^{28} - 1.4168\,10^{354}\, {s_{1,4}}^{27} \\
&+ 1.8060\,10^{357}\, {s_{1,4}}^{26} - 2.1479\,10^{360}\, {s_{1,4}}^{25} + 2.3817\,10^{363}\, {s_{1,4}}^{24} - 2.4603\,10^{366}\, {s_{1,4}}^{23} \\
&+ 2.3655\,10^{369}\, {s_{1,4}}^{22} - 2.1141\,10^{372}\, {s_{1,4}}^{21} + 1.7540\,10^{375}\, {s_{1,4}}^{20} - 1.3487\,10^{378}\, {s_{1,4}}^{19} \\
&+ 9.5930\,10^{380}\, {s_{1,4}}^{18} - 6.2979\,10^{383}\, {s_{1,4}}^{17} + 3.8066\,10^{386}\, {s_{1,4}}^{16} - 2.1121\,10^{389}\, {s_{1,4}}^{15} \\
&+ 1.0722\,10^{392}\, {s_{1,4}}^{14} - 4.9598\,10^{394}\, {s_{1,4}}^{13} + 2.0812\,10^{397}\, {s_{1,4}}^{12} - 7.8783\,10^{399}\, {s_{1,4}}^{11} \\
&+ 2.6731\,10^{402}\, {s_{1,4}}^{10} - 8.0665\,10^{404}\, {s_{1,4}}^{9} + 2.1442\,10^{407}\, {s_{1,4}}^{8} - 4.9610\,10^{409}\, {s_{1,4}}^{7} \\
&+ 9.8395\,10^{411}\, {s_{1,4}}^{6} - 1.6396\,10^{414}\, {s_{1,4}}^{5} + 2.2327\,10^{416}\, {s_{1,4}}^{4} - 2.3865\,10^{418}\, {s_{1,4}}^{3} \\
&+ 1.8780\,10^{420}\, {s_{1,4}}^{2} - 9.6768\,10^{421}\, s_{1,4} + 2.4499\,10^{423}.
\end{aligned}
$$

This polynomial has 14 real roots, a result in agreement with the solution reported in [198]. The values of these roots, as well as the corresponding assembly modes, for the case in which $P_1 = (0,0)^T$, $P_3 = (0, \frac{1}{3}\sqrt{6610})^T$, and $P_8 = (-\frac{3}{10}\sqrt{6610}, \frac{13}{30}\sqrt{6610})^T$, appear in Fig. 3.12. To the author's knowledge, this is the first time that the characteristic polynomial of a $9/B_{28}$ Baranov truss is explicitly obtained.

3.4.2 All four-loop Baranov trusses

When the bilateration technique is applied to the position analysis of all the four-loop Baranov trusses, one observes that the problem is reduced to solve a single scalar radical equation in one variable for all cases, except for trusses $9/B_{25}$, $9/B_{26}$, $9/B_{27}$, and $9/B_{28}$, for which the resulting system is formed by two scalar radical equations in two variables. This is in agreement with the coupling degree of the four-loop Baranov trusses presented in [223].

Since for the Baranov trusses with coupling degree 1 the obtained system of kinematic equations is a single scalar radical equation, their characteristic polynomials are obtained by simply clearing square roots, as it was already explained for trusses $5/B_1$, $7/B_1$, $7/B_2$, and $7/B_3$ in this chapter. Obtaining the characteristic polynomials of trusses $9/B_{25}$, $9/B_{26}$, $9/B_{27}$, and $9/B_{28}$ requires converting the resulting scalar radical equations in bivariate polynomials, by clearing square roots as well, and using classical elimination techniques, as it has been explained in the previous section for the $9/B_{28}$ Baranov truss. Then, it is important to realize that 197 trusses, out of the total of 239 Baranov trusses with eleven links (five loops), could also be solved in an elementary way and, for the remaining 42 trusses, the problem could be reduced to the solution of a system of two equations in two variables. Thus, compared to the approaches based on vector loop equations and elimination techniques, the application of the proposed technique to the position analysis of Baranov trusses seems clearly superior.

3.5 Compendium: All the cataloged Baranov trusses

In Appendix A, tables A.1 to A.8 present, for all the cataloged Baranov trusses[2], as a compendium, the system of kinematic equations derived using the bilateration tech-

[2]Except for the triad because, as presented in Section 3.1, recall that its position analysis is equivalent to solve the bilateration problem.

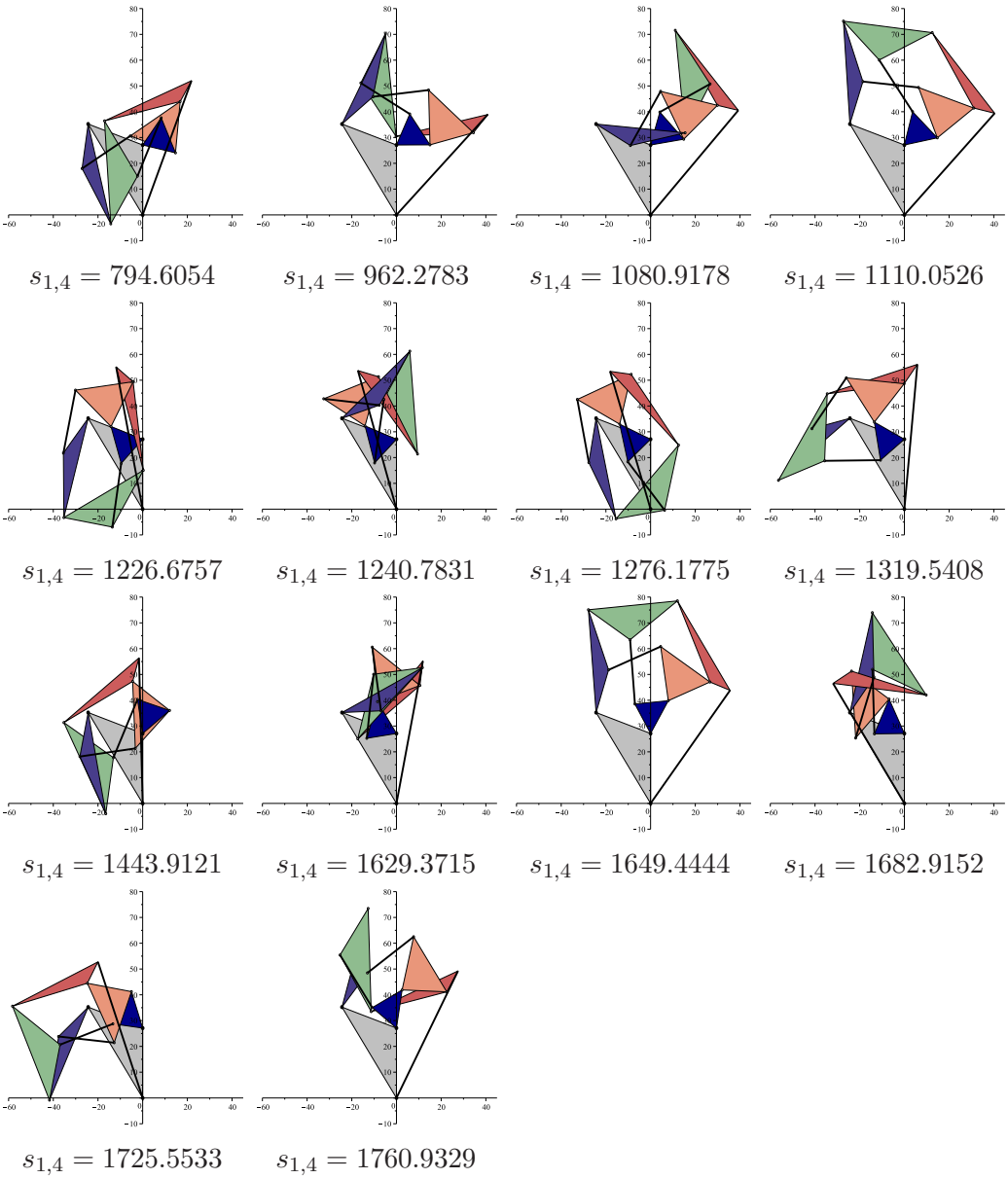

Figure 3.12. The configurations of the analyzed $9/B_{28}$ Baranov truss.

nique, the number of resulting assembly modes, and references to previous reported solutions using not only analytical approaches but also numerical ones. Using the kinematic equations presented in these tables, the closed-form position analysis of trusses $9/B_2$, $9/B_3$, $9/B_4$, $9/B_5$, $9/B_6$, $9/B_8$, $9/B_9$, $9/B_{13}$, $9/B_{18}$, $9/B_{19}$, and $9/B_{22}$, can be straightforwardly solved for the first time to the best of the author's knowledge. It can also be concluded from these tables that the number of assembly modes previously reported in the literature for trusses $9/B_4$, $9/B_8$, $9/B_{18}$, and $9/B_{19}$ do not seem accurate. In these tables, 'vector method' and 'complex number method' refer to trigonometric-based vector equations and complex-number-based vector loop equations, respectively. The equations presented for trusses $7/B_1$, $7/B_2$, and $7/B_3$ are equivalent to the ones detailed in Section 3.3.

It is worth to mention that the concept of Baranov truss has been extended to trusses with joints involving more than two links. It has been shown that there are such 125

Baranov trusses with up to four loops [35]. The closed-form solution to the position analysis of at least one of these trusses, the Dixon-Wunderlich linkage, has already been reported [189]. Although, it can be verified that the position analysis of this truss can be readily solved using bilateration techniques, the extension of the proposed method to all other members of this family of trusses is a point that deserves further attention.

3.6 Beyond four loops

As indicated at the beginning of this chapter, beyond four loops, the closed-form position analysis of only one 11-link Baranov truss has been previously reported [109, 217]. In this section, using bilateration techniques, the position analysis of the five-loop and six-loop versions of a Baranov truss of regular pattern with coupling degree 1, namely, a Watt-Baranov truss [159], is solved.

3.6.1 Baranov trusses of regular patterns

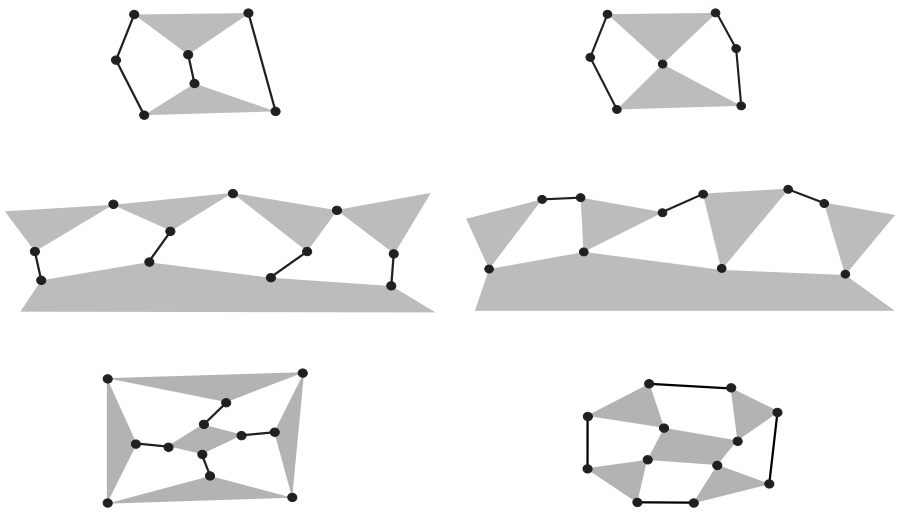

Figure 3.13. Left: The Stephenson linkage, the Stephenson pattern resulting from concatenating four Stephenson linkages, and the Stephenson-Baranov truss resulting from the circular concatenation of four Stephenson linkages. Stephenson-Baranov trusses have coupling degree 2. **Right:** The Watt linkage, the Watt pattern resulting from concatenating four Watt linkages, and the Watt-Baranov truss resulting from the circular concatenation of four Watt linkages. Watt-Baranov trusses have coupling degree 1.

At the end of the XIX century, it was known that there were only two six-link planar pin-jointed linkages of mobility 1. At a suggestion of Burmester [24], these two linkages were called the Watt linkage and the Stephenson linkage. Several Stephenson linkages can be concatenated leading to what in [40] was called a Stephenson pattern. Likewise, several Watt linkages can be concatenated to obtain what can be called, for the same reason, a Watt pattern (see [181] for their motion simulations). If these concatenations are circular, the results are Baranov trusses which will be called Stepheson-Baranov and Watt-Baranov trusses, respectively (Fig. 3.13). Observe that, regardless of the number of loops, the coupling degree of Stepheson-Baranov trusses and Watt-Baranov trusses is 2 and 1, correspondingly. As a consequence, in the case of Watt-Baranov trusses, the position analysis problem can always be reduced to solve a single scalar equation in one variable.

The position analysis of the Stepheson-Baranov truss of 4 loops, or $9/B_{26}$ Baranov truss, has been solved in closed form at least in [109, 191, 199, 201, 215], and more recently by K. Wohlhart in [218] thus reaching what the author considers to be the limit of Sylvester's elimination method. The position analysis of the Watt-Baranov truss of 4 loops, or $9/B_{10}$ Baranov truss, was solved in closed form by L. Han *et. al.* [64], Dhingra *et. al.* [44] and more recently by Borràs and Di Gregorio [19]. Elimination methods seem to reach their limit with the analysis of Baranov trusses with four, or five loops, depending on their topology. Actually, as it has been already mentioned, the closed-form position analysis of a Baranov truss with more than five loops has not been reported to the best of the author's knowledge (only the closed-form position analysis of one five-loop Baranov truss has been obtained [109, 217]). In this Section, using bilateration techniques, this challenge is addressed and the loop limit is pushed further by solving the closed-form position analysis of Watt-Baranov trusses with up to six loops.

3.6.2 Position analysis of the general n-link Watt-Baranov truss

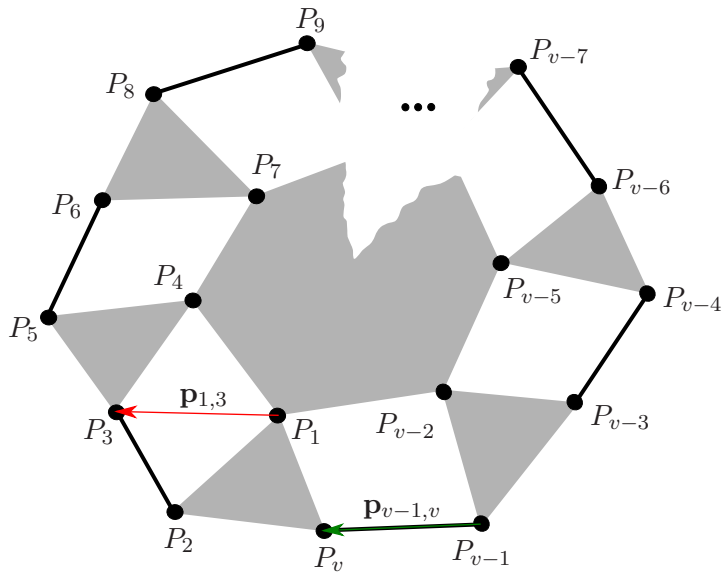

Figure 3.14. The general n-link Watt-Baranov truss has $k = \frac{n-1}{2}$ loops and $v = \frac{3}{2}(n-1)$ revolute joints. $\mathbf{p}_{v-1,v}$ can be expressed as a function of $\mathbf{p}_{1,3}$ by computing $3\,k - 2$ bilaterations.

Fig. 3.14 shows the general n-link Watt-Baranov truss, a structure with $k = \frac{n-1}{2}$ loops and $v = \frac{3}{2}(n-1)$ revolute joints. The revolute pair centers of the k-ary link define the polygon $P_1P_4P_7 \ldots P_{v-5}P_{v-2}$, and those of the k ternary links define the triangles $\triangle P_1P_vP_2$, $\triangle P_4P_3P_5$, $\triangle P_7P_6P_8$,..., $\triangle P_{v-5}P_{v-6}P_{v-4}$ and $\triangle P_{v-2}P_{v-3}P_{v-1}$. Similarly to other Baranov trusses, the position analysis problem for this structure consists in, given the dimensions of all links, calculating all relative possible transformations between them all. To solve this problem, instead of directly computing the relative Cartesian poses of all links through loop-closure equations, we will compute the set of values of $s_{1,3}$ compatible with all binary and ternary links side lengths using bilateration techniques. That is, $s_{1,3}$ is used as a parameter in terms of which the location of all other links of the truss can be expressed. Since one parameter is needed, the truss is said to have coupling degree 1.

On the one hand, according to Fig. 3.14, $\mathbf{p}_{1,4}$, $\mathbf{p}_{1,7}$, $\ldots$, $\mathbf{p}_{1,v-5}$, $\mathbf{p}_{1,v-2}$ can be expressed as a function of $\mathbf{p}_{1,3}$ using bilaterations as follows:

$$\mathbf{p}_{1,4} = \mathbf{Z}_{1,3,4}\,\mathbf{p}_{1,3} \tag{3.58}$$
$$\mathbf{p}_{1,7} = \mathbf{Z}_{1,4,7}\,\mathbf{p}_{1,4} = \mathbf{Z}_{1,4,7}\,\mathbf{Z}_{1,3,4}\,\mathbf{p}_{1,3} \tag{3.59}$$
$$\mathbf{p}_{1,10} = \mathbf{Z}_{1,7,10}\,\mathbf{p}_{1,7} = \mathbf{Z}_{1,7,10}\,\mathbf{Z}_{1,4,7},\mathbf{Z}_{1,3,4}\,\mathbf{p}_{1,3} \tag{3.60}$$
$$\vdots$$
$$\mathbf{p}_{1,v-5} = \mathbf{Z}_{1,v-8,v-5}\,\mathbf{Z}_{1,v-11,v-8}\,\ldots\,\mathbf{Z}_{1,4,7},\mathbf{Z}_{1,3,4}\,\mathbf{p}_{1,3} \tag{3.61}$$
$$\mathbf{p}_{1,v-2} = \mathbf{Z}_{1,v-5,v-2}\,\mathbf{Z}_{1,v-8,v-5}\,\ldots\,\mathbf{Z}_{1,4,7},\mathbf{Z}_{1,3,4}\,\mathbf{p}_{1,3}. \tag{3.62}$$

On the other hand, for the triangle $\triangle P_4P_3P_5$, we have

$$\begin{aligned}\mathbf{p}_{4,5} &= \mathbf{Z}_{4,3,5}\,\mathbf{p}_{4,3}\\ \mathbf{p}_{4,1} + \mathbf{p}_{1,5} &= \mathbf{Z}_{4,3,5}\,(\mathbf{p}_{4,1} + \mathbf{p}_{1,3})\\ \mathbf{p}_{1,5} &= \mathbf{p}_{1,4} + \mathbf{Z}_{4,3,5}\,(\mathbf{p}_{1,3} - \mathbf{p}_{1,4})\,.\end{aligned} \tag{3.63}$$

Likewise, for the triangles $\triangle P_7P_6P_8$, $\ldots$, $\triangle P_{v-5}P_{v-6}P_{v-4}$ and $\triangle P_{v-2}P_{v-3}P_{v-1}$, we obtain

$$\mathbf{p}_{1,6} = \mathbf{p}_{1,7} + \mathbf{Z}_{7,5,6}\,(\mathbf{p}_{1,5} - \mathbf{p}_{1,7}) \tag{3.64}$$
$$\mathbf{p}_{1,8} = \mathbf{p}_{1,7} + \mathbf{Z}_{7,6,8}\,(\mathbf{p}_{1,6} - \mathbf{p}_{1,7}) \tag{3.65}$$
$$\vdots$$
$$\mathbf{p}_{1,v-3} = \mathbf{p}_{1,v-2} + \mathbf{Z}_{v-2,v-4,v-3}\,(\mathbf{p}_{1,v-4} - \mathbf{p}_{1,v-2}) \tag{3.66}$$
$$\mathbf{p}_{1,v-1} = \mathbf{p}_{1,v-2} + \mathbf{Z}_{v-2,v-3,v-1}\,(\mathbf{p}_{1,v-3} - \mathbf{p}_{1,v-2})\,. \tag{3.67}$$

Now, substituting (3.58)-(3.62) in (3.63)-(3.67) and then replacing the resulting expression for $\mathbf{p}_{1,5}$ in that for $\mathbf{p}_{1,6}$, and the resulting expression for $\mathbf{p}_{1,6}$ after this substitution in that for $\mathbf{p}_{1,8}$, and so on till an expression is obtained for $\mathbf{p}_{1,v-1}$, we get

$$\mathbf{p}_{1,v-1} = \mathbf{Q}_n\,\mathbf{p}_{1,3}. \tag{3.68}$$

Moreover, for the triangle $\triangle P_1P_vP_2$, we have

$$\mathbf{p}_{1,v} = \mathbf{Z}_{1,2,v}\,\mathbf{Z}_{1,3,2}\,\mathbf{p}_{1,3}. \tag{3.69}$$

Finally, using equations (3.68) and (3.69), we get

$$\mathbf{p}_{v-1,v} = \mathbf{p}_{v-1,1} + \mathbf{p}_{1,v} = (-\mathbf{Q}_n + \mathbf{Z}_{1,2,v}\,\mathbf{Z}_{1,3,2})\,\mathbf{p}_{1,3}. \tag{3.70}$$

Therefore,

$$s_{v-1,v} = \det(-\mathbf{Q}_n + \mathbf{Z}_{1,2,v}\,\mathbf{Z}_{1,3,2})s_{1,3}. \tag{3.71}$$

The right hand side of the above equation is a function of the $k-1$ unknown squared distances $s_{1,3}$ and $s_{5,7}$, $s_{8,10}$, $\ldots$, $s_{v-7,v-5}$, $s_{v-4,v-2}$.

Since, using the same procedure to obtain (3.70), allows us to obtain

$$\mathbf{p}_{5,7} = -\mathbf{p}_{1,5} + \mathbf{p}_{1,7} = \mathbf{D}_{n_1}\,\mathbf{p}_{1,3} \tag{3.72}$$
$$\mathbf{p}_{8,10} = -\mathbf{p}_{1,8} + \mathbf{p}_{1,10} = \mathbf{D}_{n_2}\,\mathbf{p}_{1,3} \tag{3.73}$$
$$\vdots$$
$$\mathbf{p}_{v-7,v-5} = -\mathbf{p}_{1,v-7} + \mathbf{p}_{1,v-5} = \mathbf{D}_{n_{k-3}}\,\mathbf{p}_{1,3} \tag{3.74}$$
$$\mathbf{p}_{v-4,v-2} = -\mathbf{p}_{1,v-4} + \mathbf{p}_{1,v-2} = \mathbf{D}_{n_{k-2}}\,\mathbf{p}_{1,3}. \tag{3.75}$$

Therefore,

$$s_{5,7} = \det(\mathbf{D}_{n_1})\, s_{1,3} \tag{3.76}$$
$$s_{8,10} = \det(\mathbf{D}_{n_2})\, s_{1,3} \tag{3.77}$$
$$\vdots$$
$$s_{v-7,v-5} = \det(\mathbf{D}_{n_{k-3}})\, s_{1,3} \tag{3.78}$$
$$s_{v-4,v-2} = \det(\mathbf{D}_{n_{k-2}})\, s_{1,3}. \tag{3.79}$$

The substitution of (3.76) - (3.79) into (3.71) yields a scalar equation in a single variable: $s_{1,3}$. The roots of this equation, in the range in which the signed areas of the triangles $P_1P_2P_3$ and $P_1P_3P_4$ are real, that is, the range

$$\left[\max\{(d_{1,2}-d_{2,3})^2, (d_{1,4}-d_{3,4})^2\}, \min\{(d_{1,2}+d_{2,3})^2, (d_{1,4}+d_{3,4})^2\}\right],$$

determine the assembly modes of the general n-link Watt-Baranov truss. Similarly to what happens in some of the Baranov trusses previously analyzed, namely, the Baranov trusses with coupling degree 1, these roots can be readily obtained using, for example, an interval Newton method for the 2^k possible combinations for the signs of the signed areas of the triangles $\triangle P_1P_2P_3$, $\triangle P_1P_3P_4$, and $\triangle P_7P_5P_6$, $\triangle P_{10}P_8P_9$, ..., $\triangle P_{v-5}P_{v-7}P_{v-6}$, and $\triangle P_{v-2}P_{v-4}P_{v-3}$.

In order to obtain the characteristic polynomial it just remains to clear all square roots in the obtained scalar equation by isolating one at a time and squaring the result till no square root remains. Using a computer algebra system, it can be seen that this clearing process leads to

$$s_{1,3}^{2^{k-1}}\, s_{5,7}^{2^{k-2}}\, s_{8,10}^{2^{k-3}} \ldots s_{v-7,v-5}^{4}\, s_{v-4,v-2}^{2}\, \mathcal{P}w_n = 0 \tag{3.80}$$

where $\mathcal{P}w_n$ is a polynomial in $s_{1,3}$ of degree $2^{k+1}-2$. The extraneous roots at $s_{1,3}=0$, ..., $s_{v-4,v-2}=0$ were introduced when clearing denominators, as it happens in previous sections, so they can be dropped. For each of the real roots of polynomial $\mathcal{P}w_n$, we can determine the Cartesian position of the $v-k$ revolute pair centers of the ternary links, with respect to the n-ary link, using equations (3.63)-(3.67), equation (3.69), and the equation $\mathbf{p}_{1,3} = \mathbf{Z}_{1,4,3}\mathbf{p}_{1,4}$. This process leads up to 2^k combinations of locations for P_{v-1} and P_v, and at least one of them must satisfy the distance imposed by the binary link connecting them.

3.6.2.1 Example: A five-loop Watt-Baranov truss

Consider a 11-link Watt-Baranov truss. Since, in this case $k=5$, $v=15$, equation (3.71) reduces to

$$\det(-\mathbf{Q}_{11} + \mathbf{Z}_{1,2,15}\,\mathbf{Z}_{1,3,2}) = \frac{s_{14,15}}{s_{1,3}}, \tag{3.81}$$

where

$$\begin{aligned}\mathbf{Q}_{11} = {} & \mathbf{Z}_{1,10,13}\,\mathbf{Z}_{1,7,10}\,\mathbf{Z}_{1,4,7}\,\mathbf{Z}_{1,3,4} + \mathbf{Z}_{13,12,14}\,\mathbf{Z}_{13,11,12}\big(\mathbf{Z}_{1,7,10}\,\mathbf{Z}_{1,4,7}\,\mathbf{Z}_{1,3,4} \\ & + \mathbf{Z}_{10,9,11}\,\mathbf{Z}_{10,8,9}\big(\mathbf{Z}_{1,4,7}\,\mathbf{Z}_{1,3,4}\mathbf{Z}_{7,6,8}\,\mathbf{Z}_{7,5,6}\big(\mathbf{Z}_{1,3,4} + \mathbf{Z}_{4,3,5} + \big(\mathbf{I} - \mathbf{Z}_{1,3,4}\big) \\ & - \mathbf{Z}_{1,4,7}\,\mathbf{Z}_{1,3,4}\big) - \mathbf{Z}_{1,7,10}\,\mathbf{Z}_{1,4,7}\,\mathbf{Z}_{1,3,4}\big) - \mathbf{Z}_{1,10,13}\,\mathbf{Z}_{1,7,10}\,\mathbf{Z}_{1,4,7}\,\mathbf{Z}_{1,3,4}\big),\end{aligned}$$

and equations (3.76)-(3.79) reduce to

$$s_{5,7} = \det(\mathbf{D}_{11_1})\, s_{1,3} \tag{3.82}$$
$$s_{8,10} = \det(\mathbf{D}_{11_2})\, s_{1,3} \tag{3.83}$$
$$s_{11,13} = \det(\mathbf{D}_{11_3})\, s_{1,3}. \tag{3.84}$$

where

$$\begin{aligned}
\mathbf{D}_{11_1} &= -\mathbf{Z}_{1,3,4} - \mathbf{Z}_{4,3,5}\,(\mathbf{I} - \mathbf{Z}_{1,3,4}) + \mathbf{Z}_{1,4,7}\,\mathbf{Z}_{1,3,4} \\
\mathbf{D}_{11_2} &= -\mathbf{Z}_{1,4,7}\,\mathbf{Z}_{1,3,4} - \mathbf{Z}_{7,6,8}\,\mathbf{Z}_{7,5,6}\left(\mathbf{Z}_{1,3,4} + \mathbf{Z}_{4,3,5}\left(\mathbf{I} - \mathbf{Z}_{1,3,4}\right) - \mathbf{Z}_{1,4,7}\,\mathbf{Z}_{1,3,4}\right) \\
&\quad + \mathbf{Z}_{1,7,10}\,\mathbf{Z}_{1,4,7}\mathbf{Z}_{1,3,4} \\
\mathbf{D}_{11_3} &= -\mathbf{Z}_{1,7,10}\,\mathbf{Z}_{1,4,7}\,\mathbf{Z}_{1,3,4} - \mathbf{Z}_{10,9,11}\,\mathbf{Z}_{10,8,9}\big(\mathbf{Z}_{1,4,7}\,\mathbf{Z}_{1,3,4} + \mathbf{Z}_{7,6,8}\,\mathbf{Z}_{7,5,6}\big(\mathbf{Z}_{1,3,4} \\
&\quad + \mathbf{Z}_{4,3,5}\big(\mathbf{I} - \mathbf{Z}_{1,3,4}\big) - \mathbf{Z}_{1,4,7}\,\mathbf{Z}_{1,3,4}\big) - \mathbf{Z}_{1,7,10}\,\mathbf{Z}_{1,4,7}\,\mathbf{Z}_{1,3,4}\big) \\
&\quad + \mathbf{Z}_{1,10,13}\,\mathbf{Z}_{1,7,10}\,\mathbf{Z}_{1,4,7}\,\mathbf{Z}_{1,3,4}
\end{aligned}$$

By expanding equations (3.82)-(3.84), we get

$$s_{5,7} = {}^1\Lambda_1 + {}^1\Lambda_2\, A_{1,3,4} \tag{3.85}$$
$$s_{8,10} = \frac{1}{s_{5,7}}\left({}^2\Lambda_1 + {}^2\Lambda_2\, A_{1,3,4} + {}^2\Lambda_3\, A_{7,5,6} + {}^2\Lambda_4\, A_{1,3,4}\, A_{7,5,6}\right) \tag{3.86}$$
$$\begin{aligned}
s_{11,13} = \frac{1}{s_{5,7}\, s_{8,10}}\Big({}^3\Lambda_1 &+ {}^3\Lambda_2\, A_{1,3,4} + {}^3\Lambda_3\, A_{7,5,6} + {}^3\Lambda_4\, A_{10,8,9} + {}^3\Lambda_5\, A_{1,3,4}\, A_{7,5,6} \\
&+ {}^3\Lambda_6\, A_{1,3,4}\, A_{10,8,9} + {}^3\Lambda_7\, A_{7,5,6}\, A_{10,8,9} + {}^3\Lambda_8\, A_{1,3,4}\, A_{7,5,6}\, A_{10,8,9}\Big)
\end{aligned} \tag{3.87}$$

where ${}^1\Lambda_1$, ${}^1\Lambda_2$ are polynomials in $s_{1,3}$, ${}^2\Lambda_i$, $i = 1, \ldots, 4$ are polynomials in $s_{1,3}$ and $s_{5,7}$, and ${}^3\Lambda_i$, $i = 1, \ldots, 8$ are polynomials in $s_{1,3}$, $s_{5,7}$, and $s_{8,10}$.

Similarly, by expanding equation (3.81), we get

$$s_{14,15} = \frac{1}{s_{1,3}\, s_{5,7}\, s_{8,10}\, s_{11,13}}\,\Psi, \tag{3.88}$$

that is,

$$\Psi - s_{1,3}\, s_{5,7}\, s_{8,10}\, s_{11,13}\, s_{14,15} = 0, \tag{3.89}$$

where

$$\begin{aligned}
\Psi = \Psi_1 &+ \Psi_2\, A_{1,2,3} + \Psi_3\, A_{1,3,4} + \Psi_4\, A_{7,5,6} + \Psi_5\, A_{10,8,9} \\
&+ \Psi_6\, A_{13,11,12} + \Psi_7\, A_{1,2,3}\, A_{1,3,4} + \Psi_8\, A_{1,2,3}\, A_{7,5,6} \\
&+ \Psi_9\, A_{1,2,3}\, A_{10,8,9} + \Psi_{10}\, A_{1,2,3}\, A_{13,11,12} + \Psi_{11}\, A_{1,3,4}\, A_{7,5,6} \\
&+ \Psi_{12}\, A_{1,3,4}\, A_{10,8,9} + \ldots + \Psi_{31}\, A_{1,3,4}\, A_{7,5,6}\, A_{10,8,9}\, A_{13,11,12} \\
&+ \Psi_{32}\, A_{1,2,3}\, A_{1,3,4}\, A_{7,5,6}\, A_{10,8,9}\, A_{13,11,12},
\end{aligned}$$

with Ψ_i, $i = 1, \ldots, 2^5$, polynomials in $s_{1,3}$, $s_{5,7}$, $s_{8,10}$, and $s_{11,13}$.

Now, by expressing equation (3.89) as a linear equation in $A_{13,11,12}$ —*i.e.*, $a + b\, A_{13,11,12} = 0$, properly squaring it —*i.e.*, $a^2 - b^2\, A_{13,11,12}^2 = 0$, and replacing equation (3.87) in the result, a radical equation in $s_{1,3}$, $s_{5,7}$, and $s_{8,10}$ is obtained. Repeating this process for $A_{10,8,9}$ and then for $A_{7,5,6}$, we get the scalar radical equation

$$\Phi_1 + \Phi_2\, A_{1,2,3} + \Phi_3\, A_{1,3,4} + \Phi_4\, A_{1,2,3}\, A_{1,3,4} = 0, \tag{3.90}$$

where Φ_1, Φ_2, Φ_3 and Φ_4 are polynomials in a single variable: $s_{1,3}$. If the last procedure is applied to equations (3.85), (3.86), and (3.87), we get polynomials in $s_{1,3}$ and $s_{5,7}$, say $\mathcal{P}_1(s_{1,3}, s_{5,7})$, $s_{1,3}$ and $s_{8,10}$, say $\mathcal{P}_2(s_{1,3}, s_{8,10})$, and $s_{1,3}$ and $s_{11,13}$, say $\mathcal{P}_3(s_{1,3}, s_{11,13})$, respectively.

Finally, the square roots in (3.90) can be eliminated by properly twice squaring it. This operation yields

$$\begin{aligned}
&-\Phi_4^4 A_{1,2,3}^4 A_{1,3,4}^4 + 2\Phi_4^2\Phi_2^2 A_{1,2,3}^4 A_{1,3,4}^2 + 2\Phi_4^2\Phi_3^2 A_{1,2,3}^2 A_{1,3,4}^4 - \Phi_2^4 A_{1,2,3}^4 - \Phi_3^4 A_{1,3,4}^4 \\
&-\Phi_1^4 + \left(2\Phi_2^2\Phi_3^2 - 8\Phi_2\Phi_3\Phi_4\Phi_1 + 2\Phi_4^2\Phi_1^2\right) A_{1,2,3}^2 A_{1,3,4}^2 + 2\Phi_1^2\Phi_2^2 A_{1,2,3}^2 + 2\Phi_1^2\Phi_3^2 A_{1,3,4}^2 = 0
\end{aligned} \tag{3.91}$$

which, when fully expanded, leads to

$$\begin{aligned}
s_{1,3}^{16}\, P_1(s_{1,3},0)^8\, P_2(s_{1,3},0)^4\, P_3(s_{1,3},0)^2\, \mathcal{P}w_{11} &= 0 \\
s_{1,3}^{16}\, s_{5,7}^{8}\, s_{8,10}^{4}\, s_{11,13}^{2}\, \mathcal{P}w_{11} &= 0
\end{aligned} \tag{3.92}$$

where $\mathcal{P}w_{11}$ is a polynomial in $s_{1,3}$ of degree 62. The extraneous roots at $s_{5,7} = 0$, $s_{8,10} = 0$, and $s_{11,13} = 0$ were introduced when clearing denominators to obtain equation (3.89), so they can be dropped.

Finally, let us suppose that $s_{1,2} = 40$, $s_{1,4} = 13$, $s_{1,7} = 26$, $s_{1,10} = 34$, $s_{1,13} = 17$, $s_{1,15} = 13$, $s_{2,3} = 50$, $s_{2,15} = 17$, $s_{3,4} = 81$, $s_{3,5} = 9$, $s_{4,5} = 90$, $s_{4,7} = 13$, $s_{4,10} = 49$, $s_{4,13} = 52$, $s_{5,6} = 125$, $s_{6,7} = 40$, $s_{6,8} = 9$, $s_{7,8} = 37$, $s_{7,10} = 20$, $s_{7,13} = 45$, $s_{8,9} = 136$, $s_{9,10} = 53$, $s_{9,11} = 9$, $s_{10,11} = 50$, $s_{10,13} = 17$, $s_{11,12} = 181$, $s_{12,13} = 50$, $s_{12,14} = 9$, $s_{13,14} = 65$, and $s_{14,15} = 29$. Then, proceeding as explained above, we obtain the characteristic polynomial

$$\begin{aligned}
&{s_{1,3}}^{62} - 4091.5078\, {s_{1,3}}^{61} + 8.3074\, 10^{6}\, {s_{1,3}}^{60} - 1.1186\, 10^{10}\, {s_{1,3}}^{59} + 1.1260\, 10^{13}\, {s_{1,3}}^{58} \\
&- 9.0519\, 10^{15}\, {s_{1,3}}^{57} + 6.0604\, 10^{18}\, {s_{1,3}}^{56} - 3.4776\, 10^{21}\, {s_{1,3}}^{55} + 1.7461\, 10^{24}\, {s_{1,3}}^{54} \\
&- 7.7894\, 10^{26}\, {s_{1,3}}^{53} + 3.1238\, 10^{29}\, {s_{1,3}}^{52} - 1.1363\, 10^{32}\, {s_{1,3}}^{51} + 3.7751\, 10^{34}\, {s_{1,3}}^{50} \\
&- 1.1513\, 10^{37}\, {s_{1,3}}^{49} + 3.2360\, 10^{39}\, {s_{1,3}}^{48} - 8.4044\, 10^{41}\, {s_{1,3}}^{47} + 2.0208\, 10^{44}\, {s_{1,3}}^{46} \\
&- 4.5040\, 10^{46}\, {s_{1,3}}^{45} + 9.3129\, 10^{48}\, {s_{1,3}}^{44} - 1.7874\, 10^{51}\, {s_{1,3}}^{43} + 3.1855\, 10^{53}\, {s_{1,3}}^{42} \\
&- 5.2730\, 10^{55}\, {s_{1,3}}^{41} + 8.1092\, 10^{57}\, {s_{1,3}}^{40} - 1.1589\, 10^{60}\, {s_{1,3}}^{39} + 1.5391\, 10^{62}\, {s_{1,3}}^{38} \\
&- 1.9002\, 10^{64}\, {s_{1,3}}^{37} + 2.1807\, 10^{66}\, {s_{1,3}}^{36} - 2.3265\, 10^{68}\, {s_{1,3}}^{35} + 2.3073\, 10^{70}\, {s_{1,3}}^{34} \\
&- 2.1267\, 10^{72}\, {s_{1,3}}^{33} + 1.8215\, 10^{74}\, {s_{1,3}}^{32} - 1.4492\, 10^{76}\, {s_{1,3}}^{31} + 1.0704\, 10^{78}\, {s_{1,3}}^{30} \\
&- 7.3366\, 10^{79}\, {s_{1,3}}^{29} + 4.6623\, 10^{81}\, {s_{1,3}}^{28} - 2.7447\, 10^{83}\, {s_{1,3}}^{27} + 1.4952\, 10^{85}\, {s_{1,3}}^{26} \\
&- 7.5291\, 10^{86}\, {s_{1,3}}^{25} + 3.4992\, 10^{88}\, {s_{1,3}}^{24} - 1.4987\, 10^{90}\, {s_{1,3}}^{23} + 5.9041\, 10^{91}\, {s_{1,3}}^{22} \\
&- 2.1353\, 10^{93}\, {s_{1,3}}^{21} + 7.0731\, 10^{94}\, {s_{1,3}}^{20} - 2.1407\, 10^{96}\, {s_{1,3}}^{19} + 5.9032\, 10^{97}\, {s_{1,3}}^{18} \\
&- 1.4791\, 10^{99}\, {s_{1,3}}^{17} + 3.357\, 10^{100}\, {s_{1,3}}^{16} - 6.8819\, 10^{101}\, {s_{1,3}}^{15} + 1.271\, 10^{103}\, {s_{1,3}}^{14} \\
&- 2.111\, 10^{104}\, {s_{1,3}}^{13} + 3.149\, 10^{105}\, {s_{1,3}}^{12} - 4.2226\, 10^{106}\, {s_{1,3}}^{11} + 5.0997\, 10^{107}\, {s_{1,3}}^{10} \\
&- 5.5526\, 10^{108}\, {s_{1,3}}^{9} + 5.4328\, 10^{109}\, {s_{1,3}}^{8} - 4.7166\, 10^{110}\, {s_{1,3}}^{7} + 3.5398\, 10^{111}\, {s_{1,3}}^{6} \\
&- 2.2029\, 10^{112}\, {s_{1,3}}^{5} + 1.0721\, 10^{113}\, {s_{1,3}}^{4} - 3.7586\, 10^{113}\, {s_{1,3}}^{3} + 8.4177\, 10^{113}\, {s_{1,3}}^{2} \\
&- 1.0258\, 10^{114}\, s_{1,3} + 7.3862\, 10^{113} = 0.
\end{aligned}$$

The above polynomial has 16 real roots. The values of these roots as well as the corresponding assembly modes, for the case in which $P_1 = (12, 10)^T$, $P_4 = (10, 13)^T$, $P_7 = (13, 15)^T$, $P_{10} = (17, 13)^T$, and $P_{13} = (16, 9)^T$, appear in Fig. 3.15.

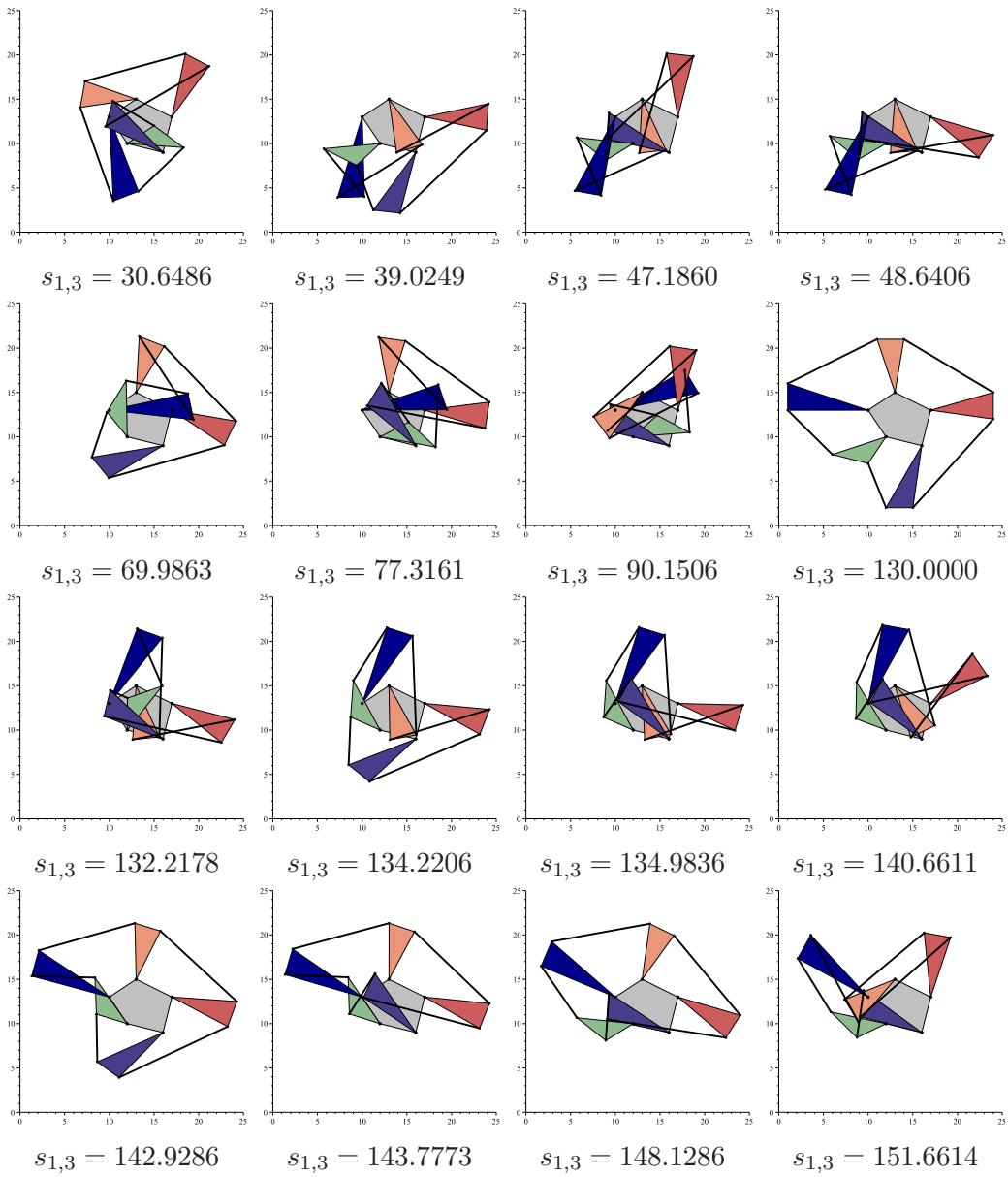

Figure 3.15. The configurations of the analyzed 11-link Watt-Baranov truss.

3.6.2.2 Example: A six-loop Watt-Baranov truss

Let us consider a 13-link Watt-Baranov truss where $s_{1,2} = 58$, $s_{1,4} = 18$, $s_{1,7} = 40$, $s_{1,10} = 53$, $s_{1,13} = 50$, $s_{1,16} = 20$, $s_{1,18} = 41$, $s_{2,3} = 52$, $s_{2,18} = 13$, $s_{3,4} = 64$, $s_{3,5} = 18$, $s_{4,5} = 34$, $s_{4,7} = 10$, $s_{4,10} = 41$, $s_{4,13} = 68$, $s_{4,16} = 50$, $s_{5,6} = 50$, $s_{6,7} = 74$, $s_{6,8} = 10$, $s_{7,8} = 68$, $s_{7,10} = 17$, $s_{7,13} = 50$, $s_{7,16} = 52$, $s_{8,9} = 65$, $s_{9,10} = 68$, $s_{9,11} = 9$, $s_{10,11} = 89$, $s_{10,13} = 13$, $s_{10,16} = 29$, $s_{11,12} = 61$, $s_{12,13} = 65$, $s_{12,14} = 26$, $s_{13,14} = 65$, $s_{13,16} = 10$, $s_{14,15} = 113$, $s_{15,16} = 40$, $s_{15,17} = 13$, $s_{16,17} = 81$, and $s_{17,18} = 68$. Then, proceeding as explained in the previous example, the following characteristic polynomial is obtained

$$
\begin{aligned}
&{s_{1,3}}^{126} - 9.4336\,10^{3}\,{s_{1,3}}^{125} + 4.3965\,10^{7}\,{s_{1,3}}^{124} - 1.3499\,10^{11}\,{s_{1,3}}^{123} + 3.0727\,10^{14}\,{s_{1,3}}^{122} \\
&- 5.5326\,10^{17}\,{s_{1,3}}^{121} + 8.2112\,10^{20}\,{s_{1,3}}^{120} - 1.0335\,10^{24}\,{s_{1,3}}^{119} + 1.1265\,10^{27}\,{s_{1,3}}^{118} \\
&- 1.0804\,10^{30}\,{s_{1,3}}^{117} + 9.2339\,10^{32}\,{s_{1,3}}^{116} - 7.1053\,10^{35}\,{s_{1,3}}^{115} + 4.9645\,10^{38}\,{s_{1,3}}^{114}
\end{aligned}
$$

$$
\begin{aligned}
&- 3.1727\,10^{41}\, {s_{1,3}}^{113} + 1.8663\,10^{44}\, {s_{1,3}}^{112} - 1.0162\,10^{47}\, {s_{1,3}}^{111} + 5.1482\,10^{49}\, {s_{1,3}}^{110} \\
&- 2.4382\,10^{52}\, {s_{1,3}}^{109} + 1.0843\,10^{55}\, {s_{1,3}}^{108} - 4.5474\,10^{57}\, {s_{1,3}}^{107} + 1.8055\,10^{60}\, {s_{1,3}}^{106} \\
&- 6.8124\,10^{62}\, {s_{1,3}}^{105} + 2.4508\,10^{65}\, {s_{1,3}}^{104} - 8.4319\,10^{67}\, {s_{1,3}}^{103} + 2.7813\,10^{70}\, {s_{1,3}}^{102} \\
&- 8.8139\,10^{72}\, {s_{1,3}}^{101} + 2.6874\,10^{75}\, {s_{1,3}}^{100} - 7.8923\,10^{77}\, {s_{1,3}}^{99} + 2.2337\,10^{80}\, {s_{1,3}}^{98} \\
&- 6.0942\,10^{82}\, {s_{1,3}}^{97} + 1.6026\,10^{85}\, {s_{1,3}}^{96} - 4.0606\,10^{87}\, {s_{1,3}}^{95} + 9.9090\,10^{89}\, {s_{1,3}}^{94} \\
&- 2.3274\,10^{92}\, {s_{1,3}}^{93} + 5.2579\,10^{94}\, {s_{1,3}}^{92} - 1.1418\,10^{97}\, {s_{1,3}}^{91} + 2.3816\,10^{99}\, {s_{1,3}}^{90} \\
&- 4.7688\,10^{101}\, {s_{1,3}}^{89} + 9.1613\,10^{103}\, {s_{1,3}}^{88} - 1.6877\,10^{106}\, {s_{1,3}}^{87} + 2.9804\,10^{108}\, {s_{1,3}}^{86} \\
&- 5.0434\,10^{110}\, {s_{1,3}}^{85} + 8.1760\,10^{112}\, {s_{1,3}}^{84} - 1.2695\,10^{115}\, {s_{1,3}}^{83} + 1.8879\,10^{117}\, {s_{1,3}}^{82} \\
&- 2.6886\,10^{119}\, {s_{1,3}}^{81} + 3.6665\,10^{121}\, {s_{1,3}}^{80} - 4.7884\,10^{123}\, {s_{1,3}}^{79} + 5.9887\,10^{125}\, {s_{1,3}}^{78} \\
&- 7.1733\,10^{127}\, {s_{1,3}}^{77} + 8.2296\,10^{129}\, {s_{1,3}}^{76} - 9.0435\,10^{131}\, {s_{1,3}}^{75} + 9.5199\,10^{133}\, {s_{1,3}}^{74} \\
&- 9.6005\,10^{135}\, {s_{1,3}}^{73} + 9.2758\,10^{137}\, {s_{1,3}}^{72} - 8.5868\,10^{139}\, {s_{1,3}}^{71} + 7.6163\,10^{141}\, {s_{1,3}}^{70} \\
&- 6.4729\,10^{143}\, {s_{1,3}}^{69} + 5.2711\,10^{145}\, {s_{1,3}}^{68} - 4.1128\,10^{147}\, {s_{1,3}}^{67} + 3.0746\,10^{149}\, {s_{1,3}}^{66} \\
&- 2.2020\,10^{151}\, {s_{1,3}}^{65} + 1.5107\,10^{153}\, {s_{1,3}}^{64} - 9.9266\,10^{154}\, {s_{1,3}}^{63} + 6.2462\,10^{156}\, {s_{1,3}}^{62} \\
&- 3.7628\,10^{158}\, {s_{1,3}}^{61} + 2.1696\,10^{160}\, {s_{1,3}}^{60} - 1.1969\,10^{162}\, {s_{1,3}}^{59} + 6.3154\,10^{163}\, {s_{1,3}}^{58} \\
&- 3.1856\,10^{165}\, {s_{1,3}}^{57} + 1.5353\,10^{167}\, {s_{1,3}}^{56} - 7.0650\,10^{168}\, {s_{1,3}}^{55} + 3.1020\,10^{170}\, {s_{1,3}}^{54} \\
&- 1.2984\,10^{172}\, {s_{1,3}}^{53} + 5.1748\,10^{173}\, {s_{1,3}}^{52} - 1.9615\,10^{175}\, {s_{1,3}}^{51} + 7.0595\,10^{176}\, {s_{1,3}}^{50} \\
&- 2.4079\,10^{178}\, {s_{1,3}}^{49} + 7.7641\,10^{179}\, {s_{1,3}}^{48} - 2.3591\,10^{181}\, {s_{1,3}}^{47} + 6.7261\,10^{182}\, {s_{1,3}}^{46} \\
&- 1.7886\,10^{184}\, {s_{1,3}}^{45} + 4.3961\,10^{185}\, {s_{1,3}}^{44} - 9.8442\,10^{186}\, {s_{1,3}}^{43} + 1.9561\,10^{188}\, {s_{1,3}}^{42} \\
&- 3.2556\,10^{189}\, {s_{1,3}}^{41} + 3.7746\,10^{190}\, {s_{1,3}}^{40} + 3.7789\,10^{190}\, {s_{1,3}}^{39} - 1.9038\,10^{193}\, {s_{1,3}}^{38} \\
&+ 7.1734\,10^{194}\, {s_{1,3}}^{37} - 1.8751\,10^{196}\, {s_{1,3}}^{36} + 3.8834\,10^{197}\, {s_{1,3}}^{35} - 6.3099\,10^{198}\, {s_{1,3}}^{34} \\
&+ 6.6906\,10^{199}\, {s_{1,3}}^{33} + 2.0383\,10^{200}\, {s_{1,3}}^{32} - 3.5351\,10^{202}\, {s_{1,3}}^{31} + 1.2135\,10^{204}\, {s_{1,3}}^{30} \\
&- 3.0316\,10^{205}\, {s_{1,3}}^{29} + 6.3595\,10^{206}\, {s_{1,3}}^{28} - 1.1749\,10^{208}\, {s_{1,3}}^{27} + 1.9535\,10^{209}\, {s_{1,3}}^{26} \\
&- 2.9560\,10^{210}\, {s_{1,3}}^{25} + 4.0962\,10^{211}\, {s_{1,3}}^{24} - 5.2162\,10^{212}\, {s_{1,3}}^{23} + 6.1146\,10^{213}\, {s_{1,3}}^{22} \\
&- 6.6023\,10^{214}\, {s_{1,3}}^{21} + 6.5653\,10^{215}\, {s_{1,3}}^{20} - 6.0073\,10^{216}\, {s_{1,3}}^{19} + 5.0514\,10^{217}\, {s_{1,3}}^{18} \\
&- 3.8970\,10^{218}\, {s_{1,3}}^{17} + 2.7528\,10^{219}\, {s_{1,3}}^{16} - 1.7765\,10^{220}\, {s_{1,3}}^{15} + 1.0450\,10^{221}\, {s_{1,3}}^{14} \\
&- 5.5886\,10^{221}\, {s_{1,3}}^{13} + 2.7106\,10^{222}\, {s_{1,3}}^{12} - 1.1893\,10^{223}\, {s_{1,3}}^{11} + 4.7079\,10^{223}\, {s_{1,3}}^{10} \\
&- 1.6757\,10^{224}\, {s_{1,3}}^{9} + 5.3402\,10^{224}\, {s_{1,3}}^{8} - 1.5139\,10^{225}\, {s_{1,3}}^{7} + 3.7811\,10^{225}\, {s_{1,3}}^{6} \\
&- 8.2030\,10^{225}\, {s_{1,3}}^{5} + 1.5138\,10^{226}\, {s_{1,3}}^{4} - 2.3010\,10^{226}\, {s_{1,3}}^{3} + 2.7265\,10^{226}\, {s_{1,3}}^{2} \\
&- 2.2556\,10^{226}\, s_{1,3} + 9.7893\,10^{225} = 0.
\end{aligned}
$$

The above polynomial has 76 real roots. The values of these roots as well as the corresponding configurations, for the case in which $P_1 = (12, 8)^T$, $P_4 = (9, 11)^T$, $P_7 = (10, 14)^T$, $P_{10} = (14, 15)^T$, $P_{13} = (17, 13)^T$, and $P_{16} = (16, 10)^T$, appear in Figs. 3.16, 3.17, and 3.18.

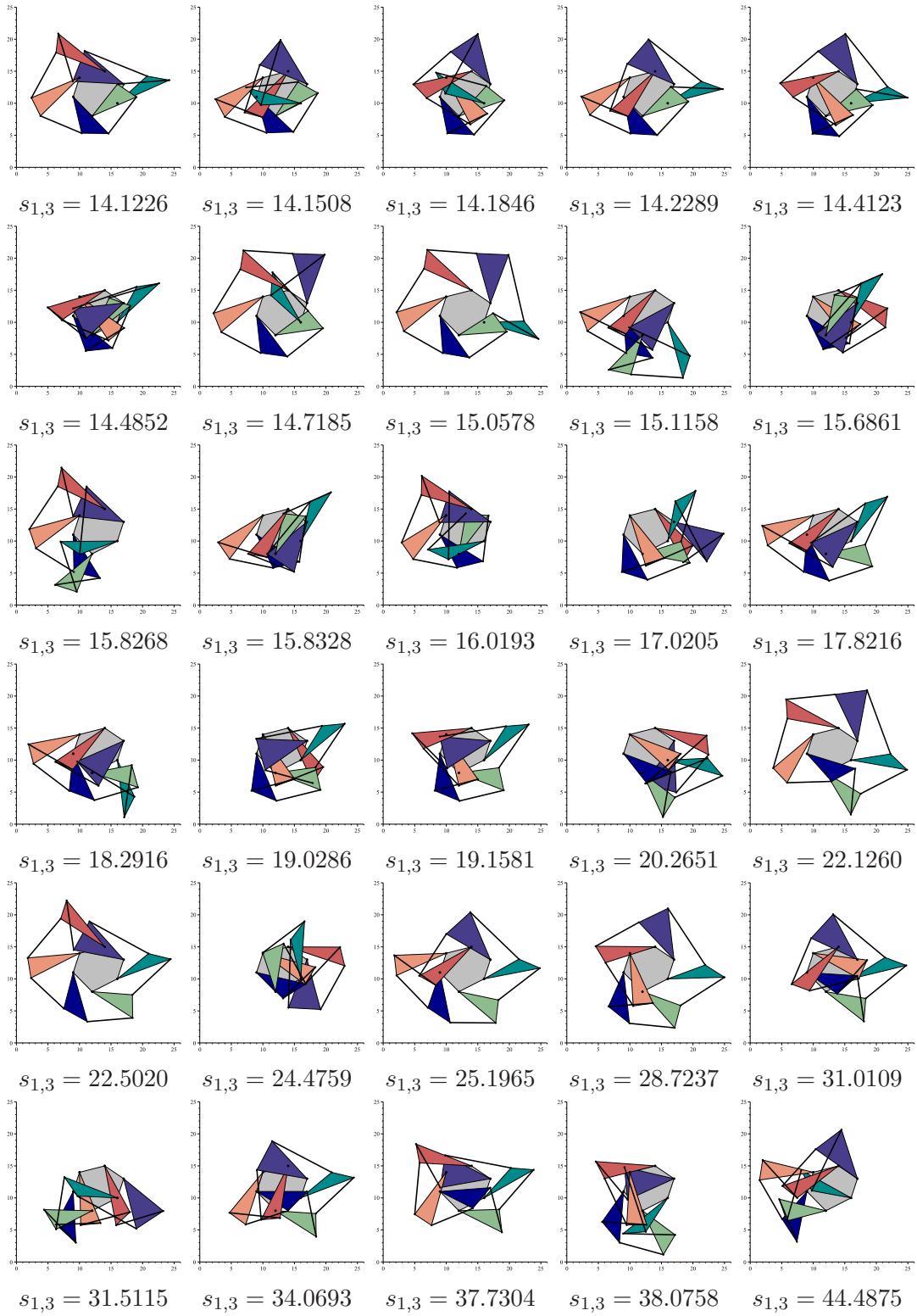

Figure 3.16. The configurations of the analyzed 13-link Watt-Baranov truss (Part 1/3).

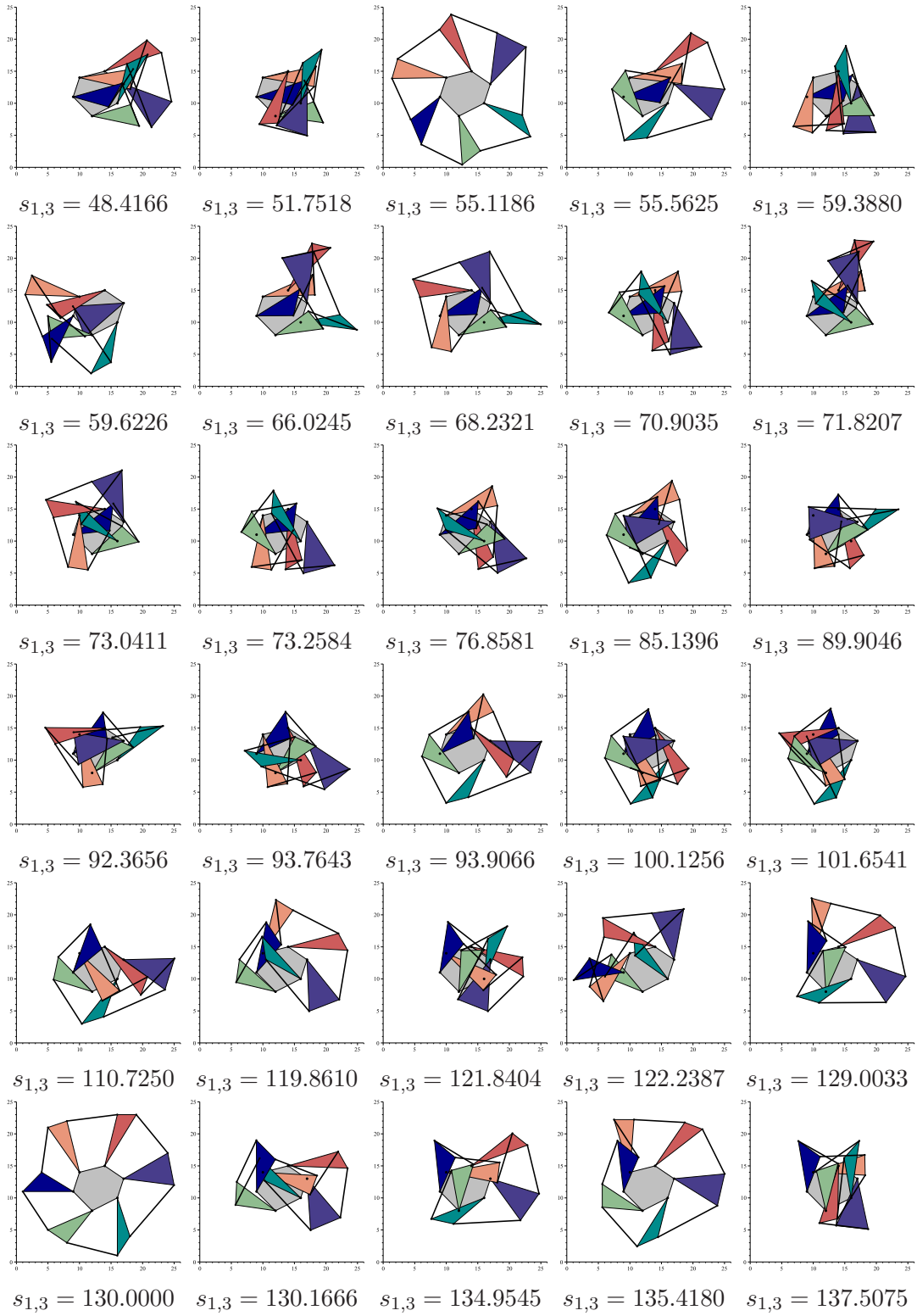

Figure 3.17. The configurations of the analyzed 13-link Watt-Baranov truss (Part 2/3).

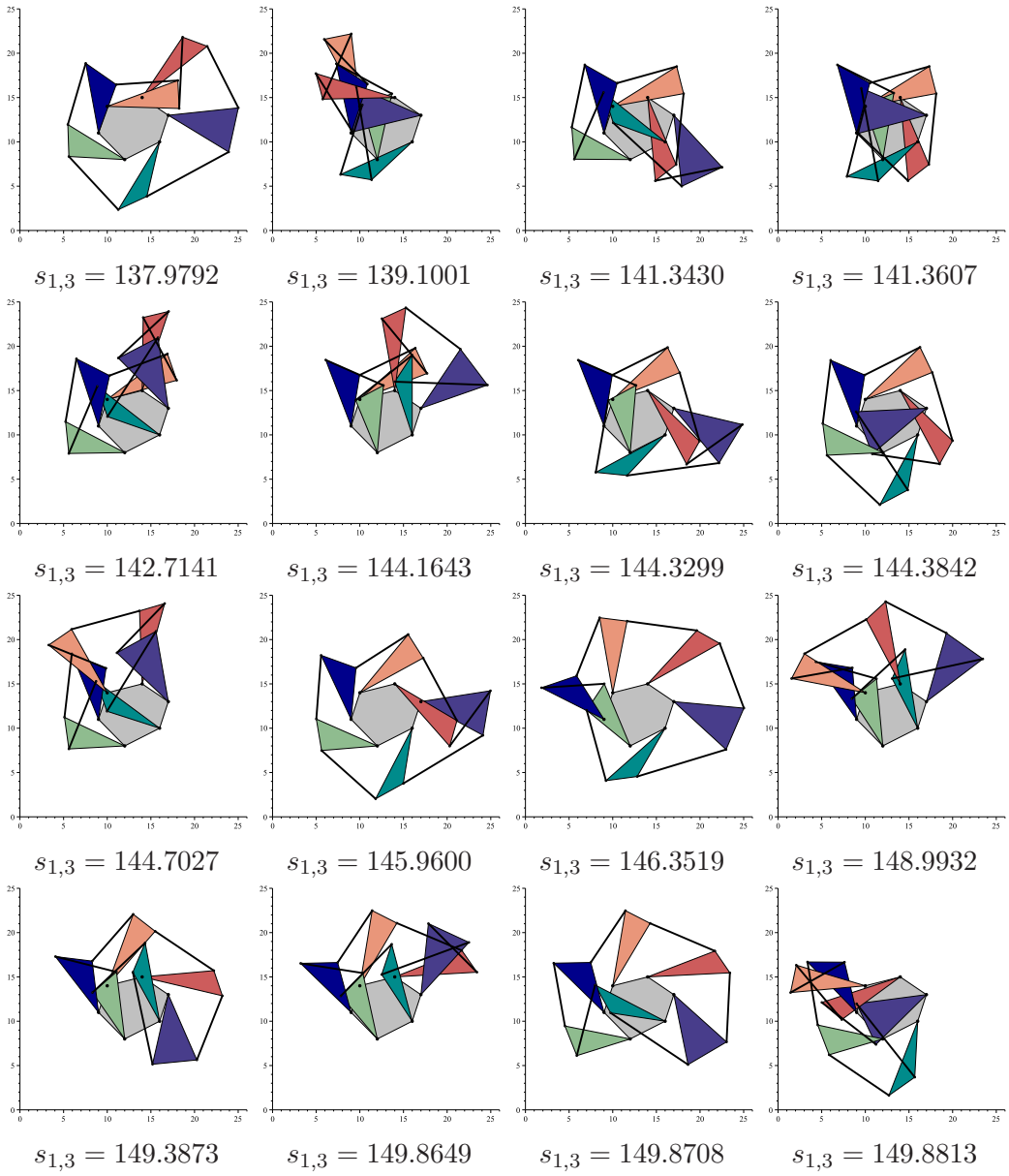

Figure 3.18. The configurations of the analyzed 13-link Watt-Baranov truss (Part 3/3).

Chapter 4

Position analysis of Assur kinematic chains

As already stated, a non-overconstrained closed planar linkage with zero-mobility from which an Assur group can be obtained by removing any of its links is defined as an Assur kinematic chain, basic truss [30, 50], or Baranov truss if no slider joints are considered [138]. Baranov trusses, that were widely studied in Chapter 3, play a fundamental role in *kinematics of mechanisms* principally because if the position analysis of a Baranov truss is solved, the same process can be applied to solve the position analysis of all its corresponding Assur groups. Moreover, all Assur kinematic chains can be derived from Baranov trusses by replacing revolute joints by slider joints bearing in mind that loops with only slider joints cannot be considered because they would reduce in one the number of constraints that make an Assur kinematic chain rigid [93]. Therefore, three different 3-link Assur kinematic chains can be derived from the triad —the only Baranov truss with 3 links— [30] [Fig. 4.1(left)], and ten 5-link Assur kinematic chains from the pentad —the only Baranov truss with 5 links— [105] [Fig. 4.1(right)].

Closed-form solutions for the position analysis of all Assur kinematic chains with 3 and 5 links have been obtained on an ad hoc basis by several authors. For the three 3-link Assur kinematic chains, explicit solutions to the position analysis problem can be found, for instance, in [30]. The position analysis problem of the ten 5-link Assur kinematic chains was solved for the first time in closed form by Li and Matthew in [105]. Other solutions for 5-link Assur kinematic chains have been presented, at least, in [36, 76, 125–127]. An extensive research on the position analysis of Assur kinematic chains with only revolute joints, i.e. Baranov trusses, has been performed by the kinematics community in the last decades, see Tables A.1-A.8 and the references therein, to the point that a closed-form solution of a 13-link (6 loop) Baranov truss, without relying on variable eliminations nor trigonometric substitutions, has been presented in the last chapter (§3.6.2). Beyond 5 links, the closed-form position analysis of some Assur kinematic chains has only been tackled, to our knowledge, by Wohlhart in [216–218]. In these works, using the Sylvester's elimination method, he successfully solved nine 9-link and one 11-link Assur kinematic chains.

General algorithms indeed exists for the closed-form position analysis of multi-loop planar linkages but they invariably rely on resultant elimination techniques applied to sets of kinematic loop equations. For example, as it was briefly discussed in §1.2.1.1, Nielsen and Roth [133], and Wampler [191] presented general methods for the analysis of planar linkages using the Dixon's resultant. Although the uniform treatment of these elimination-based methods of all planar linkages is remarkable, the position analysis of Assur kinematic chains based on them has to be carried out on a case-by-case basis because the required variable eliminations change.

In order to analyze Assur kinematic chains and Baranov trusses in a unified way, one possibility would be to introduce some transformations that would allow us to treat the translations associated with the slider joints as rotations. To this end, at least three

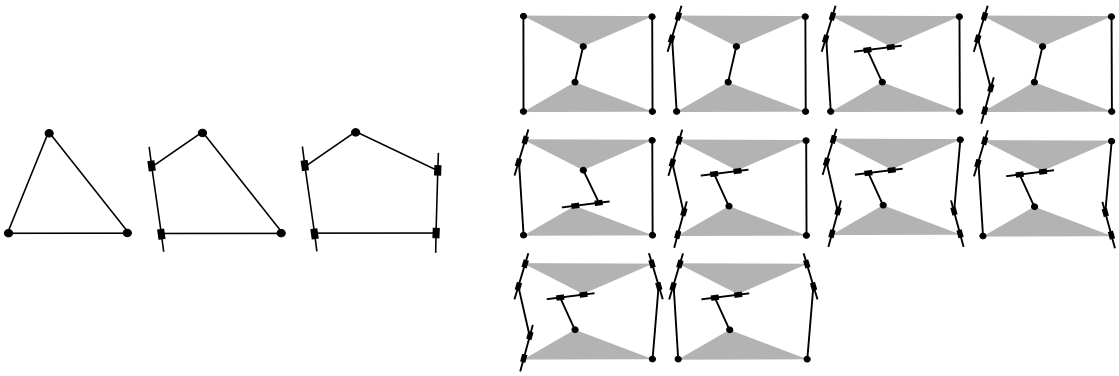

Figure 4.1. The three 3-link Assur kinematic chains **(left)**, and the ten 5-link Assur kinematic chains **(right)**.

options arise:

1. Substituting the slider joints by inversors [46, Ch. 8]. Although this would solve the problem, the resulting truss would be, in general, too complicated since one inversor should be introduced for each slider. Moreover, using this kind of substitutions, the analysis of a Baranov truss does not seem to provide any insight on the analysis of their derived Assur kinematic chains.

2. Adding one extra dimension which would permit to have an origin for the rotations which is lifted outside the 2D plane. Then, it would be possible to turn translations into rotations. This has to do with the stereographic projection. For example, in the framework of Clifford algebra, translations on a 2D plane are difficult to handle, but if one maps that plane onto the surface of a sphere in 3D, then one can identify the 2D translations with rotations on the surface of the 3D sphere. Although this approach is mathematically elegant by providing a unified treatment of Baranov trusses and Assur kinematic chains, it seems to give no clear advantage compared to the standard approach based on independent kinematic vector equations because the variables to be eliminated from the set of derived equations also change with the analyzed Assur kinematic chain.

3. Regarding a translational motion as an infinitely small rotation about a point at infinity. It is well-known that a translation in the direction (u_x, u_y) may be represented as a rotation about the ideal point given in homogeneous coordinates by $(-u_y, u_x, 0)^T$. This is probably the most intuitive and simple approach but, depending on the used formulation, it may be difficult to be accommodated. This chapter is essentially devoted to show how the intrinsic formulations based on distances and oriented areas resulting from bilateration techniques provide a framework within which this idea can be easily applied thus leading to the conclusion that the characteristic polynomials of the Baranov trusses contain all the necessary and sufficient information for solving the position analysis of all derived Assur kinematic chains [166].

4.1 Projective extensions of Baranov trusses

Let us suppose that the revolute joint centered at P_i in Fig. 4.2(a) is replaced by a slider joint as shown in Fig. 4.2(b) such that P_i is split into P_i' and P_i''. This new joint is placed

at fixed orientations with respect to the links connected to them. Once an orientation is assigned to the slider joint axis with respect to its adjacent links, a set of orientation angles can be defined (in this case α_j, α_k, α_l, and α_m) and, as a consequence, an oriented distance can be assigned to the points of the links connected by this joint with respect to this axis, as shown in Fig. 4.2(c). The sign of the considered distance will be the sign of the sine of the corresponding orientation. This defines a set of new points on the slider axis: those that realize the minimum distance to the considered points (in this case P'_j, P'_k, P'_l, and P'_m). Note that the slider joint imposes the alignment of all these points but, for the moment, let us suppose that they all are located at the same distance, say δ_i, from P_i^∞ as shown in Fig. 4.2(d). This would imply that they would lie on a circle but, if $\delta_i \to \infty$, they would again lie on a line as imposed by the slider join. The result of these geometric transformation is a joint whose topology is the same as that of the initial revolute joint, as shown in Fig. 4.2(e), but with the revolute center located at infinity.

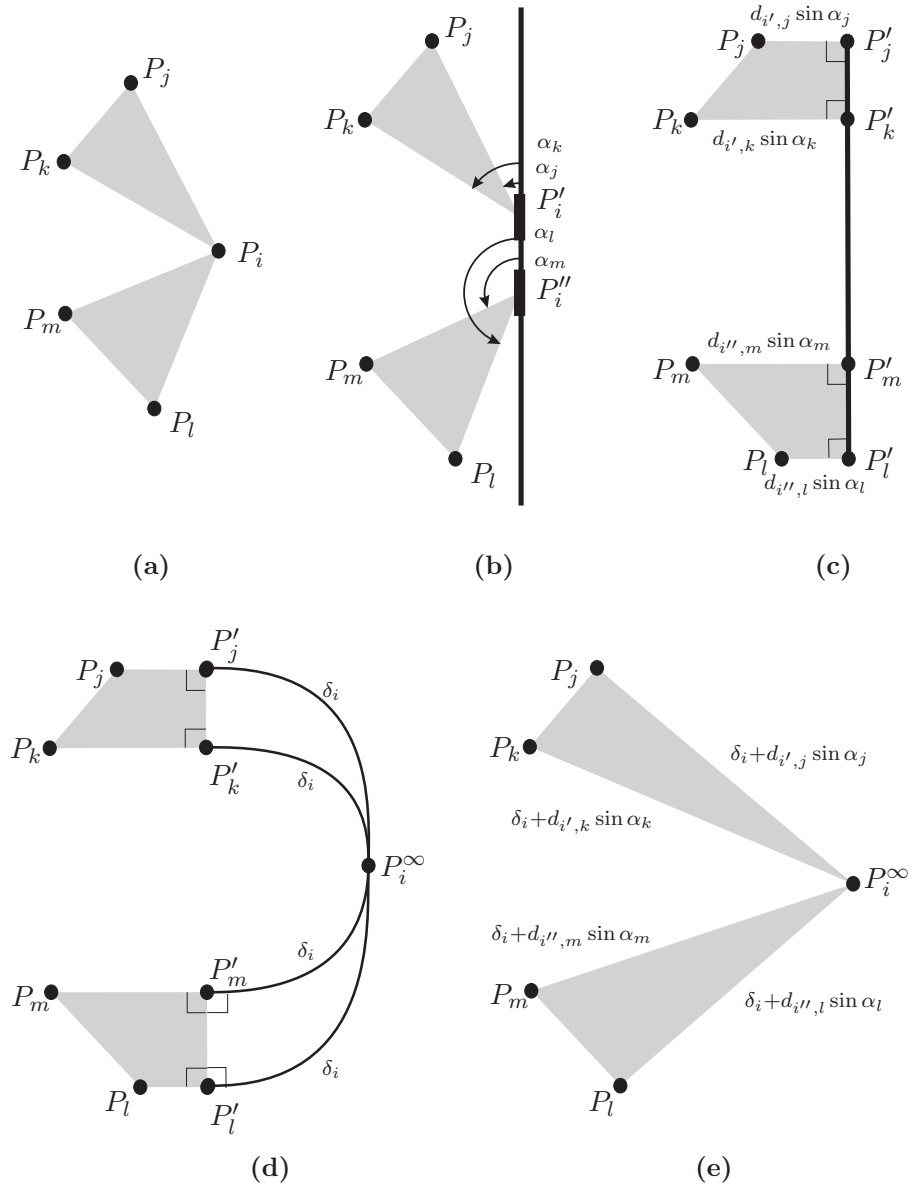

Figure 4.2. Geometric transformation that permits a slider joint that replaces a revolute joint be transformed back to a revolute joint centered at infinity.

It is worth noting that, after the described geometric transformation, it might happen that the orientations of $\triangle P_i^{\infty} P_j P_k$ or $\triangle P_i^{\infty} P_l P_m$ have changed with respect to that of $\triangle P_i P_j P_k$ or $\triangle P_i P_l P_m$, respectively, and this possible sign change has to be taken into account in the closure condition.

Although the described process is conceptually simple, three special situations arise that required a detailed analysis:

1. when two adjacent revolute joints are replaced by slider joints,
2. when a slider joint replaces a revolute joint acting as an end point of the segment whose distance is used as variable in the closure condition, and
3. when all the revolute joints of a link, different to a binary link[1], are replaced by slider joints

Handling these situations is not difficult but requires an explanation that is better understood through examples. For the first two special cases, this is carried out in the next section where the above geometric transformation is used to solve the position analysis of several seven-link Assur kinematic chains derived from the same Baranov truss. The third case is addressed in the next chapter (§5.2.1.3), for a ternary link, when solving the forward kinematics of all fully-parallel planar robots. This solution can be readily extended to higher order links because every n-ary link —*i.e.*, simple polygons of n vertices— can be triangulated[2] using $n-2$ triangles [135].

4.2 Position analysis of a family of seven-link Assur kinematic chains

The $7/B_3$ Baranov truss will be used to exemplify the ideas previously presented. First, we will recall how its characteristic polynomial and, as a consequence, their assembly modes can be derived from its closure condition given in terms of bilateration matrices. Then, we will see the effect of substituting one revolute joint by a slider joint —as shown in Fig. 4.4(a)— on this closure condition using the geometric transformations described in the previous section. This analysis leaves the way paved for the analysis of the Assur kinematic chains shown in Fig. 4.4(c), in which two adjacent revolute joints have been replaced by slider joints, and that shown in Fig. 4.8, in which one of the joints defining one of the end-points of the segment whose length is used as variable in the closure condition is replaced by a slider joint.

4.2.1 The assembly modes of the $7/B_3$ Baranov truss

Let us consider the $7/B_3$ Baranov truss in Fig. 4.3. It has three independent kinematic loops and nine joints. This truss was analyzed in detailed in Section 3.3.3. Its closure condition based on bilateration techniques, or distance-based closure condition, according to Fig. 4.3, can be written as (see Table A.1):

$$s_{2,8} = \det(\mathbf{Q})\, s_{1,6}, \tag{4.1}$$

[1]The case of a binary link is covered in the first situation

[2] Triangulation is the partition of a polygon into non-overlapping triangles using only diagonals between pairs of vertices

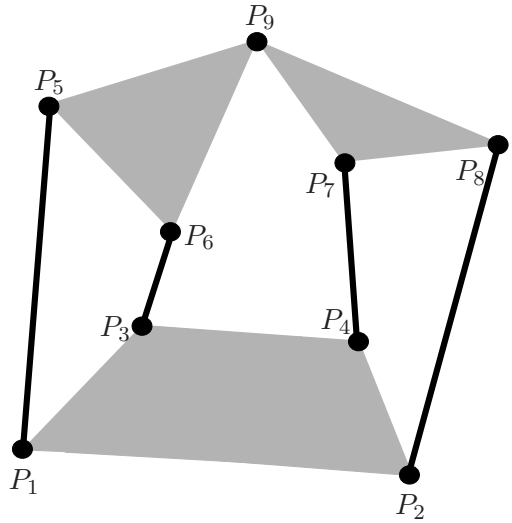

Figure 4.3. The $7/B_3$ Baranov truss.

where

$$\mathbf{Q} = \left(\mathbf{Z}_{1,3,4} - \mathbf{Z}_{1,3,2}\right)\mathbf{Z}_{1,6,3} + \left(\mathbf{I} - \mathbf{Z}_{9,7,8}\,\mathbf{Z}_{9,4,7}\right)\boldsymbol{\Omega}$$

with $\boldsymbol{\Omega} = -\mathbf{Z}_{1,3,4}\mathbf{Z}_{1,6,3} + \mathbf{I} - \mathbf{Z}_{6,5,9}\mathbf{Z}_{6,1,5}$ and $s_{4,9} = \det(\boldsymbol{\Omega})$. This equation expresses the set of values of $s_{1,6}$ compatible with all links side lengths and the signs of the oriented areas of the triangles $\triangle P_5P_6P_9$, $\triangle P_7P_8P_9$, $\triangle P_1P_2P_3$ and $\triangle P_1P_3P_4$. Once the dimensions of the truss links have been substituted in equation (4.1) and the result expanded, a scalar radical equation in function of the unknown squared distance $s_{1,6}$ is obtained which can be solved using, for example, a Newton interval method. Alternatively, a polynomial representation can be derived. For example, according to the notation used in Fig. 4.4, let us set $s_{1,2} = 49$, $s_{1,3} = 13$, $s_{1,4} = 29$, $s_{1,5} = 101$, $s_{2,3} = 34$, $s_{2,4} = 8$, $s_{2,8} = 82$, $s_{3,4} = 10$, $s_{3,6} = 36$, $s_{4,7} = 52$, $s_{5,6} = 10$, $s_{5,9} = 29$, $s_{6,9} = 13$, $s_{7,8} = 10$, $s_{7,9} = 34$, and $s_{8,9} = 20$. Substituting these values in equation (4.1), expanding it, clearing radicals, and factorizing the result, we obtain the characteristic polynomial:

$$\begin{aligned}
&s_{1,6}^{18} - 1146.0063\, s_{1,6}^{17} + 6.1754\,10^{5}\, s_{1,6}^{16} - 2.0755\,10^{8}\, s_{1,6}^{15} + 4.8684\,10^{10}\, s_{1,6}^{14} \\
&- 8.4515\,10^{12}\, s_{1,6}^{13} + 1.1239\,10^{15}\, s_{1,6}^{12} - 1.1693\,10^{17}\, s_{1,6}^{11} + 9.6369\,10^{18}\, s_{1,6}^{10} \\
&- 6.3307\,10^{20}\, s_{1,6}^{9} + 3.3187\,10^{22}\, s_{1,6}^{8} - 1.3832\,10^{24}\, s_{1,6}^{7} + 4.5432\,10^{25}\, s_{1,6}^{6} \\
&- 1.1580\,10^{27}\, s_{1,6}^{5} + 2.2360\,10^{28}\, s_{1,6}^{4} - 3.1489\,10^{29}\, s_{1,6}^{3} + 3.0382\,10^{30}\, s_{1,6}^{2} \\
&- 1.7877\,10^{31}\, s_{1,6} + 4.8226\,10^{31}.
\end{aligned}$$

The real roots of this polynomial are 88.5700 and 90.8322. The corresponding configurations, for the case in which the ground link is the quaternary link with points located at $P_1 = (1,0)^T$, $P_2 = (8,0)^T$, $P_3 = (3,3)^T$, and $P_4 = (6,2)^T$, appear in Fig. 4.5.

Next, we will see the effect of replacing a revolute joint by a slider joint on this truss.

4.2.2 Replacing one revolute joint

When the revolute joint centered at P_9 in the above Baranov truss is replaced by a slider joint as indicated in Fig. 4.4(a), an Assur kinematic chain is obtained. In accordance

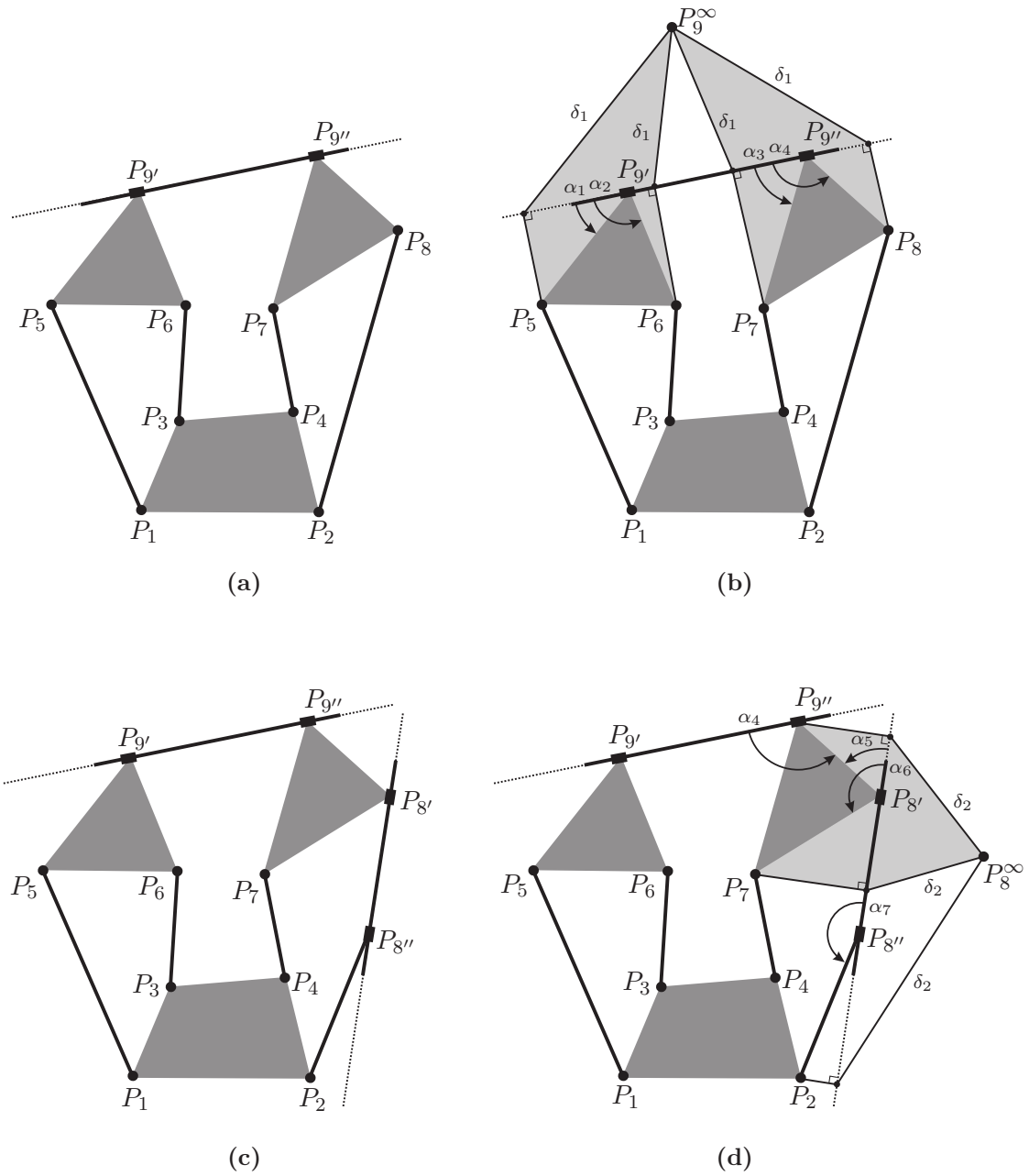

Figure 4.4. The distance-based closure condition of the seven-link Assur kinematic chain with one slider joint in **(a)** can be obtained by properly substituting in the original closure condition the square lengths $s_{5,9}$, $s_{6,9}$, $s_{7,9}$, and $s_{8,9}$, with $\delta_1 \to \infty$ **(b)**. The distance-based closure condition of the seven-link Assur kinematic chain with two slider joints **(c)** can be computed by properly substituting in the original closure condition $s_{5,9}$, $s_{6,9}$, $s_{7,9}$, $s_{7,8}$, $s_{8,9}$, and $s_{2,8}$, with $\delta_1 \to \infty$ and $\delta_2 \to \infty$ **(d)**.

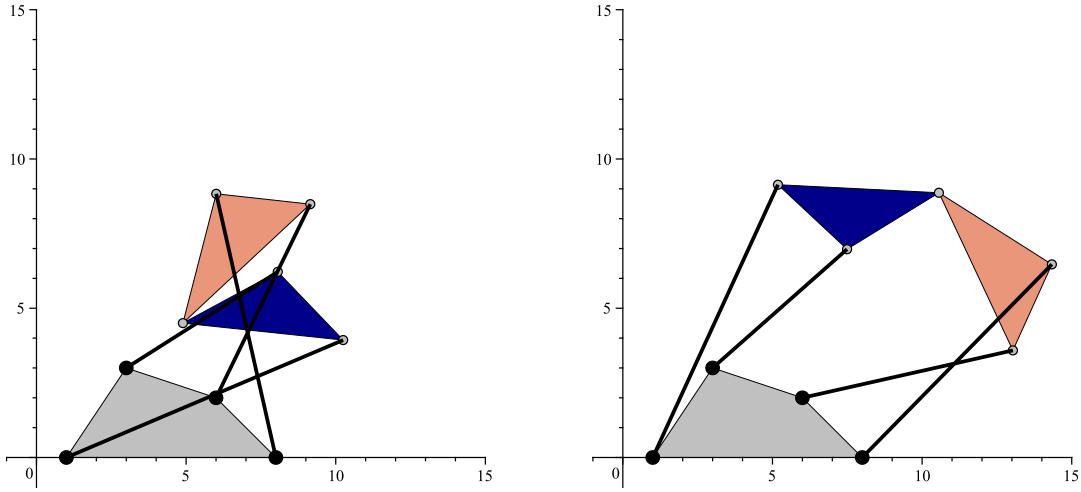

$s_{1,6} = 88.5700$ $s_{1,6} = 90.8322$

Figure 4.5. The configurations of the $7/B_3$ Baranov truss used as reference truss.

with the notation used in Fig. 4.4(b), the distance-based closure condition of this new linkage can be obtained, as explained in section 4.1, by substituting in equation (4.1):

$$\begin{aligned} d_{5,9} &= \delta_1 + d_{5,9'} \sin\alpha_1, \\ d_{6,9} &= \delta_1 + d_{6,9'} \sin\alpha_2, \\ d_{7,9} &= \delta_1 + d_{7,9''} \sin\alpha_3, \\ d_{8,9} &= \delta_1 + d_{8,9''} \sin\alpha_4, \end{aligned}$$

with $\delta_1 \to \infty$. That is,

$$\lim_{\delta_1\to\infty} \left(\det(\mathbf{Q})\, s_{1,6} - s_{2,8}\right) \Big|_{\substack{d_{5,9} = \delta_1 + d_{5,9'} \sin\alpha_1 \\ d_{6,9} = \delta_1 + d_{6,9'} \sin\alpha_2 \\ d_{7,9} = \delta_1 + d_{7,9''} \sin\alpha_3 \\ d_{8,9} = \delta_1 + d_{8,9''} \sin\alpha_4.}} \tag{4.2}$$

Note that the expression $\det(\mathbf{Q})\, s_{1,6} - s_{2,8}$, after the substitutions, can be written as a polynomial in δ_1. Therefore, the above limit can be expressed as:

$$\lim_{\delta_1\to\infty} \sum_{i=0}^{n} \phi_i(s_{1,6})\delta_1^i \Big|_{\substack{d_{5,9} = \delta_1 + d_{5,9'} \sin\alpha_1 \\ d_{6,9} = \delta_1 + d_{6,9'} \sin\alpha_2 \\ d_{7,9} = \delta_1 + d_{7,9''} \sin\alpha_3 \\ d_{8,9} = \delta_1 + d_{8,9''} \sin\alpha_4.}}$$

Then, we conclude that, for this limit to be zero, $\phi_n(s_{1,6}) = 0$. In other words, the new distance-based closure condition is indeed $\phi_n(s_{1,6}) = 0$.

Now, according to the notation of Fig. 4.4(b), let us suppose that all link dimensions of the original Baranov truss remain unaltered, that is, $s_{5,9'} = s_{5,9}$, $s_{6,9'} = s_{6,9}$, $s_{7,9''} = s_{7,9}$, and $s_{8,9''} = s_{8,9}$, and that the orientation of the new slider joint is fixed with respect to its adjacent links such that $\alpha_1 = \pi - \arctan\frac{5}{2}$ and $\alpha_3 = 2\pi - \arctan\frac{5}{3}$. Then, given the orientations of $\triangle P_5P_6P_{9'}$ and $\triangle P_7P_8P_{9''}$, it turns out that $\alpha_2 = \pi - \arctan\frac{2}{3}$ and $\alpha_4 = 2\pi - \arctan\frac{1}{2}$. Substituting these values in equation (4.2), expanding it, computing the leading coefficient of the resulting polynomial in δ_1, clearing radicals, and factorizing

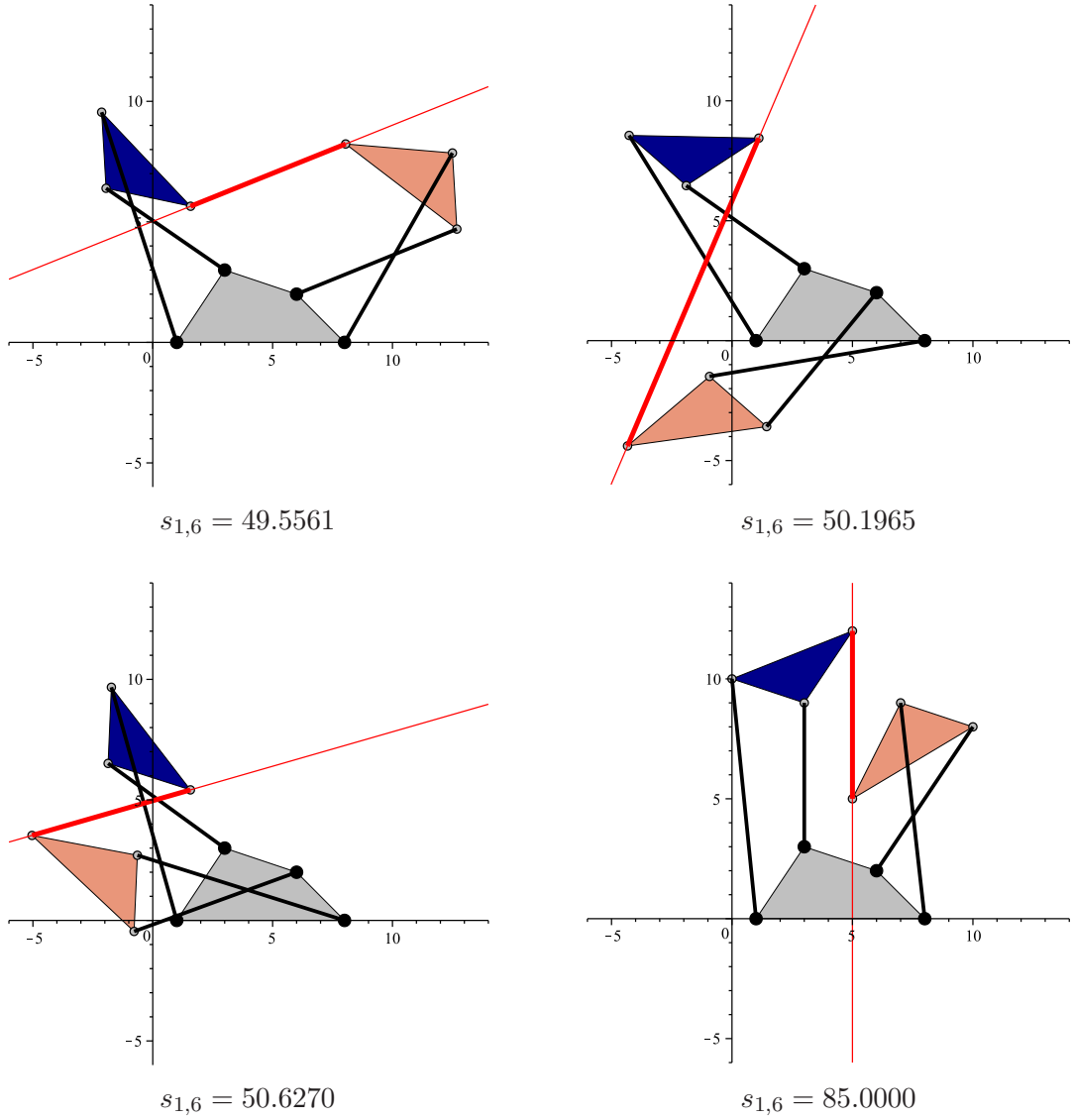

Figure 4.6. The configurations of the analyzed Assur kinematic chain with one slider joint.

the result, we obtain the characteristic polynomial

$$\begin{aligned}
&s_{1,6}^{16} - 1088.1889\, s_{1,6}^{15} + 5.5629\, 10^{5}\, s_{1,6}^{14} - 1.7759\, 10^{8}\, s_{1,6}^{13} + 3.9687\, 10^{10}\, s_{1,6}^{12} \\
&- 6.5911\, 10^{12}\, s_{1,6}^{11} + 8.4263\, 10^{14}\, s_{1,6}^{10} - 8.4748\, 10^{16}\, s_{1,6}^{9} + 6.7979\, 10^{18}\, s_{1,6}^{8} \\
&- 4.3842\, 10^{20}\, s_{1,6}^{7} + 2.2802\, 10^{22}\, s_{1,6}^{6} - 9.5228\, 10^{23}\, s_{1,6}^{5} + 3.1426\, 10^{25}\, s_{1,6}^{4} \\
&- 7.9121\, 10^{26}\, s_{1,6}^{3} + 1.4233\, 10^{28}\, s_{1,6}^{2} - 1.6169\, 10^{29}\, s_{1,6} + 8.6390\, 10^{29}.
\end{aligned}$$

The real roots of this polynomial are 49.5561, 50.1965, 50.6270, and 85.0000. The corresponding configurations associated to these new assembly modes appear in Fig. 4.6.

4.2.3 Replacing two adjacent revolute joints

Now, let us suppose that the revolute joint centered at P_8 is also replaced by a slider joint as shown in Fig. 4.4(c). Then, according to the notation used in Fig. 4.4(d), following

the same reasoning used above, the substitutions to be performed in equation (4.1) are:

$$\begin{aligned}
d_{5,9} &= \delta_1 + d_{5,9'} \sin\alpha_1,\\
d_{6,9} &= \delta_1 + d_{6,9'} \sin\alpha_2,\\
d_{7,9} &= \delta_1 + d_{7,9''} \sin\alpha_3,\\
d_{7,8} &= \delta_2 + d_{7,8'} \sin\alpha_6,\\
d_{2,8} &= \delta_2 + d_{3,8''} \sin\alpha_7,
\end{aligned}$$

with $\delta_1 \to \infty$ and $\delta_2 \to \infty$. To obtain the substitution for $d_{8,9}$, observe that the angle formed by the two slider joints is $\alpha_5 - \alpha_4$. Then,

$$\angle P_8^\infty P_7 P_9^\infty = \pi - \alpha_5 + \alpha_4.$$

Hence, using the cosine theorem, we conclude that:

$$\begin{aligned}
s_{8,9} = d_{8,9}^2 =& d_{7,8}^2 + d_{7,9}^2 - 2\, d_{7,8} d_{7,9} \cos(\pi - \alpha_5 + \alpha_4)\\
=& (\delta_2 + d_{7,8'} \sin\alpha_6)^2 + (\delta_1 + d_{7,9''} \sin\alpha_3)^2\\
&+ 2(\delta_2 + d_{7,8'} \sin\alpha_6)(\delta_1 + d_{7,9''} \sin\alpha_3) \cos(\alpha_5 - \alpha_4).
\end{aligned}$$

with $\delta_1 \to \infty$ and $\delta_2 \to \infty$. Therefore, the closure condition for the new seven-link Assur kinematic chain results from computing

$$\lim_{\delta_2\to\infty} \Big(\lim_{\delta_1\to\infty} (\det(\mathbf{Q}) s_{1,6} - s_{2,8}) \Big) \Bigg|_{\substack{d_{5,9} = \delta_1 + d_{5,9'} \sin\alpha_1\\ d_{6,9} = \delta_1 + d_{6,9'} \sin\alpha_2\\ d_{7,9} = \delta_1 + d_{7,9''} \sin\alpha_3\\ d_{7,8} = \delta_2 + d_{7,8'} \sin\alpha_6\\ d_{8,9}^2 = d_{7,8}^2 + d_{7,9}^2 + 2\, d_{7,8} d_{7,9} \cos(\alpha_5 - \alpha_4)\\ d_{2,8} = \delta_2 + d_{3,8''} \sin\alpha_7.}} \tag{4.3}$$

According to the notation used in Fig. 4.4(d), let us again suppose that the dimensions of all links remain unaltered, that is, $s_{2,8''} = s_{2,8}$, $s_{5,9'} = s_{5,9}$, $s_{6,9'} = s_{6,9}$, $s_{7,8'} = s_{7,8}$, $s_{7,9''} = s_{7,9}$, and $s_{8',9''} = s_{8,9}$, and the orientation of the second slider joint is fixed with respect to its adjacent links such that $\alpha_5 = \pi - \arctan 3$ and $\alpha_7 = \pi - \arctan 4$. Then, given the orientation of $\triangle P_7 P_{8'} P_{9''}$, it turns out that $\alpha_6 = \pi + \arctan \frac{1}{2}$. Substituting these values in equation (4.3), expanding it, computing the leading coefficient of the resulting polynomial in δ_1 and then in δ_2, and clearing radicals, we obtain the following characteristic polynomial:

$$\begin{aligned}
&s_{1,6}^{12} - 801.1113\, s_{1,6}^{11} + 2.8716\, 10^5\, s_{1,6}^{10} - 6.0970\, 10^7\, s_{1,6}^{9} + 8.5621\, 10^9\, s_{1,6}^{8}\\
&- 8.4211\, 10^{11}\, s_{1,6}^{7} + 6.0004\, 10^{13}\, s_{1,6}^{6} - 3.1645\, 10^{15}\, s_{1,6}^{5} + 1.2496\, 10^{17}\, s_{1,6}^{4}\\
&- 3.6854\, 10^{18}\, s_{1,6}^{3} + 7.8680\, 10^{19}\, s_{1,6}^{2} - 1.1067\, 10^{21}\, s_{1,6} + 7.7765\, 10^{21}.
\end{aligned}$$

The real roots of this polynomial are 48.1037, 85.0000, 88.2000, and 88.5483. The corresponding configurations associated to these assembly modes appear in Fig. 4.7.

4.2.4 Replacing a revolute joint involved in the definition of the variable distance

According to Fig. 4.8, let us now suppose that the revolute joint centered at P_1 is replaced by a slider joint in the original Baranov truss. In this case, the substitutions

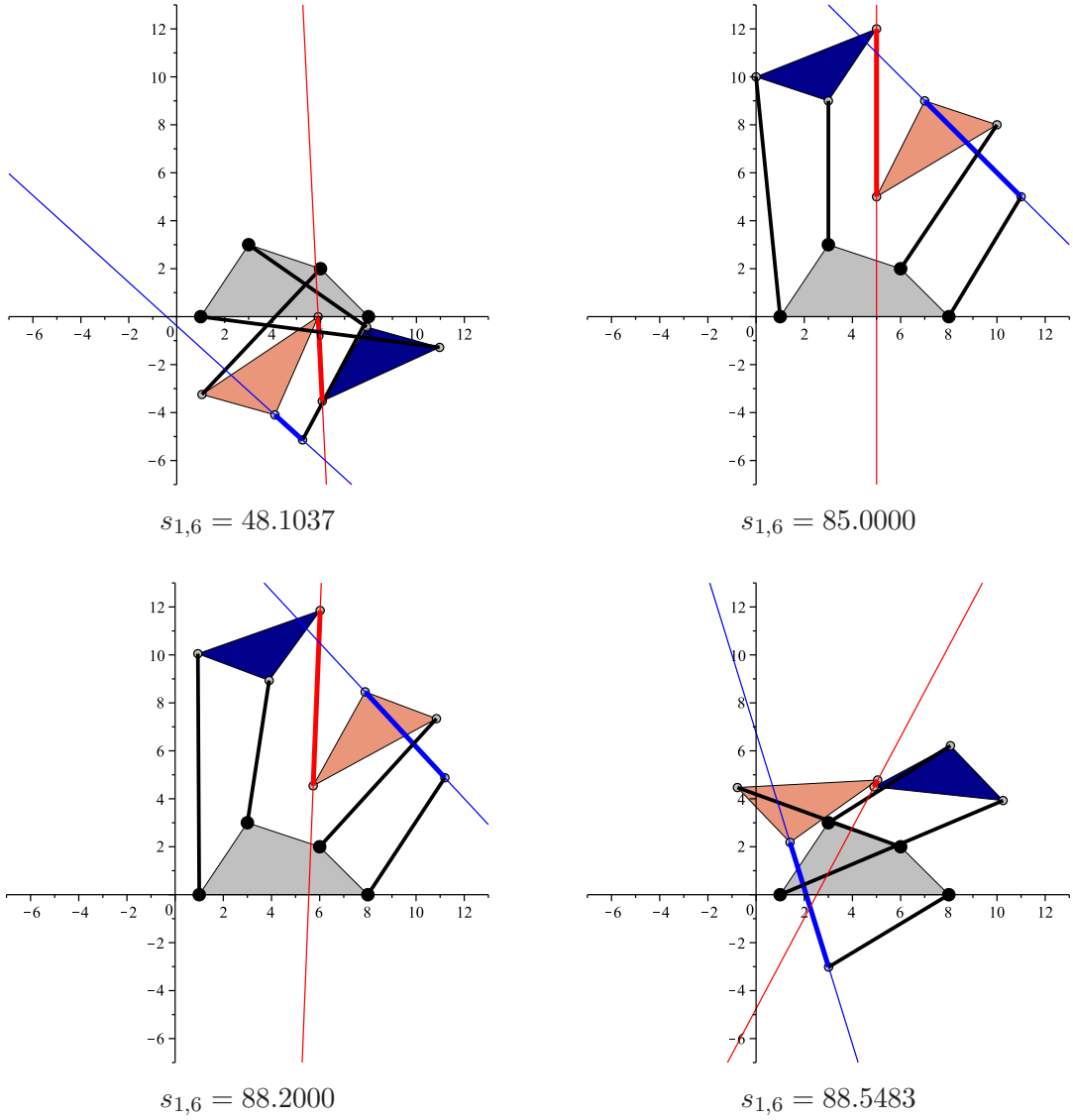

Figure 4.7. The configurations of the analyzed Assur kinematic chain with two slider joints.

to be performed in expression (4.1) are:

$$\begin{aligned} d_{1,2} &= \delta_3 + d_{1',2} \sin \alpha_1, \\ d_{1,3} &= \delta_3 + d_{1',3} \sin \alpha_3, \\ d_{1,4} &= \delta_3 + d_{1',4} \sin \alpha_2, \\ d_{1,5} &= \delta_3 + d_{1'',5} \sin \alpha_4, \\ d_{1,6} &= \delta_3 + t, \end{aligned} \tag{4.4}$$

with $\delta_3 \to \infty$. Then, the new closure condition depends on a new variable, t, the oriented distance between P_6 and the slider joint axis.

According to the notation used in Fig. 4.8, let us suppose as above that the dimension of all the original truss links remain unaltered after this substitution, that is, $s_{1',2} = s_{1,2}$, $s_{1',3} = s_{1,3}$, $s_{1',4} = s_{1,4}$, $s_{1'',5} = s_{1,5}$, and the orientation of the introduced slider joint axis with respect to its adjacent links is given by $\alpha_1 = 0$ and $\alpha_4 = \arctan 10$. Then, given the orientations of $\triangle P_{1'} P_2 P_4$ and $\triangle P_{1'} P_4 P_3$, it turns out that $\alpha_2 = \arctan \frac{2}{5}$ and

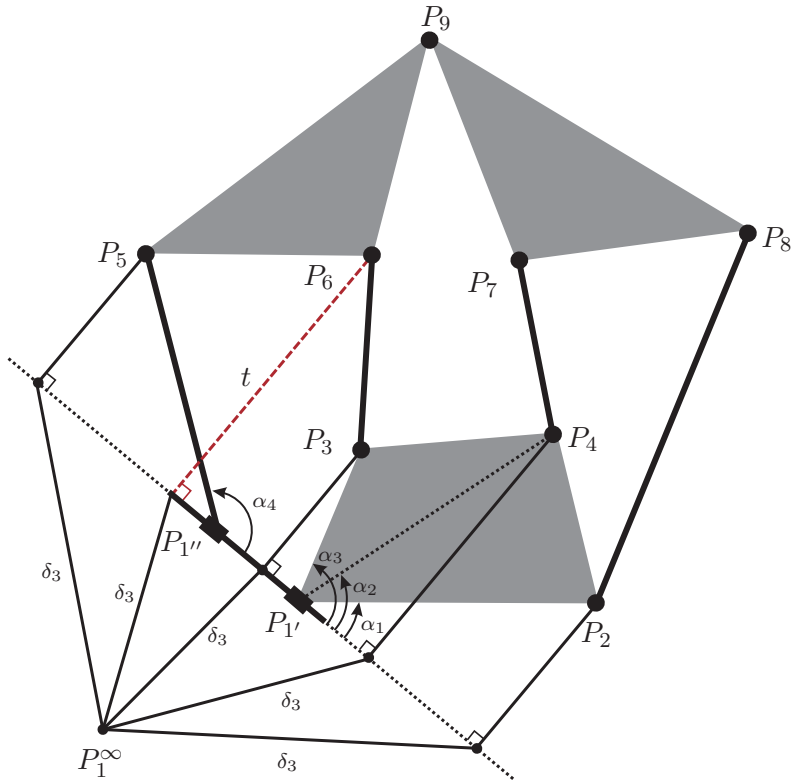

Figure 4.8. Example in which a slider replaces the revolute joint involved in the definition of the distance in which the closure condition of the truss is expressed.

$\alpha_3 = \arctan \frac{3}{2}$. Finally, performing the substitutions given in (4.4) in equation (4.1), expanding the result, computing the leading coefficient of the resulting polynomial in δ_3, and clearing radicals, we obtain the characteristic polynomial:

$$
\begin{aligned}
& t^{18} - 99.9226\, t^{17} + 4616.5154\, t^{16} - 1.3111\, 10^{5}\, t^{15} + 2.5703\, 10^{6}\, t^{14} \\
& - 3.7071\, 10^{7}\, t^{13} + 4.0975\, 10^{8}\, t^{12} - 3.5707\, 10^{9}\, t^{11} + 2.5033\, 10^{10}\, t^{10} \\
& - 1.4322\, 10^{11}\, t^{9} + 6.7649\, 10^{11}\, t^{8} - 2.6752\, 10^{12}\, t^{7} + 9.0667\, 10^{12}\, t^{6} \\
& - 2.7287\, 10^{13}\, t^{5} + 7.5300\, 10^{13}\, t^{4} - 1.8819\, 10^{14}\, t^{3} + 3.8837\, 10^{14}\, t^{2} \\
& - 5.5359\, 10^{14}\, t + 3.8671\, 10^{14}.
\end{aligned}
$$

The real roots of this polynomial are 7.4867 and 8.7825. The corresponding configurations associated to these assembly modes appear in Fig. 4.9.

Note that the case in which two slider joints replace the two revolute joints defining the endpoints of the segment whose length is used as variable in the closure condition can always be avoided because all kinematic loops of an Assur kinematic chain contain at least one revolute joint.

In this chapter, we have shown how all Assur kinematic chains can be seen as projective extensions of Baranov trusses, that is, Baranov trusses with revolute joint centers located at infinity and how this fact can be easily accommodated in a distance-based formulation. This result leads to the conclusion that the closure conditions for the Baranov trusses thus formulated can be directly used to solve the position analysis of all Assur kinematic chains derived from them. Since the distance-based closure conditions for all the cataloged Baranov trusses have been presented in Chapter 3, the position analysis

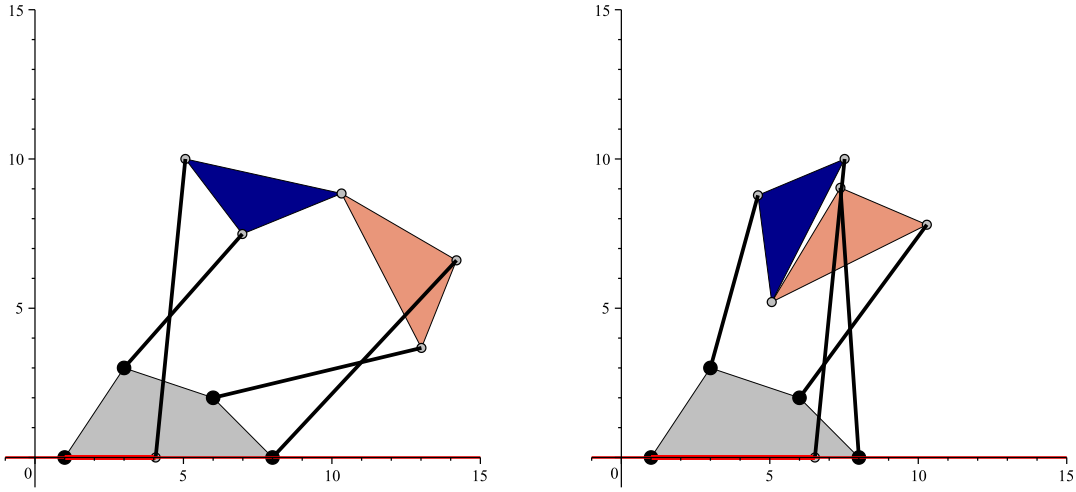

$t = 7.4867$ $t = 8.7825$

Figure 4.9. The configurations of the analyzed seven-link Assur kinematic chain whose closure condition is expressed in terms of the oriented distance between a revolute joint and the slider joint axis.

of all derived Assur kinematics chains can be carried out without having to perform new sets of variable eliminations, as it is the usual practice when deriving characteristic polynomials from sets of independent vector loop equations.

Chapter 5

The forward kinematics of all fully-parallel planar robots

5.1 The forward kinematics of 3-R$\underline{\text{P}}$R planar robots

Much has been written about the 3-R$\underline{\text{P}}$R planar parallel robot because of its practical interest, mechanical simplicity, and rich mathematical properties [123]. Such a robot consist of a moving platform connected to the ground through three revolute-prismatic-revolute kinematic chains. The prismatic joint of each chain is actuated and the forward kinematics problem consists in, given the prismatic joint lengths, calculating the Cartesian pose of the moving platform. A clever reasoning, based on the number of possible intersections between a circle and the general coupler curve of a 4-bar mechanism, permits to conclude that this problem has at most 6 different solutions [80]. That is, for fixed leg lengths, it is possible to assemble the robot in up to six different ways, known as *assembly modes*. In general, it is not possible to express analytically these six Cartesian poses as functions of the actuated joint coordinates, except for some particular cases known as *analytic robots* [54]. This chapter is devoted to the problem of finding these poses efficiently and accurately for all cases.

The usual approach to obtain the aforementioned assembly modes consists in manipulating the kinematic equations of the robot to reduce the problem to finding the roots of a polynomial in one variable, the *characteristic polynomial*, which must be of the lowest possible degree, that is, a sextic. E. Peysah is credited to be the first researcher in obtaining this sextic in 1985 [137]. The same result was obtained independently at least by G. Pennock and D. Kassner in 1990 [141], K. Wohlhart in 1992 [214], and C. Gosselin *et al.*, also in 1992 [56]. The formulation due to C. Gosselin *et al.* has become thereafter the standard one. The major step in this formulation is to find an equation only in θ (the orientation of the moving platform), that is, to eliminate all other variables from the system until an equation is obtained that contains only θ. Finally, a tangent-half-angle substitution is applied to translate sine and cosine functions of θ into rational polynomial expressions in a new variable $t = \tan(\theta/2)$.

In order to simplify as much as possible the coefficients of the resulting 6th-degree polynomial, it is possible to express the coordinates of the base attachments according to a specific coordinate frame. For example, by making one coordinate axis to coincide with the baseline between two base attachments and/or locating the origin at one base attachment. Nevertheless, this kind of simplifications has an important drawback: the numerical conditioning of the resulting formulation depends on the chosen reference frame. This is why those formulations which are not linked to a particular reference frame —or coordinate-free formulations— are preferable. In 2001, X. Kong and C. Gosselin proposed a coordinate-free formulation by deriving a sextic in $\tan(\psi/2)$, where ψ is the angle formed between one leg and one of its adjacent base sides [98]. Although

this formulation was used to study analytic instances, it is certainly superior to the one in [56] for the aforementioned reason. Nevertheless, the problems derived from the tangent-half-angle substitution still remained.

The tangent-half-angle substitution poses two well-known problems. One results from the fact that $\tan(\theta/2)$ is undefined for $\theta = \pm\pi$. Moreover, it can become difficult to reconstruct other roots, occurring in conjunction with the root $\theta = \pm\pi$ [106]. The other problem is the introduction of extraneous roots. Both problems are well known and can be handled but it complicates notably subsequent calculations [100]. One alternative to this substitution is to keep $\cos(\theta)$ and $\sin(\theta)$, both as variables, and to add the equation $\sin^2(\theta) + \cos^2(\theta) = 1$ to the elimination process.

A more elegant mathematical framework is obtained by viewing the planar moving platform displacements as points in a four-dimensional homogeneous space. This can be achieved using, for example, the kinematic mapping, as in [81] and further elaborated in [76], or Clifford algebra, as in [37]. A similar treatment may be obtained by using the substitutions $\sin(\theta) = 2sc/(c^2+s^2)$ and $\cos(\theta) = (c^2-s^2)/(c^2+s^2)$ which, after clearing denominators, lead to homogeneous equations in s and c. This noncoordinate-free formulations avoid the tangent-half-angle substitution but the problem with $\pm\pi$ turns still remains if one of the used homogeneous coordinates is normalized to 1. Alternatively, a normalizing condition involving two variables is possible thus adding one more equation to the elimination process.

An important fact that has been commonly overlooked by the robotics community is that solving the forward kinematics of the 3-R$\underline{\text{P}}$R parallel robot is equivalent to finding the distinct planar embeddings, up to Euclidean motions, of a graph with vertices subject to edge lengths constraints. This graph corresponds to what in [153] is called the *doublet*, or in [18], the *Desargues framework*. In both cases, the number of possible embeddings is obtained by formulating the problem purely in terms of distances. This kind of approach leads to undesired solutions to the original problem because the embeddings containing mirror reflections of the base and/or the moving platform also count as valid solutions. In [153], the embedding problem is tackled by assigning coordinates to two points whose distance is known and solving a system of 8 equations (the remaining 8 distances constraints) in 8 variables (the coordinates of the remaining 4 points). The resultant is a polynomial of degree 28 which factors as the product of a degree 12 and a degree 16 polynomial. Alternatively, in [18], the problem is formulated in terms of equations involving Cayley-Menger determinants which permit to conclude that there exists edge lengths which induce up to 24 embeddings, 6 for each combination of the base and the platform triangles and their mirror reflections. In this chapter, we introduce a further twist to this approach that allows us to solve the problem by a sequence of bilaterations. As a result, a 6th-degree characteristic polynomial, which is not linked to any particular reference frame, is straightforwardly obtained without variable eliminations nor tangent-half-angle substitutions. Moreover, the obtained polynomial is mathematically more tractable than the one obtained using other approaches because its coefficients are the result of operating with bilateration matrices.

5.1.1 Distance-based formulation

Figure 5.1 shows a general 3-R$\underline{\text{P}}$R planar robot platform. The center of the three grounded passive revolute joints, ◒, define the base oriented triangle $\triangle P_1P_2P_3$ and the three moving passive revolute joints centers, ●, the moving oriented triangle $\triangle P_4P_5P_6$. The squared lengths of the active prismatic joints are $s_{1,4}$, $s_{2,5}$, and $s_{3,6}$. Angles α and β have been chosen so that their signs determine the orientation of the base and platform triangles, respectively. Note that, once the active prismatic joints are locked,

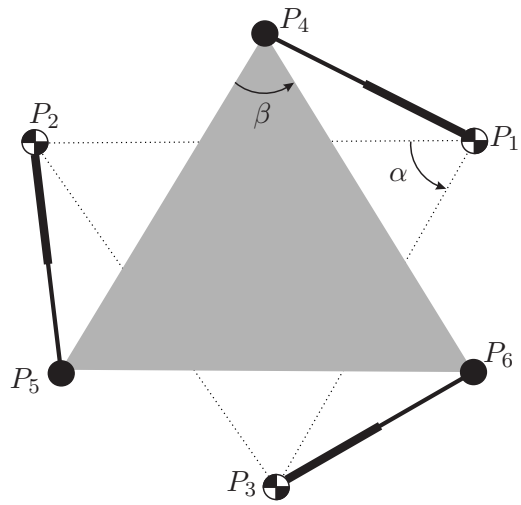

Figure 5.1. A general planar 3-R$\underline{\text{P}}$R parallel robot and its associated notation.

a general 3-R$\underline{\text{P}}$R planar robot platform is kinematically equivalent to a $5/B_1$ Baranov truss [Fig. 3.2(right)]. Hence, the forward kinematic analysis of a 3-R$\underline{\text{P}}$R robot, that is, the computation of the feasible assembly modes given fixed lengths of the active joints, can be reduced, according to the notation of Fig. 5.1, to solve the distance-based closure condition [162]:

$$s_{3,6} = \det\left(\mathbf{I} - \mathbf{Z}_{1,2,3}\mathbf{Z}_{1,5,2} - \mathbf{Z}_{5,4,6}\,\mathbf{Z}_{5,1,4}\right) T. \tag{5.1}$$

where $T = s_{1,5}$,

$$\begin{aligned}\mathbf{Z}_{1,2,3} &\triangleq \begin{pmatrix} b_1 & -b_2 \\ b_2 & b_1 \end{pmatrix} \\ &= \frac{1}{2\,s_{1,2}} \begin{pmatrix} s_{1,2} + s_{1,3} - s_{2,3} & -\mathrm{sign}(\alpha)\,4\,A_{1,2,3} \\ \mathrm{sign}(\alpha)\,4\,A_{1,2,3} & s_{1,2} + s_{1,3} - s_{2,3} \end{pmatrix}\end{aligned}$$

and

$$\begin{aligned}\mathbf{Z}_{5,4,6} &\triangleq \begin{pmatrix} d_1 & -d_2 \\ d_2 & d_1 \end{pmatrix} \\ &= \frac{1}{2\,s_{4,5}} \begin{pmatrix} s_{4,5} + s_{5,6} - s_{4,6} & \mathrm{sign}(\beta)\,4\,A_{5,4,6} \\ -\mathrm{sign}(\beta)\,4\,A_{5,4,6} & s_{4,5} + s_{5,6} - s_{4,6} \end{pmatrix},\end{aligned}$$

with $A_{1,2,3} \geq 0$ and $A_{5,4,6} \geq 0$, are constant matrices that depend only on the geometry of the base and the moving platform, respectively, and

$$\mathbf{Z}_{1,5,2} = \frac{1}{2\,T} \begin{pmatrix} T + s_{1,2} - s_{2,5} & -4\,A_{1,5,2} \\ 4\,A_{1,5,2} & T + s_{1,2} - s_{2,5} \end{pmatrix}$$

and

$$\mathbf{Z}_{5,1,4} = \frac{1}{2\,T} \begin{pmatrix} T + s_{4,5} - s_{1,4} & -4\,A_{5,1,4} \\ 4\,A_{5,1,4} & T + s_{4,5} - s_{1,4} \end{pmatrix}$$

are functions of T.

Equation (5.1) expresses the set of values of T compatible with $s_{1,4}$, $s_{2,5}$, and $s_{3,6}$, the base and the moving platform squared side lengths, $s_{1,2}$, $s_{1,3}$, $s_{2,3}$, and $s_{4,5}$, $s_{5,6}$, $s_{4,6}$,

respectively, and the orientation of the base and platform triangles. The expansion of this equation gives

$$\Phi_a + 2\,\Phi_b A_{1,5,2} + 2\,\Phi_c A_{5,1,4} + 4\,\Phi_d A_{1,5,2} A_{5,1,4} = 0 \tag{5.2}$$

where

$$\begin{aligned}
\Phi_a =& \left(\frac{1}{2}b_1 d_1 + \frac{1}{2}b_2 d_2 - b_1 - d_1 + 1\right) T^2 \\
&+ \left[s_{1,2}(b_1^2 + b_2^2) + s_{4,5}(d_1^2 + d_2^2)\right. \\
&+ \frac{1}{2}\left(-s_{1,4} + s_{4,5} + s_{1,2} - s_{2,5}\right)(b_1 d_1 + b_2 d_2) \\
&+ \left.\left(s_{2,5} - s_{1,2}\right) b_1 + \left(s_{1,4} - s_{4,5}\right) d_1 - s_{3,6}\right] T \\
&+ \frac{1}{2}(s_{4,5} - s_{1,4})(s_{1,2} - s_{2,5})(b_1 d_1 + b_2 d_2) \\
\Phi_b =& (b_1 d_2 - b_2 d_1 + 2b_2)T + (s_{4,5} - s_{1,4})(b_1 d_2 - b_2 d_1) \\
\Phi_c =& (b_2 d_1 - b_1 d_2 + 2d_2)T + (s_{1,2} - s_{2,5})(b_2 d_1 - b_1 d_2) \\
\Phi_d =& 2(b_1 d_1 + b_2 d_2).
\end{aligned}$$

The above equation is a scalar radical equation in T whose roots, in the range in which the signed areas of the triangles $\triangle P_1 P_5 P_2$ and $\triangle P_5 P_1 P_4$ are real, that is, the range

$$\left[\max\{(d_{1,2} - d_{2,5})^2, (d_{4,5} - d_{1,4})^2\}, \min\{(d_{1,2} + d_{2,5})^2, (d_{4,5} + d_{1,4})^2\}\right], \tag{5.3}$$

determine the assembly modes of the analyzed robot. After properly twice squaring equation (5.2), we obtain an expression of the form:

$$T^2\,\Gamma(T) = 0 \tag{5.4}$$

where $\Gamma(T)$, a 6th-degree polynomial in T, is the distance-based characteristic polynomial of the general 3-R$\underline{\text{P}}$R planar robot platform. For a detailed derivation of equations (5.1) and (5.4), see §3.2 applying the permutation

$$\begin{bmatrix} 1 & 2 & 3 & 4 & 5 & 6 \\ 1 & 3 & 2 & 4 & 6 & 5 \end{bmatrix}$$

to equation (3.2). In fact, observe that an alternative distance-based characteristic polynomial in $s_{1,6}$ can be derived for the general 3-R$\underline{\text{P}}$R planar robot platform. This equivalent polynomial form, called $\Gamma(s_{1,6})$, will be used in section 5.2.

5.1.2 Analytic robots

The leading coefficients of Φ_a, Φ_b, Φ_c, and Φ_d do not depend on $s_{1,4}$, $s_{2,5}$, or $s_{3,6}$. As a consequence, they can be made to be identically zero by properly choosing the dimensions of the base and the moving platform thus simplifying the formulation. For example, the maximum simplification is attained by coalescing two attachments both in the base and the platform. In this case, $\Phi_a = T^2 + b\,T$ and $\Phi_b = \Phi_c = \Phi_d = 0$. Table 5.1 compiles different geometric conditions that lead to simplifications for the resulting characteristic polynomial. All of them have already been studied on a case-by-case basis [37, 54, 89, 98, 211]. They lead to analytic robots because the roots of the resulting characteristic polynomials can be obtained using only the basic arithmetic operations and the taking of nth roots. Table 5.1 summarizes, for each case, the resulting Φ-polynomials,

the degree of the characteristic polynomial derived in the previous section, and references to related works. Since, in general, these related works use ad-hoc formulations that require solving more than one polynomial in cascade, the degrees of these polynomials are given in parenthesis besides the corresponding reference.

There have been found four families of analytic robots that satisfy at least one of the following geometric conditions:

C1: two attachments on the base, or on the platform, coincide;

C2: the attachments, both on the base and the platform, are collinear;

C3: the base and platform triangles are similar; and

C4: the base and the platform are inverted triangles (one is the mirror reflection of the other).

It is well-known that there are formulas involving radicals for finding the roots of polynomials of degree lower than 5. As a consequence, the analytic 3-R$\underline{\text{P}}$R planar parallel robots are also referred as those robots whose characteristic polynomial is of degree lower than 5 or it factors into terms of degree lower than 5. Nevertheless, it can be checked that the irreducible characteristic polynomial in T for a parallel robot satisfying the geometric condition C4 —which is known to be analytic— is of degree 6. The solution to this apparent contradiction requires Galois theory. To be precise, we recall that a polynomial equation is solvable by radicals precisely when the Galois group of the polynomial is solvable. It can be checked that the resulting sextic in T for a parallel platform satisfying the geometric condition C4 is solvable [59]. Thus, a more precise definition of analytic robots would be "robots whose characteristic polynomial Galois group is solvable".

5.1.3 Examples

The examples contained in this subsection try to highlight the advantages of the proposed distance-based formulation, first by analyzing a case in which the standard previous formulations fail to provide the correct result, and then by showing that it is valid for all specialized cases that have been previously studied on an ad hoc basis.

5.1.3.1 Example I: A comparison with previous formulations

Let us study the planar 3-R$\underline{\text{P}}$R parallel robot with geometric parameters $\alpha > 0$, $\beta > 0$, $s_{1,2} = 16$, $s_{1,3} = 65$, $s_{2,3} = 73$, $s_{4,5} = 36$, $s_{4,6} = 25$, and $s_{5,6} = 25$, and squared input joints $s_{1,4} = 1$, $s_{2,5} = 121$, and $s_{3,6} = 169$. If $P_1 = (0,0)^T$, $P_2 = (4,0)^T$, and $P_3 = (1,8)^T$, it can be verified that the characteristic polynomial of this robot, using the formulation derived in [56], reduces to:

$$1469440\,X^4 + 1755136\,X^3 + 4261376\,X^2 + 1140736\,X + 219136$$

with

$$\sin(\theta) = \frac{2\,X}{1+X^2} \quad \text{and} \quad \cos(\theta) = \frac{1-X^2}{1+X^2},$$

θ being the angle between the lines defined by $\overline{P_1P_2}$ and $\overline{P_4P_5}$. The roots of this polynomial are $-0.4573-1.5419i$, $-0.4573+1.5419i$, $-0.1399-0.1952i$, and $-0.1399+0.1952i$. Since none of them is real, it can be erroneously concluded that the robot under study cannot be assembled with the given leg lengths.

Case		Φ-polynomials	Degree $\Gamma(T)$	Previous works
Double Coincidence	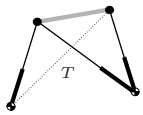	$\Phi_a = T^2 + bT$ $\Phi_b = 0$ $\Phi_c = 0$ $\Phi_d = 0$	1	
Coincidence	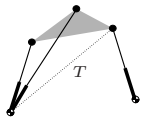	$\Phi_a = aT^2 + bT$ $\Phi_b = 0$ $\Phi_c = fT$ $\Phi_d = 0$	2	Collins [37] (1 quartic)
	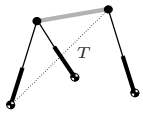	$\Phi_a = aT^2 + bT$ $\Phi_b = dT$ $\Phi_c = 0$ $\Phi_d = 0$	2	
Coincidence + Collinearity	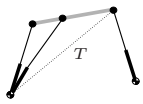	$\Phi_a = aT^2 + bT$ $\Phi_b = 0$ $\Phi_c = 0$ $\Phi_d = 0$	1	Collins [37] (1 quadratic) Gosselin & Merlet [54] (2 quadratics)
	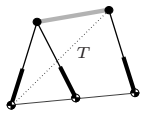	$\Phi_a = aT^2 + bT$ $\Phi_b = 0$ $\Phi_c = 0$ $\Phi_d = 0$	1	
Collinearity	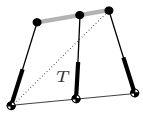	$\Phi_a = aT^2 + bT + c$ $\Phi_b = 0$ $\Phi_c = 0$ $\Phi_d = h$	3	Collins [37] (1 cubic) Gosselin & Merlet [54] (1 sextic) Kong & Gosselin [98] (1 cubic + 1 quadratic)
Collinearity + Similarity	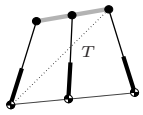	$\Phi_a = aT^2 + bT + c$ $\Phi_b = 0$ $\Phi_c = 0$ $\Phi_d = 4a$	2	Kong & Gosselin [98] (2 quadratics)
Similarity	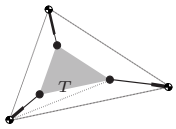	$\Phi_a = aT^2 + bT + c$ $\Phi_b = dT + e$ $\Phi_c = -dT + g$ $\Phi_d = 4a$	4	Kong & Gosselin [98] (2 quadratics) Collins [37] (1 quadratic) Ji & Wu [89] (2 quadratics) Gosselin & Merlet [54] (1 cubic + 1 quadratic)
Mirror reflection	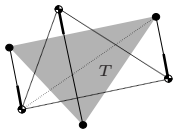	$\Phi_a = aT^2 + bT + c$ $\Phi_b = dT + e$ $\Phi_c = fT + g$ $\Phi_d = 4a$	6^*	Wenger *et al.* [211] (1 cubic + 1 quadratic) (*Solvable)

Table 5.1. The known 3-R<u>P</u>R analytic planar robots.

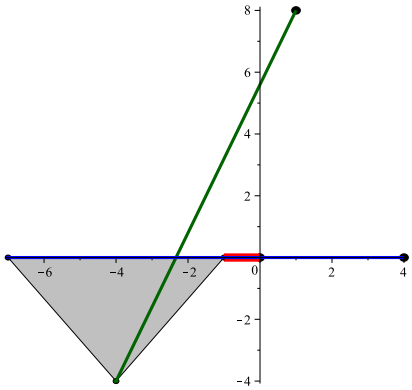

Figure 5.2. Configuration analyzed in Example I using the formulations presented in [56], [98], and [81]. The lines in red, blue, and green correspond to the legs associated to $\overline{P_1P_4}$, $\overline{P_2P_5}$, and $\overline{P_3P_6}$, respectively.

Alternately, using the formulation derived in [98], the following characteristic polynomial is obtained:

$$4408320Y^4 - 1744896Y^3 + 7788032Y^2 - 1464320Y + 3564544$$

where

$$\sin(\psi) = \frac{2Y}{1+Y^2} \quad \text{and} \quad \cos(\psi) = \frac{1-Y^2}{1+Y^2},$$

ψ being the angle between the lines defined by $\overline{P_1P_4}$ and $\overline{P_1P_2}$. The roots of this polynomial are $-0.0363 - 0.9243i$, $-0.0363 + 0.9243i$, $0.2342 - 0.9435i$, and $0.2342 + 0.9435i$. Again, since none of them is real, it can be erroneously concluded that the robot under study cannot be assembled with the given leg lengths thus confirming the results obtained using the formulation proposed in [56]. The formulation described in [81] leads to an analogous situation when one of the homogeneous coordinates is normalized to 1. Using the implementation for this formulation reported in [71], and choosing the moving reference frame such that $P_4 = (0,0)^T$ and $P_5 = (6,0)^T$ in it, the resulting polynomial is:

$$1469440Z^4 + 1755136Z^3 + 4261376Z^2 + 1140736Z + 219136,$$

where Z is a component of the kinematic image space coordinates (referenced as x_1 in [71]). The roots of this polynomial are $-0.4573 - 1.5419i$, $-0.4573 + 1.5419i$, $-0.1399 - 0.1952i$, and $-0.1399 + 0.1952i$. Again, none of them is real. Nevertheless, substituting the geometric parameters of the robot under study and the values of the input variables given above in the polynomial derived in Section 5.1.1, the following characteristic polynomial is obtained

$$\begin{aligned} &-7738000T^6 + 4843775840T^5 - 1068953603696T^4 + 100805055226688T^3 \\ &-4600887845553776T^2 + 101331227980892000T - 876950498856250000. \end{aligned}$$

The roots of this polynomial are $27.4034 - 8.5802i$, $27.4034 + 8.5802i$, $236.5829 - 35.6700i$, $236.5829 + 35.6700i$, and a double root at 49.0000. It can be checked that the obtained double real root corresponds to a valid configuration of the analyzed 3-R$\underline{\text{P}}$R parallel robot, in clear contradiction with what was concluded using the formulations proposed

T	θ	P_4
0.0000	-0.6524	$(-2.1785, 2.4284)^T$
0.0000	0.5236	$(-2.4641, -2.0000)^T$
23.0400	-0.7634	$(4.4641, 2.0000)^T$
44.3077	-1.4420	$(4.4641, 2.0000)^T$

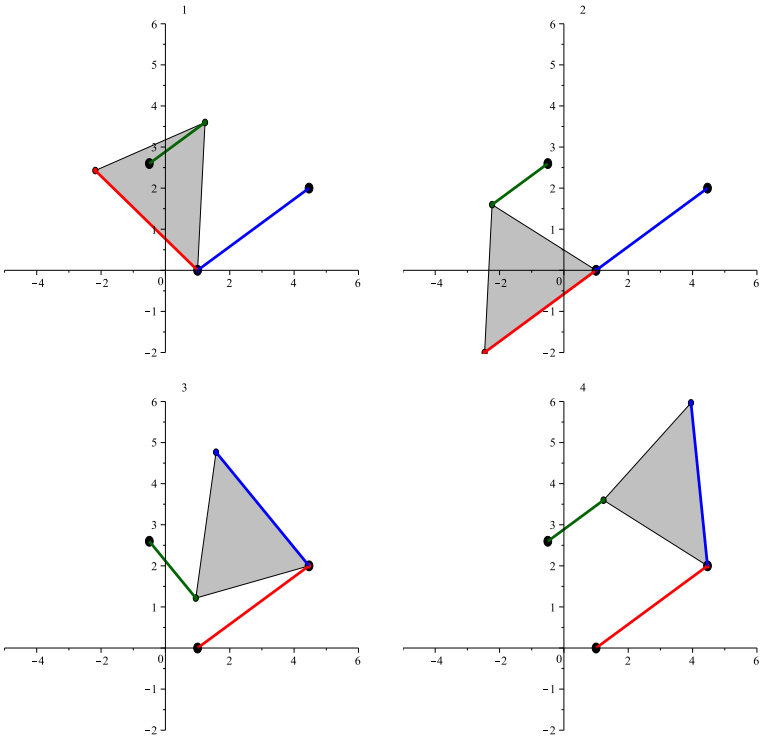

Figure 5.3. The four moving platform poses obtained in Example II and their graphical representation.

in [56], [98], and [81]. In the moving platform pose associated with this double root, $\theta = \pi$, $\psi = \pi$, and $P_4 = (-1, 0)^T$. Fig. 5.2 depicts this configuration.

The obtained results confirm that the previous formulations might incur into robustness problems. This is a highly relevant fact for the kinematic analysis and non-singular assembly-mode change studies of 3-R$\underline{\text{P}}$R parallel robots [82, 225]. The presented distance-based formulation does not exhibit this kind of undesirable behavior [158].

5.1.3.2 Example II: Roots at $T = 0$

Consider the robot with geometric parameters $\alpha > 0$, $\beta > 0$, $s_{1,2} = 16$, $s_{1,3} = 9$, $s_{2,3} = 25$, $s_{4,5} = 16$, $s_{4,6} = 13$, and $s_{5,6} = 13$, and squared input joints $s_{1,4} = 16$, $s_{2,5} = 16$, and $s_{3,6} = 4$. Substituting these values in $\Gamma(T)$, the following polynomial is obtained

$$-83200T^6 + 5603328T^5 - 84934656T^4.$$

It has a quadruple root at $T = 0$ that leads to two valid configurations. The moving platform poses associated with each root of the above polynomial for the case in which $P_1 = (1, 0)^T$, $P_2 = (2\sqrt{3} + 1, 2)^T$, and $P_3 = (-\frac{1}{2}, \frac{3}{2}\sqrt{3})^T$ appear in Fig. 5.3.

Analogously to the previous example, this one cannot either be properly analyzed

T	θ	P_4
20	-1.2490	$(2.0000, -1.0000)^T$
20	-0.3218	$(6.0000, 3.0000)^T$
$\frac{196}{5}$	1.0362	$(2.6913, -2.1610)^T$
$\frac{196}{5}$	-0.7524	$(3.3887, 2.7210)^T$

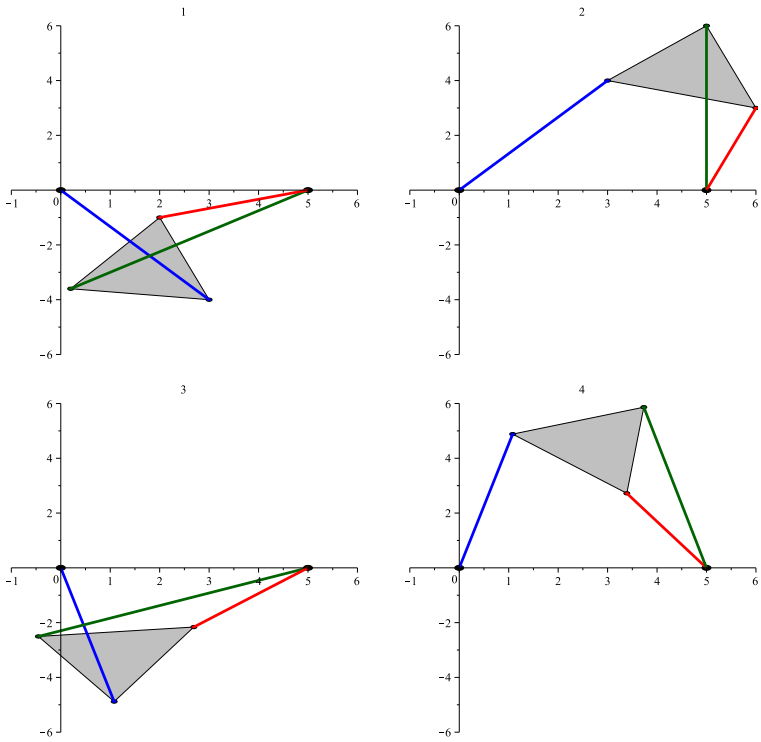

Figure 5.4. The four moving platform poses obtained in Example III and their graphical representation.

using the formulation presented in [98] and, depending on the location of the chosen reference frames, using the formulations derived in [56] and [81].

Finally, observe that, if $T = 0$, the moving platform pose can be obtained by only two bilaterations which determine up to four possible values for P_6 and at least one of them must satisfy the distance constraint between P_3 and P_6.

5.1.3.3 Example III: Coalescence of two attachments

Consider the manipulator with geometric parameters $\alpha > 0$, $\beta < 0$, $s_{1,2} = 25$, $s_{1,3} = 0$, $s_{2,3} = 25$, $s_{4,5} = 10$, $s_{4,6} = 10$, and $s_{5,6} = 8$, and squared input joints $s_{1,4} = 10$, $s_{2,5} = 25$, and $s_{3,6} = 36$. Substituting these values in $\Gamma(T)$, the following polynomial is obtained:

$$10T^2 - 592T + 7840,$$

whose roots are 20 and $\frac{196}{5}$. Each of them have two associated moving platform poses. The four resulting poses for the case in which $P_1 = P_3 = (5, 0)^T$ and $P_2 = (0, 0)^T$ appear in Fig. 5.4.

T	θ	P_4
4	1.3181	$(-0.2500, -0.9682)^T$
4	-1.3181	$(-0.2500, 0.9682)^T$
$\frac{11}{2}$	0.7227	$(-1.0000, 0.0000)^T$
$\frac{11}{2}$	-0.7227	$(-1.0000, 0.0000)^T$

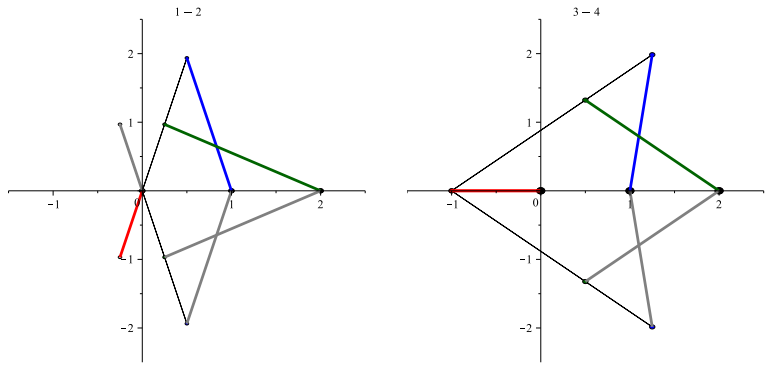

Figure 5.5. The two moving platform poses obtained in Example IV and their graphical representation.

5.1.3.4 Example IV: Collinearity of base and platform attachments

The collinear of the base and platform attachments imply that $d_{1,2} \pm d_{1,3} \pm d_{2,3} = 0$ and $d_{4,5} \pm d_{4,6} \pm d_{5,6} = 0$ for a certain combination of signs. As an example, consider the robot with geometric parameters $\alpha > 0$, $\beta > 0$, $s_{1,2} = 1$, $s_{1,3} = 4$, $s_{2,3} = 1$, $s_{4,5} = 9$, $s_{4,6} = 4$, and $s_{5,6} = 1$, and squared input joints $s_{1,4} = 1$, $s_{2,5} = 4$, and $s_{3,6} = 4$. This robot was also used as an example in [56] and [98]. Substituting these values in $\Gamma(T)$, the following polynomial is obtained:

$$8T^3 - 78T^2 + 195T - 44,$$

whose roots are $\frac{1}{4}$, 4, and $\frac{11}{2}$. However, note that the root at $T = \frac{1}{4}$ is outside the interval given by (5.3), therefore it does not correspond to a valid configuration. The moving platform poses for the case in which $P_1 = (0,0)^T$, $P_2 = (1,0)^T$, and $P_3 = (2,0)^T$ appear in Fig. 5.5.

If, in addition to the collinearity condition, the base and the moving platform are similar, the characteristic polynomial reduces to a polynomial of second degree.

5.1.3.5 Example V: Similar base and platform

In terms of the geometric parameters, the similarity constraint implies that $d_{4,5} = kd_{1,2}$, $d_{4,6} = kd_{1,3}$, and $d_{5,6} = kd_{2,3}$, with $k > 0$. Substituting these expressions in $\Gamma(T)$, it reduces to a quartic. As an example of this analytic family, consider the robot presented in [98], whose geometric parameters are $\alpha > 0$, $\beta > 0$, $s_{1,2} = 1600$, $s_{1,3} = 400$, $s_{2,3} = 400\,(5 - 2\sqrt{3})$, $s_{4,5} = 400$, $s_{4,6} = 100$, and $s_{5,6} = 100\,(5 - 2\sqrt{3})$. Substituting these values in the resulting quartic, with squared input variables $s_{1,4} = 4$, $s_{2,5} = 1936$, and $s_{3,6} = 441$, the following characteristic polynomial is obtained:

$$1.7916T^4 - 2752.8830T^3 + 1.5749\,10^6 T^2 - 3.9782\,10^8 T + 3.7457\,10^{10}.$$

The platform poses associated with each root of the above polynomial, for the case in which $P_1 = (0,0)^T$, $P_2 = (40,0)^T$, and $P_3 = (10\sqrt{3}, 10)^T$, appear in Fig. 5.6.

T	θ	P_4
329.4937	-1.5351	$(-0.7943, 1.8355)^T$
345.1531	1.5040	$(1.4501, 1.3774)^T$
387.5845	-1.5040	$(1.9805, -0.2787)^T$
474.3144	1.5351	$(1.0160, 1.7227)^T$

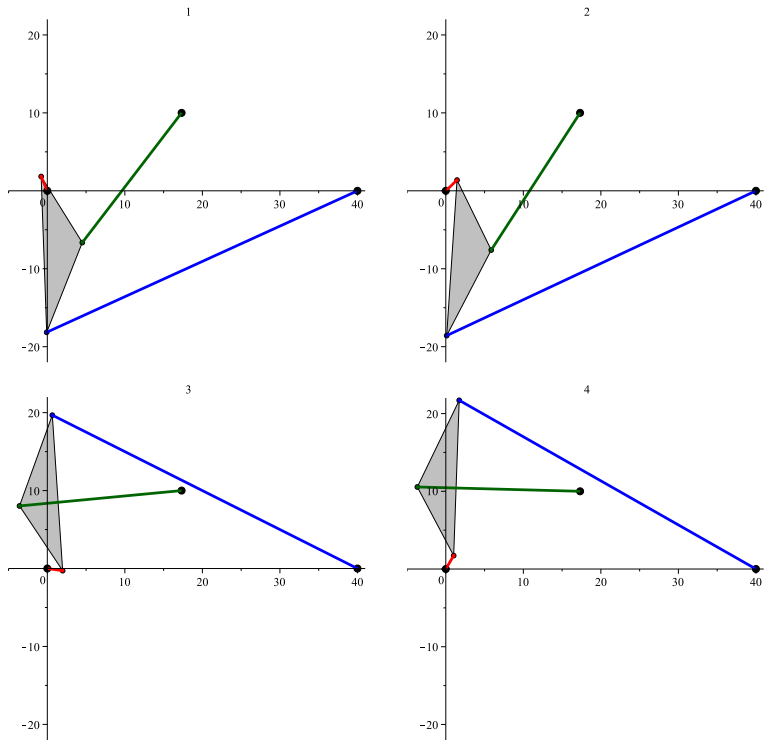

Figure 5.6. The four moving platform poses obtained in Example V and their graphical representation.

5.1.3.6 Example VI: Mirrored base and platform

Consider the manipulator with geometric parameters $\alpha > 0$, $\beta < 0$, $s_{1,2} = 1$, $s_{1,3} = 1$, $s_{2,3} = 2$, $s_{4,5} = 1$, $s_{4,6} = 1$, and $s_{5,6} = 2$, and squared input joints $s_{1,4} = 4$, $s_{2,5} = \frac{1}{4}$, and $s_{3,6} = 1$, the resulting irreducible characteristic polynomial in T is:

$$-32\,T^6 + 432\,T^5 - \frac{4455}{2}\,T^4 + \frac{39839}{8}\,T^3 - \frac{339993}{64}\,T^2 + \frac{110565}{32}\,T - \frac{47385}{32}.$$

This example, which leads to a degeneration of Gosselin's formulation [56], corresponds to the robot presented in [212] where it is shown to be analytic. Indeed, it can be checked that the Galois group of the above polynomial is solvable.

5.2 All fully-parallel planar robots and their forward kinematics

A fully-parallel planar robot consists of a *moving platform* connected to a *fixed base* by three serial kinematic chains, or *legs*. Each chain consists of three independent 1-degree-of-freedom lower pair joints, one of which is driven by an *actuator*. Thus, each chain provides the control of one of the three degrees of freedom of the moving platform —the

Type RR	Type RP	Type PR	Type PP
$\underline{R}$RR	RP$\underline{R}$	$\underline{R}$PR	
R$\underline{R}$R	R$\underline{P}$P	P$\underline{R}$R	$\underline{R}$PP
RR$\underline{R}$	RP$\underline{P}$	PR$\underline{R}$	P$\underline{R}$P
R$\underline{P}$R	$\underline{P}$RP	PR$\underline{P}$	PP$\underline{R}$
$\underline{P}$RR	$\underline{R}$RP	$\underline{P}$PR	
RR$\underline{P}$	R$\underline{R}$P	P$\underline{P}$R	

Table 5.2. Fully-parallel planar robot leg types.

number of degrees of freedom of an object is the number of its possible independent displacements. Since the movement of the moving platform is confined to a plane, only revolute (R) and prismatic (P) pairs are considered. Then, the topology of each serial kinematic chain can be described by three letters. There are seven possible combinations: RRR, RPR, RRP, PRR, RPP, PRP, and PPR. The chain PPP is not considered because three P pairs represent three translations in the plane which cannot be independent. The actuated joint is identified by underlying it. Then, since any of the three joints can be actuated, there are twenty one possible legs which can be grouped in four leg architectures —known as the RR, PR, RP and PP legs (see Table 5.2)— attending to the sequence of passive joints. The number of passive prismatic joints in a loop cannot be more than three, otherwise the robot would gain one degree of freedom. This fact limits the number of possible PP legs to one. Then, since there are $\binom{18}{3} = 1140$ feasible combinations of legs of type RR, PR, and RP, and $3 \cdot \binom{18}{2} = 513$ feasible combinations of one leg of type PP with any two legs of the other three types, the total number of different fully-parallel planar robots is 1653. When the three actuators are locked, the robot becomes a rigid structure —*i.e.*, a kinematic chain of mobility zero— provided that it is not in a singularity. This permits to classify these 1653 robots into 10 classes attending to the topology of the resulting structure (see Table 5.3). Up to this point, we have followed the standard discourse used in Robotics to present all possible fully-parallel planar robots but observe that the resulting structures are nothing more than the 5-link Assur kinematic chains, also known as the planar Assur II groups [30].

The forward kinematics of parallel robots consists in finding the possible assemblages, usually called *assembly modes*, of the mobile platform, for specified values of the actuated joint coordinates, with respect to the fixed base. Thus, it reduces to the position analysis of one of the ten possible structures in Table 5.3. Numerical solutions to this problem are enough for many applications but yield little insight into the problem. The alternative are the exact methods which rely on the computation of a characteristic polynomial thus providing what its is usually called a *closed-form solution* to the problem.

In 1987, Li and Matthew solved the position analysis problem of the ten 5-link Assur kinematic chains in closed form for the first time [105]. Their approach corresponded in realizing that every Assur II group consisted of two kinematically independent loops which can be classified into only six types: RRRR, RPRR, RPPR, RPRP, RRPP, and RPPP. Then, they reduced the problem to obtain the loop equations for these six loops in general form and compute the resultant in a single variable for the ten feasible combinations. Although outstanding in many ways for its time (the authors even envisaged the possibility of applying their results to planar and spherical robots), this work has been overlooked by the Robotics community. In 1996, Merlet tackled the same problem from a different point of view which resulted in a case-by-case analysis [121]. Other solutions for some 5-link Assur kinematic chains have been presented, at least, in [36, 125–127].

Robot family (# of different robot topologies)	**Associated structure**	**Leg types**
I (56)	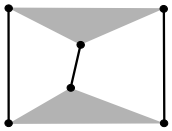	RR-RR-RR
II (252)	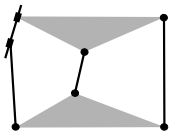	RP-RR-RR PR-RR-RR
III (216)	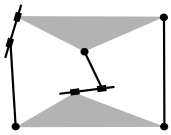	RP-PR-RR
IV (252)	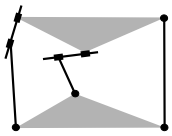	RP-RP-RR PR-PR-RR
V (252)	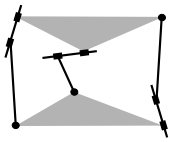	RP-RP-PR PR-PR-RP
VI (63)	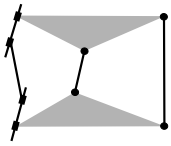	PP-RR-RR
VII (216)	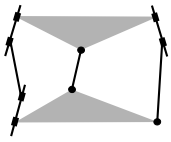	PP-RR-RP PP-RR-PR
VIII (112)	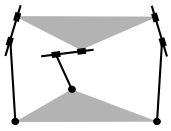	RP-RP-RP PR-PR-PR
IX (108)	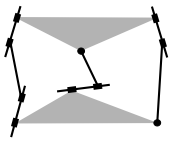	PP-PR-RP
X (126)	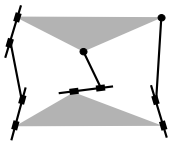	PP-RP-RP PP-PR-PR

Table 5.3. The 10 fully-parallel planar robot families.

The development of a remarkable unified formulation for the forward kinematics of all fully-parallel planar robots started in 1995 with Husty's first use of the Grünwald-Blaschke kinematic mapping to solve the forward kinematics of the 3-R$\underline{\text{P}}$R robot [81]. This formulation was thereafter extended by Hayes, Chen, Zsombor-Murray, and Husty himself who presented their results in a series of publications that culminated with a recent monograph [33, 34, 71–76, 228]. The approach followed by these authors is based on examining the motion of each leg separately which can be represented by only three types of surfaces: an hyperbolic paraboloid (for legs of type PR and RP), a hyperboloid of one sheet (for legs of type RR), or a plane (for legs of type PP). Then, the forward kinematics problem boils down to find the points of intersection of these three such surfaces. The result is indeed a uniform procedure for solving the forward kinematics of all fully-parallel planar robots but an elimination process is still required to obtain a univariate polynomial for 6 different cases.

A different unifying approach stems from regarding a translational motion as an infinitely small rotation about a point at infinity. It is well-known that a translation in the direction (u_x, u_y) may be represented as a rotation about the ideal point given in homogeneous coordinates by $(-u_y, u_x, 0)$. This is probably the most simple unifying approach to deal with revolute and prismatic joints simultaneously but, using the standard formulations such as those based on independent loop equations, it is difficult to be accommodated. This section is essentially devoted to show how a coordinate-free formulation based on distances and oriented areas provides a framework within which this idea can be easily applied. This will allow us to conclude that the characteristic polynomial of the 3-R$\underline{\text{P}}$R robot contains all the necessary and sufficient information for solving the forward kinematics of all fully-parallel planar robots.

To this end, section 5.2.1, following the ideas presented in Chapter 4, shows how to transform any fully-parallel robot with passive prismatic joints into a 3-R$\underline{\text{P}}$R robot with some revolute joint centers located at infinity. Section 5.2.2 shows through examples how to solve —using the characteristic polynomial of the 3-R$\underline{\text{P}}$R robot— the position analysis of different fully-parallel planar robots.

5.2.1 Replacing revolute by prismatic joints

In this point, we will consider the case in which the three revolute joints connected to the moving platform in a 3-R$\underline{\text{P}}$R robot are replaced by prismatic joints. We will proceed progressively by replacing first one, then two, and finally the three revolute joints. At the end, it will become clear that all other cases can be easily deduced from this analysis [164].

5.2.1.1 Replacing one revolute joint

Let us suppose that the revolute joint centered at P_4 in Fig. 5.1 is replaced by a prismatic joint, as shown in Fig. 5.7(top), such that P_4 is split into P_4' and P_4''. This new joint is placed at fixed orientations with respect to the links connected to them. Once an orientation is assigned to the prismatic joint axis with respect to its adjacent links, a set of orientation angles can be defined (in this case α_1, α_2 and α_3) and, as a consequence, an oriented distance can be defined between P_1, P_5 and P_6 and the prismatic joint axis. This defines a set of new points on this axis: those that realize the minimum distance to P_1, P_5 and P_6 which are denoted by $\otimes$ in Fig. 5.7(bottom). Note that the prismatic joint imposes the alignment of these points but, for the moment, let us suppose that they all are located at the same distance, say δ_i, from P_4^∞. This would imply that they would lie on a circle but, if $\delta_i \to \infty$, they would again lie on a line as imposed by the prismatic

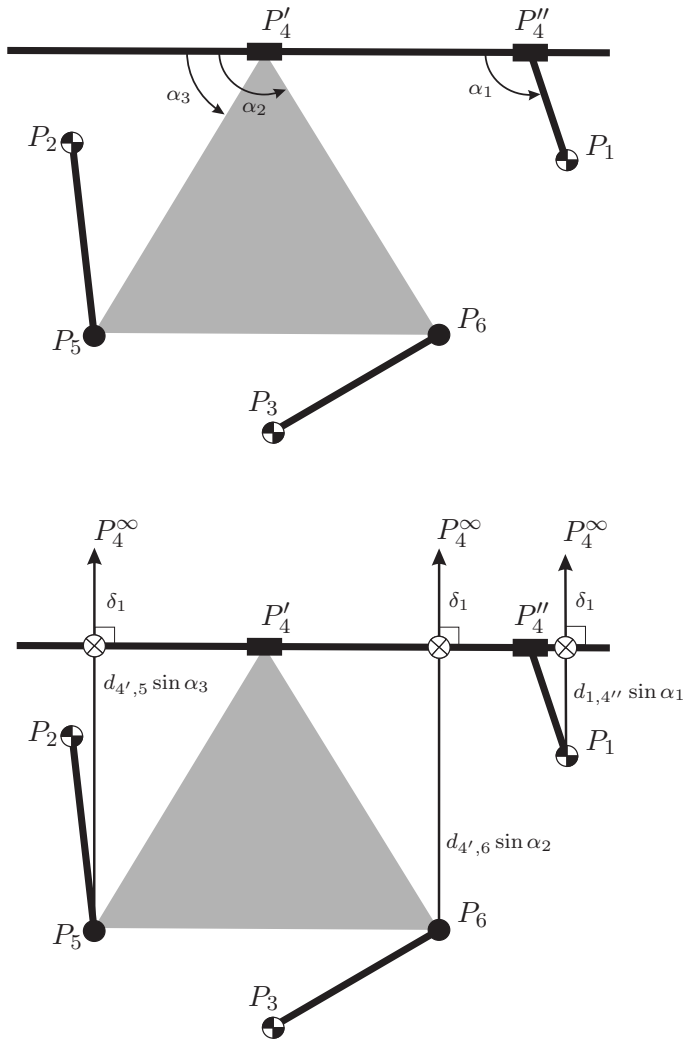

Figure 5.7. One revolute joint in the moving platform is substituted by a prismatic joint.

join. Actually, the presented geometric transformation simply consists in replacing P_4 by P_4^∞ and substituting the distances between P_4 and P_1, P_5, and P_6, by

$$\begin{aligned} d_{4,1} &= \delta_1 + d_{1,4''}\sin\alpha_1, \\ d_{4,5} &= \delta_1 + d_{4',5}\sin\alpha_3, \\ d_{4,6} &= \delta_1 + d_{4',6}\sin\alpha_2, \end{aligned}$$

with $\delta_1 \to \infty$, respectively.

As it was already stood out in §4.1, it is worth noting that, after the described geometric transformation, it might happen that the orientation of $\triangle P_4^\infty P_5 P_6$ have changed with respect to that of $\triangle P_4 P_5 P_6$. This has to be taken into account in the characteristic polynomial by changing the sign of $A_{6,4,5}$ if needed.

The characteristic polynomial for the resulting robot after the introduction of a prismatic joint results from computing

$$\lim_{\delta_1\to\infty} \Gamma(s_{1,6})\Big|_{\substack{d_{1,4} = \delta_1 + d_{1,4''}\sin\alpha_1 \\ d_{4,5} = \delta_1 + d_{4',5}\sin\alpha_3 \\ d_{4,6} = \delta_1 + d_{4',6}\sin\alpha_2,}}$$

where $\Gamma(s_{1,6})$ is the distance-based characteristic polynomial in $s_{1,6}$ of the 3-R$\underline{\text{P}}$R planar robot platform. Now, rewriting $\Gamma(s_{1,6})$, after the substitutions, as a polynomial in δ_1, the above limit can be expressed as:

$$\lim_{\delta_1 \to \infty} \sum_{i=0}^{n} \gamma_i(s_{1,6})\delta_1^i \Big|_{\substack{d_{1,4} = \delta_1 + d_{1,4''} \sin\alpha_1 \\ d_{4,5} = \delta_1 + d_{4',5} \sin\alpha_3 \\ d_{4,6} = \delta_1 + d_{4',6} \sin\alpha_2.}}$$

Then, we conclude that, for this limit to be zero, $\gamma_n(s_{1,6}) = 0$. In other words, the new characteristic polynomial is $\gamma_n(s_{1,6})$.

5.2.1.2 Replacing two revolute joints

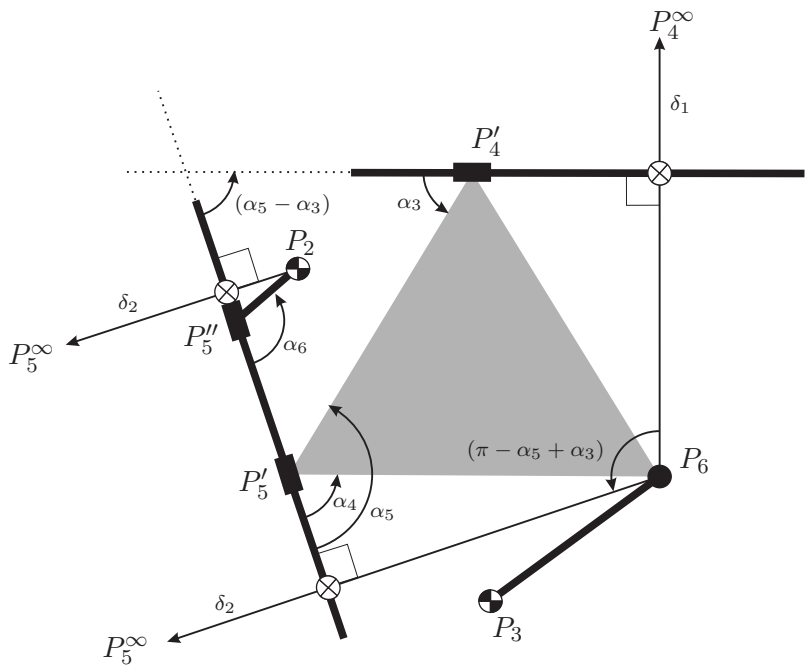

Figure 5.8. Two revolute joints connected to the moving platform are substituted by prismatic joints.

Now, let us suppose that the revolute joint centered at P_5 is also replaced by a prismatic joint as indicated in Fig. 5.8. Following the same reasoning used above, this is equivalent to replace P_5 by a point at infinity, P_5^∞, and substituting the distances between P_5 and P_2, and P_6, by

$$d_{5,2} = \delta_2 + d_{5'',2} \sin\alpha_6,$$
$$d_{5,6} = \delta_2 + d_{5',6} \sin\alpha_4,$$

with $\delta_2 \to \infty$, respectively. To obtain the substitution for $d_{4,5}$, observe that the angle formed by the two prismatic joints is $\alpha_5 - \alpha_3$. Then,

$$\angle P_5^\infty P_6 P_4^\infty = \pi - \alpha_5 + \alpha_3.$$

Therefore, using the cosine theorem, we conclude that:

$$\begin{aligned} d_{4,5}^2 =& d_{5,6}^2 + d_{4,6}^2 - 2\, d_{5,6} d_{4,6} \cos(\pi - \alpha_5 + \alpha_3) \\ =& (\delta_2 + d_{5',6} \sin\alpha_4)^2 + (\delta_1 + d_{4',6} \sin\alpha_2)^2 \\ &+ 2(\delta_2 + d_{5',6} \sin\alpha_4)(\delta_1 + d_{4',6} \sin\alpha_2) \cos(\alpha_5 - \alpha_3) \end{aligned}$$

with $\delta_1 \to \infty$ and $\delta_2 \to \infty$.

5.2.1.3 Replacing three revolute joints

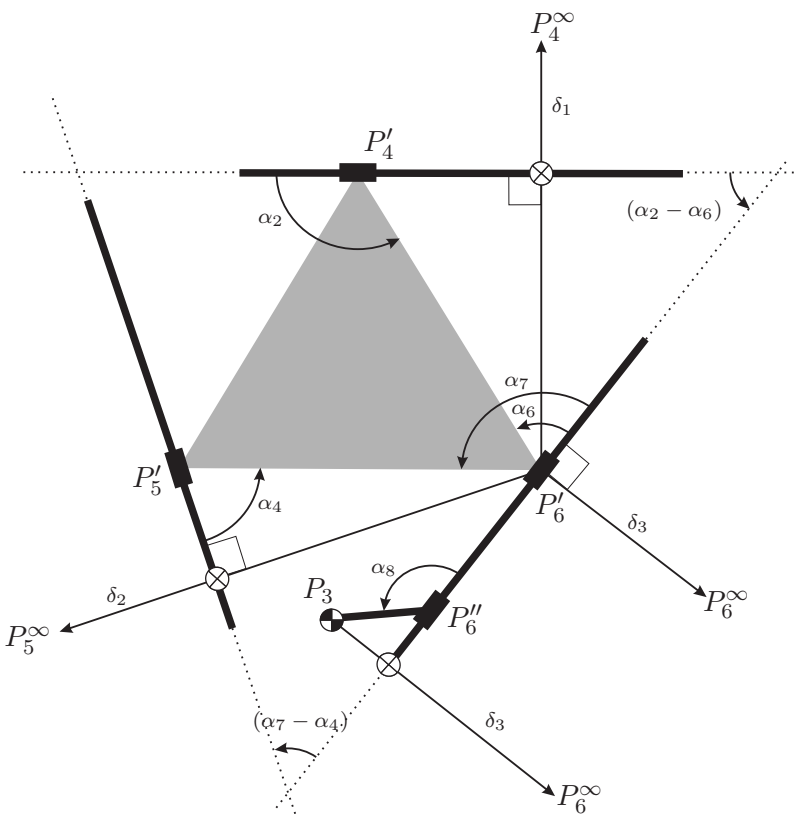

Figure 5.9. The three revolute joints connected to the moving platform are substituted by prismatic joints.

Finally, let us assume that the revolute joint centered at P_6 is also replaced by a prismatic joint with the orientation angles indicated in Fig. 5.9. Using the same reasoning as above, this is equivalent to take P_6 to infinity and substitute the distance between P_6 and P_3 by

$$d_{3,6} = \delta_3 + d_{3,6''} \sin \alpha_8. \tag{5.5}$$

In this case, to obtain the substitutions for the distances between P_6 and P_5, and P_4, observe that the angles formed by the new prismatic joint axis with those defined by the other two are $\alpha_7 - \alpha_4$ and $\alpha_2 - \alpha_6$ (see Fig. 5.9). Then,

$$\begin{aligned} \angle P_5^\infty P_6' P_6^\infty &= \pi - \alpha_7 + \alpha_4, \\ \angle P_6^\infty P_6' P_4^\infty &= \pi - \alpha_2 + \alpha_6. \end{aligned}$$

Consequently, using the cosine theorem,

$$\begin{aligned} d_{5,6}^2 =& (\delta_2 + d_{5',6'} \sin \alpha_4)^2 + \delta_3^2 + 2(\delta_2 + d_{5',6'} \sin \alpha_4)\delta_3 \cos(\alpha_7 - \alpha_4), \\ d_{6,4}^2 =& (\delta_1 + d_{4',6'} \sin \alpha_2)^2 + \delta_3^2 + 2(\delta_1 + d_{4',6'} \sin \alpha_2)\delta_3 \cos(\alpha_2 - \alpha_6), \end{aligned}$$

and

$$d_{4,5}^2 = d_{5,6}^2 + d_{4,6}^2 + 2\, d_{5,6} d_{4,6} \cos(\alpha_5 - \alpha_3).$$

The required substitutions for all other cases can be derived following the same procedure. Tables 5.4 to 5.6 compile them all thus concluding that the characteristic

polynomials of all fully-parallel planar robots can be deduced from the characteristic polynomial of the 3-R$\underline{\text{P}}$R robot when expressed in terms of distances and oriented areas. The degree of the resulting characteristic polynomial for each family, that is, the maximum number of assembly modes, is also included in Tables 5.4 to 5.6 and denoted by AM. The practical consequences of the presented formulation are better understood through an example.

5.2.2 Example

Let us consider the planar 3-R$\underline{\text{P}}$R parallel robot used as example in section 5.1.3.1. Substituting the geometrical parameters and squared input joints of this robot in $\Gamma(s_{1,6})$, the following characteristic polynomial is obtained

$$\begin{aligned} & s_{1,6}^6 - 293.1486\, s_{1,6}^5 + 54084.9111\, s_{1,6}^4 - 3.5587\, 10^6\, s_{1,6}^3 \\ & + 1.0004\, 10^8\, s_{1,6}^2 - 1.2240\, 10^9\, s_{1,6} + 5.3843\, 10^9. \end{aligned}$$

This polynomial has a double real root at 32.0000, a result in agreement with that obtained using $\Gamma(T)$ (§5.1.3.1). The corresponding moving platform pose, for the case in which $P_1 = (0,0)^T$, $P_2 = (4,0)^T$, and $P_3 = (1,8)^T$, is depicted again in the first row of Fig. 5.10 to facilitate its comparison with the configurations obtained when the revolute joints of the moving platform are replaced by prismatic joints.

If the revolute joint centered at P_4 is replaced by a prismatic joint, a R$\underline{\text{P}}$P-R$\underline{\text{P}}$R-R$\underline{\text{P}}$R planar robot is obtained. This kind of robot belongs to the type II robot family in Table 5.4. If the orientation of the passive prismatic joint with respect to its adjacent links, according to the notation used in Table 5.4, is given by

$$\alpha_1 = \frac{3}{4}\pi,\ \alpha_2 = \frac{5}{4}\pi + \arctan\frac{4}{3},\ \text{and}\ \alpha_3 = \frac{5}{4}\pi,$$

then

$$d_{1,4} = \delta_1 + \frac{1}{\sqrt{2}},\ d_{4,5} = \delta_1 - 3\sqrt{2},\ \text{and}\ d_{4,6} = \delta_1 - \frac{7}{\sqrt{2}}.$$

Substituting these distances in $\Gamma(s_{1,6})$, while keeping all other distances unaltered, and computing the leading coefficient of the resulting polynomial in δ_1, we get the characteristic polynomial

$$\begin{aligned} & s_{1,6}^6 - 672.0638\, s_{1,6}^5 + 1.4983\, 10^5\, s_{1,6}^4 - 1.4372\, 10^7\, s_{1,6}^3 \\ & + 6.1729\, 10^8\, s_{1,6}^2 - 1.2023\, 10^{10}\, s_{1,6} + 8.7934\, 10^{10}. \end{aligned}$$

The real roots of the above polynomial are 32.0000, 112.2332, 141.1726, and 342.8691. The corresponding moving platform poses appear in the second row of Fig. 5.10.

Now, if the revolute joint centered at P_6 is also replaced by a prismatic joint, a R$\underline{\text{P}}$P-R$\underline{\text{P}}$P-R$\underline{\text{P}}$R robot is obtained. This kind of robot belongs to the type IV robot family in Table 5.4. If the orientation of the new prismatic joint with respect to its adjacent links, according to the notation of Table 5.4, is given by

$$\alpha_4 = 2\pi - \arctan\frac{4}{3},\ \alpha_5 = \pi + \arctan\frac{4}{3},\ \text{and}\ \alpha_6 = \pi + \arctan\frac{12}{5},$$

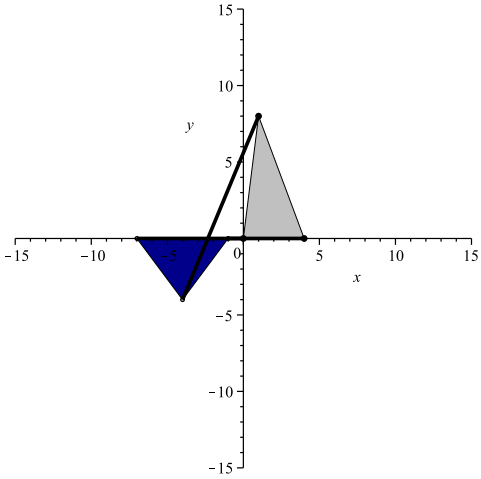

$s_{1,6} = 32.0000$

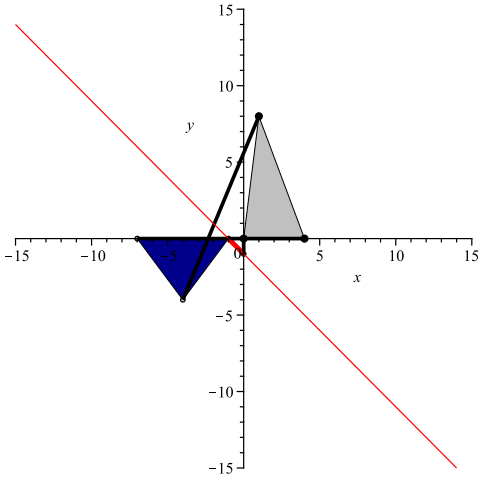

$s_{1,6} = 32.0000$

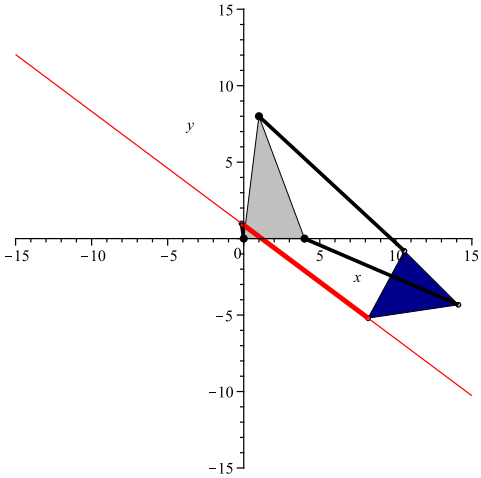

$s_{1,6} = 112.2332$

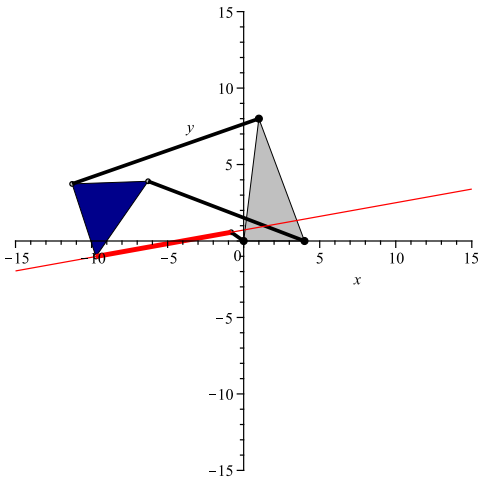

$s_{1,6} = 141.1726$

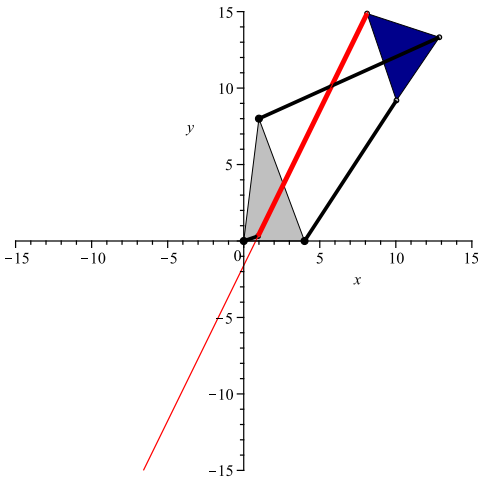

$s_{1,6} = 342.8691$

Figure 5.10. The moving platform poses of the analyzed fully-parallel planar robots (Part 1/2).

	Robot family and associated structure	AM	Substitutions
I	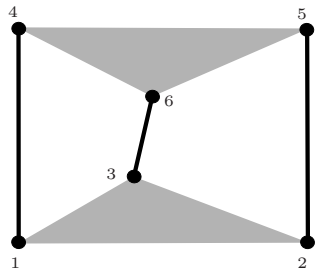	6	None
II	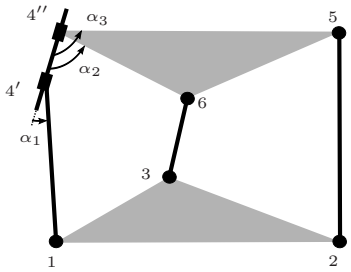	6	$d_{1,4} = \delta_1 + d_{1,4'} \sin\alpha_1$ $d_{4,6} = \delta_1 + d_{4'',6} \sin\alpha_2$ $d_{4,5} = \delta_1 + d_{4'',5} \sin\alpha_3$
III	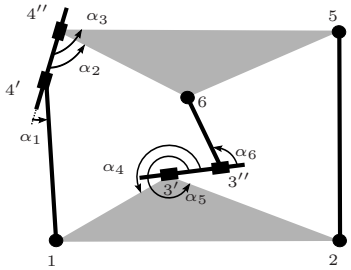	6	$d_{1,4} = \delta_1 + d_{1,4'} \sin\alpha_1$ $d_{4,6} = \delta_1 + d_{4'',6} \sin\alpha_2$ $d_{4,5} = \delta_1 + d_{4'',5} \sin\alpha_3$ $d_{1,3} = \delta_2 + d_{1,3'} \sin\alpha_4$ $d_{2,3} = \delta_2 + d_{2,3'} \sin\alpha_5$ $d_{3,6} = \delta_2 + d_{3'',6} \sin\alpha_6$
IV	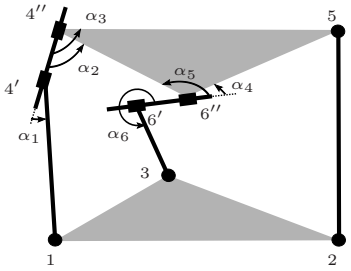	4	$d_{1,4} = \delta_1 + d_{1,4'} \sin\alpha_1$ $d_{4,5} = \delta_1 + d_{4'',5} \sin\alpha_3$ $d_{5,6} = \delta_2 + d_{5,6''} \sin\alpha_4$ $d_{4,6}^2 = d_{4,5}^2 + d_{5,6}^2 + 2\, d_{4,5}\, d_{5,6} \cos(\alpha_2 - \alpha_5)$ $d_{3,6} = \delta_2 + d_{3,6'} \sin\alpha_6$ $d_{1,6} = \delta_2 + t$
V	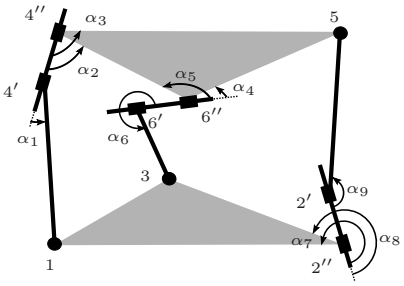	4	$d_{1,4} = \delta_1 + d_{1,4'} \sin\alpha_1$ $d_{4,5} = \delta_1 + d_{4'',5} \sin\alpha_3$ $d_{5,6} = \delta_2 + d_{5,6''} \sin\alpha_4$ $d_{4,6}^2 = d_{4,5}^2 + d_{5,6}^2 + 2\, d_{4,5}\, d_{5,6} \cos(\alpha_2 - \alpha_5)$ $d_{3,6} = \delta_2 + d_{3,6'} \sin\alpha_6$ $d_{1,6} = \delta_2 + t$ $d_{1,2} = \delta_3 + d_{1,2''} \sin\alpha_7$ $d_{2,3} = \delta_3 + d_{2'',3} \sin\alpha_8$ $d_{2,5} = \delta_3 + d_{2',5} \sin\alpha_9$

Table 5.4. Distance substitutions for each robot family (Part 1/3).

Robot family and associated structure	AM	Substitutions
VI 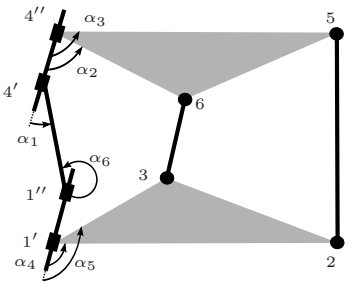	2	$d_{1,4}^2 = \delta_1^2 + \eta^2 - 2\,\delta_1\,\eta\,\cos(\alpha_6 - \alpha_1)$, with $\eta = \delta_2 + d_{1'',4'}\,\sin\alpha_6$ $d_{4,6} = \delta_1 + d_{4'',6}\,\sin\alpha_2$ $d_{4,5} = \delta_1 + d_{4'',5}\,\sin\alpha_3$ $d_{1,2} = \delta_2 + d_{1',2}\,\sin\alpha_4$ $d_{1,3} = \delta_2 + d_{1',3}\,\sin\alpha_5$ $d_{1,6} = \delta_2 + t$
VII 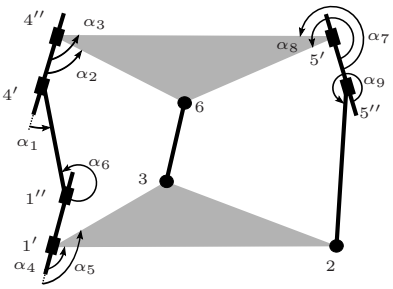	2	$d_{1,4}^2 = \delta_1^2 + \eta^2 - 2\,\delta_1\,\eta\,\cos(\alpha_6 - \alpha_1)$, with $\eta = \delta_2 + d_{1'',4'}\,\sin\alpha_6$ $d_{4,6} = \delta_1 + d_{4'',6}\,\sin\alpha_2$ $d_{1,2} = \delta_2 + d_{1',2}\,\sin\alpha_4$ $d_{1,3} = \delta_2 + d_{1',3}\,\sin\alpha_5$ $d_{1,6} = \delta_2 + t$ $d_{5,6} = \delta_3 + d_{5',6}\,\sin\alpha_8$ $d_{4,5}^2 = d_{4,6}^2 + d_{5,6}^2 - 2\,d_{4,6}\,d_{5,6}\,\cos(\alpha_7 - \alpha_3)$ $d_{2,5} = \delta_3 + d_{2,5''}\,\sin\alpha_9$
VIII 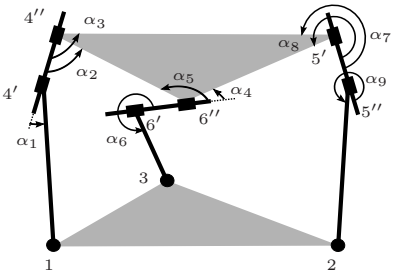	2	$d_{1,4} = \delta_1 + d_{1,4'}\,\sin\alpha_1$ $d_{3,6} = \delta_2 + d_{3,6'}\,\sin\alpha_6$ $d_{1,6} = \delta_2 + t$ $d_{4,5}^2 = \delta_3^2 + {\eta_1}^2 - 2\,\delta_3\,\eta_1\,\cos(\alpha_7 - \alpha_3)$, with $\eta_1 = \delta_1 + d_{4'',5'}\,\sin\alpha_3$ $d_{5,6}^2 = \delta_3^2 + {\eta_2}^2 - 2\,\delta_3\,\eta_2\,\cos(\alpha_4 - \alpha_8)$, with $\eta_2 = \delta_2 + d_{5',6''}\,\sin\alpha_4$ $d_{4,6}^2 = d_{4,5}^2 + d_{5,6}^2 + 2\,d_{4,5}\,d_{5,6}\,\cos(\alpha_2 - \alpha_5)$ $d_{2,5} = \delta_3 + d_{2,5''}\,\sin\alpha_9$

Table 5.5. Distance substitutions for each robot family (Part 2/3).

then

$$
\begin{aligned}
d_{1,4} &= \delta_1 + \frac{1}{\sqrt{2}},\\
d_{4,5} &= \delta_1 - 3\sqrt{2},\\
d_{5,6} &= \delta_2 - 4,\\
d_{4,6}^2 &= \delta_1^2 + \delta_2^2 + \sqrt{2}\,\delta_1\delta_2 - 10\sqrt{2}\,\delta_1 - 14\,\delta_2 + 58,\\
d_{3,6} &= \delta_2 - 12,\\
d_{1,6} &= \delta_2 - t.
\end{aligned}
$$

Substituting these values in $\Gamma(s_{1,6})$, while keeping all other distances unchanged, and

Robot family and associated structure	AM	Substitutions
IX 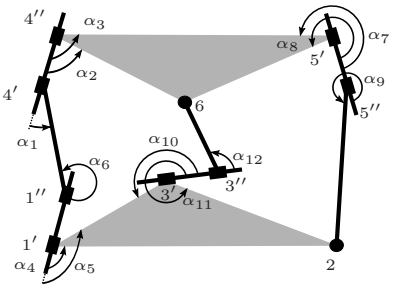	1	$d_{1,4}^2 = \delta_1^2 + \eta^2 - 2\,\delta_1\,\eta\,\cos(\alpha_6 - \alpha_1)$, with $\eta = \delta_2 + d_{1'',4'}\,\sin\alpha_6$ $d_{4,6} = \delta_1 + d_{4'',6}\,\sin\alpha_2$ $d_{1,2} = \delta_2 + d_{1',2}\,\sin\alpha_4$ $d_{1,6} = \delta_2 + t$ $d_{5,6} = \delta_3 + d_{5',6}\,\sin\alpha_8$ $d_{4,5}^2 = d_{4,6}^2 + d_{5,6}^2 - 2\,d_{4,6}\,d_{5,6}\,\cos(\alpha_7 - \alpha_3)$ $d_{2,5} = \delta_3 + d_{2,5''}\,\sin\alpha_9$ $d_{2,3} = \delta_4 + d_{2,3'}\,\sin\alpha_{11}$ $d_{1,3}^2 = d_{1,2}^2 + d_{2,3}^2 - 2\,d_{1,2}\,d_{2,3}\,\cos(\alpha_{10} - \alpha_5)$ $d_{3,6} = \delta_4 + d_{3'',6}\,\sin\alpha_{12}$
X 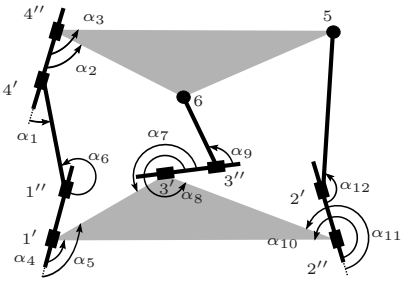	1	$d_{1,4}^2 = \delta_1^2 + \eta^2 - 2\,\delta_1\,\eta\,\cos(\alpha_6 - \alpha_1)$, with $\eta = \delta_2 + d_{1'',4'}\,\sin\alpha_6$ $d_{4,6} = \delta_1 + d_{4'',6}\,\sin\alpha_2$ $d_{4,5} = \delta_1 + d_{4'',5}\,\sin\alpha_3$ $d_{1,6} = \delta_2 + t$ $d_{2,3} = \delta_3 + d_{2,3'}\,\sin\alpha_8$ $d_{3,6} = \delta_3 + d_{3'',6}\,\sin\alpha_9$ $d_{1,2}^2 = \delta_4^2 + {\eta_1}^2 - 2\,\delta_4\,\eta_1\,\cos(\alpha_{10} - \alpha_4)$, with $\eta_1 = \delta_2 + d_{1',2''}\,\sin\alpha_4$ $d_{2,3}^2 = \delta_4^2 + {\eta_2}^2 + 2\,\delta_4\,\eta_2\,\cos(\alpha_{11} - \alpha_8)$, with $\eta_2 = \delta_3 + d_{2'',3'}\,\sin\alpha_8$ $d_{1,3}^2 = d_{1,2}^2 + d_{2,3}^2 - 2\,d_{1,2}\,d_{2,3}\,\cos(\alpha_7 - \alpha_5)$ $d_{2,5} = \delta_4 + d_{2',5}\,\sin\alpha_{12}$

Table 5.6. Distance substitutions for each robot family (Part 3/3).

computing the leading coefficient of the resulting polynomial in δ_1, and then the leading coefficient of the resulting polynomial in δ_2, we get the characteristic polynomial

$$t^4 - 35.1765\,t^3 + 410.7778\,t^2 - 1849.7255\,t + 2821.7516,$$

where t is the oriented distance between P_1 and the axis of the prismatic joint that substitutes the revolute joint centered at P_6. The real roots of this polynomial are 3.9529, 4.0000, 11.0000, and 16.2235. The corresponding moving platform poses appear in the first row of Fig. 5.11.

Finally, if the revolute joint centered at P_5 is also replaced by a prismatic joint, a 3-R$\underline{\text{P}}$P planar robot platform is obtained. This kind of robot platform belongs to the type VIII robot family in Table 5.5. If the orientation of this passive prismatic joint

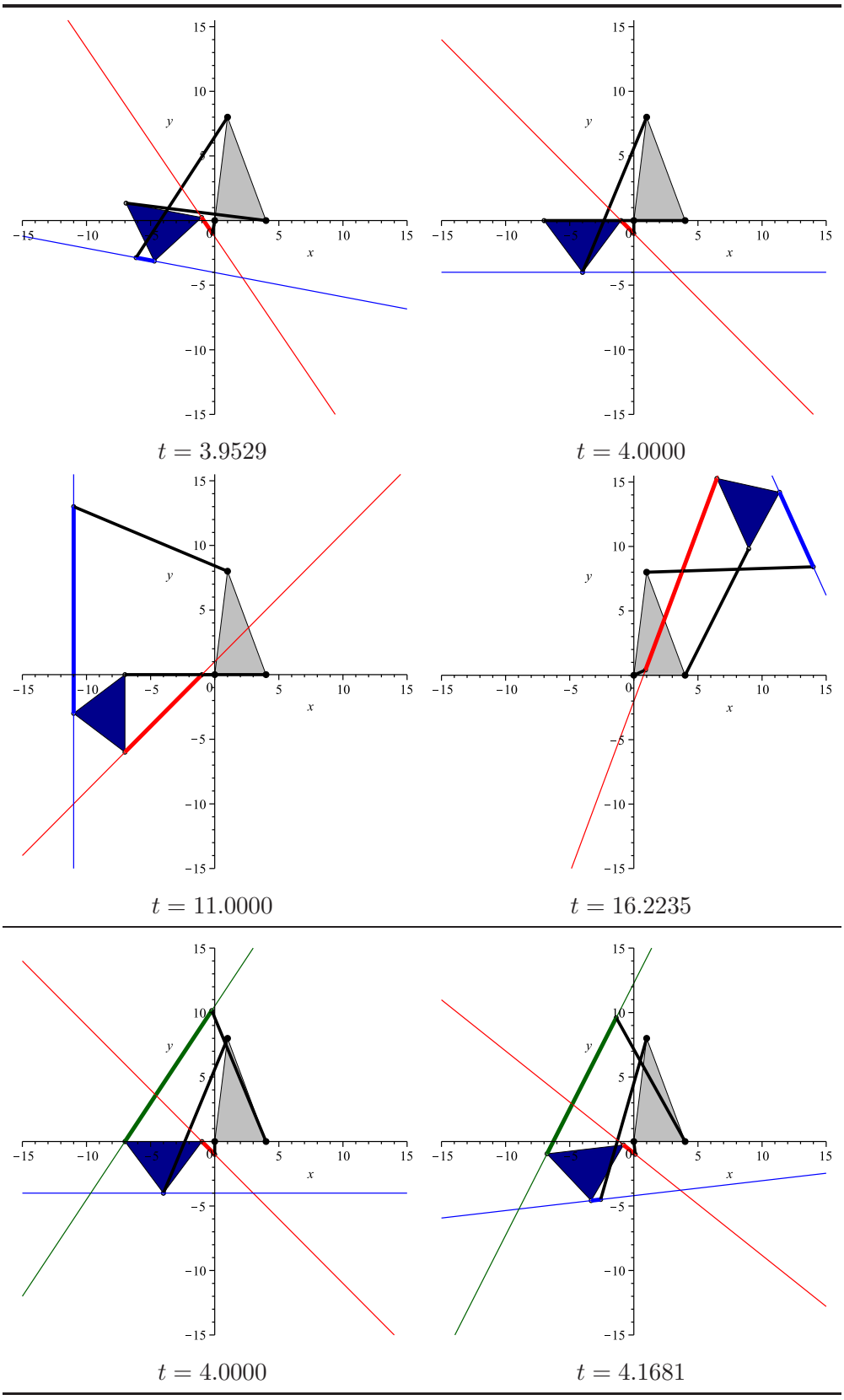

Figure 5.11. The moving platform poses of the analyzed fully-parallel planar robots (Part 2/2).

with respect to its adjacent links, according to the notation of Table 5.5, is given by

$$\begin{aligned}
\alpha_7 &= 2\pi - \arctan\frac{3}{2},\\
\alpha_8 &= 2\pi - \arctan\frac{3}{2} - \arctan\frac{4}{3},\\
\alpha_9 &= \pi + \arcsin\frac{3}{\sqrt{13}},
\end{aligned}$$

then

$$\begin{aligned}
d_{1,4} &= \delta_1 + \frac{1}{\sqrt{2}},\\
d_{3,6} &= \delta_2 - 12,\\
d_{1,6} &= \delta_2 - t,\\
d_{4,5}^2 &= \delta_1^2 + \delta_3^2 + \sqrt{\frac{2}{13}}\,\delta_1\delta_3 - 6\sqrt{2}\,\delta_1 - \frac{6}{\sqrt{13}}\,\delta_3 + 18,\\
d_{5,6}^2 &= \delta_2^2 + \delta_3^2 + \frac{4}{\sqrt{13}}\,\delta_2\delta_3 - 8\,\delta_2 - \frac{16}{\sqrt{13}}\,\delta_3 + 16,\\
d_{4,6}^2 &= \delta_1^2 + \delta_2^2 + 2\delta_3^2 + \sqrt{\frac{2}{13}}\,\delta_1\delta_3 + \frac{4}{\sqrt{13}}\,\delta_2\delta_3 - 6\sqrt{2}\,\delta_1 - 8\,\delta_2 - \frac{22}{\sqrt{13}}\,\delta_3\\
&\quad + 34 + \sqrt{2}\,d_{4,5}\,d_{5,6},\\
d_{2,5} &= \delta_3 - \frac{33}{\sqrt{13}}.
\end{aligned}$$

Substituting these values in $\Gamma(s_{1,6})$, while keeping all other distances unaltered, and iteratively computing the leading coefficients of the resulting polynomial in δ_1, and then in δ_2, and finally in δ_3, we get the characteristic polynomial

$$t^2 - 8.1681\,t + 16.6723.$$

The real roots of this polynomial are 4.000 and 4.1681. The corresponding moving platform poses appear in the second row of Fig. 5.11.

Regarding a translational motion as an infinitely small rotation about a point at infinity has been a common device to analyze some simple kinematics problems. Applying it to the position analysis of multi-loop linkages did not seem to provide any advantage with respect to existing approaches. Nevertheless, it has been shown that, when this idea is combined with a formulation based on distances and oriented areas, the result is a powerful tool that allowed us to conclude that the characteristic polynomial of the 3-R$\underline{\text{P}}$R robot contains the necessary and sufficient information to solve the position analysis of all fully-parallel planar robots. No new sets of variable eliminations are required.

Chapter 6

Configuration spaces and coupler curves

The kinematic chains, or linkages, considered under the title *linkwork* or *articulated systems* are closed planar kinematic chains involving turning pairs only. That is, sets of planar links articulated through pins. For kinematic chains of this type, the equation of the curve generated by an arbitrary point on the kinematic chain —the *tracer point*— can be obtained by solving a finite number of simultaneous equations expressing constancy of distance between pin centers which include the tracer point. Then, the coordinates of all moving pin points, other than those of the tracer, can be seen as unknowns. If we only considered pin-jointed Grübler kinematic chains —*i.e.*, closed planar kinematic chains with mobility one connected by revolute joints—, the number of independent quadratic equations will exceed the number of unknowns by unity. The curve generated by the tracer point —usually known as a *coupler curve*— is, therefore, the eliminant of these equations. This reasoning permits to conclude that the curve generated by any point on a closed planar pin-jointed kinematic chain possessing a finite number of links of finite size is necessarily algebraic [48]. The same result can be attained, in a more compact way, by computing the eliminant of the set of independent loop equations [41, 133, 190]. All coupler curves can be seen as a group of manifold curves joined through singular points usually classified in kinematics as *crunodes* and *cusps* [103, 174]. The interested reader is addressed to the treatise *Cinematica Della Biella Piana* [5] written by the Italian engineering scientist Lorenzo Allievi, a pioneer in *theoretical kinematics of mechanisms*, for a detailed classification of these points in coupler curves, as discussed in [29]. Figure 6.1 shows some types of singular points of algebraic plane curves as presented in [188, pp. 56-58].

The problem of tracing a coupler curve is essentially that of connecting sampled points to give rise to its graph. Sampling a coupler curve is not a difficult task compared to that of connecting the samples, mainly for high-order coupler curves. *Continuation methods* are one of the major approaches reported in the literature to solve this problem [4]. Since, in our case, the curves to be traced are algebraic, *polynomial continuation* can be used [176]. These methods are *global*, that is, they are able to trace all the connected components of a coupler curve but, depending on the application, one does not need to trace all components, but rather one of them starting from a given point. Actually, this is the encountered problem when simulating the motion of a planar kinematic chain [78]. In this case, a very popular method is the so-called *predictor-corrector method* [53]. It consists of two major stages. In the first stage, called the predictor step, a point in the tangent line to the curve at the current given point is estimated [Fig. 6.2(a)]. In the second stage, the corrector step, the predicted point is adjusted onto the curve, using typically a Newton-like method, to get a new point of the curve [Fig. 6.2(b)]. In the case of closed curves, a third stage, called the filling step, is implemented to avoid overlaps.

The predictor-corrector algorithm is simple to implement and hence its popularity. Unfortunately, it exhibits, in general, the undesirable phenomenon known as *drifting*

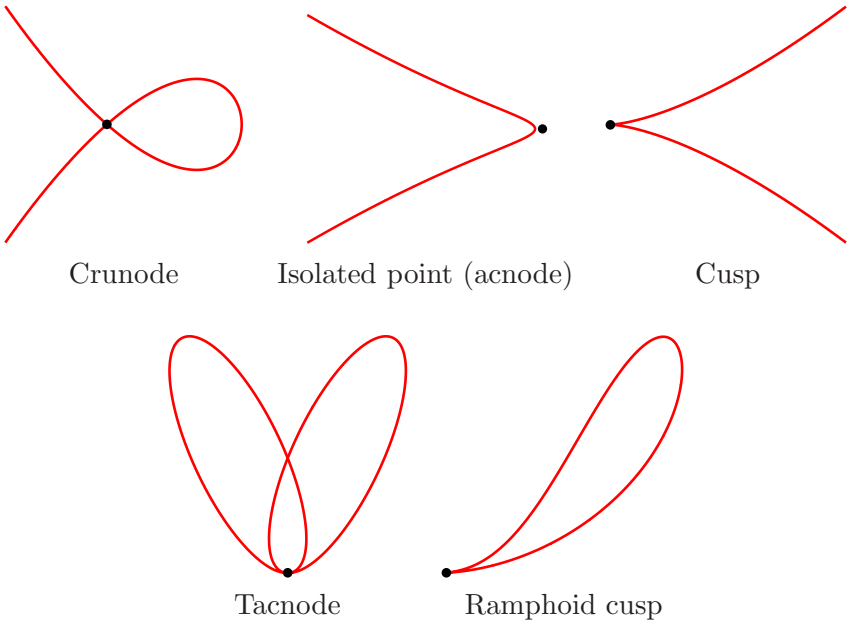

Figure 6.1. Some types of singular points of algebraic plane curves: crunode, isolated point, cusp, tacnode, and ramphoid cusp.

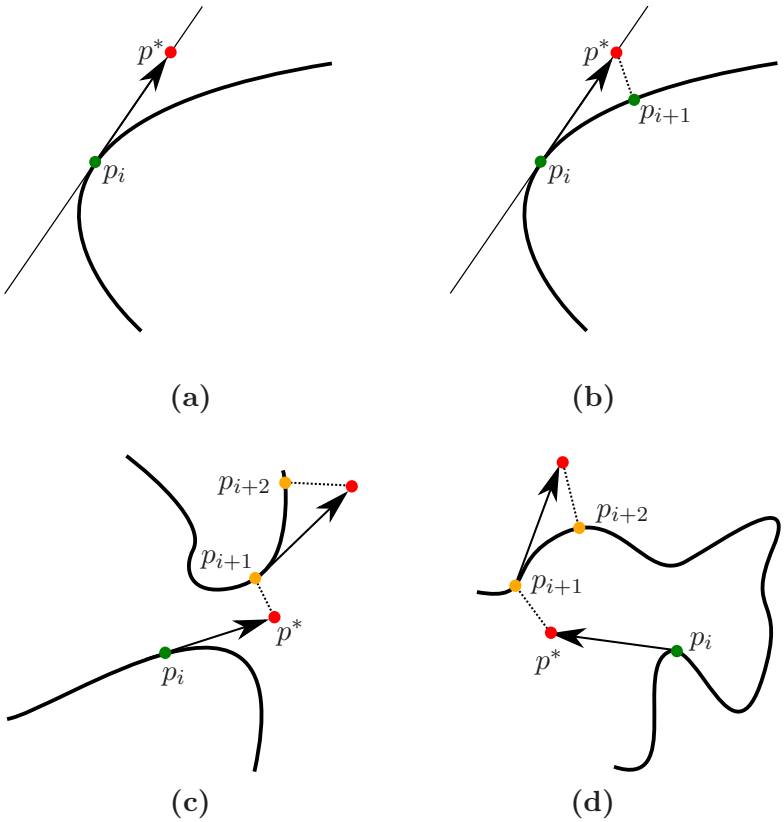

Figure 6.2. **(a)** In the predictor step, a point p^* in the tangent line to the curve at the current point p_i is estimated. **(b)** In the corrector step, the predicted point p^* is adjusted onto the curve producing a new point p_{i+1}. **(c)** The drifting problem. **(d)** The cycling problem

in which the procedure fails to keep moving along a given branch of the curve and drift to another [Fig. 6.2(c)]. In most dramatic cases this might even lead to cycling [Fig. 6.2(d)]. This drawback can be resolved using more sophisticated mathematical tools, than the first order approximations used in standard predictor-corrector algorithms, such as Runge-Kutta or Adam's method [102]. Another important drawback of predictor-corrector algorithms arises when the plane curve to be traced has singular points because the tangent is undefined at them. An approach to overcome this issue is by first computing the singular points with symbolic processing techniques for then use them as starting points of a predictor-corrector algorithm. A simpler and more elegant alternative, valid only for plane curves, is the use of derivative-free methods such as the Morgado-Gomes false position numerical method [130].

The possibility of drifting, cycling, and having problems with singular points, increases dramatically with the number of independent kinematic loops of the linkage because the order of the coupler curves to be traced grows exponentially with it. For example, while the coupler curves of the well-known single-loop four-bar linkage are of the sixth order [79], that of the three-loop double butterfly linkage can be up to the forty-eighth order [140].

In this chapter, instead of focusing on a better algorithm for tracing coupler curves able to deal with all mentioned problems in the workspace of the kinematic chain, an approach based on bilateration techniques and geometrical arguments that first traces the configuration space of the kinematic chain in a distance space and then maps it onto the workspace to obtained the desired coupler curves is proposed. To get an intuitive idea of this approach and its advantages, in the next Section the main clues without going into mathematical details are presented. Section 6.2 concentrates on the case study of tracing the coupler curves of the double butterfly linkage. Section 6.4 discusses how the presented approach can be applied to other pin-jointed Grübler kinematic chains.

6.1 Overview of the proposed approach

A *linkage configuration* is given by a set of parameters uniquely specifying the position of each of its links. The *configuration space* of a linkage is thus simply the set of all its configurations. Then, since all points of a linkage of mobility one trace plane curves which can readily be expressed in terms of the configuration parameters of the linkage itself, an alternative approach, other than directly tracing coupler curves in the linkage workspace, naturally arises: first trace the configuration space of the kinematic chain and then compute the desired curves from it.

To exemplify this idea, let us consider the four-bar linkage in Fig. 6.3(a). The coupler curve traced by any point linked to one of its bars, while taking the opposite bar as fixed, are algebraic curves of the sixth order; *i.e.*, a straight line will cut it in not more than six points [79] [Fig. 6.3(b)]. The configuration space of this linkage can be easily derived by expressing the location of the line segments $\overline{P_1P_3}$ and $\overline{P_2P_4}$ as a function of θ_1 and θ_2, respectively, and imposing the distance between P_3 and P_4 as closure condition [118, pp. 26-27]. Thus, all possible configurations of this linkage defines a curve in the space defined by θ_1 and θ_2.

Unfortunately, the above idea cannot be applied, in general, to multi-loop linkages. Actually, the valid configurations of a multi-loop linkage is usually represented by the solution set of an independent set of its vector loop equations [41, 133, 190]. This requires introducing a variable for each link representing its orientation with respect to the fixed link. For the case of the four-bar linkage, its vector loop equation defines a one-dimension variety in the space defined by $\{\theta_1, \theta_2, \theta_3\}$ which seems quite complicated for

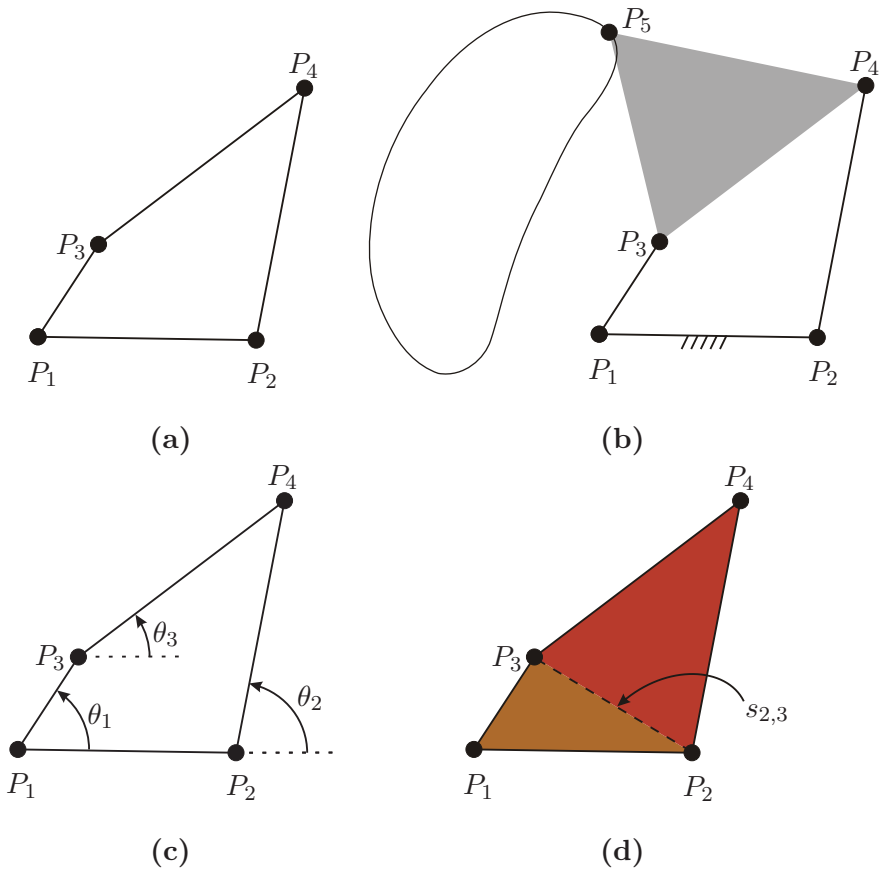

Figure 6.3. **(a)** A four-bar linkage and **(b)** the coupler curve traced by a point affixed to one of its bars while taking the opposite one as fixed. **(c)** Any coupler curve generated by this linkage can be expressed in terms of its configuration space which can be represented by a one-dimension variety in the space defined by $\{\theta_1, \theta_2, \theta_3\}$, or by $\{\theta_1, \theta_2\}$ if the distance constraint between P_3 and P_4 is used as closure condition instead of the standard loop equation. **(d)** Alternatively, this configuration space can be represented by value ranges of a single variable, $s_{2,3}$, one range for each combination of signs of the oriented areas of the triangles $\triangle P_1P_2P_3$ and $\triangle P_2P_4P_3$.

such a simple linkage [Fig. 6.3(c)]. Alternatively, the configuration space of a four-bar linkage can be represented by a single distance variable, for example the distance between P_2 and P_3, provided that the sign of the oriented areas of the triangles $\triangle P_1P_2P_3$ and $\triangle P_2P_4P_3$ are given [Fig. 6.3(d)]. Besides an important reduction in the dimensionality of the problem, the configuration space of the linkage is thus decomposed into up to four components, one for each combination of signs for the two oriented areas. Most importantly, this idea of using distances and signs of oriented areas can be applied to characterize the configuration spaces of arbitrary multi-loop linkages [160, 165].

For example, let us consider the three-loop linkage, commonly known as *double butterfly linkage*, depicted in Fig. 6.4(a). Using the standard formulation based in vector loop equations, its configuration space is determined by the root locus of a system of six scalar equations in the space defined by $\{\theta_1, \ldots, \theta_7\}$. Using the approach proposed in this chapter, it will be shown how this configuration space can be characterized by a plane curve in the space defined by the lengths of $\overline{P_1P_6}$ and $\overline{P_2P_4}$, and how this curve is decomposed into 16 components, one for each combination of signs of the oriented areas of the triangles $\triangle P_2P_4P_{10}$, $\triangle P_1P_3P_6$, $\triangle P_1P_6P_5$ and $\triangle P_4P_9P_7$. This decomposition, to-

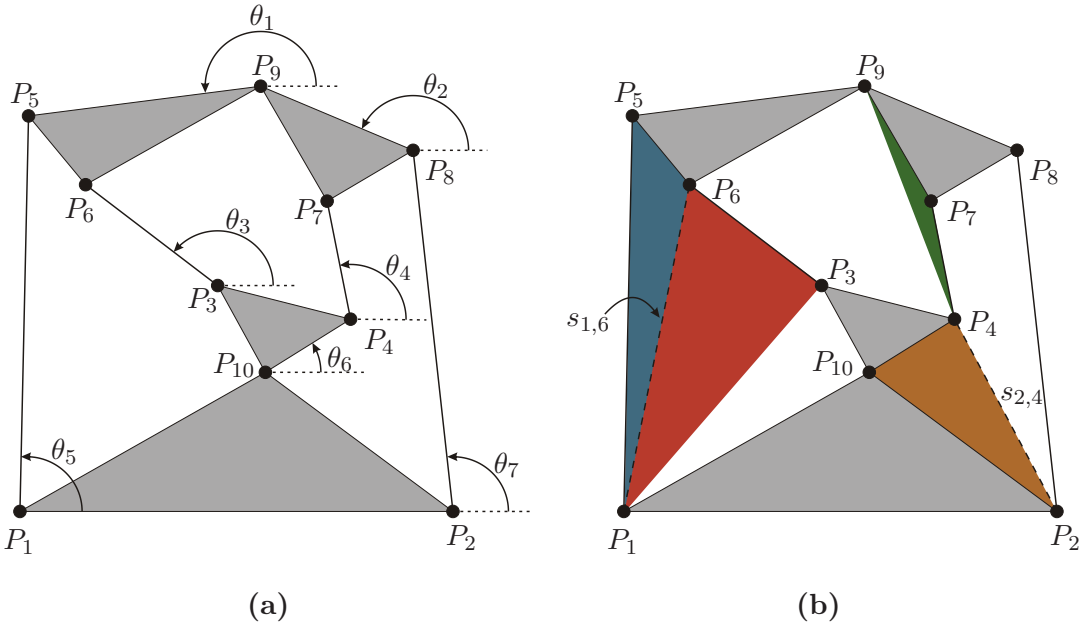

Figure 6.4. **(a)** Using the standard vector loop formulation, the configuration space of a double butterfly linkage can be represented by a one-dimensional variety in the space defined by $\{\theta_1, \ldots, \theta_7\}$. **(b)** Alternatively, using the proposed approach, this configuration space can be represented by a one-dimensional variety in the space defined by $\{s_{1,6}, s_{2,4}\}$ which can be decomposed into 16 varieties, one for each combination of signs of the oriented areas of the triangles $\triangle P_2P_4P_{10}$, $\triangle P_1P_3P_6$, $\triangle P_1P_6P_5$ and $\triangle P_4P_9P_7$.

gether with the reduction of the dimensionality of the ambient space from 7 to 2, greatly simplifies the process of tracing the configuration space of this linkage while retaining, at the same time, the geometric flavor of the problem contrarily to what happens to the fully algebraic current approaches.

6.2 Tracing the double butterfly linkage configuration space

The double butterfly linkage has one of the sixteen topologies available for eight-bar Grübler kinematic chains [118]. In the context of classical kinematics of mechanisms, the input-output problem for this linkage leads to either sixteenth order or eighteenth order polynomials depending on the selected fix and input links [41]. This input-output problem is equivalent to the position analysis problem of the $7/B_2$ and $7/B_3$ Baranov trusses. A polynomial equation for the path of a point located in a coupler link of the double butterfly linkage was presented in [140] for the first time. The resulting polynomial was shown to be, at most, of forty-eighth order. A sampled plot of this curve is presented in [145]. The interested reader is referred to [143] for more details on this kinematic chain.

Fig. 6.5(a) shows a double butterfly linkage. It consists of four binary links and four ternary links with three independent loops. The centers of the revolute joints of the binary links define the line segments $\overline{P_1P_5}$, $\overline{P_3P_6}$, $\overline{P_4P_7}$, and $\overline{P_2P_8}$, and those for the ternary links define the triangles $\triangle P_1P_{10}P_2$, $\triangle P_{10}P_3P_4$, $\triangle P_6P_5P_9$, and $\triangle P_7P_9P_8$. Instead of computing its configuration space in terms of joint angles through loop-closure equations, we will use bilateration techniques to compute the set of values of $s_{2,4}$ and

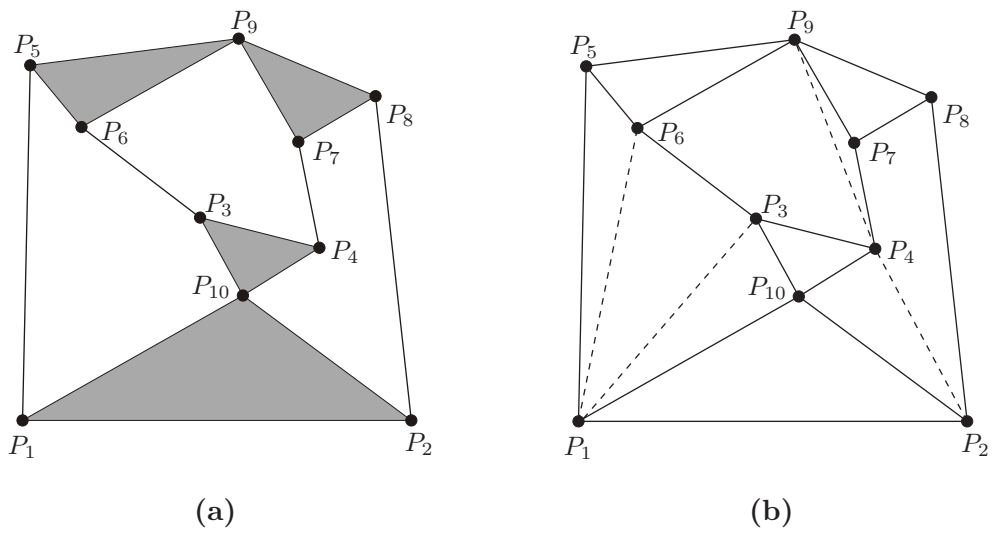

Figure 6.5. **(a)** A double butterfly linkage. **(b)** If the lengths of dotted segments were known, this double butterfly linkage would be equivalent to the structure formed by the strips of triangles presented in Fig. 2.4(bottom).

$s_{1,6}$ compatible with all binary and ternary link side lengths.

It can be verified that, if the distances $s_{1,3}$, $s_{1,6}$, $s_{4,9}$, and $s_{2,4}$ of the double butterfly linkage in Fig. 6.5(a) were fixed, the structure formed by the strips of triangles presented in Fig. 2.4(bottom) would be obtained [Fig. 6.5(b)]. Then, if we rewrite equations (2.21), (2.22), and (2.23), leaving these distances as variables, we get the following system of equations:

$$s_{1,3} = f_1(s_{2,4}) = \det\Big(\mathbf{\Omega}_1\Big) s_{2,4} \tag{6.1a}$$

$$s_{4,9} = f_2(s_{2,4}, s_{1,6}, s_{1,3}) = \det\Big(\mathbf{\Omega}_2\Big) s_{2,4} \tag{6.1b}$$

$$s_{2,8} = f_3(s_{2,4}, s_{1,6}, s_{1,3}, s_{4,9}) = \det\Big(\mathbf{\Omega}_3\Big) s_{2,4} \tag{6.1c}$$

where

$$\begin{aligned}
\mathbf{\Omega}_1 &= -\mathbf{Z}_{2,10,1}\,\mathbf{Z}_{2,4,10} + \mathbf{I} - \mathbf{Z}_{4,10,3}\,\mathbf{Z}_{4,2,10} \\
\mathbf{\Omega}_2 &= -\mathbf{I} + \mathbf{Z}_{2,10,1}\,\mathbf{Z}_{2,4,10} + (\mathbf{I} - \mathbf{Z}_{6,5,9}\,\mathbf{Z}_{6,1,5})\mathbf{Z}_{1,3,6}\,\mathbf{\Omega}_1 \\
\mathbf{\Omega}_3 &= \mathbf{I} + (\mathbf{I} - \mathbf{Z}_{9,7,8}\,\mathbf{Z}_{9,4,7})\,\mathbf{\Omega}_2.
\end{aligned}$$

See §2.6.2 and §2.6.3 for a detailed derivation of these expressions. Computing a resultant from the above triangular system becomes a trivial task that yields a scalar radical equation in two variables: $s_{2,4}$ and $s_{1,6}$.

By expanding (6.1c), we get

$$s_{2,8} = \frac{1}{s_{1,6}\, s_{1,3}\, s_{4,9}}\,\Psi, \tag{6.2}$$

where

$$\begin{aligned}
\Psi =& \Psi_1 + \Psi_2 A_{2,4,10} + \Psi_3 A_{1,3,6} + \Psi_4 A_{1,6,5} + \Psi_5 A_{4,9,7} + \Psi_6 A_{2,4,10} A_{1,3,6} \\
&+ \Psi_7 A_{2,4,10} A_{1,6,5} + \Psi_8 A_{2,4,10} A_{4,9,7} + \Psi_9 A_{1,3,6} A_{1,6,5} + \Psi_{10} A_{1,3,6} A_{4,9,7} \\
&+ \Psi_{11} A_{1,6,5} A_{4,9,7} + \Psi_{12} A_{2,4,10} A_{1,3,6} A_{1,6,5} + \Psi_{13} A_{2,4,10} A_{1,3,6} A_{4,9,7} \\
&+ \Psi_{14} A_{2,4,10} A_{1,6,5} A_{4,9,7} + \Psi_{15} A_{1,3,6} A_{1,6,5} A_{4,9,7} + \Psi_{16} A_{2,4,10} A_{1,3,6} A_{1,6,5} A_{4,9,7},
\end{aligned}$$

with Ψ_i, $i = 1, \ldots, 16$, being polynomials in $s_{2,4}$, $s_{1,6}$, $s_{1,3}$, and $s_{4,9}$, and $A_{2,4,10}$, $A_{1,3,6}$, $A_{1,6,5}$, and $A_{4,9,7}$, the oriented areas of $\triangle P_2P_4P_{10}$, $\triangle P_1P_6P_3$, $\triangle P_1P_6P_5$, and $\triangle P_4P_9P_7$, respectively, and substituting (6.1a) and (6.1b) which account for the unknown squared distances $s_{1,3}$ and $s_{4,9}$.

Equation (6.2) is the closure condition for the double butterfly linkage. This equation contains four variable oriented areas, namely, $A_{2,4,10}$, $A_{1,3,6}$, $A_{1,6,5}$, and $A_{4,9,7}$. Hence, strictly speaking, this closure condition encompasses sixteen different scalar equations, one per each combination of signs for these areas. Each set of solutions to these sixteen equations correspond to different families of assembly modes. Therefore, the configuration space of the double butterfly linkage can be decomposed into sixteen varieties, one for each combination of signs of the oriented areas $A_{2,4,10}$, $A_{1,3,6}$, $A_{1,6,5}$ and $A_{4,9,7}$, in the space defined by $\{s_{1,6}, s_{2,4}\}$. Next, we show a simple procedure, that explodes this fact, for tracing the configuration space of the double butterfly linkage.

According to (6.1c), let us define

$$f_\eta(s_{2,4}, s_{1,6}) = \frac{1}{s_{1,6}\, s_{1,3}\, s_{4,9}}\, \Psi - s_{2,8}, \tag{6.3}$$

where $\eta = 0, \ldots, 15$ specifies the combination of signs for the areas $A_{2,4,10}$, $A_{1,3,6}$, $A_{1,6,5}$, and $A_{4,9,7}$. Thus, for example, $\eta = 10 = (1010)_2$ implies that $A_{2,4,10} > 0$, $A_{1,3,6} < 0$, $A_{1,6,5} > 0$, and $A_{4,9,7} < 0$. Given a initial configuration for the double butterfly linkage identified by the tuple $({s_{2,4}}^{(0)}, {s_{1,6}}^{(0)}, \eta)$ where $f_\eta({s_{2,4}}^{(0)}, {s_{1,6}}^{(0)}) = 0$, the configuration space can be traced from this point following these steps:

1. Use a predictor-corrector method for computing a new ordered pair $({s_{2,4}}^{(k)}, {s_{1,6}}^{(k)})$ such that $f_\eta({s_{2,4}}^{(k)}, {s_{1,6}}^{(k)}) = 0$ and $|{s_{2,4}}^{(k)} - {s_{2,4}}^{(k-1)}| < \delta$, where δ is a specified resolution step.

2. Evaluate the oriented areas $A_{2,4,10}$, $A_{1,3,6}$, $A_{1,6,5}$, and $A_{4,9,7}$ for $({s_{2,4}}^{(k)}, {s_{1,6}}^{(k)})$. If any of them is *close enough* to zero, the current configuration given by $({s_{2,4}}^{(k)}, {s_{1,6}}^{(k)}, \eta)$ belongs to more than one family of assembly modes and the linkage movement may evolve along different paths. Identify all these families, that is, determine all feasible values that η can assume.

3. Repeat steps 1 and 2 for each tuple $({s_{2,4}}^{(k)}, {s_{1,6}}^{(k)}, \eta)$ until the initial tuple $({s_{2,4}}^{(0)}, {s_{1,6}}^{(0)}, \eta)$ is reached or it is not possible to compute any new ordered pair $({s_{2,4}}^{(k+1)}, {s_{1,6}}^{(k+1)})$.

To exemplify this algorithm, a detailed example is presented next.

6.3 Example

According to the notation used in Fig. 6.5(a), let us set $s_{1,2} = 169$, $s_{1,5} = 145$, $s_{1,10} = 65$, $s_{2,8} = 200$, $s_{2,10} = 52$, $s_{3,4} = 5$, $s_{3,6} = 50$, $s_{3,10} = 5$, $s_{4,7} = 36$, $s_{4,10} = 10$, $s_{5,6} = 5$, $s_{5,9} = 53$, $s_{6,9} = 34$, $s_{7,8} = 10$, $s_{7,9} = 5$, and $s_{8,9} = 25$. Using triangular inequalities, $s_{2,4}$ can be bound to lie in the interval $[62 - 4\sqrt{13}\sqrt{10}, 62 + 4\sqrt{13}\sqrt{10}]$. Fig. 6.6(left) shows the root locus of (6.2) for sampled values of $s_{2,4}$ in its range using increments of $\frac{1}{100}$. The result contains no information on the connectivity of each sample to its neighbors. Actually, finding this connectivity is the difficult point. This sampled curve has been included here for comparison purposes with the results obtained by tracing as shown next.

Let us suppose that we are interested in tracing the configuration space followed by the linkage from the following three initial configurations:

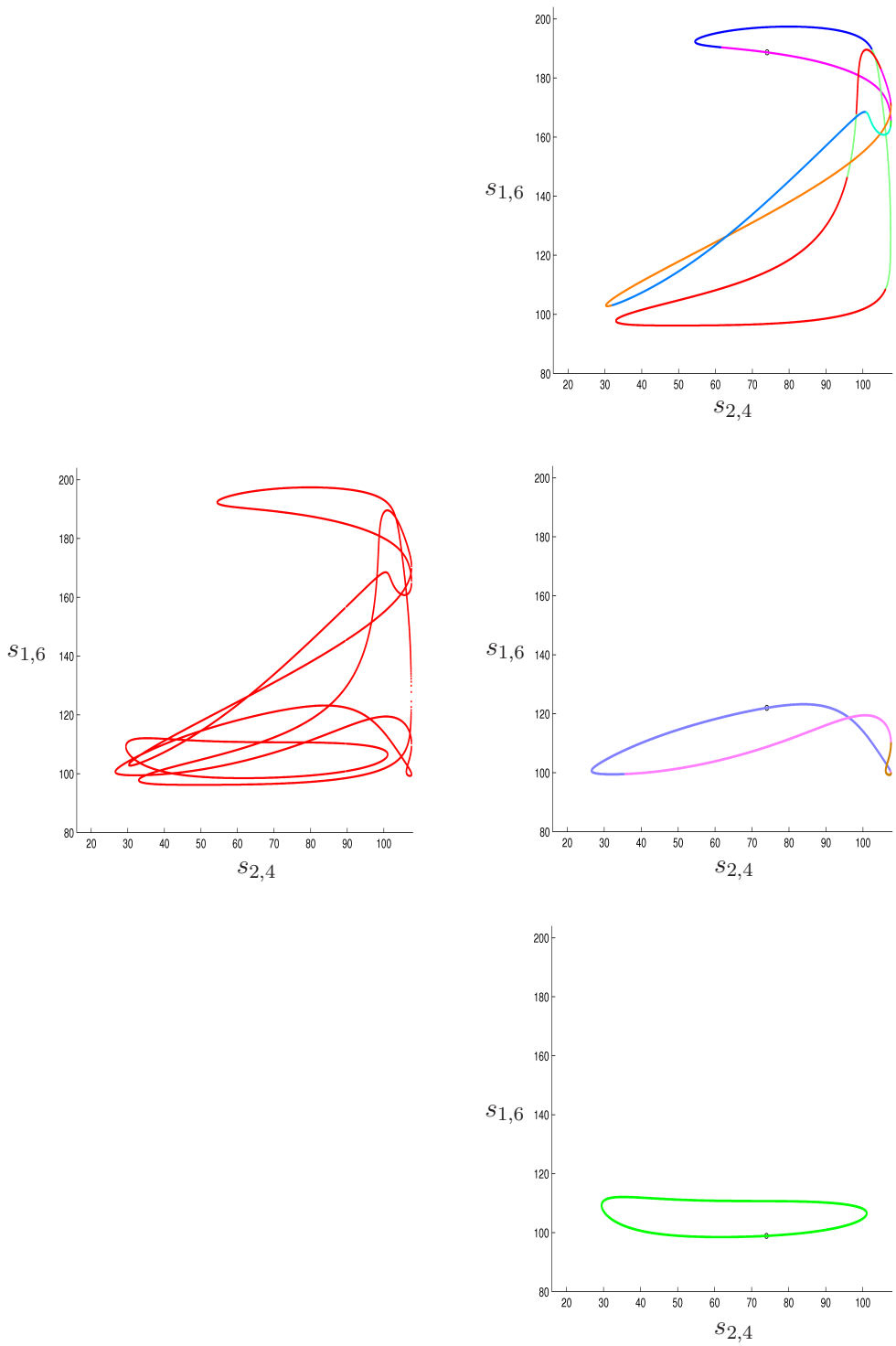

Figure 6.6. Left: The root locus of equation (6.2) in the plane defined by $s_{2,4}$ and $s_{1,6}$ for sampled values of $s_{2,4}$. **Right:** From top to bottom, the connected components of the configuration space traced when starting from the initial configurations $s_{2,4} = 74$, $s_{1,6} = 188.68$, and $\eta = 8$ ($A_{2,4,10} > 0$, $A_{1,3,6} < 0$, $A_{1,6,5} < 0$, and $A_{4,9,7} < 0$), $s_{2,4} = 74$, $s_{1,6} = 122$, and $\eta = 14$ ($A_{2,4,10} > 0$, $A_{1,3,6} > 0$, $A_{1,6,5} > 0$, and $A_{4,9,7} < 0$), and $s_{2,4} = 74$, $s_{1,6} = 98.92$, and $\eta = 0$ ($A_{2,4,10} < 0$, $A_{1,3,6} < 0$, $A_{1,6,5} < 0$, and $A_{4,9,7} < 0$), respectively.

Color	$A_{2,4,10}$	$A_{1,3,6}$	$A_{1,6,5}$	$A_{4,9,7}$
	$-$	$-$	$-$	$-$
	$-$	$-$	$-$	$+$
	$-$	$+$	$-$	$-$
	$-$	$+$	$-$	$+$
	$-$	$+$	$+$	$+$
	$+$	$-$	$-$	$-$
	$+$	$-$	$-$	$+$
	$+$	$+$	$-$	$-$
	$+$	$+$	$-$	$+$
	$+$	$+$	$+$	$-$
	$+$	$+$	$+$	$+$

Table 6.1. Code of colors used in Figs. 6.6 and 6.7 for the signs of $A_{2,4,10}$, $A_{1,3,6}$, $A_{1,6,5}$, and $A_{4,9,7}$.

1. $s_{2,4} = 74$, $s_{1,6} = 188.68$, and $\eta = 8$ ($A_{2,4,10} > 0$, $A_{1,3,6} < 0$, $A_{1,6,5} < 0$, and $A_{4,9,7} < 0$),

2. $s_{2,4} = 74$, $s_{1,6} = 122$, and $\eta = 14$ ($A_{2,4,10} > 0$, $A_{1,3,6} > 0$, $A_{1,6,5} > 0$, and $A_{4,9,7} < 0$),

3. $s_{2,4} = 74$, $s_{1,6} = 98.92$, and $\eta = 0$ ($A_{2,4,10} < 0$, $A_{1,3,6} < 0$, $A_{1,6,5} < 0$, and $A_{4,9,7} < 0$).

The results using the procedure presented in the previous section appear in Figure 6.6(right), from top to bottom, respectively. In the three plots, colors indicate the signs of the oriented areas according to Table 6.1.

6.3.1 Coupler curves

In order to determine the coupler curve of a selected tracer of the linkage using the computed configuration space, we proceed to calculate the position of the linkage's revolute pair centers using bilateration. Let us suppose that $\triangle P_1 P_2 P_{10}$ is the fixed link. Then, for example, we can set $P_1 = (4,0)^T$, $P_2 = (17,0)^T$, and $P_{10} = (11,4)^T$, and the path traced by P_3, P_4, P_5, P_6, P_7, P_8, and P_9 can be obtained by replacing each previously computed tuple $(s_{2,4}, s_{1,6}, \eta)$ in the sequence of bilaterations given by:

$$\begin{aligned}
\mathbf{p}_{2,4} &= \mathbf{Z}_{2,10,4}\,\mathbf{p}_{2,10},\\
\mathbf{p}_{10,3} &= \mathbf{Z}_{10,4,3}\,\mathbf{p}_{10,4},\\
\mathbf{p}_{1,6} &= \mathbf{Z}_{1,3,6}\,\mathbf{p}_{1,3},\\
\mathbf{p}_{1,5} &= \mathbf{Z}_{1,6,5}\,\mathbf{p}_{1,6},\\
\mathbf{p}_{5,9} &= \mathbf{Z}_{5,6,9}\,\mathbf{p}_{5,6},\\
\mathbf{p}_{4,7} &= \mathbf{Z}_{4,9,7}\,\mathbf{p}_{4,9},\\
\mathbf{p}_{7,8} &= \mathbf{Z}_{7,9,8}\,\mathbf{p}_{7,9}.
\end{aligned}$$

Fig. 6.7(top) shows the path followed by P_9 from the first initial configuration. It can be observed how the mapping from configuration space to workspace is surjective —*i.e.*, two points of the configuration space can be mapped onto the same point in the workspace— and how this fact is actually the underlying reason that makes coupler curves so difficult to be traced directly in the linkage workspace. The zoomed-in areas in Fig. 6.7(top) present this effect by showing how two overlapping branches next to

a ramphoid cusp, which leads to a reciprocating motion of the linkage, and a near-quadruple point are generated. Similar situations arise for the path followed by P_9 from the second initial configuration. In this case a cusp and a tacnode can be identified [Fig. 6.7(center)]. The curve traced when starting from the third initial configuration appears in [Fig. 6.7(bottom)]. Observe how in this case a smooth simple curve in the configuration space maps onto the linkage workspace as a curve with several singular points in a reduced area which would be very difficult to be directly traced using a standard predictor-corrector procedure without highly increasing its resolution.

If we were interested in the curve traced by a coupler point different from the revolute pair centers, we could compute its location by introducing one extra bilateration with reference to the revolute pair centers of the corresponding coupler link.

For the curves traced in a different kinematic inversion of the linkage, that is, taking as fixed another link, we simply have to calculate the Euclidean transformation between the constant values of the corresponding fixed link and the values computed with the above set of bilaterations, and use it to recompute the values for the other revolute pair centers. With this simple procedure, the coupler curves of any kinematic inversion of the double butterfly linkage can be computed.

As it has been shown in this example, the main advantage of the proposed method for tracing the coupler curves is that the configuration space of Grübler kinematic chains can be decomposed into easy-to-trace branches. Actually, in the presented example all singularities arise when mapping these branches onto the linkage workspace.

6.4 Other pin-jointed Grübler kinematic chains

The proposed method for tracing configuration spaces and coupler curves can be easily applied to any pin-jointed Grübler kinematic chain. It can be verified that tracing the coupler curves of the four-bar linkage and the two six-bar linkages —the Watt and the Stephenson linkages— becomes trivial because their configuration spaces correspond to ranges of a single distance, one range for each combination of sign of two or three oriented areas, depending on the case. A similar situation occurs for twelve of the sixteen possible topologies for eight-bar Grübler kinematic chains (these topologies can be found in [118, p. 144]). In these cases, four oriented areas are needed. For the remaining four topologies —in which the double butterfly linkage is included— the one-dimensional configuration space is embedded in a two-dimensional distance space. Since the signs of four oriented areas are needed in all these four cases to uniquely identify a configuration, the configuration space is naturally decomposed into 16 components. Table 6.2 presents the equations representing the corresponding configuration spaces for these four cases.

As a final remark, it is relevant to stand out that the current approaches for tracing the coupler curves of planar kinematic chains provide a rapid algebraization of the problem thus becoming blind to the underlying geometry. A new approach, based on bilateration techniques and geometrical arguments, that first computes the linkage configuration space embedded in a space of squared distances and then maps it onto the linkage workspace has been presented in this chapter. The used formulation involves products, additions, and square roots. The presence of square roots permits a more compact representation than the standard techniques based on polynomials. Square roots actually play a fundamental role in the presented approach because their sign represent the orientation of triangles formed by sets of three joints of the linkage thus retaining important geometric information. Configuration spaces are thus decomposed into components for which the signs of the oriented areas of the involved triangles remain invariant. This decomposition, besides providing a new insight in the analysis of

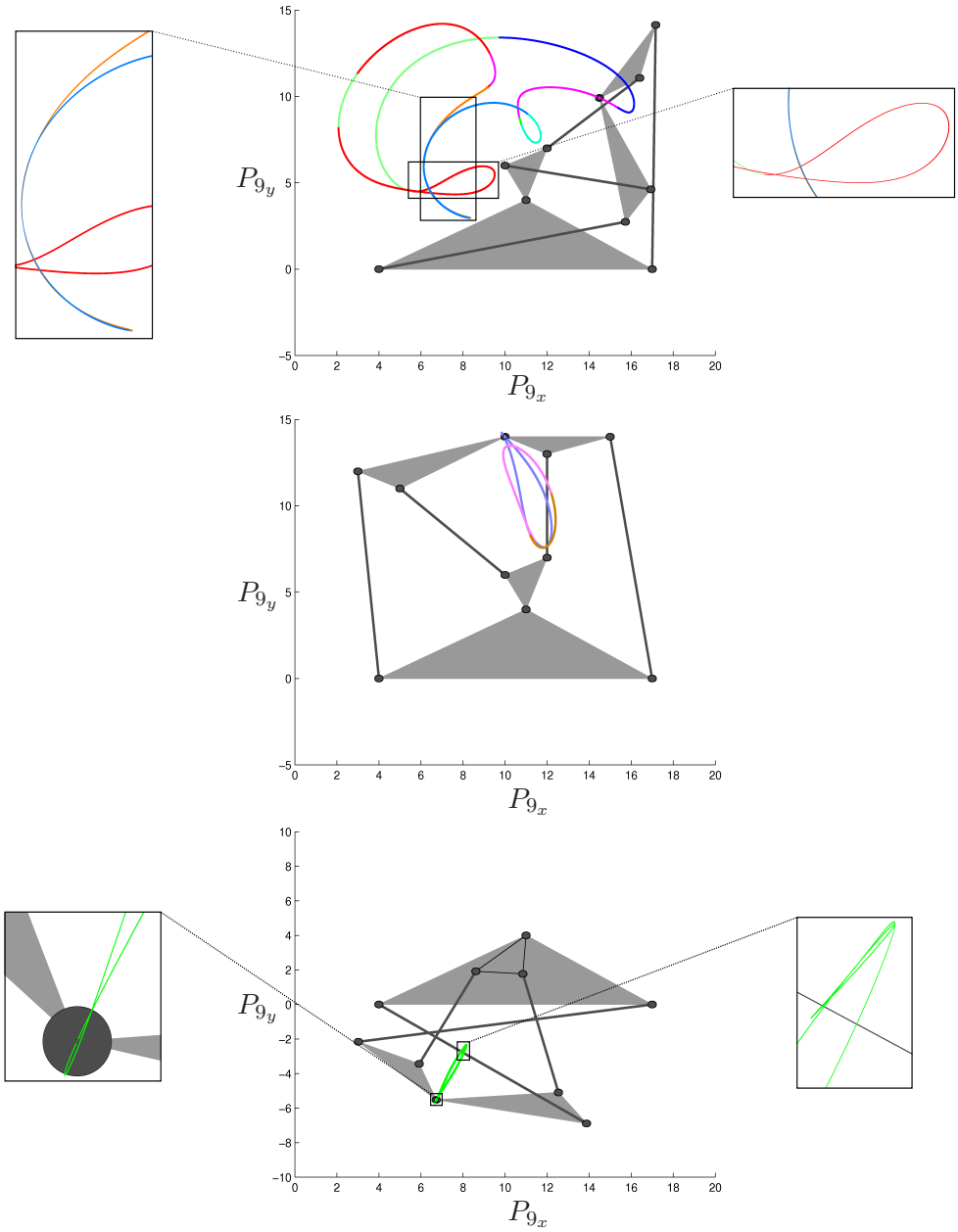

Figure 6.7. The paths followed by the revolute pair center P_9 from different initial configurations. **Top:** For the curve traced from the initial configuration $s_{2,4} = 74$, $s_{1,6} = 188.68$, and $\eta = 8$, zoomed-in areas show how, after mapping the configuration space onto the workspace, a ramphoid cusp and near-quadruple point are generated. **Center:** For the curve traced from the initial configuration $s_{2,4} = 74$, $s_{1,6} = 122$, and $\eta = 14$, a cusp and a tacnode can be identified. **Bottom:** For the curve traced from the initial configuration $s_{2,4} = 74$, $s_{1,6} = 98.92$, and $\eta = 0$, zoomed-in areas show how, after mapping the configuration space onto the workspace, several singular points are generated in a reduced region.

coupler curves, avoids most of the possible drifts that could arise when using a standard predictor-corrector method directly in the linkage workspace.

Linkage	**Distance space & oriented areas**	**Closure conditions**
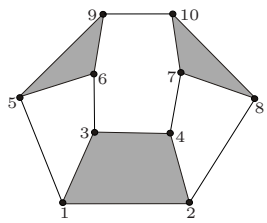	$(s_{1,6}, s_{2,7})$ $A_{1,6,3}, A_{1,6,5},$ $A_{2,4,7}, A_{2,7,8}$	$s_{9,10} = f(s_{1,6}, s_{2,7}) =$ $\det\Big(-\mathbf{I}+\mathbf{Z}_{6,5,9}\mathbf{Z}_{6,1,5}+\mathbf{Z}_{1,3,4}\mathbf{Z}_{1,6,3}-\mathbf{Z}_{4,1,2}\mathbf{Z}_{1,3,4}\mathbf{Z}_{1,6,3}-$ $(\mathbf{I}-\mathbf{Z}_{7,8,10}\mathbf{Z}_{7,2,8})\,\mathbf{Z}_{4,2,7}\mathbf{Z}_{4,1,2}\mathbf{Z}_{1,3,4}\mathbf{Z}_{1,6,3}\Big)s_{1,6}$
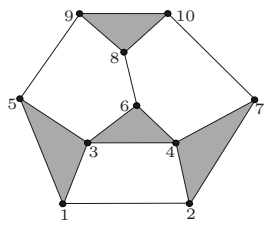	$(s_{1,4}, s_{6,9})$ $A_{1,4,3}, A_{1,4,2},$ $A_{5,6,9}, A_{6,9,8}$	$s_{7,10} = f(s_{1,4}, s_{6,9}, s_{5,6}) =$ $\det\Big(\mathbf{Z}_{4,2,7}\mathbf{Z}_{4,1,2}-\mathbf{Z}_{4,3,6}\mathbf{Z}_{4,1,3}-(\mathbf{I}-\mathbf{Z}_{9,8,10}\mathbf{Z}_{9,6,8})$ $\mathbf{Z}_{6,5,9}\mathbf{\Omega}_1\Big)s_{1,4}$ $s_{5,6} = f(s_{1,4}) = \det\big(\mathbf{\Omega}_1\big)s_{1,4} =$ $\det\Big(-\mathbf{Z}_{1,3,5}\mathbf{Z}_{1,4,3}+\mathbf{I}-\mathbf{Z}_{4,3,6}\mathbf{Z}_{4,1,3}\Big)s_{1,4}$
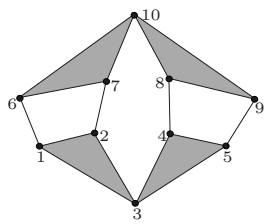	$(s_{1,7}, s_{4,10})$ $A_{1,7,6}, A_{1,7,2},$ $A_{3,10,4}, A_{4,10,8}$	$s_{5,9} = f(s_{1,7}, s_{4,10}, s_{3,10}) =$ $\det\Big((\mathbf{I}-\mathbf{Z}_{4,3,5}\mathbf{Z}_{4,10,3}-\mathbf{Z}_{10,8,9}\mathbf{Z}_{10,4,8})\,\mathbf{Z}_{10,3,4}\mathbf{\Omega}_1\Big)s_{1,7}$ $s_{3,10} = f(s_{1,7}) = \det\big(\mathbf{\Omega}_1\big)s_{1,7} =$ $\det\Big(-\mathbf{Z}_{1,2,3}\mathbf{Z}_{1,7,2}+\mathbf{I}-\mathbf{Z}_{7,6,10}\mathbf{Z}_{7,1,6}\Big)s_{1,7}$
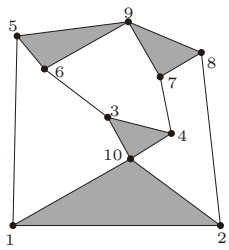	$(s_{2,4}, s_{1,6})$ $A_{2,4,10}, A_{1,3,6},$ $A_{1,6,5}, A_{4,9,7}$	$s_{2,8} = f(s_{2,4}, s_{1,6}, s_{1,3}, s_{4,9}) =$ $\det\Big(\mathbf{I}+(\mathbf{I}-\mathbf{Z}_{9,7,8}\,\mathbf{Z}_{9,4,7})\,\mathbf{\Omega}_2\Big)s_{2,4}$ $s_{4,9} = f(s_{2,4}, s_{1,6}) = \det\big(\mathbf{\Omega}_2\big)s_{2,4} =$ $\det\Big(-\mathbf{I}+\mathbf{Z}_{2,10,1}\,\mathbf{Z}_{2,4,10}+(\mathbf{I}-\mathbf{Z}_{6,5,9}\,\mathbf{Z}_{6,1,5})\,\mathbf{Z}_{1,3,6}\,\mathbf{\Omega}_1\Big)s_{2,4}$ $s_{1,3} = f(s_{2,4}) = \det\big(\mathbf{\Omega}_1\big)s_{2,4} =$ $\det\Big(-\mathbf{Z}_{2,10,1}\,\mathbf{Z}_{2,4,10}+\mathbf{I}-\mathbf{Z}_{4,10,3}\,\mathbf{Z}_{4,2,10}\Big)s_{2,4}$

Table 6.2. The four eight-bar Grübler kinematic chains whose configuration space can be embedded in a two-dimensional distance space. Since four oriented areas are needed in the four cases to uniquely identify a configuration, the corresponding configuration spaces are decomposed into 16 components. The equations representing the corresponding configuration spaces in implicit form are given on the right column.

Chapter 7
Conclusions

In this thesis, the position analysis of kinematic chains has been studied based on the idea of obtaining their closure conditions using n-laterations and constructive geometry arguments for the first time. The developed techniques fall inside of what is known as distance geometry, that is, the study of geometric spaces by means of the metrics which can be defined on them without resorting to arbitrary reference frames —*i.e*, an intrinsic characterization of the spaces studied. In order to develop the basics, theory, and verify the applicability of the proposed approach, this thesis focuses on the analysis of the most fundamental planar kinematic chains, namely, Baranov trusses, Assur kinematic chains, and pin-jointed Grübler kinematic chains.

The techniques developed in this thesis have shown to be novel and promising tools for the position analysis of kinematic chains and related problems because, principally, the resulting system of kinematic equations is i) free from arbitrary coordinate frames, ii) free from transcendental functions, iii) reduced in the number of variables and equations —in comparison with standard methods, and iv) geometrically interpretable in a straightforward way —all equations are posed in terms of distances and oriented areas. In fact, the development of the proposed approach and its application to planar kinematic chains have opened the door to what seems a fruitful field in *kinematics of mechanisms*.

7.1 Summary of contributions

In Chapter 2, a matrix-form expression for the bilateration problem is deduced. From this linear algebra representation emerges what has been called in this thesis the bilateration matrix, the key element of the developed techniques. It is shown that bilateration matrices can be seen as perpendicular matrices, a name coined from the fact that their columns and rows are orthogonal vectors of the same magnitude. Using the scaling property of these matrices and the condition that they constitute a commutative group under product and addition operations, the fundamental technique of computing squared distances between any pair of points in strips of triangles is developed. The use of this technique to compute closure conditions of kinematic chains, as well as the application of permutations to closure conditions, are also presented. All these results can be seen as contributions to distance plane geometry.

Chapter 3 discusses how the constraints arisen from the procedure to compute the coupling degree of a truss can be straightforwardly implemented by applying squared distances in strips of triangles, that is, using the technique to compute closure conditions of kinematic chains presented in Chapter 2. In this way it is shown how, using bilateration techniques, the position analysis problem of all the cataloged Baranov trusses is greatly simplified when compared with state-of-the-art methods, specially to those based on independent loop equations, because the system of kinematic equations is reduced to

a single scalar radical equation in one variable in all of them, except for the Baranov trusses $9/B_{25}$, $9/B_{26}$, $9/B_{27}$, and $9/B_{28}$ for which the system is formed by two scalar equations in two variables. In this chapter is presented how to algebraically manipulate the resulting system of equations to obtain a polynomial expression. The simplification achieved with the use of bilateration techniques is highlighted by solving classical problems of *theoretical kinematics of mechanisms*, such as the closed-form position analysis of the seven-link Baranov trusses, and other that remained still open, such as the closed-form position analysis of the $9/B_{28}$ Baranov truss or the closed-form position analysis of a Baranov truss of more than five loops.

A well-known fact in *theoretical kinematics* is that a translational motion can be considered as an infinitely small rotation about a point at infinity. However, applying this property to solve the position analysis of Assur kinematic chains, is not, in general, simple. Chapter 4 essentially shows how the intrinsic formulations based on distances and oriented areas resulting from bilateration techniques provide a framework within which the aforementioned property can be easily applied thus leading to the conclusion that the distance-based closure conditions of Baranov trusses contain all the necessary and sufficient information for solving the position analysis of all derived Assur kinematic chains. In fact, it is shown how all Assur kinematic chains can be seen as projective extensions of Baranov trusses, that is, Baranov trusses with revolute joint centers located at infinity. This contribution to *theoretical kinematics of mechanisms* is relevant because the position analysis of all derived Assur kinematics chains from a single Baranov truss can be carried out without having to perform new sets of variable eliminations, as it is the usual practice when deriving characteristic polynomials from sets of independent loop equations.

In Chapter 5, a contribution to robot kinematics is done by applying and extending the ideas presented in Chapters 3 and 4 to solve the forward kinematic analysis of fully-parallel planar robots. It is shown that the characteristic polynomial of any fully-parallel planar robot can be derived directly from the characteristic polynomial expressed in terms of distances and oriented areas of the well-studied 3-R$\underline{\text{P}}$R robot, thus escaping from the case-by-case treatment for the closed-form solution of the forward kinematics of fully-parallel planar robots that typically requires new sets of variable eliminations. In addition, it is presented that the mentioned characteristic polynomial derived using bilateration techniques for the 3-R$\underline{\text{P}}$R parallel robot is valid, without modifications, for any instance of this robot, including the special architectures and configurations that cannot be properly handled by previous formulations.

Finally, Chapter 6 presents a new approach to trace the coupler curves of pin-jointed Grübler kinematic chains. The proposed method, instead of focusing on finding better algorithms for tracing curves, avoids a rapid algebraization of the problem, as it happens in current approaches, by tracing first the linkage configuration space in a distance space and then mapping it onto the linkage workspace to obtain the desired coupler curves. It is shown that tracing the configuration space of a linkage in the proposed distance space is simpler because the equation that implicitly defines this space can be straightforwardly obtained using bilateration techniques, and the configuration space embedded in this distance space naturally decomposes into components corresponding to different combinations of signs for the oriented areas of the triangles involved in the bilaterations. Actually, this decomposition provides a new insight in the analysis of coupler curves, a fundamental topic in *kinematics of mechanisms*. The advantages of the proposed two-step method are exemplified by tracing the coupler curves of a double butterfly linkage.

7.2 Directions for future work

The research line started with this thesis seems a promising one for the analysis of mechanisms. Some prospects for further research can be identified. They are briefly discussed next:

1. Application to trusses with joints involving more than two links

The concept of Baranov truss has been extended to trusses with joints involving more than two links —there are indeed 125 such trusses with up to four loops [35]. The closed-form solution to the position analysis of at least one of these trusses, the Dixon-Wunderlich linkage, was reported in [189]. It can be verified that the position analysis of this truss can be readily solved using bilateration techniques. However, the extension of the method proposed in this thesis to all other members of this family of trusses is a point that deserves more attention. This topic was already discussed in Chapter 3.

2. Position analysis of spherical kinematic chains

The position analysis of spherical kinematic chains could be solved by extending the ideas developed in this thesis for the position analysis of planar kinematic chains. Two approaches to address this problem can be identified. The first approach consists in considering spherical kinematic chains as special cases of spatial kinematic chains to solve their position analysis problem using trilaterations. The second approach, geometrically more elegant, would be based on obtaining a matrix-form expression for bilateration on the sphere to compute closure conditions —*i.e*, to use angles instead of distances. In any case, since planar kinematic chains can be seen as particular cases of spherical kinematic chains [192], the result could be used to solve the spherical versions of Baranov trusses and Assur kinematic chains.

3. Position analysis of spatial kinematic chains

The ideas developed in this thesis for the position analysis of planar kinematic chains could be extended to solve the position analysis of spatial kinematic chains. To this end, it is necessary first to derive a matrix-form expression for trilateration that facilitates the algebraic manipulations needed to obtain closure conditions, that is, in this case, the computation of square distances in strips of tetrahedra. This is a relevant step because, the vector expression for trilateration presented in [184] can be used to obtain closure conditions but, as it can be verified, its manipulation becomes very cumbersome even to solve the position analysis of simple spatial structures such as an octahedron. This matrix-form expression for trilateration could be used to solve the position analysis of spatial Assur groups [170].

4. Implementation of numerical procedures

The research reported in this thesis has focused on algebraically manipulating the distance-based closure conditions of Baranov trusses, and Assur kinematic chains, to obtain closed-form solutions to the position analysis problem. As it has been repeatedly suggested throughout this thesis, these closure conditions could be solved using numerical approaches like, for instance, interval Newton methods. The use of interval techniques is highlighted because of they naturally accommodate to the expressions with geometrical meaning. The implementation of such numerical procedure seems promising for the

position analysis of Baranov trusses with a large number of independent loops —think, for example, of Watt-Baranov trusses with more than 13 links.

5. Coupler curves of planar linkages with slider joints

Combining the results presented in Chapters 4 and 5 with the algorithm developed in Chapter 6 to trace the configuration spaces and coupler curves of complex planar kinematic chains with slider joints is an interesting problem that needs further research. Up to the author's knowledge, there are no previous works on the analysis of coupler curves of planar kinematic chains with slider joints beyond those of the well-known four-bar linkages. Moreover, although in theory the algorithm of Chapter 6 can be straightforwardly applied to kinematic chains with mobility greater than one, the extension to compute workspaces actually demands additional work.

6. Singularity analysis of all fully-parallel planar robots

The singularities of a fully-parallel planar robot can be obtained by computing the discriminant of its characteristic polynomial. Then, according to the results presented in Chapter 5, these singularities could be obtained from those of the 3-R$\underline{\text{P}}$R robot through a limit process. In this sense, it can be said that the ideas presented in Chapters 4 and 5 have far-ranging implications as they can be applied to solve other problems than those tackled in this thesis.

Chapter 8

List of publications

The publications resulting from the research reported in this thesis are listed below:

Journals

1. **N. Rojas** and F. Thomas, *On Closed-Form Solutions to the Position Analysis of Baranov Trusses*, Mechanism and Machine Theory, Vol. 50, pp. 179-196, April **2012**

2. **N. Rojas** and F. Thomas, *Closed-Form Solution to the Position Analysis of Watt-Baranov Trusses Using the Bilateration Method*, ASME Journal of Mechanisms and Robotics, Vol. 3, No. 3, 031001, August **2011**

3. **N. Rojas** and F. Thomas, *Distance-Based Position Analysis of the Three Seven-Link Assur Kinematic Chains*, Mechanism and Machine Theory, Vol. 46, No. 2, pp. 112-126, February **2011**

4. **N. Rojas** and F. Thomas, *The Forward Kinematics of 3-R$\underline{P}$R Planar Robots: A Review and a Distance-Based Formulation*, IEEE Transactions on Robotics, Vol. 27, No. 1, pp. 143-150, **2011**

Submitted

5. **N. Rojas** and F. Thomas, *A Distance Geometry Approach to the Computation of Pin-Jointed Linkage Configuration Spaces: Application to Tracing High-Order Coupler Curves*

6. **N. Rojas** and F. Thomas, *Formulating Assur Kinematic Chains as Projective Extensions of Baranov Trusses*

7. **N. Rojas** and F. Thomas, *The Characteristic Polynomials of All Fully-Parallel Planar Robots Derived From a Single Polynomial*

Conferences

1. **N. Rojas** and F. Thomas, *A Coordinate-Free Approach to Tracing the Coupler Curves of Pin-Jointed Linkages*, Proceedings of the ASME 2011 International Design Engineering Technical Conferences & Computers and Information in Engineering Conference, IDECTC/CIE 2011, Washington DC, August 28-31, **2011**
   Honorable mention, finalist of the Mechanisms and Robotics Committee Best Paper Award

2. **N. Rojas** and F. Thomas, *A Robust Forward Kinematics Analysis of 3-R$\underline{P}$R Planar Platforms*, in Advances in Robot Kinematics, J. Lenarcic and M. Stanisic (editors), Springer Verlag, **2010**.

Appendix A

All the cataloged Baranov trusses

Baranov truss		AM	Reported solutions
$5/B_1$	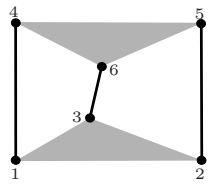	6	***Analytical*:** Peisach [137], Pennock and Kassner [142], Gosselin *et. al.* [55], [56], Wohlhart [214], Husty [81], Kong and Gosselin [98], Collins [37] (Basic elimination theory), Han *et. al.* [66], Liu *et. al.* [108], Luo [110] (Wu method). ***Numerical*:** Hang *et. al.* [67] (Vector method with homotopy continuation), Luo *et. al.* [111] (Newton iterative method), Chandra and Rolland [31] (Hybrid metaheuristics)
$s_{2,5} = f(s_{1,6}) = \det\left(\mathbf{I} - \mathbf{Z}_{1,3,2}\mathbf{Z}_{1,6,3} - \mathbf{Z}_{6,4,5}\,\mathbf{Z}_{6,1,4}\right) s_{1,6}$			
$7/B_1$	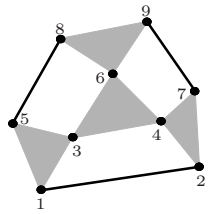	14	***Analytical*:** Kong and Yang [99], Innocenti [87] (Vector method with Sylvester resultant), Dhingra *et. al.* [41] (Vector method with Sylvester resultant). ***Numerical*:** Liu and Yang [107] (Homotopy continuation), Hang *et. al.* [67] (Vector method with homotopy continuation)
$s_{5,8} = f(s_{1,4}, s_{6,7}) = \det\left(-\mathbf{Z}_{1,3,5}\mathbf{Z}_{1,4,3} + \mathbf{I} - \mathbf{Z}_{4,3,6}\,\mathbf{Z}_{4,1,3} + \mathbf{Z}_{6,9,8}\mathbf{Z}_{6,7,9}\mathbf{\Omega}_1\right) s_{1,4}$ $s_{6,7} = f(s_{1,4}) = \det\left(\mathbf{\Omega}_1\right) = \det\left(\mathbf{Z}_{4,3,6}\mathbf{Z}_{4,1,3} - \mathbf{Z}_{4,2,7}\mathbf{Z}_{4,1,2}\right) s_{1,4}$			
$7/B_2$	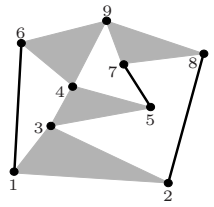	16	***Analytical*:** Innocenti [85] (Vector method with an ad-hoc elimination procedure), Almadi *et. al.* [7] (Vector method with Sylvester resultant), Dhingra *et. al.* [41] (Vector method with Sylvester resultant), Dhingra *et. al.* [42] (Vector method with Gröbner basis and Sylvester resultant), Wampler [191] (Complex number method with Dixon resultant). ***Numerical*:** Hang *et. al.* [67] (Vector method with homotopy continuation), Shen *et. al.* [172] (Single-opened-chains iterative method)
$s_{1,6} = f(s_{4,7}, s_{3,8}) = \det\left(-\mathbf{Z}_{3,2,1}\mathbf{Z}_{3,8,2}\mathbf{\Omega}_1 - \mathbf{Z}_{4,5,3}\mathbf{Z}_{4,7,5} + \mathbf{Z}_{4,9,6}\mathbf{Z}_{4,7,9}\right) s_{4,7}$ $s_{3,8} = f(s_{4,7}) = \det\left(\mathbf{\Omega}_1\right) = \det\left(-\mathbf{Z}_{4,5,3}\mathbf{Z}_{4,7,5} + \mathbf{I} - \mathbf{Z}_{7,9,8}\mathbf{Z}_{7,4,9}\right) s_{4,7}$			
$7/B_3$	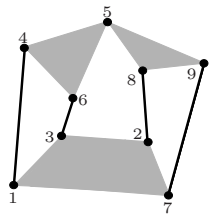	18	***Analytical*:** Innocenti [84], [86] (Vector method with Sylvester resultant), Han *et. al.* [61] (Complex number method with Sylvester resultant), Dhingra *et. al.* [41] (Vector method with Sylvester resultant), Wang *et. al.* [196] (Complex number method with Wu method), Ni *et. al.* [132] (Conformal geometric algebra with Dixon resultant). ***Numerical*:** Hang *et. al.* [67] (Vector method with homotopy continuation)
$s_{7,9} = f(s_{1,6}, s_{2,5}) = \det\left(\left(\mathbf{Z}_{1,3,2} - \mathbf{Z}_{1,3,7}\right)\mathbf{Z}_{1,6,3} + \left(\mathbf{I} - \mathbf{Z}_{5,8,9}\,\mathbf{Z}_{5,2,8}\right)\mathbf{\Omega}_1\right) s_{1,6}$ $s_{2,5} = f(s_{1,6}) = \det\left(\mathbf{\Omega}_1\right) = \det\left(-\mathbf{Z}_{1,3,2}\mathbf{Z}_{1,6,3} + \mathbf{I} - \mathbf{Z}_{6,4,5}\mathbf{Z}_{6,1,4}\right) s_{1,6}$			

Table A.1. Position analysis of all the cataloged Baranov trusses (Part 1/8).

Baranov truss		AM	Reported solutions
$9/B_1$	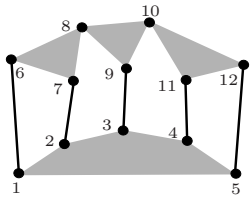	54	***Analytical*:** Lösch [109] (Vector method with Gröbner basis), Dhingra *et. al.* [45] (Vector method with Gröbner basis), Wei *et. al.* [208] (Complex number method with Sylvester resultant), Wohlhart [216] (Vector method with Sylvester resultant). ***Numerical*:** Hang *et. al.* [67] (Vector method with homotopy continuation)
$s_{5,12} = f(s_{1,7}, s_{3,8}, s_{4,10}) = \det\Big(\mathbf{Z}_{4,1,5}\mathbf{Z}_{1,3,4}\mathbf{Z}_{1,2,3}\mathbf{Z}_{1,7,2} + \big(\mathbf{I} - \mathbf{Z}_{10,11,12}\,\mathbf{Z}_{10,4,11}\big)\mathbf{\Omega}_2\Big)s_{1,7}$			
$s_{4,10} = f(s_{1,7}, s_{3,8}) = \det(\mathbf{\Omega}_2) = \det\big(-\mathbf{Z}_{1,3,4}\mathbf{Z}_{1,2,3}\mathbf{Z}_{1,7,2} + \mathbf{Z}_{1,2,3}\mathbf{Z}_{1,7,2} + \big(\mathbf{I} - \mathbf{Z}_{8,9,10}\mathbf{Z}_{8,3,9}\big)\mathbf{\Omega}_1\big)s_{1,7}$			
$s_{3,8} = f(s_{1,7}) = \det(\mathbf{\Omega}_1) = \det\left(-\mathbf{Z}_{1,2,3}\mathbf{Z}_{1,7,2} + \mathbf{I} - \mathbf{Z}_{7,6,8}\mathbf{Z}_{7,1,6}\right)s_{1,7}$			
$9/B_2$	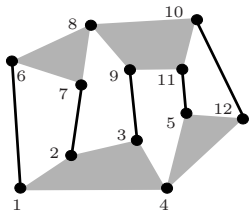	54	***Numerical*:** Hang *et. al.* [67] (Vector method with homotopy continuation)
$s_{10,12} = f(s_{1,7}, s_{3,8}, s_{4,11}) = \det\Big(-\mathbf{Z}_{1,2,3}\mathbf{Z}_{1,7,2} - \left(\mathbf{I} - \mathbf{Z}_{8,9,10}\mathbf{Z}_{8,3,9}\right)\mathbf{\Omega}_1 + \mathbf{Z}_{1,3,4}\mathbf{Z}_{1,2,3}\mathbf{Z}_{1,7,2} + \mathbf{Z}_{4,5,12}\mathbf{Z}_{4,11,5}\mathbf{\Omega}_2\Big)s_{1,7}$			
$s_{4,11} = f(s_{1,7}, s_{3,8}) = \det(\mathbf{\Omega}_2) = \det\big(-\mathbf{Z}_{1,3,4}\mathbf{Z}_{1,2,3}\mathbf{Z}_{1,7,2} + \mathbf{Z}_{1,2,3}\mathbf{Z}_{1,7,2} + \big(\mathbf{I} - \mathbf{Z}_{8,9,11}\mathbf{Z}_{8,3,9}\big)\mathbf{\Omega}_1\big)s_{1,7}$			
$s_{3,8} = f(s_{1,7}) = \det(\mathbf{\Omega}_1) = \det\left(-\mathbf{Z}_{1,2,3}\mathbf{Z}_{1,7,2} + \mathbf{I} - \mathbf{Z}_{7,6,8}\mathbf{Z}_{7,1,6}\right)s_{1,7}$			
$9/B_3$	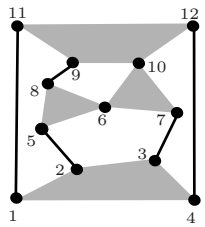	48	***Numerical*:** Hang *et. al.* [67] (Vector method with homotopy continuation)
$s_{8,9} = f(s_{1,12}, s_{3,10}, s_{2,6}) = \det\Big(-\mathbf{Z}_{1,4,3}\mathbf{Z}_{1,12,4} - \left(\mathbf{I} - \mathbf{Z}_{10,7,6}\mathbf{Z}_{10,3,7}\right)\mathbf{\Omega}_1 + \mathbf{Z}_{6,5,8}\mathbf{Z}_{6,2,5}\mathbf{\Omega}_2 + \mathbf{I} - \mathbf{Z}_{12,11,9}\mathbf{Z}_{12,1,11}\Big)s_{1,12}$			
$s_{2,6} = f(s_{1,12}, s_{3,10}) = \det(\mathbf{\Omega}_2) = \det\left(-\mathbf{Z}_{1,4,2}\mathbf{Z}_{1,12,4} + \mathbf{Z}_{1,4,3}\mathbf{Z}_{1,12,4} + \left(\mathbf{I} - \mathbf{Z}_{10,7,6}\mathbf{Z}_{10,3,7}\right)\mathbf{\Omega}_1\right)s_{1,12}$			
$s_{3,10} = f(s_{1,12}) = \det(\mathbf{\Omega}_1) = \det\left(-\mathbf{Z}_{1,4,3}\mathbf{Z}_{1,12,4} + \mathbf{I} - \mathbf{Z}_{12,11,10}\mathbf{Z}_{12,1,11}\right)s_{1,12}$			
$9/B_4$	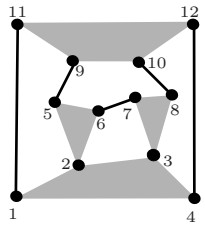	42	***Numerical*:** Hang *et. al.* [67] (Vector method with homotopy continuation, the reported number of AM is incorrect (38))
$s_{6,7} = f(s_{1,12}, s_{3,10}, s_{2,9}) = \det\Big(-\mathbf{Z}_{1,4,2}\mathbf{Z}_{1,12,4} - \mathbf{Z}_{2,5,6}\mathbf{Z}_{2,9,5}\mathbf{\Omega}_2 + \mathbf{Z}_{1,4,3}\mathbf{Z}_{1,12,4} + \mathbf{Z}_{3,8,7}\mathbf{Z}_{3,10,8}\mathbf{\Omega}_1\Big)s_{1,12}$			
$s_{2,9} = f(s_{1,12}) = \det(\mathbf{\Omega}_2) = \det\left(-\mathbf{Z}_{1,4,2}\mathbf{Z}_{1,12,4} + \mathbf{I} - \mathbf{Z}_{12,11,9}\mathbf{Z}_{12,1,11}\right)s_{1,12}$			
$s_{3,10} = f(s_{1,12}) = \det(\mathbf{\Omega}_1) = \det\left(-\mathbf{Z}_{1,4,3}\mathbf{Z}_{1,12,4} + \mathbf{I} - \mathbf{Z}_{12,11,10}\mathbf{Z}_{12,1,11}\right)s_{1,12}$			

Table A.2. Position analysis of all the cataloged Baranov trusses (Part 2/8).

Baranov truss		AM	Reported solutions
$9/B_5$	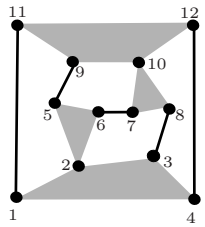	48	***Numerical*:** Hang *et. al.* [67] (Vector method with homotopy continuation)

$$s_{6,7} = f(s_{1,12}, s_{3,10}, s_{2,9}) = \det\Big(- \mathbf{Z}_{1,4,2}\mathbf{Z}_{1,12,4} - \mathbf{Z}_{2,5,6}\mathbf{Z}_{2,9,5}\mathbf{\Omega}_2 + \mathbf{Z}_{1,4,3}\mathbf{Z}_{1,12,4} + (\mathbf{I} - \mathbf{Z}_{10,8,7}\mathbf{Z}_{10,3,8})\,\mathbf{\Omega}_1\Big) s_{1,12}$$

$$s_{2,9} = f(s_{1,12}) = \det(\mathbf{\Omega}_2) = \det(-\mathbf{Z}_{1,4,2}\mathbf{Z}_{1,12,4} + \mathbf{I} - \mathbf{Z}_{12,11,9}\mathbf{Z}_{12,1,11})\, s_{1,12}$$

$$s_{3,10} = f(s_{1,12}) = \det(\mathbf{\Omega}_1) = \det(-\mathbf{Z}_{1,4,3}\mathbf{Z}_{1,12,4} + \mathbf{I} - \mathbf{Z}_{12,11,10}\mathbf{Z}_{12,1,11})\, s_{1,12}$$

$9/B_6$	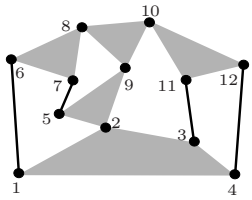	48	***Numerical*:** Hang *et. al.* [67] (Vector method with homotopy continuation)

$$s_{4,12} = f(s_{7,9}, s_{2,6}, s_{3,10}) = \det((-\mathbf{Z}_{2,3,4} + \mathbf{I})\,\mathbf{Z}_{2,1,3}\mathbf{Z}_{2,6,1}\mathbf{\Omega}_1 + (\mathbf{I} - \mathbf{Z}_{10,11,12}\mathbf{Z}_{10,3,11})\,\mathbf{\Omega}_2)\, s_{7,9}$$

$$s_{3,10} = f(s_{7,9}, s_{2,6}) = \det(\mathbf{\Omega}_2) = \det(\mathbf{Z}_{9,5,2}\mathbf{Z}_{9,7,5} - \mathbf{Z}_{2,1,3}\mathbf{Z}_{2,6,1}\mathbf{\Omega}_1 - \mathbf{Z}_{9,8,10}\mathbf{Z}_{9,7,8})\, s_{7,9}$$

$$s_{2,6} = f(s_{7,9}) = \det(\mathbf{\Omega}_1) = \det(-\mathbf{I} + \mathbf{Z}_{9,5,2}\mathbf{Z}_{9,7,5} + \mathbf{Z}_{7,8,6}\mathbf{Z}_{7,9,8})\, s_{7,9}$$

$9/B_7$	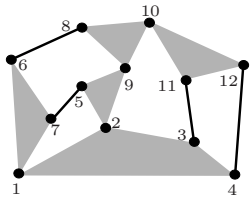	48	***Analytical*:** Han *et. al.* [65] (Complex number method with Sylvester resultant). ***Numerical*:** Hang *et. al.* [67] (Vector method with homotopy continuation)

$$s_{4,12} = f(s_{1,5}, s_{6,9}, s_{3,10}) = \det(-\mathbf{Z}_{1,3,4}\mathbf{Z}_{1,2,3}\mathbf{Z}_{1,5,2} + \mathbf{Z}_{1,2,3}\mathbf{Z}_{1,5,2} + (\mathbf{I} - \mathbf{Z}_{10,11,12}\mathbf{Z}_{10,3,11})\,\mathbf{\Omega}_2)\, s_{1,5}$$

$$s_{3,10} = f(s_{1,5}, s_{6,9}) = \det(\mathbf{\Omega}_2) = \det(-\mathbf{Z}_{1,2,3}\mathbf{Z}_{1,5,2} + \mathbf{Z}_{1,7,6}\mathbf{Z}_{1,5,7} + (\mathbf{I} - \mathbf{Z}_{9,8,10}\mathbf{Z}_{9,6,8})\,\mathbf{\Omega}_1)\, s_{1,5}$$

$$s_{6,9} = f(s_{1,5}) = \det(\mathbf{\Omega}_1) = \det(-\mathbf{Z}_{1,7,6}\mathbf{Z}_{1,5,7} + \mathbf{I} - \mathbf{Z}_{5,2,9}\mathbf{Z}_{5,1,2})\, s_{1,5}$$

$9/B_8$	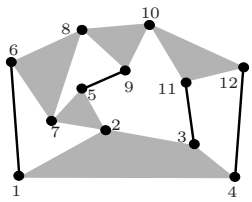	48	***Numerical*:** Hang *et. al.* [67] (Vector method with homotopy continuation, the reported number of AM is incorrect (44))

$$s_{4,12} = f(s_{1,7}, s_{5,8}, s_{3,10}) = \det(-\mathbf{Z}_{1,3,4}\mathbf{Z}_{1,2,3}\mathbf{Z}_{1,7,2} + \mathbf{Z}_{1,2,3}\mathbf{Z}_{1,7,2} + (\mathbf{I} - \mathbf{Z}_{10,11,12}\mathbf{Z}_{10,3,11})\,\mathbf{\Omega}_2)\, s_{1,7}$$

$$s_{3,10} = f(s_{1,7}, s_{5,8}) = \det(\mathbf{\Omega}_2) = \det(-\mathbf{Z}_{1,2,3}\mathbf{Z}_{1,7,2} + \mathbf{I} - \mathbf{Z}_{7,2,5}\mathbf{Z}_{7,1,2} + (\mathbf{I} - \mathbf{Z}_{8,9,10}\mathbf{Z}_{8,5,9})\,\mathbf{\Omega}_1)\, s_{1,7}$$

$$s_{5,8} = f(s_{1,7}) = \det(\mathbf{\Omega}_1) = \det(\mathbf{Z}_{7,2,5}\mathbf{Z}_{7,1,2} - \mathbf{Z}_{7,6,8}\mathbf{Z}_{7,1,6})\, s_{1,7}$$

Table A.3. Position analysis of all the cataloged Baranov trusses (Part 3/8).

Baranov truss		AM	Reported solutions
$9/B_9$	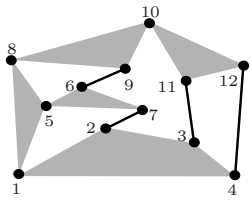	42	***Numerical*:** Hang *et. al.* [67] (Vector method with homotopy continuation)
$s_{4,12} = f(s_{1,7}, s_{6,8}, s_{3,10}) = \det\left(-\mathbf{Z}_{1,3,4}\mathbf{Z}_{1,2,3}\mathbf{Z}_{1,7,2} + \mathbf{Z}_{1,2,3}\mathbf{Z}_{1,7,2} + \left(\mathbf{I} - \mathbf{Z}_{10,11,12}\mathbf{Z}_{10,3,11}\right)\mathbf{\Omega}_2\right) s_{1,7}$			
$s_{3,10} = f(s_{1,7}, s_{6,8}) = \det\left(\mathbf{\Omega}_2\right) = \det\left(-\mathbf{Z}_{1,2,3}\mathbf{Z}_{1,7,2} + \mathbf{I} - \mathbf{Z}_{7,5,6}\mathbf{Z}_{7,1,5} + \left(\mathbf{I} - \mathbf{Z}_{8,9,10}\mathbf{Z}_{8,6,9}\right)\mathbf{\Omega}_1\right) s_{1,7}$			
$s_{6,8} = f(s_{1,7}) = \det\left(\mathbf{\Omega}_1\right) = \det\left(-\mathbf{I} + \mathbf{Z}_{7,5,6}\mathbf{Z}_{7,1,5} + \mathbf{Z}_{1,5,8}\mathbf{Z}_{1,7,5}\right) s_{1,7}$			
$9/B_{10}$	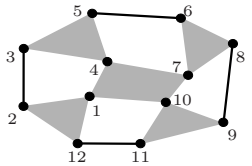	30	***Analytical*:** Han *et. al.* [64] (Complex number method with Sylvester resultant), Dhingra *et. al.* [44] (Vector method with Sylvester resultant), Borràs and Di Gregorio [19] (Vector method with Sylvester dialytic elimination method). ***Numerical*:** Liu and Yang [107] (Homotopy continuation), Hang *et. al.* [67] (Vector method with homotopy continuation), Cai *et. al.* [25]
$s_{11,12} = f(s_{1,3}, s_{5,7}, s_{8,10}) = \det\left(-\mathbf{Z}_{1,7,10}\mathbf{Z}_{1,4,7}\mathbf{Z}_{1,3,4} + \mathbf{Z}_{10,9,11}\mathbf{Z}_{10,8,9}\mathbf{\Omega}_2 + \mathbf{Z}_{1,2,12}\mathbf{Z}_{1,3,2}\right) s_{1,3}$			
$s_{8,10} = f(s_{1,3}, s_{5,7}) = \det\left(\mathbf{\Omega}_2\right) = \det\left(-\mathbf{Z}_{1,4,7}\mathbf{Z}_{1,3,4} + \mathbf{Z}_{7,6,8}\mathbf{Z}_{7,5,6}\mathbf{\Omega}_1 + \mathbf{Z}_{1,7,10}\mathbf{Z}_{1,4,7}\mathbf{Z}_{1,3,4}\right) s_{1,3}$			
$s_{5,7} = f(s_{1,3}) = \det\left(\mathbf{\Omega}_1\right) = \det\left(\mathbf{Z}_{1,4,7}\mathbf{Z}_{1,3,4} - \mathbf{I} + \mathbf{Z}_{3,4,5}\mathbf{Z}_{3,1,4}\right) s_{1,3}$			
$9/B_{11}$	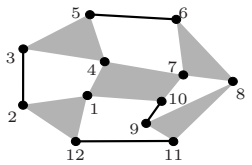	36	***Analytical*:** Wei *et. al.* [207] (Complex number method with Sylvester resultant). ***Numerical*:** Hang *et. al.* [67] (Vector method with homotopy continuation, the reported number of AM is incorrect (34))
$s_{11,12} = f(s_{1,3}, s_{5,7}, s_{8,10}) = \det\left(-\mathbf{Z}_{1,7,10}\mathbf{Z}_{1,4,7}\mathbf{Z}_{1,3,4} + \left(\mathbf{I} - \mathbf{Z}_{8,9,11}\mathbf{Z}_{8,10,9}\right)\mathbf{\Omega}_2 + \mathbf{Z}_{1,2,12}\mathbf{Z}_{1,3,2}\right) s_{1,3}$			
$s_{8,10} = f(s_{1,3}, s_{5,7}) = \det\left(\mathbf{\Omega}_2\right) = \det\left(-\mathbf{Z}_{1,4,7}\mathbf{Z}_{1,3,4} + \mathbf{Z}_{7,6,8}\mathbf{Z}_{7,5,6}\mathbf{\Omega}_1 + \mathbf{Z}_{1,7,10}\mathbf{Z}_{1,4,7}\mathbf{Z}_{1,3,4}\right) s_{1,3}$			
$s_{5,7} = f(s_{1,3}) = \det\left(\mathbf{\Omega}_1\right) = \det\left(\mathbf{Z}_{1,4,7}\mathbf{Z}_{1,3,4} - \mathbf{I} + \mathbf{Z}_{3,4,5}\mathbf{Z}_{3,1,4}\right) s_{1,3}$			
$9/B_{12}$	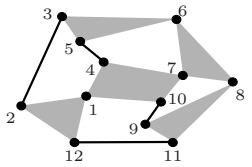	40	***Analytical*:** Dhingra *et. al.* [44] (Vector method with Sylvester resultant). ***Numerical*:** Hang *et. al.* [67] (Vector method with homotopy continuation, the reported number of AM is incorrect, (54))
$s_{2,3} = f(s_{4,6}, s_{8,10}, s_{1,11}) = \det\left(-\mathbf{Z}_{4,7,1}\mathbf{Z}_{4,6,7} - \mathbf{Z}_{1,12,2}\mathbf{Z}_{1,11,12}\mathbf{\Omega}_2 + \mathbf{I} - \mathbf{Z}_{6,5,3}\mathbf{Z}_{6,4,5}\right) s_{4,6}$			
$s_{1,11} = f(s_{4,6}, s_{8,10}) = \det\left(\mathbf{\Omega}_2\right) = \det\left(-\mathbf{Z}_{4,7,1}\mathbf{Z}_{4,6,7} + \mathbf{I} - \mathbf{Z}_{6,7,8}\mathbf{Z}_{6,4,7} + \mathbf{Z}_{8,9,11}\mathbf{Z}_{8,10,9}\mathbf{\Omega}_1\right) s_{4,6}$			
$s_{8,10} = f(s_{4,6}) = \det\left(\mathbf{\Omega}_1\right) = \det\left(-\mathbf{I} + \mathbf{Z}_{6,7,8}\mathbf{Z}_{6,4,7} + \mathbf{Z}_{4,7,10}\mathbf{Z}_{4,6,7}\right) s_{4,6}$			
$9/B_{13}$	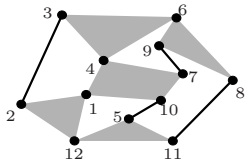	40	***Numerical*:** Hang *et. al.* [67] (Vector method with homotopy continuation)
$s_{8,11} = f(s_{2,4}, s_{6,7}, s_{10,12}) = \det\Big(\mathbf{Z}_{4,3,6}\mathbf{Z}_{4,2,3} - \mathbf{Z}_{6,9,8}\mathbf{Z}_{6,7,9}\mathbf{\Omega}_1 - \mathbf{Z}_{4,1,10}\mathbf{Z}_{4,2,1} + \left(\mathbf{I} - \mathbf{Z}_{12,5,11}\mathbf{Z}_{12,10,5}\right)\mathbf{\Omega}_2\Big) s_{2,4}$			
$s_{10,12} = f(s_{2,4}, s_{6,7}) = \det\left(\mathbf{\Omega}_2\right) = \det\left(-\mathbf{I} + \mathbf{Z}_{4,1,10}\mathbf{Z}_{4,2,1} + \mathbf{Z}_{2,1,12}\mathbf{Z}_{2,4,1}\right) s_{2,4}$			
$s_{6,7} = f(s_{2,4}) = \det\left(\mathbf{\Omega}_1\right) = \det\left(\mathbf{Z}_{4,3,6}\mathbf{Z}_{4,2,3} - \mathbf{Z}_{4,1,7}\mathbf{Z}_{4,2,1}\right) s_{2,4}$			

Table A.4. Position analysis of all the cataloged Baranov trusses (Part 4/8).

Baranov truss		AM	Reported solutions
$9/B_{14}$	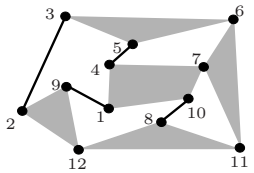	42	***Analytical*:** Han *et. al.* [60] (Complex number method with Sylvester resultant). ***Numerical*:** Hang *et. al.* [67] (Vector method with homotopy continuation, the reported number of AM is incorrect (52))
	$s_{2,3} = f(s_{4,6}, s_{10,11}, s_{1,12}) = \det\left(-\mathbf{Z}_{4,7,1}\mathbf{Z}_{4,6,7} - (\mathbf{I} - \mathbf{Z}_{12,9,2}\mathbf{Z}_{12,1,9})\,\mathbf{\Omega}_2 + \mathbf{I} - \mathbf{Z}_{6,5,3}\mathbf{Z}_{6,4,5}\right) s_{4,6}$		
	$s_{1,12} = f(s_{4,6}, s_{10,11}) = \det(\mathbf{\Omega}_2) = \det\left(-\mathbf{Z}_{4,7,1}\mathbf{Z}_{4,6,7} + \mathbf{Z}_{4,7,10}\mathbf{Z}_{4,6,7} + (\mathbf{I} - \mathbf{Z}_{11,8,12}\mathbf{Z}_{11,10,8})\,\mathbf{\Omega}_1\right) s_{4,6}$		
	$s_{10,11} = f(s_{4,6}) = \det(\mathbf{\Omega}_1) = \det\left(-\mathbf{Z}_{4,7,10}\mathbf{Z}_{4,6,7} + \mathbf{I} - \mathbf{Z}_{6,7,11}\mathbf{Z}_{6,4,7}\right) s_{4,6}$		
$9/B_{15}$	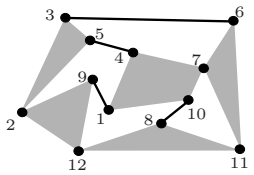	52	***Analytical*:** Dhingra *et. al.* [44] (Vector method with Sylvester resultant), ***Numerical*:** Hang *et. al.* [67] (Vector method with homotopy continuation, the reported number of AM is incorrect (26))
	$s_{3,6} = f(s_{10,11}, s_{1,12}, s_{2,4}) = \det\Big(-\mathbf{Z}_{10,7,1}\mathbf{Z}_{10,11,7} - (\mathbf{I} - \mathbf{Z}_{12,9,2}\mathbf{Z}_{12,1,9})\,\mathbf{\Omega}_1 - \mathbf{Z}_{2,5,3}\mathbf{Z}_{2,4,5}\mathbf{\Omega}_2 + \mathbf{I} - \mathbf{Z}_{11,7,6}\mathbf{Z}_{11,10,7}\Big) s_{10,11}$		
	$s_{2,4} = f(s_{10,11}, s_{1,12}) = \det(\mathbf{\Omega}_2) = \det\Big(-\mathbf{Z}_{10,7,1}\mathbf{Z}_{10,11,7} - (\mathbf{I} - \mathbf{Z}_{12,9,2}\mathbf{Z}_{12,1,9})\,\mathbf{\Omega}_1 + \mathbf{Z}_{10,7,4}\mathbf{Z}_{10,11,7}\Big) s_{10,11}$		
	$s_{1,12} = f(s_{10,11}) = \det(\mathbf{\Omega}_1) = \det\left(-\mathbf{Z}_{10,7,1}\mathbf{Z}_{10,11,7} + \mathbf{I} - \mathbf{Z}_{11,8,12}\mathbf{Z}_{11,10,8}\right) s_{10,11}$		
$9/B_{16}$	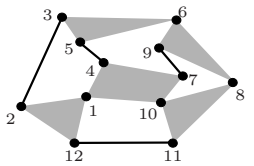	44	***Analytical*:** Han *et. al.* [63] (Complex number method with Sylvester resultant). ***Numerical*:** Hang *et. al.* [67] (Vector method with homotopy continuation)
	$s_{2,3} = f(s_{7,8}, s_{4,6}, s_{1,11}) = \det\Big(-\mathbf{Z}_{7,10,1}\mathbf{Z}_{7,8,10} - \mathbf{Z}_{1,12,2}\mathbf{Z}_{1,11,12}\mathbf{\Omega}_2 + \mathbf{Z}_{7,10,4}\mathbf{Z}_{7,8,10} + (\mathbf{I} - \mathbf{Z}_{6,5,3}\mathbf{Z}_{6,4,5})\,\mathbf{\Omega}_1\Big) s_{7,8}$		
	$s_{1,11} = f(s_{7,8}, s_{4,6}) = \det(\mathbf{\Omega}_2) = \det\left(-\mathbf{Z}_{7,10,1}\mathbf{Z}_{7,8,10} + \mathbf{I} - \mathbf{Z}_{8,10,11}\mathbf{Z}_{8,7,10}\right) s_{7,8}$		
	$s_{4,6} = f(s_{7,8}) = \det(\mathbf{\Omega}_1) = \det\left(-\mathbf{Z}_{7,10,4}\mathbf{Z}_{7,8,10} + \mathbf{I} - \mathbf{Z}_{8,9,6}\mathbf{Z}_{8,7,9}\right) s_{7,8}$		
$9/B_{17}$	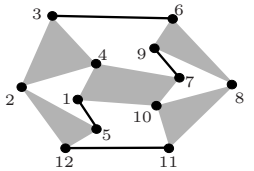	44	***Analytical*:** Han *et. al.* [62] (Complex number method with Sylvester resultant). ***Numerical*:** Hang *et. al.* [67] (Vector method with homotopy continuation, the reported number of AM is incorrect (66))
	$s_{3,6} = f(s_{1,2}, s_{10,12}, s_{7,8}) = \det\left(-\mathbf{I} + \mathbf{Z}_{2,4,3}\mathbf{Z}_{2,1,4} + \mathbf{Z}_{1,4,7}\mathbf{Z}_{1,2,4} + (\mathbf{I} - \mathbf{Z}_{8,9,6}\mathbf{Z}_{8,7,9})\,\mathbf{\Omega}_2\right) s_{1,2}$		
	$s_{7,8} = f(s_{1,2}, s_{10,12}) = \det(\mathbf{\Omega}_2) = \det\left(-\mathbf{Z}_{1,4,7}\mathbf{Z}_{1,2,4} + \mathbf{Z}_{1,4,10}\mathbf{Z}_{1,2,4} + \mathbf{Z}_{10,11,8}\mathbf{Z}_{10,12,11}\mathbf{\Omega}_1\right) s_{1,2}$		
	$s_{10,12} = f(s_{1,2}) = \det(\mathbf{\Omega}_1) = \det\left(-\mathbf{Z}_{1,4,10}\mathbf{Z}_{1,2,4} + \mathbf{I} - \mathbf{Z}_{2,5,12}\mathbf{Z}_{2,1,5}\right) s_{1,2}$		

Table A.5. Position analysis of all the cataloged Baranov trusses (Part 5/8).

Baranov truss		AM	Reported solutions
$9/B_{18}$	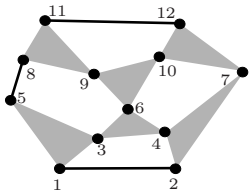	38	***Numerical*:** Hang *et. al.* [67] (Vector method with homotopy continuation, the reported number of AM is incorrect (34))
$s_{11,12} = f(s_{1,4}, s_{6,7}, s_{5,9}) = \det\Big(- \mathbf{Z}_{1,3,5}\mathbf{Z}_{1,4,3} - (\mathbf{I} - \mathbf{Z}_{9,8,11}\mathbf{Z}_{9,5,8})\,\mathbf{\Omega}_2 + \mathbf{I} - \mathbf{Z}_{4,3,6}\mathbf{Z}_{4,1,3} + (\mathbf{I} - \mathbf{Z}_{7,10,12}\mathbf{Z}_{7,6,10})\,\mathbf{\Omega}_1\Big) s_{1,4}$			
$s_{5,9} = f(s_{1,4}, s_{6,7}) = \det(\mathbf{\Omega}_2) = \det(-\mathbf{Z}_{1,3,5}\mathbf{Z}_{1,4,3} + \mathbf{I} - \mathbf{Z}_{4,3,6}\mathbf{Z}_{4,1,3} + \mathbf{Z}_{6,10,9}\mathbf{Z}_{6,7,10}\mathbf{\Omega}_1)\, s_{1,4}$			
$s_{6,7} = f(s_{1,4}) = \det(\mathbf{\Omega}_1) = \det(\mathbf{Z}_{4,3,6}\mathbf{Z}_{4,1,3} - \mathbf{Z}_{4,2,7}\mathbf{Z}_{4,1,2})\, s_{1,4}$			
$9/B_{19}$	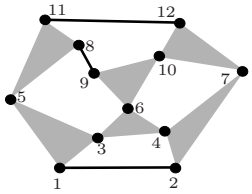	46	***Numerical*:** Hang *et. al.* [67] (Vector method with homotopy continuation, the reported number of AM is incorrect (62))
$s_{11,12} = f(s_{1,4}, s_{6,7}, s_{5,9}) = \det\Big(- \mathbf{Z}_{1,3,5}\mathbf{Z}_{1,4,3} - \mathbf{Z}_{5,8,11}\mathbf{Z}_{5,9,8}\mathbf{\Omega}_2 + \mathbf{I} - \mathbf{Z}_{4,3,6}\mathbf{Z}_{4,1,3} + (\mathbf{I} - \mathbf{Z}_{7,10,12}\mathbf{Z}_{7,6,10})\,\mathbf{\Omega}_1\Big) s_{1,4}$			
$s_{5,9} = f(s_{1,4}, s_{6,7}) = \det(\mathbf{\Omega}_2) = \det(-\mathbf{Z}_{1,3,5}\mathbf{Z}_{1,4,3} + \mathbf{I} - \mathbf{Z}_{4,3,6}\mathbf{Z}_{4,1,3} + \mathbf{Z}_{6,10,9}\mathbf{Z}_{6,7,10}\mathbf{\Omega}_1)\, s_{1,4}$			
$s_{6,7} = f(s_{1,4}) = \det(\mathbf{\Omega}_1) = \det(\mathbf{Z}_{4,3,6}\mathbf{Z}_{4,1,3} - \mathbf{Z}_{4,2,7}\mathbf{Z}_{4,1,2})\, s_{1,4}$			
$9/B_{20}$	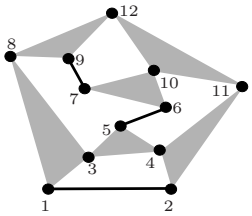	46	***Analytical*:** Wang *et. al.* [200] (Complex number method with Dixon resultant and Sylvester resultant), Wang *et. al.* [197] (Complex number method with Sylvester resultant). ***Numerical*:** Hang *et. al.* [67] (Vector method with homotopy continuation, the reported number of AM is incorrect (64)), Luo and Liu [112] (Complex number method with chaos least square method)
$s_{5,6} = f(s_{1,4}, s_{8,11}, s_{9,10}) = \det\Big(- \mathbf{I} + \mathbf{Z}_{4,3,5}\mathbf{Z}_{4,1,3} + \mathbf{Z}_{1,3,8}\mathbf{Z}_{1,4,3} + \mathbf{Z}_{8,12,9}\mathbf{Z}_{8,11,12}\mathbf{\Omega}_1 + (\mathbf{I} - \mathbf{Z}_{10,7,6}\mathbf{Z}_{10,9,7})\,\mathbf{\Omega}_2\Big) s_{1,4}$			
$s_{9,10} = f(s_{1,4}, s_{8,11}) = \det(\mathbf{\Omega}_2) = \det((-\mathbf{Z}_{8,12,9}\mathbf{Z}_{8,11,12} + \mathbf{I} - \mathbf{Z}_{11,12,10}\mathbf{Z}_{11,8,12})\,\mathbf{\Omega}_1)\, s_{1,4}$			
$s_{8,11} = f(s_{1,4}) = \det(\mathbf{\Omega}_1) = \det(-\mathbf{Z}_{1,3,8}\mathbf{Z}_{1,4,3} + \mathbf{I} - \mathbf{Z}_{4,2,11}\mathbf{Z}_{4,1,2})\, s_{1,4}$			
$9/B_{21}$	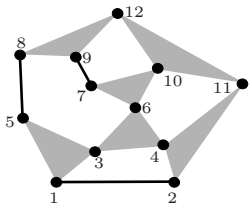	40	***Analytical*:** Wang *et. al.* [195] (Complex number method with Dixon resultant and Sylvester resultant). ***Numerical*:** Hang *et. al.* [67] (Vector method with homotopy continuation, the reported number of AM is incorrect (30))
$s_{5,8} = f(s_{1,4}, s_{6,11}, s_{7,12}) = \det\Big(- \mathbf{Z}_{1,3,5}\mathbf{Z}_{1,4,3} + \mathbf{I} - \mathbf{Z}_{4,3,6}\mathbf{Z}_{4,1,3} + \mathbf{Z}_{6,10,7}\mathbf{Z}_{6,11,10}\mathbf{\Omega}_1 + (\mathbf{I} - \mathbf{Z}_{12,9,8}\mathbf{Z}_{12,7,9})\,\mathbf{\Omega}_2\Big) s_{1,4}$			
$s_{7,12} = f(s_{1,4}, s_{6,11}) = \det(\mathbf{\Omega}_2) = \det((-\mathbf{Z}_{6,10,7}\mathbf{Z}_{6,11,10} + \mathbf{I} - \mathbf{Z}_{11,10,12}\mathbf{Z}_{11,6,10})\,\mathbf{\Omega}_1)\, s_{1,4}$			
$s_{6,11} = f(s_{1,4}) = \det(\mathbf{\Omega}_1) = \det(\mathbf{Z}_{4,3,6}\mathbf{Z}_{4,1,3} - \mathbf{Z}_{4,2,11}\mathbf{Z}_{4,1,2})\, s_{1,4}$			

Table A.6. Position analysis of all the cataloged Baranov trusses (Part 6/8).

Baranov truss		AM	Reported solutions
$9/B_{22}$	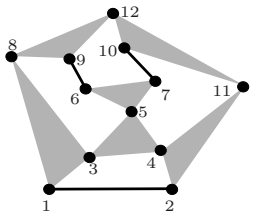	50	***Numerical*:** Hang *et. al.* [67] (Vector method with homotopy continuation)
$s_{7,10} = f(s_{1,4}, s_{8,11}, s_{5,9}) = \det\Big(-\mathbf{I} + \mathbf{Z}_{4,3,5}\mathbf{Z}_{4,1,3} - \mathbf{Z}_{5,6,7}\mathbf{Z}_{5,9,6}\mathbf{\Omega}_2 + \mathbf{Z}_{1,3,8}\mathbf{Z}_{1,4,3} + (\mathbf{I} - \mathbf{Z}_{11,12,10}\mathbf{Z}_{11,8,12})\,\mathbf{\Omega}_1\Big) s_{1,4}$			
$s_{5,9} = f(s_{1,4}, s_{8,11}) = \det(\mathbf{\Omega}_2) = \det(-\mathbf{I} + \mathbf{Z}_{4,3,5}\mathbf{Z}_{4,1,3} + \mathbf{Z}_{1,3,8}\mathbf{Z}_{1,4,3} + \mathbf{Z}_{8,12,9}\mathbf{Z}_{8,11,12}\mathbf{\Omega}_1)\, s_{1,4}$			
$s_{8,11} = f(s_{1,4}) = \det(\mathbf{\Omega}_1) = \det(-\mathbf{Z}_{1,3,8}\mathbf{Z}_{1,4,3} + \mathbf{I} - \mathbf{Z}_{4,2,11}\mathbf{Z}_{4,1,2})\, s_{1,4}$			
$9/B_{23}$	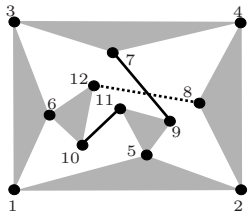	46	***Analytical*:** Zhuang *et. al.* [226] (Complex number method with Sylvester resultant), Wang *et. al.* [204] (Complex number method with Dixon resultant and Sylvester resultant). ***Numerical*:** Hang *et. al.* [67] (Vector method with homotopy continuation)
$s_{10,11} = f(s_{1,4}, s_{6,8}, s_{5,7}) = \det\Big(-\mathbf{Z}_{6,12,10}\mathbf{Z}_{6,8,12}\mathbf{\Omega}_1 - \mathbf{Z}_{1,3,6}\mathbf{Z}_{1,4,3} + \mathbf{Z}_{1,2,5}\mathbf{Z}_{1,4,2} + \mathbf{Z}_{5,9,11}\mathbf{Z}_{5,7,9}\mathbf{\Omega}_2\Big) s_{1,4}$			
$s_{5,7} = f(s_{1,4}, s_{6,8}) = \det(\mathbf{\Omega}_2) = \det(-\mathbf{Z}_{1,2,5}\mathbf{Z}_{1,4,2} + \mathbf{I} - \mathbf{Z}_{4,3,7}\mathbf{Z}_{4,1,3})\, s_{1,4}$			
$s_{6,8} = f(s_{1,4}) = \det(\mathbf{\Omega}_1) = \det(-\mathbf{Z}_{1,3,6}\mathbf{Z}_{1,4,3} + \mathbf{I} - \mathbf{Z}_{4,2,8}\mathbf{Z}_{4,1,2})\, s_{1,4}$			
$9/B_{24}$	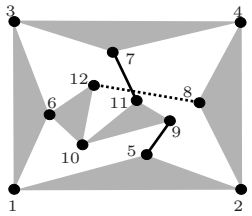	50	***Analytical*:** Wang *et. al.* [194] (Complex number method with Dixon resultant and Sylvester resultant). ***Numerical*:** Hang *et. al.* [67] (Vector method with homotopy continuation)
$s_{7,11} = f(s_{1,4}, s_{6,8}, s_{5,10}) = \det(-\mathbf{I} + \mathbf{Z}_{4,3,7}\mathbf{Z}_{4,1,3} + \mathbf{Z}_{1,2,5}\mathbf{Z}_{1,4,2} + (\mathbf{I} - \mathbf{Z}_{10,9,11}\mathbf{Z}_{10,5,9})\,\mathbf{\Omega}_2)\, s_{1,4}$			
$s_{5,10} = f(s_{1,4}, s_{6,8}) = \det(\mathbf{\Omega}_2) = \det(-\mathbf{Z}_{1,2,5}\mathbf{Z}_{1,4,2} + \mathbf{Z}_{1,3,6}\mathbf{Z}_{1,4,3} + \mathbf{Z}_{6,12,10}\mathbf{Z}_{6,8,12}\mathbf{\Omega}_1)\, s_{1,4}$			
$s_{6,8} = f(s_{1,4}) = \det(\mathbf{\Omega}_1) = \det(-\mathbf{Z}_{1,3,6}\mathbf{Z}_{1,4,3} + \mathbf{I} - \mathbf{Z}_{4,2,8}\mathbf{Z}_{4,1,2})\, s_{1,4}$			
$9/B_{25}$	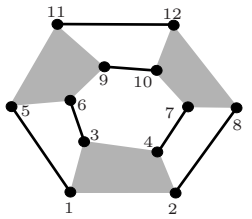	52	***Analytical*:** Wang *et. al.* [203] (Complex number method with Dixon resultant and Sylvester resultant). ***Numerical*:** Hang *et. al.* [67] (Vector method with homotopy continuation)
$s_{9,10} = f(s_{1,6}, s_{2,7}) = \det\Big(-\mathbf{I} + \mathbf{Z}_{6,5,9}\,\mathbf{Z}_{6,1,5} + \mathbf{Z}_{1,3,2}\mathbf{Z}_{1,6,3} + (\mathbf{I} - \mathbf{Z}_{7,8,10}\,\mathbf{Z}_{7,2,8})\, \mathbf{Z}_{2,4,7}\,(-\mathbf{Z}_{1,3,2}\mathbf{Z}_{1,6,3} + \mathbf{Z}_{1,3,4}\mathbf{Z}_{1,6,3})\Big) s_{1,6}$			
$s_{11,12} = f(s_{1,6}, s_{2,7})$ is obtained applying the permutation $\begin{bmatrix} 1 & 2 & 3 & 4 & 5 & 6 & 7 & 8 & 9 & 10 & 11 & 12 \\ 1 & 2 & 3 & 4 & 5 & 6 & 7 & 8 & 11 & 12 & 9 & 10 \end{bmatrix}$ to the above equation			

Table A.7. Position analysis of all the cataloged Baranov trusses (Part 7/8).

Baranov truss	AM	Reported solutions
$9/B_{26}$ 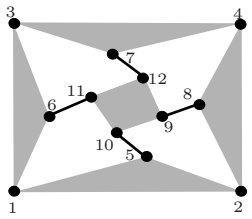	56	***Analytical*:** Wohlhart [215], [218] (Vector method with Sylvester resultant), Lösch [109] (Vector method with Gröbner basis), Wampler [191] (Complex number method with Dixon resultant), Wang *et. al.* [199] (Complex number method with Dixon resultant), Wang *et. al.* [201] (Complex number method with Dixon resultant and Sylvester resultant). ***Numerical*:** Hang *et. al.* [67] (Vector method with homotopy continuation, the reported number of AM is incorrect (38)), He *et. al.* [77] (Complex number method with hyper-chaotic Newton downhill method)
$s_{5,10} = f(s_{3,11}, s_{3,12}, s_{1,4}) = \det\left(-\mathbf{Z}_{11,12,10}\mathbf{Z}_{11,3,12} + \mathbf{I} - \mathbf{Z}_{3,6,1}\mathbf{Z}_{3,11,6} + \mathbf{Z}_{1,2,5}\mathbf{Z}_{1,4,2}\mathbf{\Omega}_1\right) s_{3,11}$		
$s_{1,4} = f(s_{3,11}, s_{3,12}) = \det\left(\mathbf{\Omega}_1\right) = \det\left(\mathbf{Z}_{3,6,1}\mathbf{Z}_{3,11,6} - \mathbf{Z}_{3,7,4}\mathbf{Z}_{3,12,7}\mathbf{Z}_{3,11,12}\right) s_{3,11}$		
$s_{8,9} = f(s_{3,12}, s_{3,11}, s_{1,4})$ and $s_{1,4} = f(s_{3,12}, s_{3,11})$ are obtained applying the permutation		
$\begin{bmatrix} 1 & 2 & 3 & 4 & 5 & 6 & 7 & 8 & 9 & 10 & 11 & 12 \\ 4 & 2 & 3 & 1 & 8 & 7 & 6 & 5 & 10 & 9 & 12 & 11 \end{bmatrix}$ to the above equations		
$9/B_{27}$ 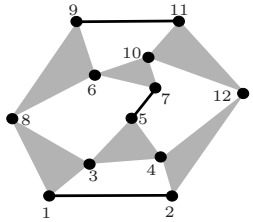	50	***Analytical*:** Wang *et. al.* [202] (Complex number method with Dixon resultant and Sylvester resultant). ***Numerical*:** Hang *et. al.* [67] (Vector method with homotopy continuation, the reported number of AM is incorrect (36))
$s_{9,11} = f(s_{5,12}, s_{7,12}, s_{3,6}) = \det\left(-\mathbf{Z}_{7,10,6}\mathbf{Z}_{7,12,10} + \mathbf{Z}_{6,8,9}\mathbf{Z}_{6,3,8}\mathbf{\Omega}_1 + \mathbf{I} - \mathbf{Z}_{12,10,11}\mathbf{Z}_{12,7,10}\right) s_{7,12}$		
$s_{3,6} = f(s_{5,12}, s_{7,12}) = \det\left(\mathbf{\Omega}_1\right) = \det\left(-\mathbf{Z}_{5,4,3}\mathbf{Z}_{5,12,4}\left(-\mathbf{Z}_{7,12,5} + \mathbf{I}\right) - \mathbf{Z}_{7,12,5} + \mathbf{Z}_{7,10,6}\mathbf{Z}_{7,12,10}\right) s_{7,12}$		
$s_{1,2} = f(s_{7,12}, s_{5,12}, s_{3,6})$ and $s_{3,6} = f(s_{7,12}, s_{5,12})$ are obtained applying the permutation		
$\begin{bmatrix} 1 & 2 & 3 & 4 & 5 & 6 & 7 & 8 & 9 & 10 & 11 & 12 \\ 9 & 11 & 6 & 10 & 7 & 3 & 5 & 8 & 1 & 4 & 2 & 12 \end{bmatrix}$ to the above equations		
$9/B_{28}$ 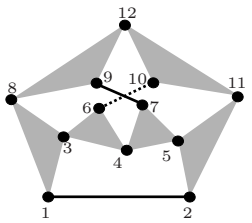	58	***Analytical*:** Wang *et. al.* [198] (Complex number method with Dixon resultant). ***Numerical*:** Almadi *et. al.* [6] (Homotopy continuation), Hang *et. al.* [67] (Vector method with homotopy continuation), Luo and Liu [113] (Complex number method with hyper-chaotic Newton downhill method)
$s_{6,10} = f(s_{1,4}, s_{2,4}, s_{8,11}) = \det\left(-\mathbf{I} + \mathbf{Z}_{4,3,6}\mathbf{Z}_{4,1,3} + \mathbf{Z}_{1,3,8}\mathbf{Z}_{1,4,3} + \left(\mathbf{I} - \mathbf{Z}_{11,12,10}\mathbf{Z}_{11,8,12}\right)\mathbf{\Omega}_1\right) s_{1,4}$		
$s_{8,11} = f(s_{1,4}, s_{2,4}) = \det\left(\mathbf{\Omega}_1\right) = \det\left(-\mathbf{Z}_{1,3,8}\mathbf{Z}_{1,4,3} + \mathbf{I} - \mathbf{Z}_{4,1,2} + \mathbf{Z}_{2,5,11}\mathbf{Z}_{2,4,5}\mathbf{Z}_{4,1,2}\right) s_{1,4}$		
$s_{7,9} = f(s_{2,4}, s_{1,4}, s_{8,11})$ and $s_{8,11} = f(s_{2,4}, s_{1,4})$ are obtained applying the permutation		
$\begin{bmatrix} 1 & 2 & 3 & 4 & 5 & 6 & 7 & 8 & 9 & 10 & 11 & 12 \\ 2 & 1 & 5 & 4 & 3 & 7 & 6 & 11 & 10 & 9 & 8 & 12 \end{bmatrix}$ to the above equations		

Table A.8. Position analysis of all the cataloged Baranov trusses (Part 8/8).

Bibliography

[1] A. Alfakih. On the uniqueness of Euclidean distance matrix completions. *Linear Algebra and its Applications*, 370(0):1 – 14, 2003.

[2] A. Alfakih. On the uniqueness of Euclidean distance matrix completions: the case of points in general position. *Linear Algebra and its Applications*, 397:265 – 277, 2005.

[3] A. Alfakih, A. Khandani, and H. Wolkowicz. Solving Euclidean distance matrix completion problems via semidefinite programming. *Computational Optimization Applications*, 12(1-3):13 – 30, 1999.

[4] E. Allgower and K. Georg. *Introduction to Numerical Continuation Methods.* SIAM, 2003.

[5] L. Allievi. *Cinematica Della Biella Piana.* Regia Tipografia Francesco Giannini & Figli, Naples, Italy, 1895.

[6] A. Almadi, A. Dhingra, and D. Kohli. Displacement analysis of ten-link kinematic chains using homotopy. In *Proceedings of 9th World Congress on Theory of Machines and Mechanisms*, 1:90 – 94, 1995.

[7] A. Almadi, A. Dhingra, and D. Kohli. Closed-form displacement analysis of SDOF 8-link mechanisms. In *Proceedings of the ASME 1996 International Design Engineering Technical Conferences & Computers in Engineering Conference, Paper No. 96-DETC/MECH-1206*, 1996.

[8] A. Ampère. *Essai sur la Philosophie des Sciences: ou, Exposition Analytique d'une Classification Naturelle de Toutes les Connaissances Humaines, Volum 1.* Bachelier, 1834.

[9] J. Angeles. *Fundamentals of Robotic Mechanical Systems. Theory, Methods, and Algorithms.* Second Edition. Mechanical Engineering Series. Springer-Verlag, New York, 2003.

[10] R. Ball. *The Theory of Screws: A Study in the Dynamics of a Rigid Body.* Hodges, Foster, and Co., 1876.

[11] G. Baranov. Classification, formation, kinematics, and kinetostatics of mechanisms with pairs of the first kind (in Russian). In *Proceedings of Seminar on the Theory of Machines and Mechanisms, Moscow*, 2:15 – 39, 1952.

[12] G. Baranov. *Curso de la Teoría de Mecanismos y Máquinas.* Editorial Mir, 1979.

[13] L. Basañez, J. Rosell, L. Palomo, E. Nuño, and H. Portilla. A framework for robotized teleoperated tasks. In *ROBOT 2011 Robótica Experimental, November 28 - 29, Sevilla, Spain*, 573 – 580, 2011.

[14] D. Bates, J. Hauenstein, A. Sommese, and C. Wampler. Bertini: Software for numerical algebraic geometry. available at http://www.nd.edu/~sommese/bertini/.

[15] L. Blumenthal. *Distance Geometries: A Study of the Development of Abstract Metrics.* University of Missouri Studies, 13(2), 1938.

[16] L. Blumenthal. *Theory and Applications of Distance Geometry.* Oxford University

Press, 1953.

[17] C. Borcea and I. Streinu. On the number of embeddings of minimally rigid graphs. In *SCG '02: Proceedings of the eighteenth annual symposium on Computational geometry*, 25 – 32, New York, NY, USA, 2002.

[18] C. Borcea and I. Streinu. The number of embeddings of minimally rigid graphs. *Discrete and Computational Geometry*, 31(2):287 – 303, 2004.

[19] J. Borràs and R. Di Gregorio. Polynomial solution to the position analysis of two Assur kinematic chains with four loops and the same topology. *Journal of Mechanisms and Robotics*, 1(2):021003, 2009.

[20] O. Bottema. Some remarks on theoretical kinematics, I. on instantaneous invariants, II. on the application of elliptic functions in kinematics. In *Proceedings of an International Conference for Teachers of Mechanisms*, 159 – 167, 1961.

[21] O. Bottema and B. Roth. *Theoretical Kinematics*. Dover books on engineering. Dover Publications, 1979.

[22] R. Bricard. *Leçons de Cinématique: Cinématique Appliquée*, volume 2 of *Leçons de Cinématique*. Gauthier-Villars, Paris, France, 1926-1927.

[23] B. Buchberger. *An Algorithm for Finding the Basis Elements of the Residue Class Ring Modulo a Zero Dimensional Polynomial Ideal (in German)*. PhD thesis, Universität Innsbruck, 1966.

[24] L. Burmester. *Lehrbuch der Kinematik*. Verlag Von Arthur Felix, Leipzig, Germany, 1888.

[25] S. Cai, Y. Zuo, and N. Chen. Position analysis of planar complex mechanisms using triangular vector loop method. *Journal of Lanzhou University of Technology*, 31(5):35 – 38, 2005.

[26] A. Castellet. *Solving Inverse Kinematics Problems Using an Interval Method*. PhD thesis, Institut de Robòtica i Informàtica Industrial (CSIC-UPC), 1998.

[27] A. Castellet and F. Thomas. An algorithm for the solution of inverse kinematics problems based on an interval method. In J. Lenarcic and M. Husty, editors, *Advances in Robot Kinematics*, 393 – 403. Kluwer Academic Publishers, 1998.

[28] M. Ceccarelli. Evolution of TMM (theory of machines and mechanisms) to MMS (machine and mechanism science): An illustration survey. In *Proceedings of the 11th World Congress in Mechanism and Machine Science*, 13 – 24, 2003.

[29] M. Ceccarelli and T. Koetsier. Burmester and Allievi: A theory and its application for mechanism design at the end of 19th century. *Journal of Mechanical Design*, 130(7):072301, 2008.

[30] E. Ceresole, P. Fanghella, and C. Galletti. Assur's groups, AKCs, basic trusses, SOCs, etc.: Modular kinematics of planar linkages. In *Proceedings of the ASME 1996 International Design Engineering Technical Conferences & Computers in Engineering Conference, Paper No. 96-DETC/MECH-1027*, 1996.

[31] R. Chandra and L. Rolland. On solving the forward kinematics of 3RPR planar parallel manipulator using hybrid metaheuristics. *Applied Mathematics and Computation*, 217(22):8997 – 9008, 2011.

[32] M. Chasles. *Mémoire de Géométrie sur la Construction des Normales à Plusieurs Courbes Mécaniques*. Bulletin de la Société Mathématique de France, 1878.

[33] C. Chen. A direct kinematic computation algorithm for all planar 3-legged platforms. Master's thesis, Department of Mechanical Engineering and Centre for Intelligent Machines, McGill University, 2001.

[34] C. Chen and P. Zsombor-Murray. *Direct Kinematics for All Planar Three-Legged*

Parallel Platforms. VDM Verlag Publishing House, Saarbrücken, Germany, 2009.

[35] J. Chu, W. Cao, and T. Yang. Type synthesis of Baranov truss with multiple joints and multiple-joint links. In *Proceedings of the ASME 1998 Design Engineering Technical Conferences and Computers in Engineering Conference, Paper No. DETC98/MECH-5972*, 1998.

[36] W. Chung. The position analysis of Assur kinematic chain with five links. *Mechanism and Machine Theory*, 40(9):1015 – 1029, 2005.

[37] C. Collins. Forward kinematics of planar parallel manipulators in the Clifford algebra of p2. *Mechanism and Machine Theory*, 37(8):799 – 813, 2002.

[38] J. Dai, D. Wang, and L. Cui. Orientation and workspace analysis of the multifingered metamorphic hand - metahand. *IEEE Transactions on Robotics*, 25(4):942 – 947, 2009.

[39] J. Dattorro. *Convex Optimization & Euclidean Distance Geometry*. Meboo, 2006.

[40] A. Dhingra, A. Almadi, and D. Kohli. A closed-form approach to coupler-curves of multi-loop mechanisms. *Journal of Mechanical Design*, 122(4):464 – 471, 2000.

[41] A. Dhingra, A. Almadi, and D. Kohli. Closed-form displacement analysis of 8, 9 and 10-link mechanisms: Part I: 8-link 1-DOF mechanisms. *Mechanism and Machine Theory*, 35(6):821 – 850, 2000.

[42] A. Dhingra, A. Almadi, and D. Kohli. Closed-form displacement analysis of 8, 9 and 10-link mechanisms: Part II: 9-link 2-DOF and 10-link 3-DOF mechanisms. *Mechanism and Machine Theory*, 35(6):851 – 869, 2000.

[43] A. Dhingra, A. Almadi, and D. Kohli. A Gröbner-Sylvester hybrid method for closed-form displacement analysis of mechanisms. *Journal of Mechanical Design*, 122(4):431 – 438, 2000.

[44] A. Dhingra, A. Almadi, and D. Kohli. Closed-form displacement analysis of 10-link 1-DOF mechanisms: Part 2 - polynomial solutions. *Mechanism and Machine Theory*, 36(1):57 – 75, 2001.

[45] A. Dhingra, A. Almadi, and D. Kohli. Closed-form displacement and coupler curve analysis of planar multi-loop mechanisms using Gröbner bases. *Mechanism and Machine Theory*, 36(2):273 – 298, 2001.

[46] E. Dijksman. *Motion Geometry of Mechanisms*. Cambridge University Press, 1976.

[47] F. Freudenstein. Approximate synthesis of four-bar linkages. *Transactions of the ASME*, 77(8):853 – 861, 1955.

[48] F. Freudenstein. On the variety of motions generated by mechanisms. *Journal of Engineering for Industry*, 39(February):156 – 160, 1962.

[49] C. Galletti. On the position analysis of Assur's groups of high class. *Meccanica*, 14:6 – 10, 1979.

[50] C. Galletti. A note on modular approaches to planar linkage kinematic analysis. *Mechanism and Machine Theory*, 21(5):385 – 391, 1986.

[51] D. Gan, Q. Liao, J. Dai, S. Wei, and L. Seneviratne. Forward displacement analysis of the general 6-6 Stewart mechanism using Gröbner bases. *Mechanism and Machine Theory*, 44(9):1640 – 1647, 2009.

[52] G. Gogu. Mobility of mechanisms: a critical review. *Mechanism and Machine Theory*, 40(9):1068 – 1097, 2005.

[53] A. Gomes, I. Voiculescu, J. Jorge, B. Wyvill, and C. Galbraith. *Implicit Curves and Surfaces: Mathematics, Data Structures and Algorithms*. Springer Publishing Company, Incorporated, 1st edition, 2009.

[54] C. Gosselin and J. Merlet. The direct kinematics of planar parallel manipulators: Special architectures and number of solutions. *Mechanism and Machine Theory*, 29(8):1083 – 1097, 1994.

[55] C. Gosselin and J. Sefrioui. Polynomial solutions for the direct kinematic problem of planar three-degree-of-freedom parallel manipulators. In *5th International Conference on Advanced Robotics, 'Robots in Unstructured Environments', ICAR*, 1124 – 1129 vol.2, Jun 1991.

[56] C. Gosselin, J. Sefrioui, and M. Richard. Solutions polynomiales au problème de la cinématique des manipulateurs parallèles plans à trois degrés de liberté. *Mechanism and Machine Theory*, 27(2):107 – 119, 1992.

[57] J. Graver. *Counting on Frameworks: Mathematics to Aid the Design of Rigid Structures*. The Mathematical Association of America, 2001.

[58] I. Grooms, R. Michael, and M. Trosset. Molecular embedding via a second order dissimilarity parameterized approach. *SIAM Journal on Scientific Computing*, 31(4):2733 – 2756, 2009.

[59] T. Hagedorn. General formulas for solving solvable sextic equations. *Journal of Algebra*, 233(2):704 – 757, 2000.

[60] L. Han, Q. Liao, and C. Liang. Closed-form displacement analysis of a planar fifth-class group with lower pairs. *Journal of Beijing University of Aeronautics and Astronautics*, 24(5):603 – 606, 1998.

[61] L. Han, Q. Liao, and C. Liang. The closed form displacement analysis of a seven-link Barranov-truss and all the Assur groups connected with it. *Mechanical Science and Technology*, 17(5):785 – 788, 1998.

[62] L. Han, Q. Liao, and C. Liang. Complex number method for kinematic analysis of planar Assur groups. *Mechanical Science and Technology*, 17(3):410 – 412, 1998.

[63] L. Han, Q. Liao, and C. Liang. Closed-form displacement analysis of an eight links planer Assur group. In *Proceedings of the 10th World Congress on the Theory of Machine and Mechanisms, June 20-24, Oulu, Finland*, 168 – 173, 1999.

[64] L. Han, Q. Liao, and C. Liang. A kind of algebraic solution for the position analysis of a planar basic kinematic chain. *Journal of Machine Design*, 16(3):16 – 18, 1999.

[65] L. Han, Q. Liao, and C. Liang. Closed-form displacement analysis for a nine-link Barranov truss or a eight-link Assur group. *Mechanism and Machine Theory*, 35(3):379 – 390, 2000.

[66] L. Han, Y. Zhang, and C. Liang. Wu's method for forward displacement analysis of the planar parallel mechanisms. *Journal of Beijing University of Aeronautics and Astronautics*, 24(1):116 – 119, 1998.

[67] L. Hang, Q. Jin, J. Wu, and T. Yang. A general study of the number of assembly configurations for multi-circuit planar linkages. *Journal of Southeast University (English edition)*, 16(1):46 – 51, 2000.

[68] E. Hansen. *Global Optimization Using Interval Analysis*. Marcel Dekker, New York, USA, 1992.

[69] T. Havel. The use of distances as coordinates in computer-aided proofs of theorems in Euclidean geometry. In *Symbolic Computations in Geometry*, 389:54 – 68. IMA Preprint Series, 1988.

[70] T. Havel. Some examples of the use of distances as coordinates for Euclidean geometry. *Journal of Symbolic Computation*, 11(5-6):579 – 593, 1991.

[71] M. Hayes. *Kinematics of General Planar Stewart-Gough Platforms*. PhD thesis, Department of Mechanical Engineering and Centre for Intelligent Machines, McGill University, 1999.

[72] M. Hayes and M. Husty. On the kinematic constraint surfaces of general three-legged planar robot platforms. *Mechanism and Machine Theory*, 38(5):379 – 394, 2003.

[73] M. Hayes, M. Husty, and P. Zsombor-Murray. Kinematic mapping of planar Stewart-Gough platforms. In *Proceedings of the 17th Canadian Congress of Applied Mechanics (CANCAM 1999)*, 319 – 320, 1999.

[74] M. Hayes, M. Husty, and P. Zsombor-Murray. Solving the forward kinematics of a planar three-legged platform with holonomic higher pairs. *Journal of Mechanical Design*, 121(2):212 – 219, 1999.

[75] M Hayes and P. Zsombor-Murray. A planar parallel manipulator with holonomic higher pairs: Inverse kinematics. In *Proceedings of the CSME Forum 1996*, 109 – 116, 1996.

[76] M. Hayes, P. Zsombor-Murray, and C. Chen. Unified kinematic analysis of general planar parallel manipulators. *Journal of Mechanical Design*, 126(5):866 – 874, 2004.

[77] Z. He, Y. Luo, and Q. Liu. Forward displacement analysis of a kind of nine-link Barranov truss based on hyper-chaotic Newton downhill method. In *2nd International Conference on Intelligent Human-Machine Systems and Cybernetics (IHMSC)*, 2:137 – 142, 2010.

[78] A. Hernández and V. Petuya. Position analysis of planar mechanisms with R-pairs using a geometrical-iterative method. *Mechanism and Machine Theory*, 39(2):133 – 152, 2004.

[79] K. Hunt. *Kinematic Geometry of Mechanisms*. Clarendon Press, Oxford, 1978.

[80] K. Hunt. Structural kinematics of in-parallel actuated robot arms. *ASME Journal of Mechanisms, Transmissions, and Automation in Design*, 105:705 – 712, 1983.

[81] M. Husty. Kinematic mapping of planar three-legged platforms. In *Proceedings of 15th Canadian Congress of Applied Mechanics (CANCAM 1995)*, 2:876 – 877, 1995.

[82] M. Husty. Non-singular assembly mode change in 3-RPR-parallel manipulators. In A. Kecskeméthy and A. Müller, editors, *Computational Kinematics*, 51 – 60. Springer Berlin Heidelberg, 2009.

[83] IFToMM. Terminology for the theory of machines and mechanisms. *Mechanism and Machine Theory*, 26(5):435 – 539, 1991.

[84] C. Innocenti. Analytical determination of the intersections of two coupler-point curves generated by two four-bar linkages. In J. Angeles, G. Hommel, and P. Kovács, editors, *Computational Kinematics*, 251 – 262. Kluwer Academic Publishers, 1993.

[85] C. Innocenti. Analytical-form position analysis of the 7-link Assur kinematic chain with four serially-connected ternary links. *Journal of Mechanical Design*, 116(2):622 – 628, 1994.

[86] C. Innocenti. Polynomial solution to the position analysis of the 7-link Assur kinematic chain with one quaternary link. *Mechanism and Machine Theory*, 30(8):1295 – 1303, 1995.

[87] C. Innocenti. Position analysis in analytical form of the 7-link Assur kinematic chain featuring one ternary link connected to ternary links only. *Mechanism and Machine Theory*, 32(4):501 – 509, 1997.

[88] J. Jalón and E. Bayo. *Kinematic and Dynamic Simulation of Multibody Systems: The Real-time Challenge*. Mechanical engineering series. Springer-Verlag, 1994.

[89] P. Ji and H. Wu. An efficient approach to the forward kinematics of a planar

parallel manipulator with similar platforms. *IEEE Transactions on Robotics and Automation*, 18(4):647 – 649, Aug 2002.

[90] D. Kapur and T. Saxena. Comparison of various multivariate resultant formulations. In *ISSAC '95: Proceedings of the 1995 International Symposium on Symbolic and Algebraic Computation*, 187 – 194. ACM Press, 1995.

[91] N. Kazarinoff. *Ruler and the Round: Classic Problems in Geometric Constructions.* Dover Publications, 2003.

[92] Kinematics and Robot Design Group at IRI. The CUIK project. Available at http://www.iri.upc.edu/research/webprojects/cuikweb/index.php.

[93] A. Klein. *Kinematics of Machinery.* McGraw-Hill Book Company, Inc., New York., 1917.

[94] T. Koetsier. A contribution to the history of kinematics - I. *Mechanism and Machine Theory*, 18(1):37 – 42, 1983.

[95] T. Koetsier. A contribution to the history of kinematics - II. *Mechanism and Machine Theory*, 18(1):43 – 48, 1983.

[96] T. Koetsier. From kinematically generated curves to instantaneous invariants: Episodes in the history of instantaneous planar kinematics. *Mechanism and Machine Theory*, 21(6):489 – 498, 1986.

[97] R. Kolodny, L. Guibas, M. Levitt, and P. Koehl. Inverse kinematics in biology: The protein loop closure problem. *International Journal of Robotics Research*, 24:151 – 163, 2005.

[98] X. Kong and C. Gosselin. Forward displacement analysis of third-class analytic 3-RPR planar parallel manipulators. *Mechanism and Machine Theory*, 36(9):1009 – 1018, 2001.

[99] X. Kong and T. Yang. Closed-form displacement analysis of 3-loop Baranov trussed. In *Proceedings of International Conference on Spatial Mechanisms and High Class Mechanisms (Theory and Practice)*, 1994.

[100] P. Kovács and G. Hommel. On the tangent-half-angle substitution. In J. Angeles, G. Hommel, and P. Kovács, editors, *Computational Kinematics*, 27 – 39. Kluwer Academic Publishers, 1993.

[101] S. Ku and R. Adler. Computing polynomial resultants: Bezout's determinant vs. Collins' reduced P.R.S. algorithm. *Communications of the ACM*, 12(1):23 – 30, 1969.

[102] J. Lambert. *Numerical Methods for Ordinary Differential Systems: The Initial Value Problem.* John Wiley and Sons, 1991.

[103] Z. Lan, Z. Huijun, and L. Liuming. Kinematic decomposition of coupler plane and the study on the formation and distribution of coupler curves. *Mechanism and Machine Theory*, 37(1):115 – 126, 2002.

[104] M. Laurent. A connection between positive semidefinite and Euclidean distance matrix completion problems. *Linear Algebra and its Applications*, 273(1-3):9 – 22, 1998.

[105] S. Li and G. Matthew. Closed form kinematic analysis of planar Assur II groups. In *Proceedings of the 7th IFToMM World Congress on the Theory of Machines and Mechanisms, September 17 - 22, Sevilla, Spain*, 1:141 – 145, 1987.

[106] H. Lipkin and J. Duffy. A vector analysis of robot manipulators. In G. Beni and S. Hackwood, editors, *Recent Advances in Robotics*, 175 – 242. John Wiley & Sons, Inc., New York, NY, USA, 1985.

[107] A. Liu and T. Yang. Displacement analysis of planar complex mechanisms using

continuation method. *Mechanical Science and Technology*, 13(2):55 – 62, 1994.

[108] H. Liu, T. Zhang, and H. Ding. Forward solutions of the 3-RPR planar parallel mechanism with Wu's method. *Journal of Beijing Institute of Technology*, 20(5):565 – 569, 2000.

[109] S. Lösch. Parallel redundant manipulators based on open and closed normal Assur chains. In J. Merlet and B. Ravani, editors, *Computational Kinematics*, 251 – 260. Kluver Academic Publishers, 1995.

[110] Y. Luo. Forward solutions of the 3-RPR planar parallel mechanism with Wu's method. *Journal of Hunan University of Arts and Science (Science and Technology)*, (2):27 – 29, 2004.

[111] Y. Luo, X. Li, L. Luo, and D. Liao. The research of Newton iterative method based on chaos mapping and its application to forward solutions of the 3-RPR planar parallel mechanism. *Machine Design and Research*, 23(2):37 – 39, 2007.

[112] Y. Luo and Q. Liu. Forward displacement analysis of 25th nine-link Barranov truss based on chaos least square method. In *2nd International Conference on Computer Modeling and Simulation (ICCMS)*, 1:184 – 188, 2010.

[113] Y. Luo and Q. Liu. Forward displacement analysis of non-plane two coupled degree nine-link Barranov truss based on hyper-chaotic Newton downhill method. *Applied Mechanics and Materials*, 20 - 23:659 – 664, 2010.

[114] N. Manolescu. A method based on Baranov trusses, and using graph theory to find the set of planar jointed kinematic chains and mechanisms. *Mechanism and Machine Theory*, 8(1):3 – 22, 1973.

[115] N. Manolescu and T. Erdelean. La determination des fermes Baranov avec e=9 elements en utilisant la methode de graphisation inverse, paper D-12. In *Proceedings of the 3rd IFToMM World Congress on the Theory of Machines and Mechanisms, September, Kupari, Yugoslavia*, D:177 – 188, 1971.

[116] A. Markov and N. Sonin (Editors). *Œuvres de P.L. Tchebychef*. Commissionaires de l'Académie impériale des sciences, 1907.

[117] J. McCarthy. Kinematics, polynomials, and computers—a brief history. *Journal of Mechanisms and Robotics*, 3(1):010201, 2011.

[118] J. McCarthy and G. Soh. *Geometric Design of Linkages*. Springer, 2011.

[119] K. Menger. Untersuchungen über allgemeine metrik. *Mathematische Annalen*, 100:75 – 163, 1928.

[120] K. Menger. New foundation of Euclidean geometry. *American Journal of Mathematics*, 53(4):721 – 745, 1931.

[121] J. Merlet. Direct kinematics of planar parallel manipulators. In *Proceedings of the IEEE International Conference on Robotics and Automation*, 4:3744 – 3749, Apr 1996.

[122] J. Merlet. ALIAS: An interval analysis based library for solving and analyzing system of equations. In *Proceedings of the SEA*, Toulouse, France, June 14 - 16 2000.

[123] J. Merlet. *Parallel Robots*. Springer, Dordrecht, The Netherlands, 2006.

[124] D. Michelucci and S. Foufou. Using Cayley-Menger determinants for geometric constraint solving. In *SM '04: Proceedings of the 9th ACM Symposium on Solid Modeling and Applications*, 285 – 290, Aire-la-Ville, Switzerland, 2004. Eurographics Association.

[125] S. Mitsi, K.-D. Bouzakis, and G. Mansour. Position analysis in polynomial form of planar mechanism with an Assur group of class 4 including one prismatic joint.

Mechanism and Machine Theory, 39(3):237 – 245, 2004.

[126] S. Mitsi, K.-D. Bouzakis, G. Mansour, and I. Popescu. Position analysis in polynomial form of planar mechanisms with Assur groups of class 3 including revolute and prismatic joints. *Mechanism and Machine Theory*, 38(12):1325 – 1344, 2003.

[127] S. Mitsi, K.-D. Bouzakis, G. Mansour, and I. Popescu. Position analysis in polynomial form of class-three Assur groups with two or three prismatic joints. *Mechanism and Machine Theory*, 43(11):1401 – 1415, 2008.

[128] F. Moon. Franz Reuleaux: Contributions to 19th century kinematics and theory of machines. *Applied Mechanics Reviews*, 56(2):261 – 285, 2003.

[129] F. Moon. Robert Willis and Franz Reuleaux: pioneers in the theory of machines. *Notes and Records of the Royal Society of London*, 57(2):209 – 230, 2003.

[130] J. Morgado and A. Gomes. A derivative-free tracking algorithm for implicit curves with singularities. In *International Conference on Computational Science*, 221 – 228, 2004.

[131] A. Müller. Generic mobility of rigid body mechanisms. *Mechanism and Machine Theory*, 44(6):1240 – 1255, 2009.

[132] Z. Ni, Q. Liao, and S. Wei. New research of forward displacement analysis of 6-link Assur group. In *2nd International Conference on Information Science and Engineering (ICISE)*, 5187 – 5190, 2010.

[133] J. Nielsen and B. Roth. Solving the input/output problem for planar mechanisms. *Journal of Mechanical Design*, 121(2):206 – 211, 1999.

[134] H. Nolle. Linkage coupler curve synthesis: A historical review - I. developments up to 1875. *Mechanism and Machine Theory*, 9(2):147 – 168, 1974.

[135] J. O'Rourke. *Art Gallery Theorems and Algorithms*. The International Series of Monographs on Computer Science. Oxford University Press, 1987.

[136] J. Owen and S. Power. The nonsolvability by radicals of generic 3-connected planar Laman graphs. *Transactions of the American Mathematical Society*, 359(5):2269 – 2303, 2007.

[137] E. Peisach. Determination of the position of the member of three-joint and two-joint four member Assur groups with rotational pairs (in Russian). *Machinowedenie*, (5):55 – 61, 1985.

[138] E. Peisach. On Assur groups, Baranov trusses, Grübler chains, planar linkages and on their structural (number) synthesis. In *The 22th Working Meeting of the IFToMM Permanent Commission for Standardization of Terminology*, 33 – 41, LaMCoS - INSA de LYON, Villeurbanne, France, June 29 - July 4, 2008.

[139] S. Pellegrino, editor. *Deployable structures*. CISM Courses and Lectures No. 412, International Centre for Mechanical Sciences. Springer, 2001.

[140] G. Pennock and A. Hasan. A polynomial equation for a coupler curve of the double butterfly linkage. *Journal of Mechanical Design*, 124(1):39 – 46, 2002.

[141] G. Pennock and D. Kassner. Kinematic analysis of a planar eight-bar linkage: application to a platform-type robot. In *Proceedings of the 21th ASME Biennial Mechanisms Conference*, 37 – 43, Chicago, USA, 1990.

[142] G. Pennock and D. Kassner. Kinematic analysis of a planar eight-bar linkage: Application to a platform-type robot. *Journal of Mechanical Design*, 114(1):87 – 95, 1992.

[143] G. Pennock and N. Raje. Curvature theory for the double flier eight-bar linkage. *Mechanism and Machine Theory*, 39(7):665 – 679, 2004.

[144] J. Porta. CuikSLAM: A kinematics-based approach to SLAM. In *Proceedings*

of the 2005 IEEE International Conference on Robotics and Automation, 2425 – 2431, 2005.

[145] J. Porta, L. Ros, T. Creemers, and F. Thomas. Box approximations of planar linkage configuration spaces. *Journal of Mechanical Design*, 129(4):397 – 405, 2007.

[146] J. Porta, L. Ros, and F. Thomas. Inverse kinematics by distance matrix completion. In *Proceedings of the International Workshop on Computational Kinematics*, Cassino, Italy, May 4-6 2005.

[147] J. Porta, L. Ros, and F. Thomas. On the trilaterable six-degree-of-freedom parallel and serial manipulators. In *Proceedings of the 2005 IEEE International Conference on Robotics and Automation*, 960 – 967, 2005.

[148] J. Porta, L. Ros, and F. Thomas. Multi-loop position analysis via iterated linear programming. In *Proceedings of Robotics: Science and Systems*, Philadelphia, USA, August 2006.

[149] J. Porta, L. Ros, and F. Thomas. A linear relaxation technique for the position analysis of multiloop linkages. *IEEE Transactions on Robotics*, 25(2):225 – 239, 2009.

[150] J. Porta, L. Ros, F. Thomas, F. Corcho, J. Canto, and J. Perez. Complete maps of molecular-loop conformational spaces. *Journal of Computational Chemistry*, 28(13):2170 – 2189, 2007.

[151] J. Porta, L. Ros, F. Thomas, and C. Torras. A branch-and-prune solver for distance constraints. *IEEE Transactions on Robotics*, 21(2):176 – 187, 2005.

[152] J. Porta, F. Thomas, L. Ros, and C. Torras. A branch-and-prune algorithm for solving systems of distance constraints. In *Proceedings of the IEEE International Conference on Robotics and Automation*, 1:342 – 348, 2003.

[153] S. Power and J. Owen. The nonsolvability by radicals of generic 3-connected planar Laman graphs. *Transactions of the American Mathematical Society*, 359(5):2269 – 2303, 2007.

[154] H. Résal. *Traité de Cinématique Pure*. Imprimerie de Mallet-Bachelier, Paris, France, 1862.

[155] F. Reuleaux. *The Kinematics of Machinery: Outlines of a Theory of Machines (translated and edited by A. Kennedy)*. Macmillan, 1876.

[156] S. Roberts. On three-bar motion in plane space. *Proceedings of the London Mathematical Society*, 7:14 – 23, 1875.

[157] A. Rodriguez, L. Basañez, and E. Celaya. A relational positioning methodology for robot task specification and execution. *IEEE Transactions on Robotics*, 24(3):600 –611, 2008.

[158] N. Rojas and F. Thomas. A robust forward kinematics analysis of 3-R$\underline{\text{P}}$R planar platforms. In J. Lenarcic and M. Stanisic, editors, *Advances in Robot Kinematics*, 23 – 32. Springer, 2010.

[159] N. Rojas and F. Thomas. Closed-form solution to the position analysis of Watt–Baranov trusses using the bilateration method. *Journal of Mechanisms and Robotics*, 3(3):031001, 2011.

[160] N. Rojas and F. Thomas. A coordinate-free approach to tracing the coupler curves of pin-jointed linkages. In *Proceedings of the ASME 2011 International Design Engineering Technical Conferences & Computers and Information in Engineering Conference, Paper No. DETC2011-48147*, 2011.

[161] N. Rojas and F. Thomas. Distance-based position analysis of the three seven-link Assur kinematic chains. *Mechanism and Machine Theory*, 46(2):112 – 126, 2011.

[162] N. Rojas and F. Thomas. The forward kinematics of 3-R$\underline{P}$R planar robots: A review and a distance-based formulation. *IEEE Transactions on Robotics*, 27(1):143 – 150, 2011.

[163] N. Rojas and F. Thomas. On closed-form solutions to the position analysis of Baranov trusses. *Mechanism and Machine Theory*, 50:179 – 196, 2012.

[164] N. Rojas and F. Thomas. The characteristic polynomials of all fully-parallel planar robots derived from a single polynomial. Submitted.

[165] N. Rojas and F. Thomas. A distance geometry approach to the computation of pin-jointed linkage configuration spaces: Application to tracing high-order coupler curves. Submitted.

[166] N. Rojas and F. Thomas. Formulating Assur kinematic chains as projective extensions of Baranov trusses. Submitted.

[167] B. Roth and F. Freudenstein. Synthesis of path-generating mechanisms by numerical methods. *ASME Journal of Engineering for Industry*, 85:298 – 307, 1963.

[168] J. Saxe. Embeddability of weighted graphs in k-space is strongly NP-hard. In *Proceedings of the 17th Allerton Conference in Communications, Control and Computing*, 480 – 489, 1979.

[169] B. Servatius, O. Shai, and W. Whiteley. Combinatorial characterization of the Assur graphs from engineering. *European Journal of Combinatorics*, 31(4):1091 – 1104, 2010.

[170] O. Shai. Topological synthesis of all 2D mechanisms through Assur graphs. In *Proceedings of the ASME 2010 International Design Engineering Technical Conferences & Computers and Information in Engineering Conference, Paper No. DETC2010-28926*, 2010.

[171] O. Shai. The correction to grubler criterion for calculating the degrees of freedoms of mechanisms. In *Proceedings of the ASME 2011 International Design Engineering Technical Conferences & Computers and Information in Engineering Conference, Paper No. DETC2011-48146*, 2011.

[172] H. Shen, K. Ting, and T. Yang. Configuration analysis of complex multiloop linkages and manipulators. *Mechanism and Machine Theory*, 35(3):353 – 362, 2000.

[173] H. Shen and T. Yang. A numerical method and automatic generation for determining the assemblage configurations of complex planar linkages based on the ordered SOCs. In *Proceedings of the ASME 1996 International Design Engineering Technical Conferences & Computers in Engineering Conference, Paper No. 96-DETC/MECH-1030*, 1996.

[174] K. Shirazi. Symmetrical coupler curve and singular point classification in planar and spherical swinging-block linkages. *Journal of Mechanical Design*, 128(2):436 – 443, 2006.

[175] A. Sljoka, O. Shai, and W. Whiteley. Checking mobility and decomposition of linkages via pebble game algorithm. In *Proceedings of the ASME 2011 International Design Engineering Technical Conferences & Computers and Information in Engineering Conference, Paper No. DETC2011-48340*, 2011.

[176] A. Sommese and C. Wampler. *The Numerical Solution of Systems of Polynomials Arising in Engineering and Science*. World Scientific, 2005.

[177] D. Sotiropoulos and T. Grapsa. Optimal centers in branch-and-prune algorithms for univariate global optimization. *Applied Mathematics and Computation*, 169(1):247 – 277, 2005.

[178] E. Study. *Geometric der Dynamen*. Teubner Verlagsgesellschaft, 1903.

[179] Bernd Sturmfels. What is a Gröbner basis? *Notices of the American Mathematical Society*, 52(10):1199 – 1200, 2005.

[180] C. Suh and C. Radcliffe. *Kinematics and Mechanism Design*. Wiley, New York, 1978.

[181] F. Thomas. Simulation of planar bar linkages using Cinderella. Web document available at http://www.iri.upc.edu/people/thomas/PlanarLinkages.html.

[182] F. Thomas. Solving geometric constraints by iterative projections and backprojections. In *Proceedings of the IEEE International Conference on Robotics and Automation*, 2:1789 – 1794, 2004.

[183] F. Thomas, J. M. Porta, and L. Ros. Distance constraints solved geometrically. In J. Lenarcic and C. Galletti, editors, *Advances in Robot Kinematics*, 123 – 132. Kluwer Academic Publishers, 2004.

[184] F. Thomas and L. Ros. Revisiting trilateration for robot localization. *IEEE Transactions on Robotics*, 21(1):93 – 101, 2005.

[185] M.. Trosset. Distance matrix completion by numerical optimization. *Computational Optimization and Applications*, 17(1):11 – 22, 2000.

[186] S. Vavasis. Condition numbers of numeric and algebraic problems. In *Fields Institute Workshop on Hybrid Methodologies for Symbolic-Numeric Computation*, The University of Waterloo, Waterloo, Ontario, Canada, November 16 - 19 2011.

[187] J. Verschelde. Algorithm 795: PHCPACK: A general-purpose solver for polynomial systems by homotopy continuation. *ACM Transactions on Mathematical Software*, 25(2):251 – 276, 1999.

[188] R. Walker. *Algebraic Curves*. Springer-Verlag, 1978.

[189] D. Walter and M. Husty. On a nine-bar mechanism, its possible configurations and conditions for flexibility. In *Proceedings of the 12th IFToMM World Congress in Mechanism and Machine Science, June 17 - 20, Besançon, France*, 2007.

[190] C. Wampler. Solving the kinematics of planar mechanisms. *Journal of Mechanical Design*, 121(3):387 – 391, 1999.

[191] C. Wampler. Solving the kinematics of planar mechanisms by Dixon determinant and a complex-plane formulation. *Journal of Mechanical Design*, 123(3):382 – 387, 2001.

[192] C. Wampler. Displacement analysis of spherical mechanisms having three or fewer loops. *Journal of Mechanical Design*, 126(1):93 – 100, 2004.

[193] C. Wampler, J. Hauenstein, and A. Sommese. Mechanism mobility and a local dimension test. *Mechanism and Machine Theory*, 46(9):1193 – 1206, 2011.

[194] P. Wang, Q. Liao, and Z. Lu. Displacement analysis of non-planar nine-link Barranov truss. *Journal of Beijing University of Posts and Telecommunications*, 31(4):10 – 14, 2008.

[195] P. Wang, Q. Liao, and Z. Lu. Displacement analysis of a nine-link Barranov truss. *Machine Design and Research*, 25(2):33 – 36, 2009.

[196] P. Wang, Q. Liao, and S. Wei. Forward displacement analysis of a seven-link Barranov truss based on Wu method. *Mechanical Science and Technology*, 25(6):748 – 752, 2006.

[197] P. Wang, Q. Liao, S. Wei, and Y. Zhuang. Displacement analysis of a kind of nine-link Barranov truss. *Journal of Beijing University of Posts and Telecommunications*, 29(3):12 – 17, 2006.

[198] P. Wang, Q. Liao, S. Wei, and Y. Zuang. Direct position analysis of nine-link Barranov truss based on Dixon resultant. *Journal of Beijing University of Aeronautics*

and Astronautics, 32(7):852 – 855,864, 2006.

[199] P. Wang, Q. Liao, S. Wei, and Y. Zuang. Forward displacement analysis of a kind of nine-link Barranov truss based on Dixon resultants. *China Mechanical Engineering*, 17(21):2034 – 2038, 2006.

[200] P. Wang, Q. Liao, Y. Zhuang, and S. Wei. Direct position analysis of a nine-link Barranov truss. *Journal of Tsinghua University (Science and Technology)*, 46(8):1373 – 1376, 2006.

[201] P. Wang, Q. Liao, Y. Zhuang, and S. Wei. A method for position analysis of a kind of nine-link Barranov truss. *Mechanism and Machine Theory*, 42(10):1280 – 1288, 2007.

[202] P. Wang, Q. Liao, Y. Zhuang, and S. Wei. Research on position analysis of a kind of nine-link Barranov truss. *Journal of Mechanical Design*, 130(1):011005, 2008.

[203] P. Wang, Q. Liao, Y. Zuang, and S. Wei. Displacement analysis of nine-link Barranov truss. *Chinese Journal of Mechanical Engineering*, 43(7):11 – 15, 2007.

[204] P. Wang, L. Wang, D. Li, J. Gu, and J. Song. Closed-form displacement analysis of a kind of non-planar nine-link Barranov truss. In *IEEE International Conference on Automation and Logistics (ICAL)*, 2397 – 2401, 2008.

[205] W. Wedemeyer and H. Scheraga. Exact analytical loop closure in proteins using polynomial equations. *Journal of Computational Chemistry*, 20(8):819 – 844, 1999.

[206] C. Wee and R. Goldman. Elimination and resultants. 1. elimination and bivariate resultants. *IEEE Computer Graphics and Applications*, 15(1):69 – 77, 1995.

[207] S. Wei, X. Zhou, and Q. Liao. Closed-form displacement analysis of one kind of nine-link Barranov trusses. In *Proceedings of the 11th IFToMM World Congress in Mechanism and Machine Science, April 1-4, Tianjin, China*, 1176 – 1177, 2004.

[208] S. Wei, X. Zhou, and Q. Liao. Research on assembly configurations for nine-link Barranov truss. *Mechanical Science and Technology*, 23(8):962 – 965, 2004.

[209] E. Weisstein. Graph embedding. From MathWorld - A Wolfram Web Resource, http://mathworld.wolfram.com/GraphEmbedding.html.

[210] E. Weisstein. Sylvester matrix. From MathWorld - A Wolfram Web Resource, http://mathworld.wolfram.com/SylvesterMatrix.html.

[211] P. Wenger and D. Chablat. Kinematic analysis of a class of analytic planar 3-RPR parallel manipulators. In A. Kecskeméthy and A. Müller, editors, *Computational Kinematics*, 43 – 50. Springer Berlin Heidelberg, 2009.

[212] P. Wenger, D. Chablat, and M. Zein. Degeneracy study of the forward kinematics of planar 3-RPR parallel manipulators. *ASME Journal of Mechanical Design*, 129(12):1265 – 1268, 2007.

[213] R. Willis. *Principles of Mechanism*. John W. Parker, 1841.

[214] K. Wohlhart. Direct kinematic solution of a general planar Stewart platform. In *Proceedings of the International Conference on Computer Integrated Manufacturing*, 403 – 411, Zakopane, Poland, 1992.

[215] K. Wohlhart. Position analysis of the rhombic Assur group 4.4. In *Proceedings of the RoManSy, CISM- IFTOMM Symposium, Gdansk, Poland*, 21 – 31, 1994.

[216] K. Wohlhart. Robots based on Assur group A(3.5). In J. Lenarcic and P. Wenger, editors, *Advances in Robot Kinematics: Analysis and Design*, 165 – 175. Springer Netherlands, 2008.

[217] K. Wohlhart. Position analyses of open normal Assur groups A(3.6). In *ASME/IFToMM International Conference on Reconfigurable Mechanisms and Robots*, 88 – 94, 2009.

[218] K. Wohlhart. Position analyses of normal quadrilateral Assur groups. *Mechanism and Machine Theory*, 45(9):1367 – 1384, 2010.

[219] Y. Yajima. Positive semidefinite relaxations for distance geometry problems. *Japan Journal of Industrial and Applied Mathematics*, 19:87 – 112, 2002.

[220] J. Yakey, S. LaValle, and L. Kavraki. Randomized path planning for linkages with closed kinematic chains. *IEEE Transactions on Robotics and Automation*, 17(6):951 – 958, 2001.

[221] L. Yang. Solving spatial constraints with global distance coordinate system. *International Journal of Computational Geometry and Applications*, 16(5-6):533 – 548, 2006.

[222] T. Yang. Structural analysis and number synthesis of spatial mechanisms. In *Proceedings of the 6th IFToMM World Congress on the Theory of Machines and Mechanisms, December 15 - 20, New Delhi, India*, 1:280 – 283, 1983.

[223] T. Yang and F. Yao. Topological characteristics and automatic generation of structural synthesis of planar mechanisms based on the ordered single-opened-chains. In *Proceedings of the ASME 1994 Mechanisms Conference*, 70:67 – 74, 1994.

[224] L. Yaohui. New method to extend Macaulay resultant. In *Second International Conference on Intelligent Computation Technology and Automation*, 4:562 – 565, 2009.

[225] M. Zein, P. Wenger, and D. Chablat. Non-singular assembly-mode changing motions for 3-RPR parallel manipulators. *Mechanism and Machine Theory*, 43(4):480 – 490, 2008.

[226] Y. Zhuang, P. Wang, and Q. Liao. Research on displacement analysis of a kind of non-planar nine link Barranov truss. *Journal of Beijing University of Posts and Telecommunications*, 29(6):13 – 16, 2006.

[227] Z. Zou, R. Bird, and R. Schnabel. A stochastic/perturbation global optimization algorithm for distance geometry problems. *Journal of Global Optimization*, 11(1):91 – 105, 1997.

[228] P. Zsombor-Murray, C. Chen, and M. Hayes. Direct kinematic mapping for general planar parallel manipulators. In *Proceedings of the CSME Forum*, 2002.